University of Southampton

Faculty of Engineering and Physical Sciences

Chemistry

Electrochemical oxidation and reduction of hydroxyalkenes

DOI

by

Domenico Romano

Thesis for the degree of Doctor of Phylosophy

April 2022

University of Southampton

Abstract

Faculty of Engineering and Physical Sciences

Chemistry

Doctor of Phylosophy

Electrochemical oxidation and reduction of hydroxyalkenes

by

Domenico Romano

Electrochemistry is the chemistry that studies all those processes that involve the transfer of electrons and organic electro-synthesis is that branch that exploits electricity for the synthesis of valuable chemical compounds. It is considered an environmentally friendly approach but it has never been largely used in synthetic organic laboratories because of lack of standardised equipment and protocols. For this reason, nowadays the use of flow equipment and flow electrolysis cells is gaining a lot of interest and is helping the development of new electro-synthetic processes.

Heterocycles are one of the most important and useful groups of organic compounds; they are found in bio-active natural compounds, agrochemical and pharmaceutical compounds. Because of that, their preparation in an efficient and economical way has been the main target in industry. Because the common approaches usually require expensive or toxic reagents, severe conditions, long reaction time, new more sustainable and convenient approaches are required. So electrochemical methods can be an interesting and environmentally friendly way to synthetize different heterocyclic structures. Recently, there has been much interest in the use of flow systems in organic synthesis, especially flow electrochemical reactors. This interest is due to the ability of microflow approach to give high selectivity and high conversion in a single pass. The main target of my first work was the synthesis of substituted tetrahydrofurans and lactones using an Ammonite electrochemical flow reactor. The approach targets a reagent free oxidative cyclisation of styrene-derivatives using microfluidic electrolysis cells. Different substrates have been tested with moderate to good yields and some mechanistic insight have been given with regard to this process.

While working on the oxidative cyclisation we discovered a side-reaction involving the reduction of the styrene double bond to single bond. Considering the importance of such reaction in synthetic chemistry and after a careful literature review we decided to focus our attention on developing an electrolysis method in the Ammonite microfluidic reactor for the reduction of styrene-double bond. Our method does not require any metal catalyst and no flammable hydrogen gas. Once optimised the electrolysis conditions, the method has been applied to different substrates, in particular on the synthesis of Gigantol a natural compound with medicinal properties. While working on the substrate scope a defluorination side-reaction was observed for substrate bearing fluorine atoms on their structure and this could be a topic to further explore in future considering the importance of such reaction especially in medicinal chemistry.

Table of Contents

Table of Tables

Table of Figures

Research Thesis: Declaration of Authorship

Print name: DOMENICO ROMANO

Title of thesis: Electrochemical oxidation and reduction of hydroxyalkenes

I declare that this thesis and the work presented in it are my own and has been generated by me as the result of my own original research.

I confirm that:

This work was done wholly or mainly while in candidature for a research degree at this University;
Where any part of this thesis has previously been submitted for a degree or any other qualification at this University or any other institution, this has been clearly stated;
Where I have consulted the published work of others, this is always clearly attributed;
Where I have quoted from the work of others, the source is always given. With the exception of such quotations, this thesis is entirely my own work;
I have acknowledged all main sources of help;
Where the thesis is based on work done by myself jointly with others, I have made clear exactly what was done by others and what I have contributed myself;
None of this work has been published before submission

Signature: ..... Date:.....

Acknowledgements

I am not really good with words but I will try.

First of all, I would like to thank my supervisor Professor Richard Brown for giving me the opportunity to be part of his research group and to work on this project that made me grow not only as a chemist but also as an individual. I would like to thank him especially for the support and the guidance through all my PhD.

I would like to really thank all the people of the Brown group, past and present, for their support and especially for the fun we shared in the lab and in the pubs, that made my life in Southampton and my studies more enjoyable, especially during rough times. Same for the people of the other groups on the floor (Harrowen's and Linclau's). I am really happy to be able to call some of these people not just colleagues but friends, in particular Ana, Sergio, Diego and George.

Also a huge thank to my family for always being supportive and being always there whenever I need it. Thanks to the LABFACT Interreg program for founding my PhD.

Definitions and Abbreviations

^{1}H-NMR	proton nuclear magnetic resonance
^{13}C-NMR	carbon-13 nuclar magnetic resonance
°C	Celsius degree(s)
A	Ampere
Ac	Acetate
atm	atmospheric
Bn	Benzyl
$CDCl_3$	deuterated chloroform
CV	Cyclic Voltammetry
d	Doublet
DMF	*N*,*N*-Dimethylformamide
e^-	electron
EI	electron ionisation
Equiv	Equivalets
ESI	Electronspray ionisation
Et	Ethyl
EWG	Electron withdrawing group
g	gram(s)
GC	Gas Chromatography
h	hour(s)
HPLC	high performance liquid chromatography
HRMS	High resolution mass spectrometry
i	current
IR	Infrared
J	Coupling constant
LRMS	Low resolution mass spectrometry

ms	mass spectrometry
m	multiplet
m	meta
Me	methyl
mmol	millimole(s)
min	minute(s)
MP	melting point
MW	molecular weight
m/z	mass/charge ratio
NMR	Nuclear Magnetic Resonance
o	ortho
p	pressure
p	para
Ph	phenyl
ppm	parts per million
PVDF	polyvinylidene fluoride
q	quartet
rt	room temperature
sat	saturated
SCE	saturated calomel electrode
t	triplet
*t*Bu	tert-butyl
THF	tetrahydrofuran
TLC	thin layer chromatography
V	volt

Chapter 1 GENERAL INTRODUCTION

1.1 Basics of electrochemistry

Electrochemistry is the field of chemistry that studies the results of the combination of chemical and electrical effects. Two main electrochemical processes can be identified: Galvanic and Electrolytic.

In a galvanic process, a spontaneous chemical reaction is used to produce electricity. The most common example is the reaction between an aqueous solution of zinc and one of copper, during which solid Zn^0 is oxidised to Zn^{2+} while Cu^{2+} is reduced to Cu^0. A galvanic cell usually consists of two chambers connected through a salt bridge in order to close the circuit; in each chamber there is an electrode, a cathode and anode. In this type of cell, the anode is indicated as negative because electrons are generated there and they start to flow through the circuit to the cathode which is positive because it is where the electrons are consumed by the reduction reaction. Electrons flow through the circuit until equilibrium is reached (Figure 1.1).

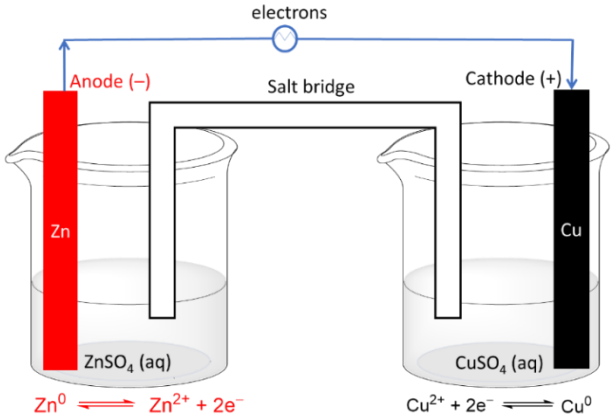

Figure 1.1: scheme of a galvanic cell.

During an electrolytic process instead, the passage of electric current is provided by an external source (battery) in order to perform a chemical red-ox reaction that normally would not occur spontaneously. An electrolytic cell can look like a galvanic one but it also can be undivided. In this case, the cathode (where the reduction happens) is indicated as negative because the battery provides the electrons that are used to reduce the compound at the cathode; at the anode (where the oxidation happens) the species get still oxidised but it is indicated as positive because the electrons generated are "removed" by the battery (Figure 1.2).[1]

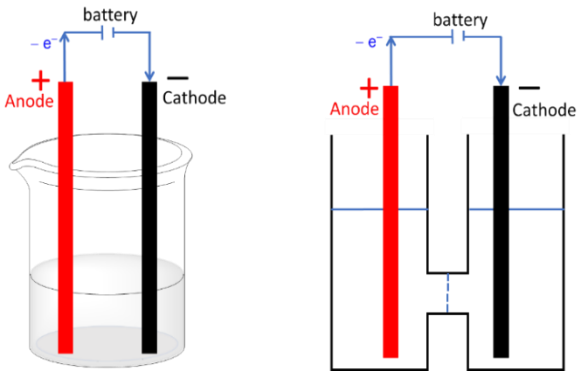

Figure 1.2: Scheme of electrolytic cells (undivided and divided).

1.2 Organic electrosynthesis

1.2.1 Fundamentals of organic electrosynthesis

The principle of electrosynthesis is to replace the electrons formally transfered between molecules in redox reactions with two separated processes: electron release at the anode and electron consumption at the cathode. In most cases, only one of these two reactions is wanted and it takes place at the working electrode, the other one is the counter-reaction and it happens at the auxiliary (counter) electrode. An electrochemical reaction occurs in a cell that is part of a broken circuit and at the ends of each break, there are the two electrodes (anode and cathode); other components of this circuit are the substrate, the solvent and the supporting electrolyte. In order to close the circuit and have the desired transformation, ions needs to flow between the electrodes. The electrolysis reaction can take place in an undivided cell or a divided one if the counter reaction can interfere with the chemistry at the working electrode (see Figure 1.2).[2–5]

An organic electrochemical reaction that proceeds directly at an electrode is made of different steps, chemical and physical: the mass transport of the substrate from the bulk solution to the electrode surface *via* diffusion or migration; a pre-reaction such as deprotonation or dissociation may take place to form an intermediate that is adsorbed on the electrode surface, followed by the electron transfer (reduction or oxidation); the intermediate formed in the electron transfer step is then desorbed and subject to the chemical step to give the final product; the last step is the diffusion of the product from the electrode surface to the bulk solution (Figure 1.3).[5,6] This is a simplified picture, and multiple electron transfers take place in many reactions with intervening chemical steps.

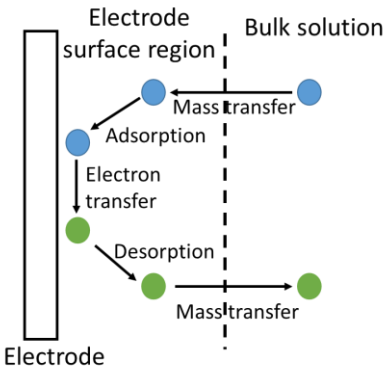

Figure 1.3: Simplified overview of the steps involved in an electrolysis reaction.

The key step of an organic electrochemical reaction is the electron transfer between the molecule and the electrode. It can be described using molecular orbitals as a transfer of an electron from the highest occupied orbital (HOMO) to the anode in case of an oxidation and as transfer of an electron from the cathode to the lowest unoccupied orbital (LUMO) for a reduction (Figure 1.4).[5,7]

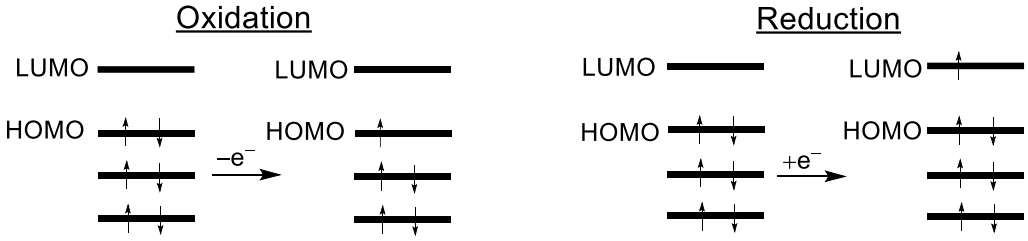

Figure 1. 4: MO's involved in electrochemical oxidation and reduction.

1.2.1.1 Electrodes and their role

The electrodes are crucial components in an electrochemical cell, and the choice of the right material is fundamental.[5] The selection of the right electrode is often based on prior experience rather than a theoretical basis, but careful attention is needed because the success and the selectivity of the electrolysis are highly dependent on it.[8] The oxidation of acetic acid,[9–12] and the reduction of acrylonitrile[9,13–15] are examples where the same starting material can be converted to different products by simply changing the working electrode; the selectivity is affected by the ability of the electrode material to adsorb the reactant, the product, the intermediates or even the species not directly involved in the transformation (solvent, additives); also the selectivity depends on the ability of the electrode to drive the main reaction at high rate and low overpotential, inhibiting possible side-reactions.[8] (Scheme 1.1).

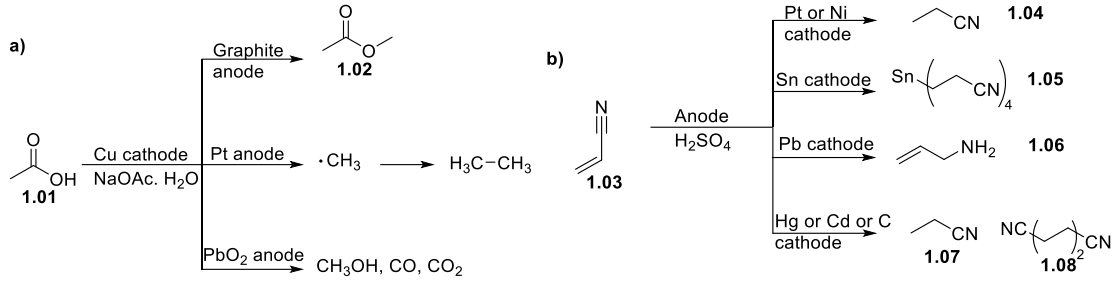

Scheme 1.1: Examples of the effect of electrode material in: (a) the oxidation of acetic acid, and (b) reduction of acrylonitrile.

The yield and the selectivity for the desired reaction are not the only parameter to consider when choosing appropriate electrode materials. The overpotential for undesired reaction is another one. In general, the overpotential is the additional potential to the equilibrium potential that needs to be applied at both electrodes in order to make the current flow through the circuit and to form the product.[2,5] Unwanted reactions may be avoided by using a specific electrode material with an overpotential that is high enough. In cases where reactions at the counter-electrode, such as anodic oxygen evolution and cathodic hydrogen evolution, are desirable it is preferable to choose a material with a low overpotential.[16–20] Moreover, when choosing suitable electrode materials, electronic conductivity, chemical and physical stability (stability at various temperatures, pressures, solvents, resistance to corrosion and to degradation) need to be taken into account. In addition, other parameters like cost, toxicity and how easily it can be worked into different shapes.[2,5,8,9,21]

As previously stated, an electrochemical reaction is made of different steps (adsorption and desorption, single or multi-electron transfer, preceding and/or subsequent chemical reactions) and all of them depend on the electrode surface and its cleanliness. To that extent passivation of the electrode surface due to formation of oxide films or polymer deposition can be a big issue affecting the kinetics of the reaction. Passivation can be detected by cyclic voltammetry experiments but in general, it is good practise to pre-treat the electrode surface before the use; this can be simple mechanical polishing or exposure to a solvent or a chemical species in order to activate the surface.[2,5,21]

When picking the cathode material, if it is going to be the working electrode, it is desirable to have a high overpotential for hydrogen evolution. Mercury has the highest hydrogen overpotential and was frequently used in the past as cathode, but its application is greatly limited nowadays due to its toxicity. An exception perhaps is application of Hg as a cathode for electrochemical measurements. Pt has the lowest hydrogen overpotential and it usually a good choice as cathode material for hydrogenation reactions; Ni can be an inexpensive alternative to Pt. Carbon is inexpensive and has a high hydrogen over-potential; stainless steel despite a

relatively low hydrogen overpotential, because of its low price and corrosion resistance has many applications.[2,5]

When choosing the anode material, not only the oxygen overpotential has to be taken into account, corrosion resistance is also a very important parameter to consider unless it is a sacrificial anode. If anode disintegration provides the counter reaction, electronegative metals such as zinc, aluminium or magnesium are commonly used as sacrificial anodes. Other anode materials include platinum because of its tendency to generate radical intermediate selectively, but its activity is very dependent on the conditions of the surface; carbon anodes are widely used in electrosynthesis and are available with different microstructures (graphite, glassy carbon, C/PVDF, diamond, nano-tubes and fibres) and at relatively low costs. Characteristic properties include the ability to enhance further oxidation forming useful cationic intermediates.[2,5,21]

When working under controlled potential conditions, a third electrode is needed to perform the role of the reference electrode. It must have a constant efficiency, providing a stable potential. The reaction at the reference electrode should be reversible and when choosing the right one it is important to consider the temperature and the pressure of the cell and if the species generated at the anode and cathode can interfere with its performance. A common reference electrode in aqueous systems is the SHE (standard hydrogen electrode) whose potential is conventionally defined as zero. Other common reference electrodes are the SCE (saturated calomel electrode; Hg/Hg_2Cl_2/sat. KCl in H_2O) and the Ag/AgCl electrode (Figure 1.5).[5,21] All reference electrodes consist of: a body (made of plastic or glass); a top seal; a junction that separates the filling solution from the external electrolyte and it can be a Teflon frit or a ceramic junction and the active component inside of the electrode (metal wire or platinum flag or metal wire/sparingly soluble salt or mercury/sparingly soluble mercury compound).[21]

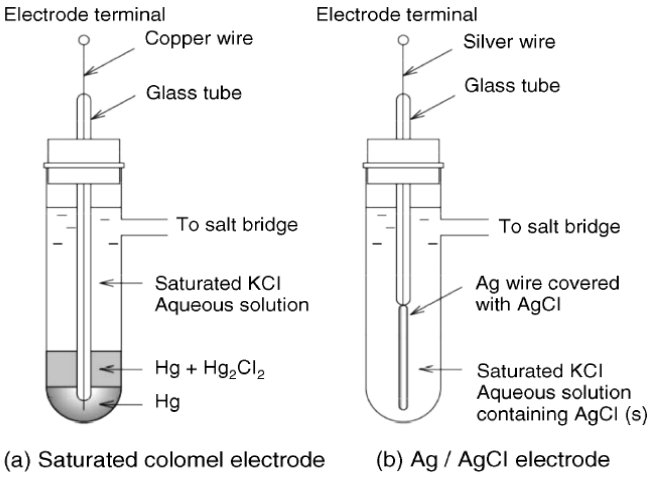

Figure 1.5: schemes of SCE and Ag/AgCl reference electrode[5].

1.2.1.2 Solvent and supporting electrolyte

Another important component of the electrolysis cell is the electrolyte. The term "electrolyte" refers to the reaction solution and supporting electrolyte, if used.[2] Different solvents can be used in organic electrochemistry, as long as they are able to dissolve the substrate(s), and reagents and the supporting electrolyte in order to afford conductivity. The solvent also needs to have a wide enough potential window in order not to get reduced or oxidised at the electrodes. It is also desirable that solvents should also have low toxicity and low viscosity; the latter is important because viscosity can strongly affect the diffusion of the substrate from the bulk solution to the electrode surface. Common protic solvents are water, methanol and ethanol; they are useful especially because they can give proton reduction to hydrogen gas as a counter reaction. Nitriles (e.g. acetonitrile) are also used in organic electrochemistry because of their stability to common redox conditions and their high polarity and good solvating power. THF is quite commonly employed in organic electrosynthesis because of its electrochemical stability, although its low polarity can make it difficult to dissolve the supporting electrolyte. Halogenated solvent have excellent solvating power, but their use is discouraged due to poor stability under some reductive conditions and especially because of their toxicity.[5,21,22]

The term supporting electrolyte refers to the salt dissolved in the reacting solution in order to provide ionic species capable of migrating between the electrodes, allowing the current to pass in the cell; it needs to be soluble in the reaction solvent and it should be stable under oxidative and reductive conditions. The most common salts that are routinely used in electrochemistry, are a combination of tetraalkylammonium cations with perchlorate or tetrafluoroborate counter ions. The tetraalkylammonium ions are used because of their organic solubility and their low electroreductive reactivity; lithium, sodium and magnesium are also used sometimes, although care may be needed to avoid plating of metals on the cathode. Selection of appropriate anion is also important; halide ions can be used but Cl^-, Br^- and I^- can be oxidised. Perchlorate salts have been widely used, although safety concerns related to explosion hazards should be considered. Tetrafluoroborates and hexafluorophosphates are a good alternatives, but are relatively expensive (Figure 1.6).[2,5,21,22]

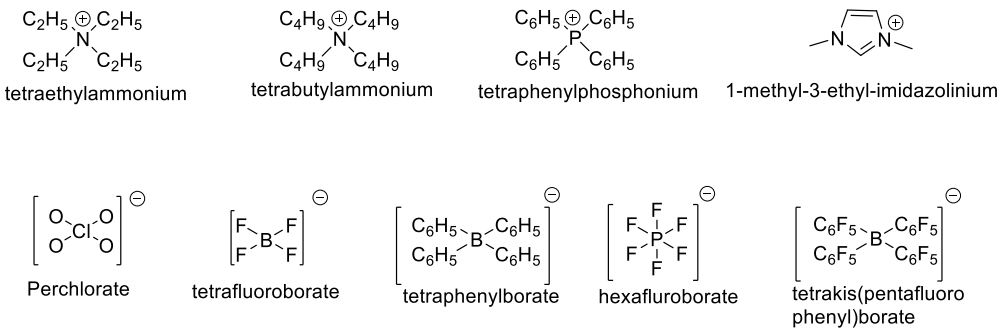

Figure 1.6: Examples of cations and anions used in supporting electrolytes.

1.2.2 Organic electrosynthesis as a sustainable approach

Electrochemistry is the chemistry that studies all those processes that involve the transfer of electrons. In particular, electro-synthesis is that branch that exploits electricity for the synthesis of valuable chemical compounds.[4,23] Electrosynthesis has the potential to provide a valuable method in organic synthesis, but its application, despite its growth in recent years, is still far from making it a routine technique.[4]

The growing interest in electrosynthesis lies to a large extent in its potential to provide a sustainable and an environmentally friendly approach to synthesis. In 1998, Paul Anastas and John Warner described in their publication "Green Chemistry, theory and practice" a list of twelve principles to follows in order to make a chemical process sustainable and green.[24] These 12 principles are:

- Prevention: it is better to prevent waste than to treat or clean up waste after it has been created.
- Atom economy: synthetic methods should be designed to maximise incorporation of all materials used in the process into the final product.
- Less hazardous chemical syntheses: wherever practicable, synthetic methods should be designed to use and generate substances that possess little or no toxicity to human health and the environment.
- Design safer chemicals: chemical products should be designed to preserve efficacy of function while reducing toxicity.
- Safer solvents and auxiliaries: the use of auxiliary substances should be made unnecessary wherever possible and innocuous when used.
- Design for energy and efficiency: energy requirements should be recognised for their environmental and economic impacts and should be minimised. Synthetic methods should be conducted at ambient temperature and pressure.
- Use of renewable feedstocks: a raw material or feedstock should be renewable rather than depleting whenever technically and economically practicable.
- Reduce derivatives: unnecessary derivatisation should be minimised or avoided if possible, because such steps require additional reagents and can generate waste.
- Catalysis: catalytic reagents are superior to stoichiometric reagents.

- Design for degradation: chemical products should be designed so that at the end of their function they break down into innocuous degradation products and do not persist in the environment.

- Real-time analysis for pollution prevention: analytical methodologies need to be further developed to allow for real-time, in-process monitoring and control prior to the formation of hazardous substances.

- Inherently safer chemistry for accident prevention: substances and the form of a substance used in a chemical process should be chosen to minimise the potential for chemical accidents, including releases, explosion and fires.

Electrosynthesis follows almost all of these principles:[7] the substrate is activated by the electron transfer so there is no need for thermal activation and the reaction rate can be controlled by adjusting the current density or the applied potential, so electrochemical reactions are generally conducted under mild conditions (room temperature and atmospheric pressure).[5,7,25–27] Instead of toxic and hazardous reducing and/or oxidising reagent (OsO_4, $Pb(OAc)_4$, NaH, Na^0, K^0) electricity is used.[28] Electricity is a cheaper and safer reagent, its use also reduce the amount of waste produced[7,23,25–27] and can be generated from renewable resources[23]. In many cases "greener" solvents like water or methanol are used.[7,25,27] Another big advantage is that selectivity can be controlled by the applied potential (controlled potential reactions) or by the choice of electrodes [see section 1.2.1.1, scheme 1.1] so it is not always necessary to activate a substrate or a particular functional group through derivatisation.[3,7,25]It is possible to reverse the reactivity of a particular group (umpolung), potentially shortening the synthetic sequence.[3,7,25,29] An example of this approach will be further discuss in Chapter two: it is the electrochemical synthesis of heterocycles based on the conversion of electron-rich olefins, that would normally serve as nucleophiles, to radical cations that instead serve as electrophiles [Chapter 2 section 2.3]. Here we just report the general scheme (Scheme 1.2).

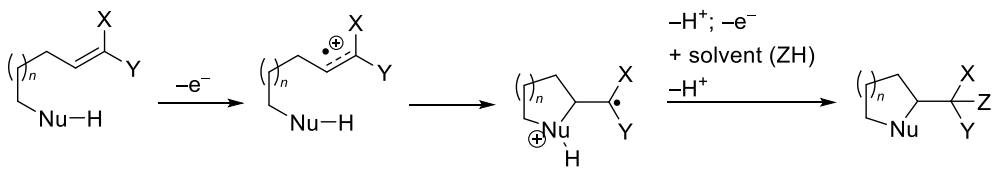

Scheme 1.2: General mechanism for the electrochemical intramolecular oxidative cyclisation.

By simply coupling electroanalytical control methods real-time monitoring is easily achieved reducing errors and costs;[7] atom economy is improved thanks to the possibility to perform direct, indirect or paired electrolysis [see section 1.2.3.2];[7,23,27] reactive intermediates, that are in most cases unstable and dangerous can be generated and directly used *in-situ* (e.g. superoxide ($O_2^{\bullet-}$) or

S^{2+}).[7,26] An example is the synthesis of carbamates reported by Moracci *et al.*[30] using a combination of CO_2 and $O_2^{\bullet-}$ electrochemically generated as carboxylating reagent (Scheme 1.3).

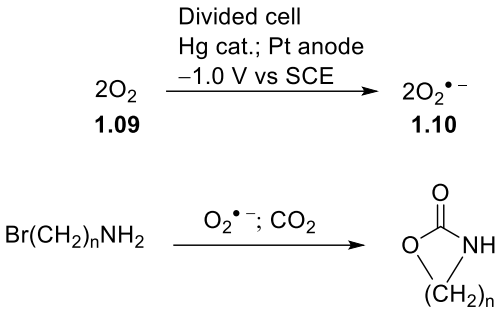

Scheme 1.3: Moracci's carbamate synthesis.

The electrodes can be considered the heterogeneous catalysts in an electrochemical reaction and they can be simply removed from the reaction mixture at the end of the process, so no-extra purification steps are needed to recover them at the end of the process.[7]

1.2.3 Methods of electrolysis

1.2.3.1 Controlled potential and constant current

We can distinguish two main types of reactions: controlled potential and constant current.

Usually, a reaction is run under controlled potential when selectivity is an issue so the potential is set to a value at which only a specific functional group is reduced or oxidised, avoiding any over reduction or over oxidation and any side reactions. A reference electrode is needed in order to keep the potential at the working electrode constant; this make the set-up a bit more complex because not only you have three electrodes but also a potentiostat is needed. Another drawback is that once the substrate is almost consumed, there is drop of current with consequent long reaction time. [2,5,7,29,31]

Most of the electrolysis reactions are run under constant current; the set-up is simple, they are easier to scale-up compared to the reactions under controlled potential and the only drawback of course is the selectivity but in most of the cases, it is not an issue. The flow of current through the circuit is kept constant while the potential between the two electrodes varies.[2,5,7,29,31] The amount of current needed for the transformation can be easily calculated by the Faraday's law. It is the law that says that the moles of a substance produced or consumed at one of the electrodes during an electrolysis is proportional to the amount of electricity that passes through the cell. This is the general formula: $I = (m \times n \times F)/t$ where I is the current, m is the number of moles, n is the number of electrons F is the faraday constant (96485 C/mol) and t is the time for which the current is applied. For a flow electrolysis is almost similar and it is: $I = n \times F \times c \times Q$ where again

I is the current, F the faraday constant and n the number of electrons exchanged, c is the concentration of the substrate and Q is the flow.[32]

1.2.3.2 Direct electrolysis and indirect electrolysis

An electrolysis process can be direct or indirect (electrocatalytic).[2,5,7] In a direct electrolysis, the electrode on whose surface the substrate is transformed has replaced the redox reagent. In an indirect or electrocatalytic process, a mediator that is regenerated at the electrode surface will act as redox reagent, so instead of the heterogeneous electron transfer between the electrode and the substrate, a homogeneous one between the activated mediator and the substrate occurs (Scheme 1.4).

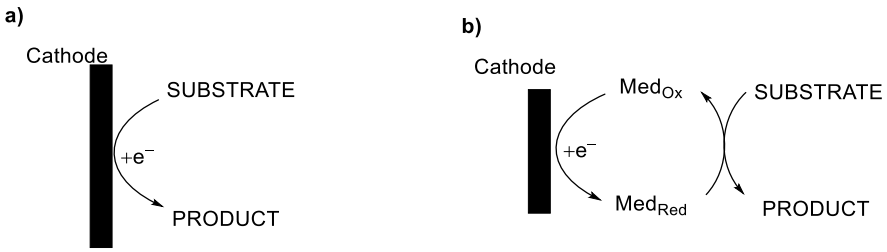

Scheme 1.4: a) Scheme of direct electrolysis; b) Scheme of electrocatalytic electrolysis.

The mediator can be activated and regenerated in the same cell where the actual process happens (in-cell approach) or in another cell (ex-cell approach). When choosing the mediator, its reduced and oxidised forms have to be inert to all the processes except the electron transfer, the electron transfer between the mediator and both the electrode and the substrate needs to be fast otherwise larger surface area electrodes and higher temperature are needed. Another important parameter is the mediator potential; if it is lower than the potential of the substrate you can operate with an in-cell approach; if it is higher you need to activate the mediator separately (ex-cell process) otherwise the substrate would get reduced or oxidised before the mediator.[33] Common redox mediators are triarylamines,[34,35] quinones,[35–37] arylimidazoles[33,35,38] and transition metal ions ($Fe^{II/III}$, $Co^{II/III}$).[35,39,40]

1.2.3.3 Paired electrolysis

Usually it is only the reaction of interest, the one happening at the working electrode that is the focus of electrochemical synthesis published in the literature. However, the counter electrode reaction is of critical importance in electrosynthesis. Usually, it involves a sacrificial process like electrolysis of the solvent. However, sometimes reaction at the counter-electrode can be usefully applied for the synthesis of valuable compounds too. In this scenario, four cases can be identified: parallel paired electrolysis, convergent paired electrolysis, divergent paired electrolysis and linear paired electrolysis.[7]

1.2.3.3.1 Parallel Paired Electrolysis

In parallel paired electrolysis two different starting materials, each react at one of the electrodes generating different products. One example is the industrial process for the synthesis of phthalide (**1.12**) and dimethylacetal **1.14** (Scheme 1.5). In an undivided cell, at the cathode, phthalic acid dimethyl ester **1.11** is reduced to give methanol and phthalide **1.12**, while simultaneously, at the anode, *tert*-butyltoulene **1.13** is oxidised to the dimethyl acetal of *tert*-butylbenzaldehyde **1.14.**[41]

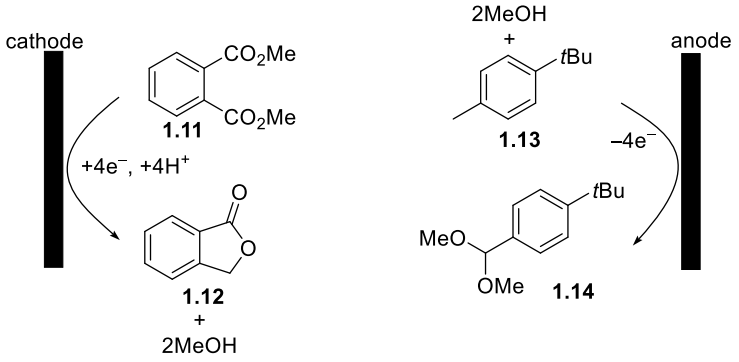

Scheme 1.5: Electrochemical synthesis of phthalide **1.12** and dimethyl acetal **1.14** by parallel paired electrolysis.

1.2.3.3.2 Convergent paired electrolysis

In the case of convergent paired electrolysis the substrates undergoing electron transfers at opposing electrodes generate two intermediates that will react together to give the final product. An example is the synthesis of cyanoacetic acid (**1.15**) starting from acetonitrile and CO_2. The conventional industrial synthesis of cyanoacetic acid is a dangerous and not green process that requires chloroacetic acid and alkaline cyanide. This convergent paired electrolysis provides a more sustainable alternative: at the anode a radical, generated from the oxidation of the supporting electrolyte anion, abstracts a hydrogen from the acetonitrile. This new radical $\cdot CH_2CN$ will then react with the reduced CO_2 generated at the cathode to give the desired product.[42]

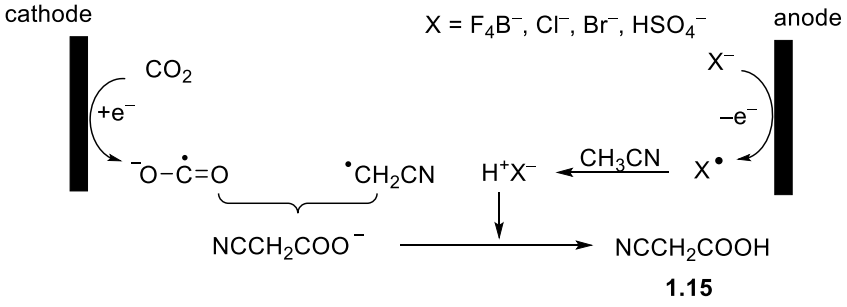

Scheme 1.6: Convergent paired electrochemical synthesis of cyanoacetic acid (**1.12**).

1.2.3.3.3 Divergent Paired Electrolysis

Two different products are produced from the same substrate in divergent paired electrolysis, where the starting material undergoes either oxidation or reduction at opposing electrodes. An example is the electrochemical synthesis of sorbitol and gluconic acid from glucose. This process, used on industrial scale, allows the simultaneous oxidation and reduction of glucose in an undivided packed-bed electrode flow reactor to afford sorbitol and gluconic acid in high yields and high current efficiency. At the anode glucose is oxidised to gluconic acid with the electrogenerated HOBr, while at the Ni-Raney cathode it is reduced to sorbitol. [43]

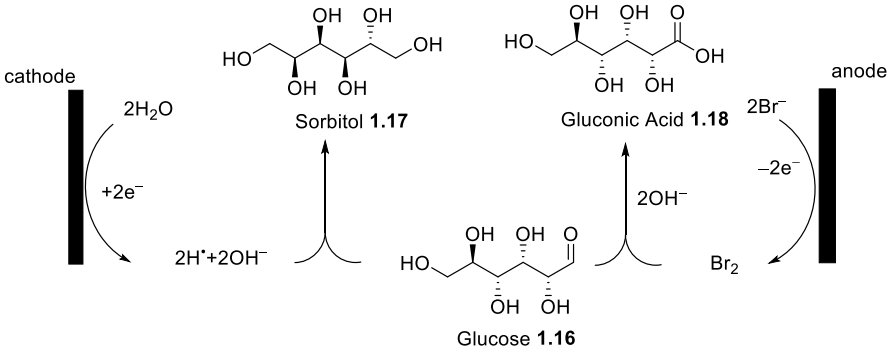

Scheme 1.7: Divergent Paired electrochemical synthesis of sorbitol and gluconic acid.

1.2.3.3.4 Linear paired electrolysis

Linear paired electrolysis converts a single substrate to the desired product by exploiting two different reactions happening at the two electrodes. One example is the electrolysis of dibutyl-*N*-hydroxylamine (**1.19**) to *N*-butylidenbutylamine (**1.20**, Scheme 1.8). WO_4^{2-}/WO_5^{2-} is used as cathodic redox mediator while Br^-/Br_2 as anodic redox mediator to oxidise *N*-hydroxy secondary amines to nitrones. Hydrogen peroxide react with WO_4^{2-} to form WO_5^{2-} that will then oxidise the substrate; on the other side, the electrogenerate Br_2 will also oxidise the N-hydroxyl amine.[44]

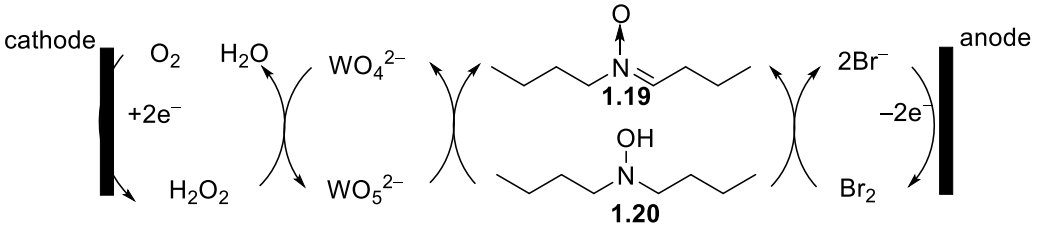

Scheme 1.8: electrochemical synthesis of *N*-butylidenbutylamine.

1.2.4 Classification of electrolysis reactions

Electrolysis reactions can be classified as cathodic reductions, cathodic cyclisation (ERC), anodic oxidation and anodic cyclisation.[4]

1.2.4.1 Cathodic reductions

Cathodic reductions do not need metals or metal hydrides with consequent economical and environmental advantages. In this regard a good example is the electrochemical reduction of vinyl halides, applied to the synthesis of inositol, by Hudlicky and co-workers (Scheme 1.9).[45] In their studies they compare the electrochemical approach with the chemical reduction using Bu_3SnH; they obtain similar yields with the two approach demonstrating how the electrochemical approach can be a valid and more sustainable method. In some cases, electrochemistry can also be used together with catalytic amounts of metals; an example is the electrochemical NHK (Nozaki-Hiyama-Kishi) reaction using two sacrificial anodes reported by Durandetti *et al*. (Scheme 1.9).[46] The NHK is a coupling reaction between allyl, vinyl or aryl halides with aldehydes (highly selective for aldehydes), that requires toxic Cr^{II} and Ni^{II} salts. Durandetti and co-workers in their modified approach, generate electrochemically the Cr^{II} and Ni^{II} catalysts from a sacrificial stainless steel anode (Stainless steel composition: iron/chromium/nickel=72/18/10); once this first transformation is complete, the stainless steel is replaced by an iron rod electrode to perform the actual NHK coupling.

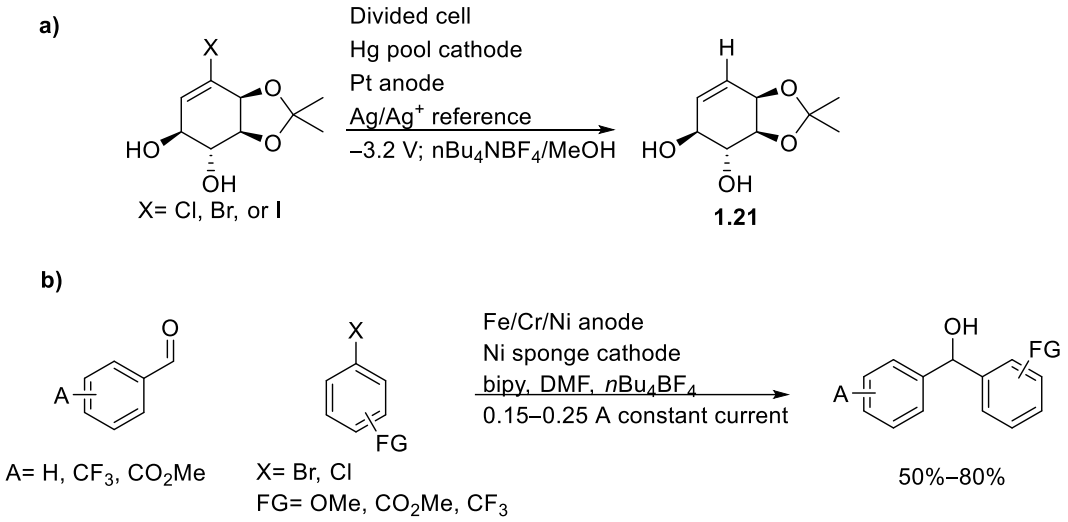

Scheme 1.9: a) Cathodic reduction of vinyl halides reported by Hudlicky and co-workers[45]; b) Electrochemical NHK coupling reaction reported by Durandetti and co-workers.[46]

1.2.4.2 Cathodic cyclisation

The definition electroreductive cyclisations (ERC), refers to all those reactions where an electron-deficient alkene undergoes an electrochemical reductive cyclisation.[47] The

advantages of the electrochemical approach are the mild conditions and the selectivity that can be achieved,[4] the fact that the polarity of a functional group can be reversed triggering umpolung reactions.[48] An example of this approach is the electroreductive cyclisation of α,β-unsaturated esters described by Little and co-workers.[49] α,β-Unsaturated esters undergo umpolung electrochemical reduction generating a nucleophilic β-carbon that then cyclise on the ketone or aldehyde at the other side of the chain in good yields (70-79%).

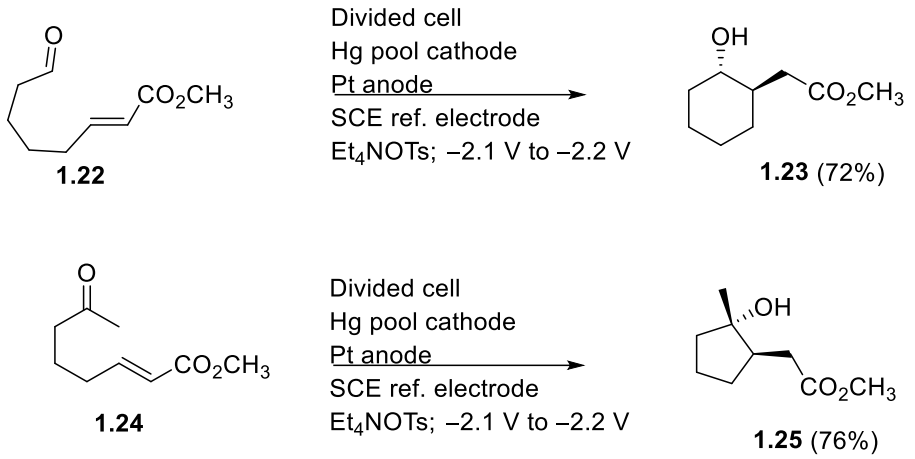

Scheme 1.10: Intramolecular electrochemically initiated cyclisation of α,β-unsaturated esters.

1.2.4.3 Anodic oxidation

Anodic electrochemistry is a powerful tool in the synthesis of organic molecules; this approach allows selective oxidation of functional groups and can reverse the polarity of nucleophiles.[3] Anodic oxidations are the largest class of organic electrosynthetic procedures, and are often carried out as constant current experiments in an undivided cells.

The Kolbe electrolysis[50,51] is the best known anodic oxidation and in general one of the most studied and reviewed electrolysis reactions.[3,52] It is an electrochemical decarboxylation of carboxylic acids that leads to the formation of a carbon-centred radical[3,4]. In the first example reported by Kolbe in 1849, the radical dimerises forming a new C—C bond (Scheme 1.11a);[50,53]but over the years the Kolbe decarboxylative coupling has been used between different carboxylic acids, decarboxylative intramolecular cyclisations and addition to alkenes.[4,53] An example of cross-coupling is the one from Haufe and co-workers,[54] shown in scheme 1.11b, where they applied the Kolbe electrolysis in the synthesis of bioactive lactones; in particular in scheme 1.11b is shown the coupling between intermediate lactono acid **1.26** and butanoic acid. An example of addition of the carbon-centred radical to an alkene is the work by Schäfer *et al*. where they exploited the Kolbe electrolysis to start a tandem intramolecular cyclisation.[55] In the particular example shown in scheme 1.11c acid **1.28** is

reacted in an undivided cell equipped with a stainless steel cathode and a platinum anode, with acetic acid; different result where obtained based on the current density.

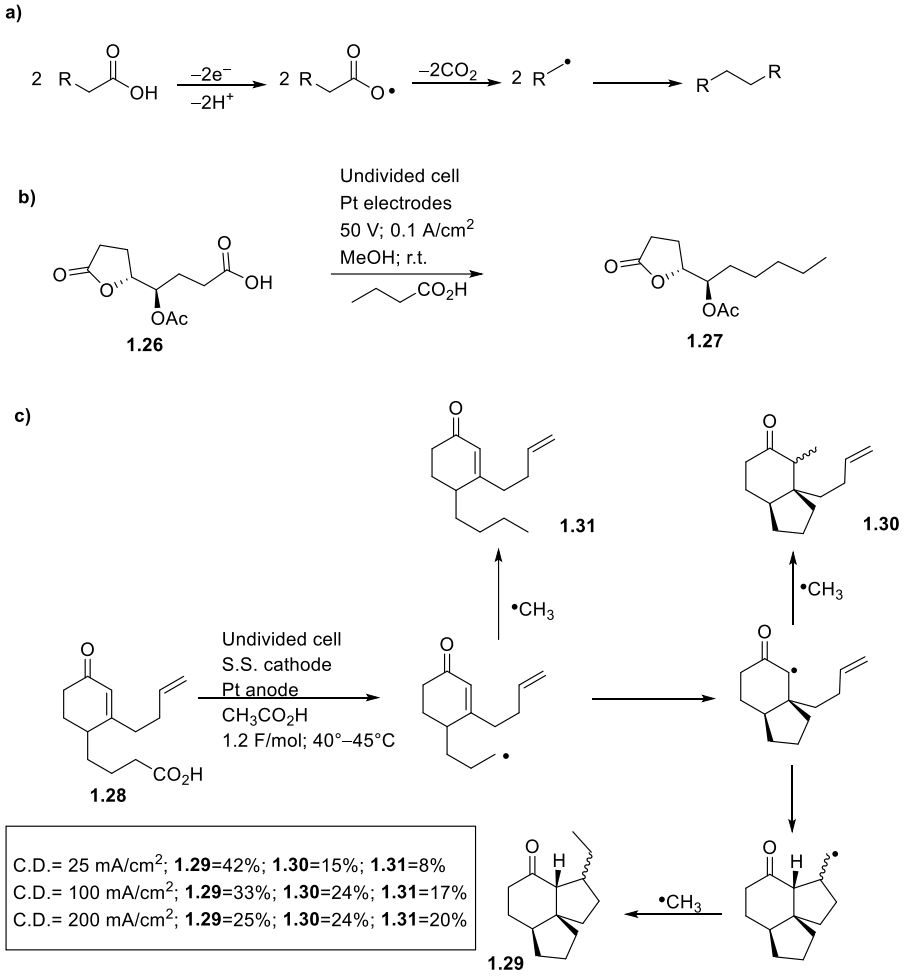

Scheme 1.11: a) General scheme of Kolbe electrolysis; b) Haufe's Kolbe cross-coupling; c) Schäfer's Kolbe tandem intramolecular cyclisation.

Another well-known example of anodic oxidation is the Shono oxidation, the electrochemical oxidation of amides to generate *N*-acyliminium ions.[56] It consists in the electrochemical oxidation of amides to *N*-acyliminium ions followed by nucleophilic attach.[3,4] This methodology has been extensively reviewed and studied over the years[56] and applied to the synthesis of complex molecules and natural products. An example, to that extent, is Moeller[57] synthesis of natural compounds (–)-A58365A (**1.34**) and (±)-A58365B by anodic amide oxidation (Scheme 1.12b).

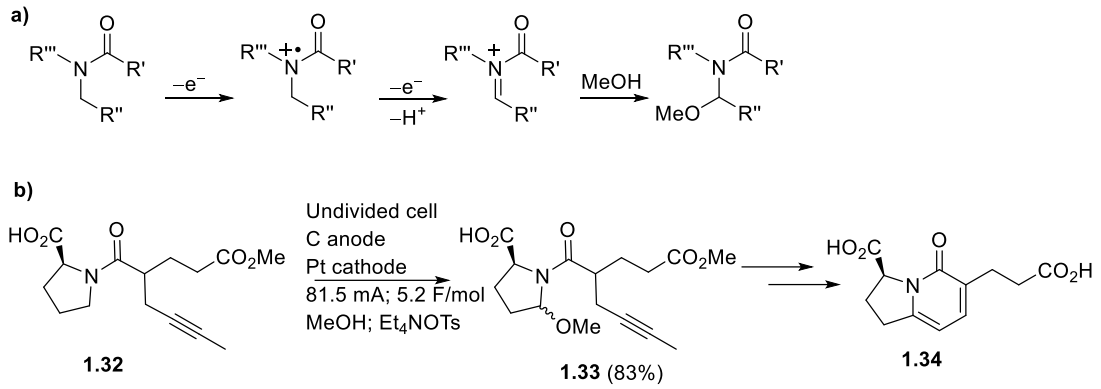

Scheme 1.12: a) General scheme of Shono electrochemical oxidation; b) Moeller's electrochemical synthesis of natural compounds (–)-A58365A and (±)-A58365B by anodic amide oxidation.

1.2.4.4 Anodic cyclisation

This methodology is based on the electrochemical formation of a radical cation followed by intramolecular attack of a nucleophile and can be applied to the synthesis of complex molecules.[4] Popular functional groups involved in EOCs are enol ethers, ketene dithioacetals and common nucleophiles are oxygen and nitrogen based.[58–60] The anodic oxidation of electron-rich olefins followed by intramolecular nucleophilic attack is an example to this regard and it will be further discussed in Chapter 2. Also a general scheme of this type of reaction has been shown before in section 1.2.2, scheme 1.2.

1.2.5 Cyclic voltammetry

A number of useful electroanalytical techniques are available to help understand physical and chemical processes taking place in electrochemical reactions.[61,62] Cyclic voltammetry is a common technique in organic electrochemistry used to investigate the red-ox processes of a substrate.[63] From a cyclic voltammetry experiment the red-ox potential can be determined. It is also possible to establish: whether a process is reversible or irreversible,[4] the presence of intermediates or side-products and hence the stability of the product, standard rate constants for electron transfer, electrode kinetics,[64] whether eventual electrode passivation occurs.[9] A cyclic voltammogram gives also information about the diffusive or the adsorptive nature of the electrode process, its kinetic and thermodynamic parameters. The resulting peak signal provides a fingerprint of the reduction and oxidation processes; the position and the shape give information about the nature of the electrochemical process.[61]

In a cyclic voltammogram current is normally plotted over potential (Figure 1.7). The potential sweep usually follows a triangular-like waveform that starts and ends at the same point. If a process is reversible, there will be a second peak beneath the oxidation one when the voltage is swept towards a positive value and then back again.[4,63]

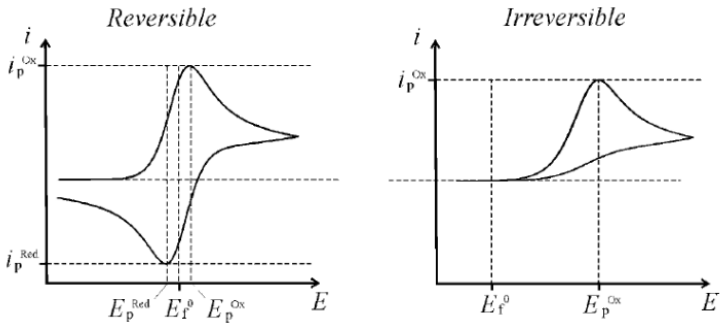

Figure 1.7: cyclic voltammetric waveshapes for a reversible and non-reversible processes.[65]

The characteristic shape of a voltammogram allows to understand the kinetic behind an electrolysis. If we consider a generic one electron reduction, at the start of the scan no current is flowing because the potential is not negative enough to reduce the species. Once the scan starts and the potential gets more negative, current starts to increase (rising section of the forward swept). At this point the reaction is under kinetic control, the rate of the electron transfer between the substrate and the electrode surface is limited by the rate of the chemical transformation. When the concentration of the starting substrate is almost zero, the current reaches is maximum; after that current starts to decrease and the reaction is under diffusional control: the rate of the electron transfer is now limited by the rate of the diffusion of fresh starting material from the bulk solution to the electrode surface (Figure 1.8).[61]

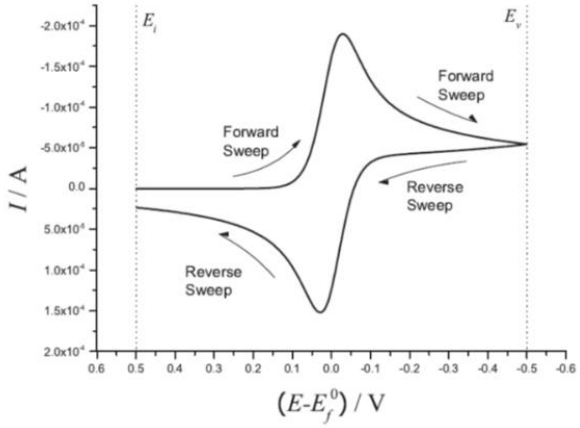

Figure 1.8: Reversible cyclic voltammogram.[61]

Important parameters are the peak potentials (E_{pc} for cathodic reduction; E_{pa} for anodic oxidation) and corresponding currents (i_{pc} and/or i_{pa}). The half-wave potential ($E°'$) for a reversible process is the potential in the middle of the E_{pc} and E_{pa}, which is specific for an electrochemical reaction.[5] When planning a CV experiment the first thing to consider is whether run it in a divided or undivided cell. To make this choice it is important to know if the products at the counter-electrode can interfere with the experiment. To perform a CV experiment, a cell, a potentiostat and three electrodes (working, counter and the reference electrodes) are required. Common

working electrodes used in CV are platinum, gold or carbon; the ideal electrode should always behave the same way, but during the experiments its surface can become contaminated, due to formation of oxides for example, so before running the experiments it is good practise to clean the electrode surface by mechanical polishing or exposure to solvent or other chemical species.[5] The counter electrode is normally a platinum, due to its high stability, and typically has a much bigger surface compared to the working one so the counter reaction is fast enough and will not limit the reaction at the working electrode. The most used reference electrodes are the saturated calomel (SCE) and the Ag/AgCl, due to their stability and reproducibility.[5]

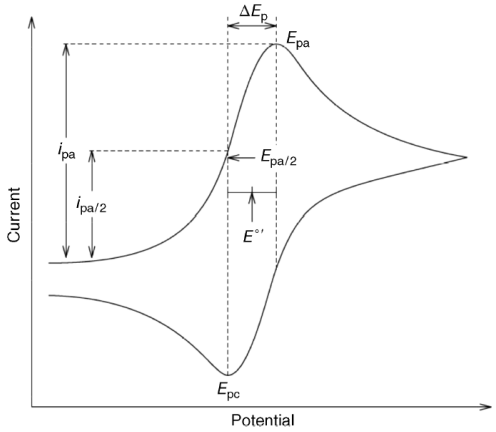

Figure 1.9: Cyclic voltammogram for a reversible process.[5]

1.3 General aspects of flow chemistry

The term "flow chemistry" refers to all those chemical processes that are performed in a tube or a pipe in a continuous stream.[66] In recent years the flow chemistry approach has gained a lot of interest in the field of organic synthesis in research laboratories but also in industrial processes[67,68]

Flow chemistry has various applications and has several advantages compared to batch chemistry as it can allow better control, efficiency, reproducibility and increased safety. Using a flow apparatus, facilitates accurate control of the reaction time and temperature, avoiding the risk of uncontrolled exothermic reactions with consequent degradation or formation of side-products. This is due to the high surface area to volume ratio present in many flow reactors, giving excellent heat transfer. The higher surface area to volume ratio, also increase the mass transfer compared to a batch system. Another big advantage is a better mixing especially for multiphasic systems; a flow approach, thanks to the small volumes involved, allows better mixing, which can reduce or even eliminate concentration gradients that may be an issue in batch processes. Using a flow system is also more advantageous when it comes to scale-up: in batch, scale-up, especially for multiphasic reactions, involves several problems like the size of the reactor, its shape, achieving

efficient stirring and mixing and controlling the temperature. With a flow system, as stated before, control of temperature and mixing can be greatly improved. What can be considered a drawback of flow chemistry is the initial investigation, which is less familiar to chemists used to working in round-bottom flasks. The design of the experiment requires additional considerations of parameters such as flow rate, concentration and residence times in the reactor. The substrates should ideally be soluble and not precipitate during the process, and the design of the reactor, and its size need to be considered. The initial optimisation work can be made easier and faster by the use of in-line analytic methods (IR, NMR, UV, GC) to check the outlet solution, although some of these technologies are quite expensive and can make the set-up of the all system more difficult.[66,67,69] A general flow set-up comprises of pumps to flow the reagents/reactants, which are mixed before entering the reactor where the chemical process takes place (Figure 1.10). The reaction mixture can then be quenched in-line and collected or sent to the analysis system. The reactor is the key part of the flow set up and can take many forms, such as chip, coil and packed bed. The nature of the reaction determines the type of reactor and its material, for example chip reactors because of their high surface to volume ratio, offer the best heat transfer. Coil reactors are generally cheaper than the chip ones, they can be made of different materials; fluoropolymers reactors have good transmission properties, so they are often used for photoreactions while stainless steel coil reactors are good for high temperature and high pressure applications. Packed bed reactors are instead used when a heterogeneous catalyst or reagents are required is a continuous chemical transformation.[66]

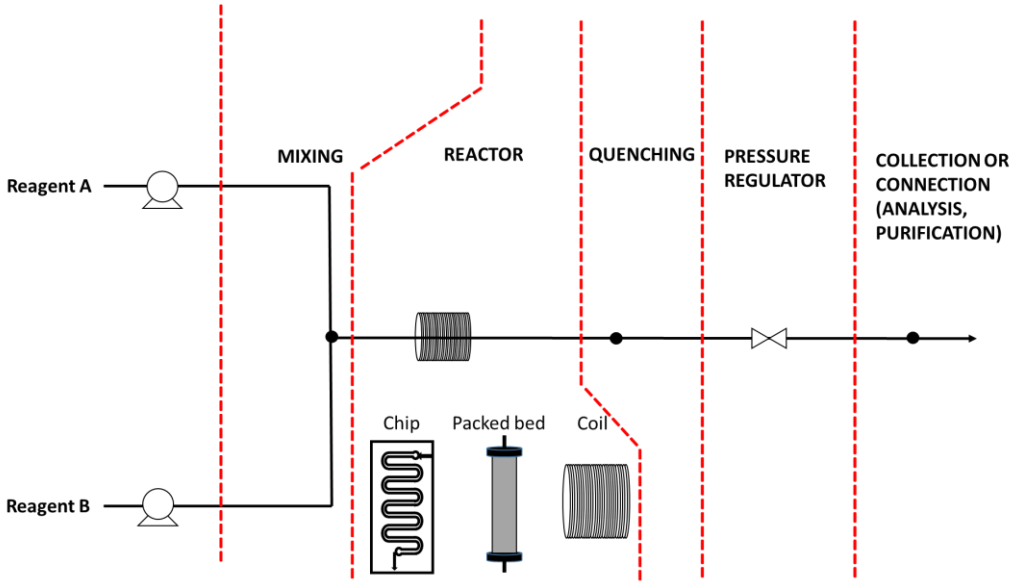

Figure 1.10: Generalised diagram of a flow chemistry set-up.

1.4 Microfluidic electrosynthesis

The use of electricity in organic synthesis is an approach that has been known since mid-1800s, but only in the recent past has organic electrosynthesis started to gain increasing interest.[70] Electrosynthesis may be considered to be a green, environmentally friendly approach where toxic and dangerous oxidising and reducing agent are avoided in favour of relatively cheaper electricity. An ideal scenario would be one where the electricity used would be generated from renewable sources like the sun or the wind, and no reagent waste would be produced and high atomic efficiency would be achieved. A further advantage of the electrochemical approach is that unstable and/or hazardous intermediates can be generated and consumed *in situ*; reactions are often run under mild conditions (e.g. atmospheric temperature and pressure).[6,70–73]

Organic chemists have shown a reluctance to apply electrosynthesis, and it has never been considered as a routine technique in synthetic organic laboratories, although this situation is changing as more researchers try electrochemical methods.[74] Historically, some of the barriers to take-up of electrosynthesis could include issues such as a lack of standardised equipment and reliable protocols. Also, many of the methods described in literature were potentiostatic and their scale-up and reproducibility was problematic due to the use of three electrodes and the long reaction time, and the cost and additional complication of working with a potentiostat. [2,5,7,29,31] Equipment commonly used in electrosynthesis is based on batch cells, that can be broadly grouped under beaker and H-cells (Figure 1.11), although a wide array of cell designs have been described.[75] Beaker cells are most widely used because they can be made of components that are more readily available to the synthetic chemist. However, they do have several drawbacks such as lack of reproducibility; slow rate of conversion, which can also lead to degradation and formation of side-products with consequent low selectivity; heat transfer issues and mixing problems are especially for heterogeneous transformations at an electrode surface. Beaker electrolysis cells are difficult to scale-up and bigger batch cells can suffer from lower surface to volume ratios and poor mass transport. As the distance between the two electrodes is frequently quite large, greater amounts of supporting electrolyte is needed, making the process less cost efficient.[70–72,74,76–78]

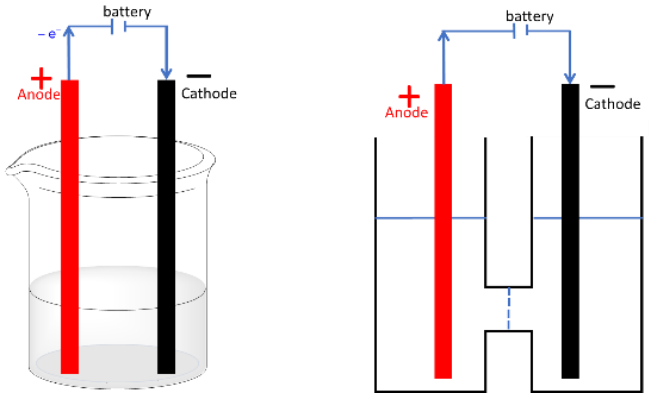

Figure 1.11: Diagrams of a beaker cell and of a H-cell.

For the reasons mentioned above, nowadays the use of flow equipment in electrosynthesis is gaining a lot of interest.[74] Flow electrolysis cells may appear to be more complex, and require additional consideration in the set-up to plan the design and the conditions of the experiment, but they offer significant advantages compared to batch cells. Flow cells can allow high selectivity and high conversion that can be achieved just by controlling the potential between the two electrodes. Due to efficient mass transport and high electrode area to reactor volume, the residence time in the reactor can be very short, often less than 1 minute, so competing chemical side-reactions or degradation can be reduced. Owing to the small interelectrode gap present in some microreactors, no additional supporting electrolyte is needed or the amount can be reduced considerably compared to batch cells. Consequently, purification and isolation of the product is easier. Superior control of temperature is possible due to the small reactor volumes involved and the higher surface area, enabling better heat transfer. The arrangement of the electrodes in a plane parallel fashion maintains a constant inter-electrode gap, and potential gradients are easier to control. The points across the surface of the working electrode are equivalent so potential gradients are minimised when low conversion occurs during each reactor pass. However, it should be noted that electrode potential is a function of conversion along the channel, so single pass and multiple pass approaches will differ in this respect.[6,70,76,79]

In many anodic electrosynthesis hydrogen evolution is used as a counter reaction with formation of a gas, which can be a disadvantage in a flow reactor.[80] In some situations, however, formation of gas bubbles in the reactor channel enhance the mass transfer and the mixing of the reaction.[76] Flow systems are also amenable towards implementation of analytical technology in-line in order to follow the course of the reaction or to analyse the outlet solution, and recent applications have been reported.[81] Flow systems also offer easy linking of reaction steps, which can be combined together in a continuous process. This can be particularly useful when unstable or very reactive or hazardous intermediate are generated, and consumed in a subsequent step.[6]

Laboratory flow cells are generally based on parallel plate arrangements and electrolysis can be carried out with high conversion by recycling the reactant through the cell multiple times, or in a single pass using microfluidic cells (Figure 1.12).[74]

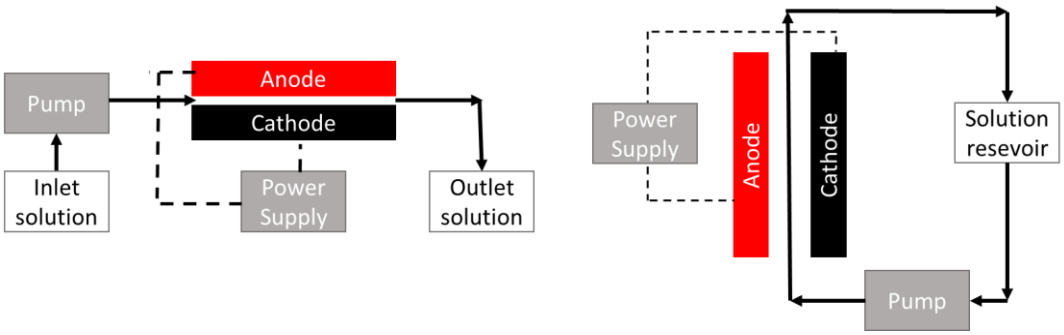

Figure 1.12: Representation of single pass and multiple pass (recycling) approaches to flow electrolysis.

A drawback of recycling approach is that the rate of the reaction drops very substantially as the reactant is consumed and its concentration decreases, requiring a reduction in the cell current towards the end of the process to avoid side reactions.[78] Cells used in recycling or single pass mode can be divided or undivided. Separators used in batch cells, such as ion bridges and glass frits, are not easily applied in flow cells, particularly those that have microfluidic dimensions. Divided reactors require a suitable separator (glass frit or iono-selective membrane) to be put between the two electrodes in order to separate their chemistry, and this is important when the counter reaction can interfere with the reaction at the working electrode. Using a divided cell system makes the set-up more complex and the separation is not total, some mixing will always happen. For this reason divided flow cells are often avoided by synthetic chemists, and undivided cells are more common. This requires careful consideration of the compatibility of the chemistries at the two electrodes that are in the same electrolyte solution. The formation of hydrogen gas as counter reaction is often convenient for anodic transformations in protic solvents such as MeOH. Alternative strategies such as synthetising the same product at both electrodes have been applied, but are limited in scope, as is the use both cathodic and anodic reactions in a chemical sequence that will lead to the final product [see discussion of “paired electrosynthesis above]. In the case of reductions, use a sacrificial anode (Mg, Al, Zn) is frequently used as a counter reaction, but formation of inorganic salts can complicate flow processes and cause blockages.[6,70,74,76,77]

1.4.1 Electrochemical microflow reactors and their applications

Over the years, different microfluidic electrolysis cells have been developed, and some illustrative studies are presented below.

In 2005,[74,82] Yoshida and co-workers reported a two compartment electrochemical microfluidic cell made of diflone and stainless steel (Figure 1.13). The two chambers were divided by a PTFE (polytetrafluoroethylene) diaphragm, with a carbon felt anode and Pt wire coil cathode.

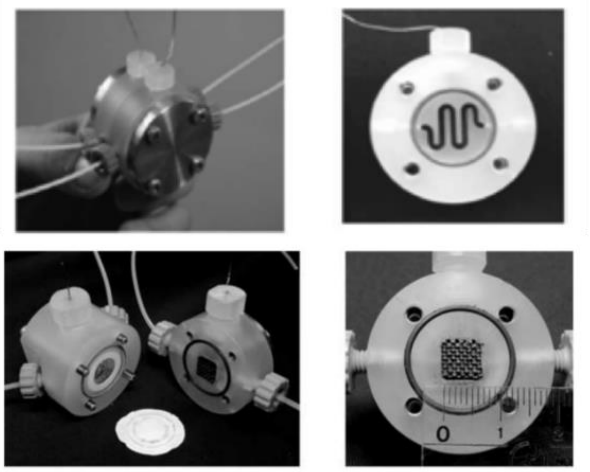

Figure 1.13: Yoshida's microfluidic cell.[82]

Despite the low volumetric flow rate, this cell has been used to perform several interesting reactions, and can be considered to be one of the pioneering approaches in microfluidic electrosynthesis. Its big advantage is the possibility to perform electrolysis at low temperature.[74] One of the interests of Yoshida and co-workers was an approach they termed "cation flow". A typical example is the oxidation of carbamates **1.35** to form *N*-acyliminium cations **1.36**, which are trapped post-reactor with different nucleophiles (scheme 1.13).[82]

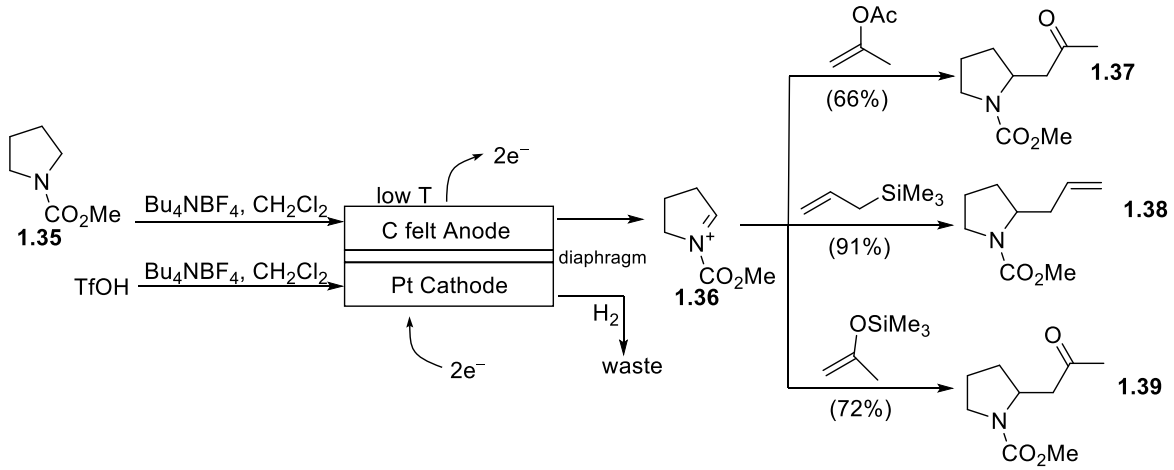

Scheme 1.13: Yoshida's electrochemical generation of *N*-acyliminium ions and application in "cation flow" syntheses.[82]

In 2015, Chapman *et al*. reported an electrochemical flow cell for the selective generation of Cu-*N*-heterocyclic carbene complexes (Scheme 1.14).[74,83]

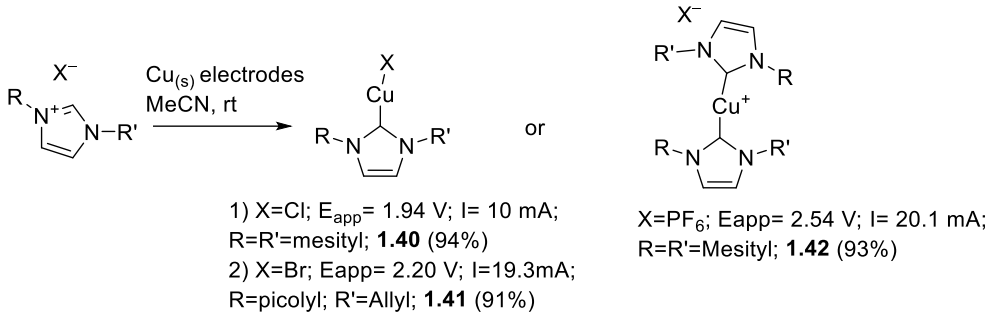

Scheme 1.14: Electrochemical generation of Cu-*N*-heterocyclic carbene complexes reported by Chapman *et al.*[83]

The cell is a monopolar stack cell made of a series of copper electrodes arranged one on top of the other and separated by PTFE gaskets to create a snaking channel. Both the electrodes participate in the chemistry: at the cathode the carbene is generated, while the sacrificial anode erodes to generate Cu(I) that combines with the carbene (Figure 1.14).

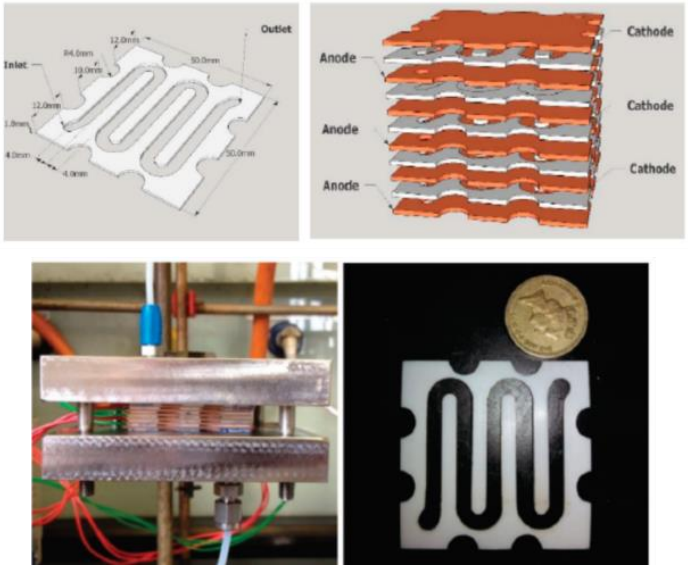

Figure 1.14: Chapman's microfluidic cell.[83]

The first commercially available extended length channel cell is the Syrris microflow cell and was reported in 2012, and was developed as part of an EPSRC-funded project involving Syrris, Pfizer Pletcher, Brown and co-workers (Figure 1.15).[74,84–86] It is made of two rectangular plate electrodes, a carbon PVDF anode (polyvinylidene fluoride) and a stainless steel cathode. The prototype design has a PFKM (perfluoroelastomer) spacer with a snaking microchannel; the stainless steel electrode has a recess, to locate the spacer and two holes for the inlet and the outlet. The commercially available version has a modified sealing arrangement, with a Teflon

spacer to create the channel and an outer O-ring to improve sealing. A range of electrode materials are available, and the cell is part of the Asia Flux flow electrochemical system.[75]

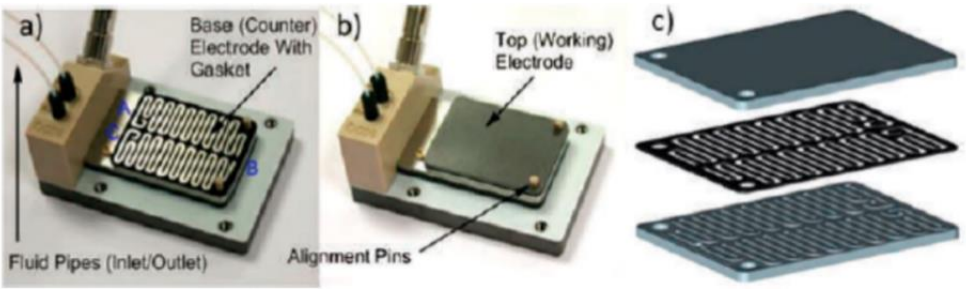

Figure 1.15: Prototype Syrris microfluidic cell showing: a) internal view of the cell; b) cell after the inclusion of the plate electrode; c) arrangement of the grooved electrode, the gasket and the plate electrode.

This cell has been used for many reactions incuding the methoxylation of *N*-formylpyrrolidine,[84,85] TEMPO mediated oxidation of alcohols to aldehydes and ketones,[87] the Kolbe reaction for the formation of dimethyladipate[76] and the α-methoxylation of *N*-protected cyclic amines (Scheme 1.15).[88]

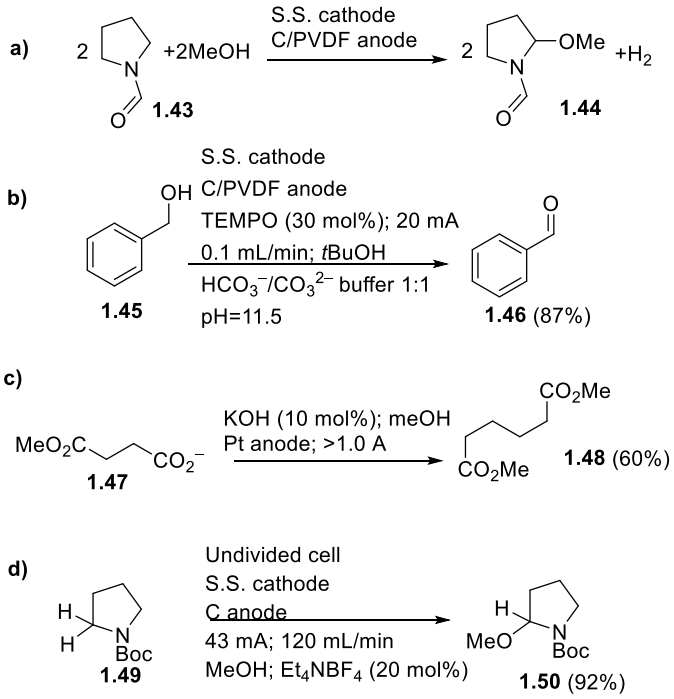

Scheme 1.15: Examples of electrosyntheses performed in the Syrris prototype cell. a) Methoxylation of *N*-formylpyrrolidine; b) TEMPO mediated oxidation of alcohols; c) Synthesis of dimethyladipate *via* Kolbe decarboxylation; d) Ley's electrochemical α-methoxylation of *N*-protected cyclic amines.

More recently a new electrolysis flow cell has been developed, the Ammonite reactor (Figure 1.16).[74,89]

Figure 1.16: Ammonite microfluidic cell.

The Ammonite electrolysis cell has a particular compact design that allows the solution to flow through a spiral channel formed by a polymer spacer between the two disk electrodes. The Ammonite reactors have been applied to a number of electrochemical reactions, and on different scales.[75] Examples include the methoxylation of *N*-formylpyrrolidine[77] and the cleavage of 4-methoxy groups from PMB ethers for alcohol deprotection.[90] [Its application and set-up will be further discussed in the following chapters, in particular in the experimental section of this thesis].

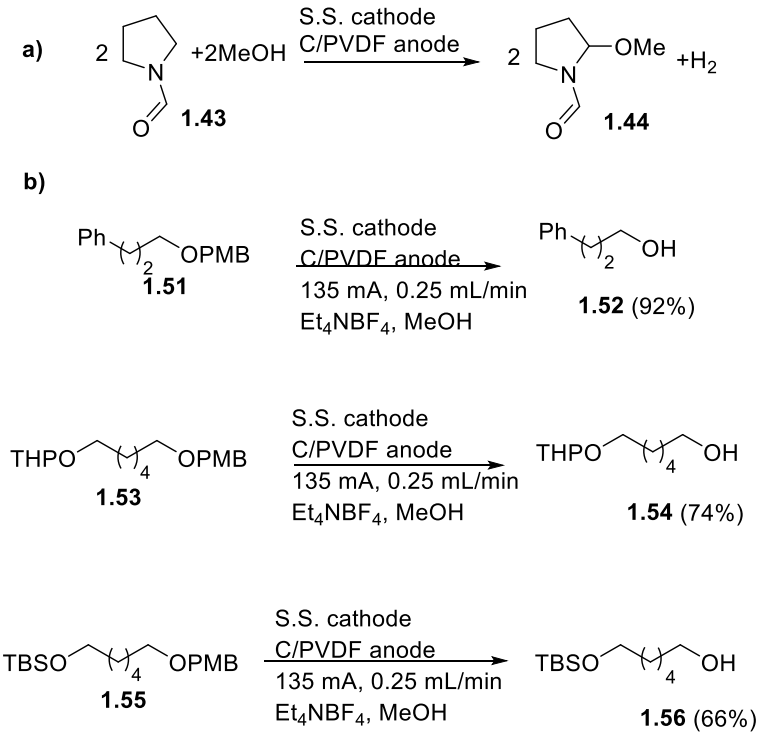

Scheme 1.16: a) Methoxylation of N-formylpyrrolidine; b) PMB deprotection.

Another commercially available electrolysis cell is the Ion electrochemical reactor by Vapourtec (Figure 1.17).[73,79,91] It consists of two electrode holders where the electrodes are held in position; the flat plates electrodes can be of different materials (platinum, glassy carbon, boron-doped

diamond, nickel, graphite); the electrodes are separated by a gasket and all the system is held together by a single-hand-screw system. This reactor can also operate on broad range of temperature (–10 to 100°C).[75]

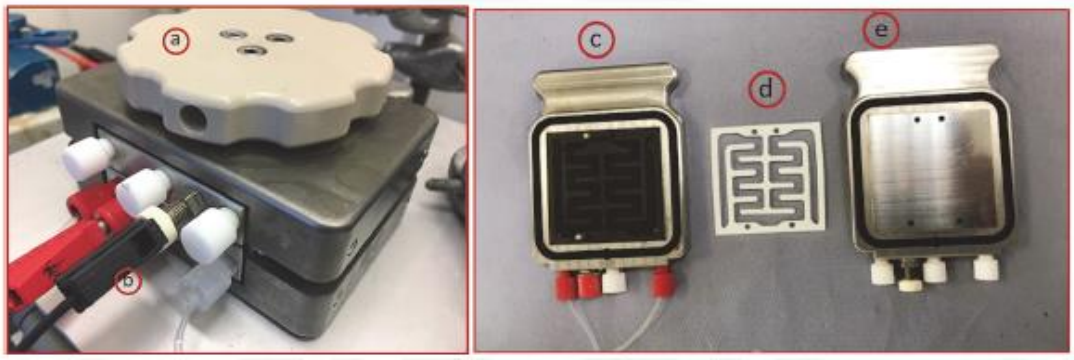

Figure 1.17: Ion electrochemical reactor by Vapourtec; a) reactor housing with cell inside; b) electrical connections; c) and e) electrodes on holders; d) spacer.[73]

Examples of reactions run in this cell are methoxylation of *N*-formyl pyrrolidine[79] and the generation of hypervalent iodine to perform a series of different oxidative transformations (Scheme 1.17), such as oxidation of dihydroquinone, [73,75] and difluoro- and trifluoromethylative coupling of electron-deficient alkenes.[92]

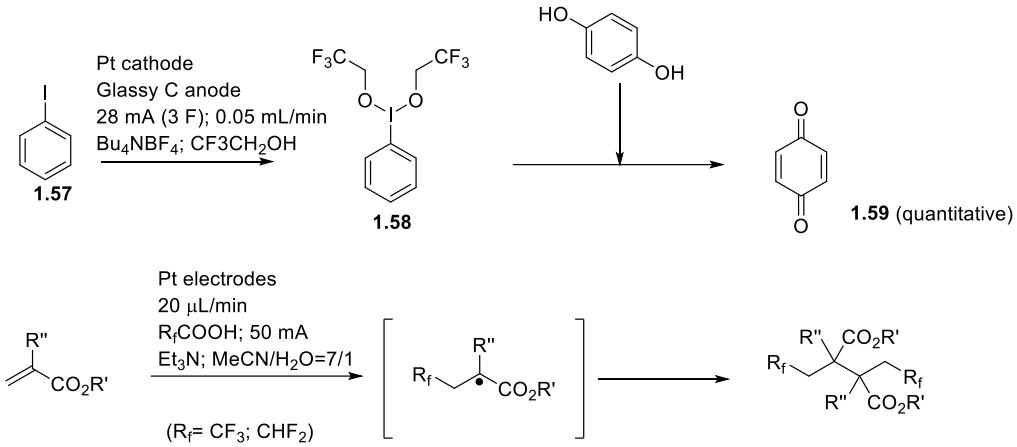

Scheme 1.17: top) electrochemical generation of hypervalent iodine for oxidative transformations; bottom) electrochemical difluoro- and trifluoromethylation of electron-deficient alkenes.

In 2017, Waldvoegel *et al.* designed a modular parallel-plate flow electrolysis cell for organic electrosynthesis (Figure 1.18).[71,75] This cell consist of two Teflon pieces with connection for tubing and a space for the electrode; a gasket around the electrical connectors avoid that the connector and the electrolyte get in contact. The electrodes are insert in the Teflon pieces by thermal expansion of the polymer that is then cooled down contracting and holding the electrode in position. Its design allows to work both in divided and undivided mode.

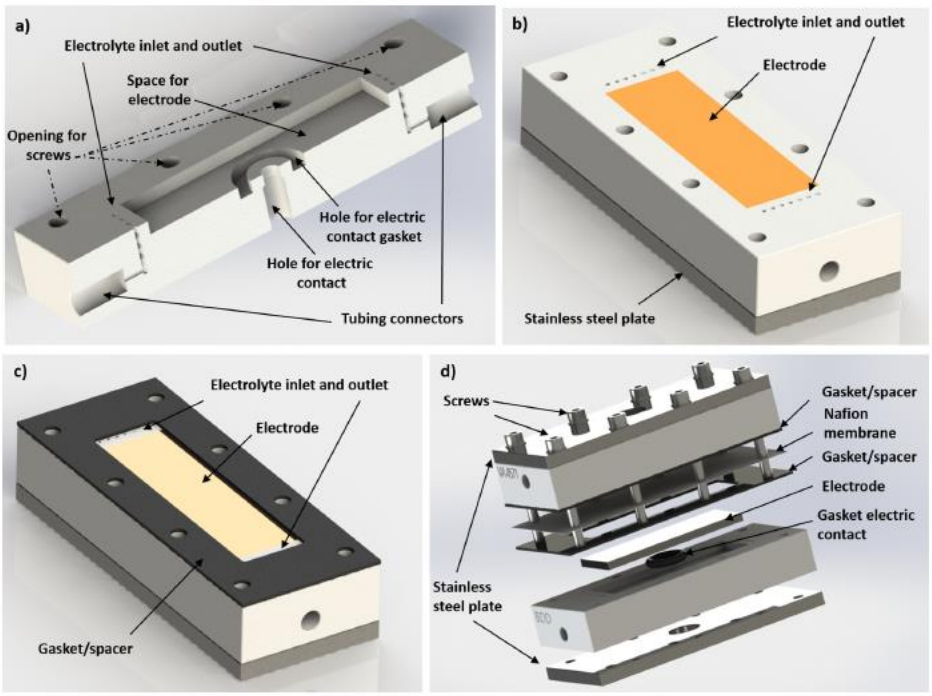

Figure 1.18: a) cross-section of the Teflon piece with connections; b) complete half-cell containing the Teflon piece, the electrode and the stainless steel plate; c) half-cell with gasket on top; d) drawing of complete divided cell.[71]

Examples of organic electrosynthesis using this modular flow cell, are the domino-oxidation-reduction of aldoximes to nitriles[93] and the selective anodic dehydrogenative cross coupling of phenols.[94]

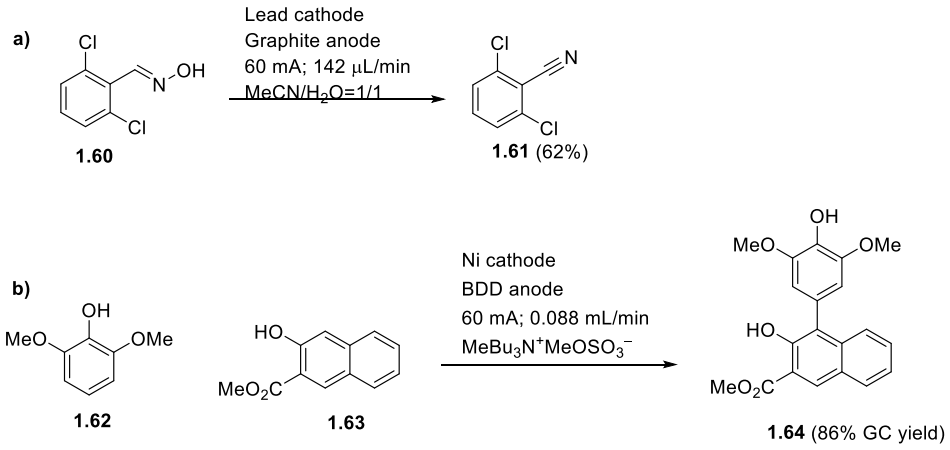

Scheme 1.18: a) electrochemical domino-oxidation-reduction of aldoximes; b) electrochemical dehydrogenative cross coupling of phenols.

1.5 Summary

The aim of this chapter was to give a just a general overview of the basic aspects of electrochemistry with a particular focus on organic electrosynthesis, its principles, and the value of its application in organic synthesis in order to prepare the reader for a better understanding of the following chapters. In the second part the focus was on flow chemistry and the application of flow reactors to organic electrosynthesis. Some examples of different flow electrolysis cells and their applications have been reviewed.

Chapter 2 OXIDATIVE CYCLISATION

2.1 Importance of oxygen heterocycles

Heterocycles are ring structures containing not just carbon atoms but also oxygen, nitrogen or sulfur. They are the building blocks of a diverse range of natural compounds like alkaloids, carbohydrates, nucleic acids and amino acids. The fundamental process that underpins drug discovery and leads to the development of a valid candidate for therapeutic treatment is essentially attempting to imitate a natural compound; for this reason, heterocycles are an important building block in the majority of commercially available drugs (Figure 2.1). However, heterocycles are also important building blocks because of their properties; introducing heteroatoms into a ring can affect the polarity, solubility and lipophilicity of the final compound, influencing its pharmacokinetic, pharmacological, toxicological and physicochemical properties.[95]

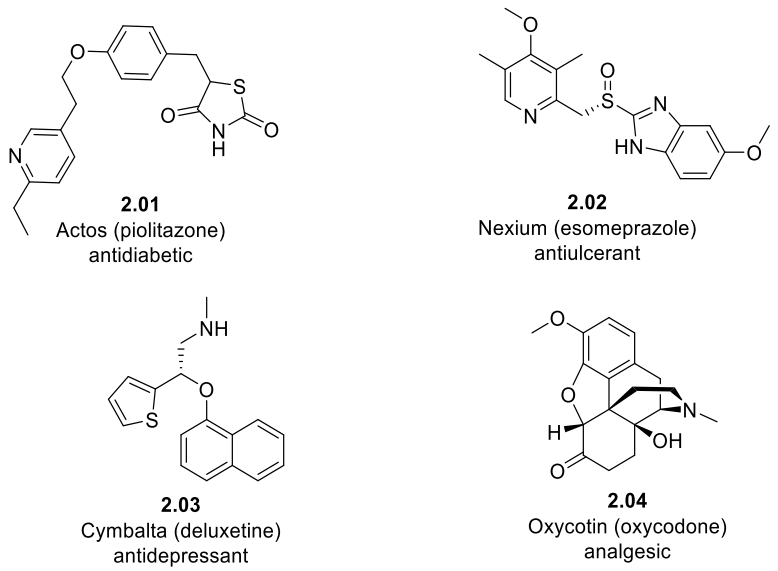

Figure 2. 1: Examples of drugs containing heterocyclic systems.

In particular, saturated heterocycles increase water solubility and create useful three-dimensional molecular shapes that are often attractive in potential drug candidates; moreover avoiding aromatic heterocycles can remove potential problems of toxic metabolites derived from arene oxidation.[96] One category of saturated heterocycles are saturated 5-member oxygen heterocycles such as tetrahydrofurans and γ-butyrolactones. They are structural units present in many naturally occurring compounds with numerous examples displaying interesting bioactivities. Examples include Amprenavir, a protease inhibitor used to treat HIV infection, oxycodone, an opioid derivative used to treat pain, Eribulin, a marine macrolide used for the treatment of breast cancer and tetrahydrofuran **2.06**, a polymerase inhibitor of the nucleoside respiratory syncytial virus (RSV), that just entered phase II clinical trials (Figure 2.2).[95,96,105–107,97–104]

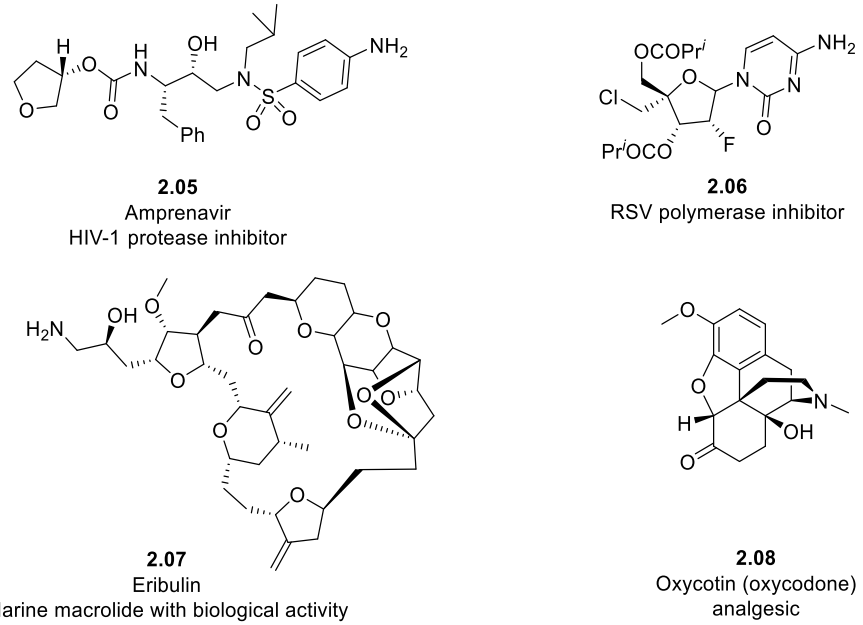

Figure 2. 2: Examples of bioactive compounds containing oxygen heterocycles.

2.2 Synthesis of THFs and γ-lactones

A wide variety of approaches have been described to synthesise THFs[100,101,108–113] and γ-lactones,[108,109,114] from acyclic precursors involving C—C and C—O bond formations to create the 5-membered ring.

In terms of C—C bond formation the ene-type cyclisation with the use of a metal catalyst (Pd, Rh, Ru, Ti) is a well-known approach (Scheme 2.1).[115]

For example in 2012, Evans and co-workers reported a highly diastereoselective Rhodium-catalysed ene-cycloisomerisation of carbon and heteroatom-tethered alkenylidenecyclopropanes (ACPs) for the synthesis of 5-member rings containing two stereo-centres (Scheme 2.1a). The diastereoselectivity and efficiency of this reaction are independent of the nature of the starting material, the alkene geometry and substitution. Based on their proposed mechanism is the carbometalation the stereoselective step; as shown in Scheme 2.1, the reaction starts with the oxidative addition of the Rh catalyst, the intermediate **2.09a** rearrange to **2.09b**; at this point a stereoselective carbometalation leads to the formation of intermediate **2.09c** that undergoes β-hydride elimination to give **20.9d**; the final product is then afforded by reductive elimination.[116]

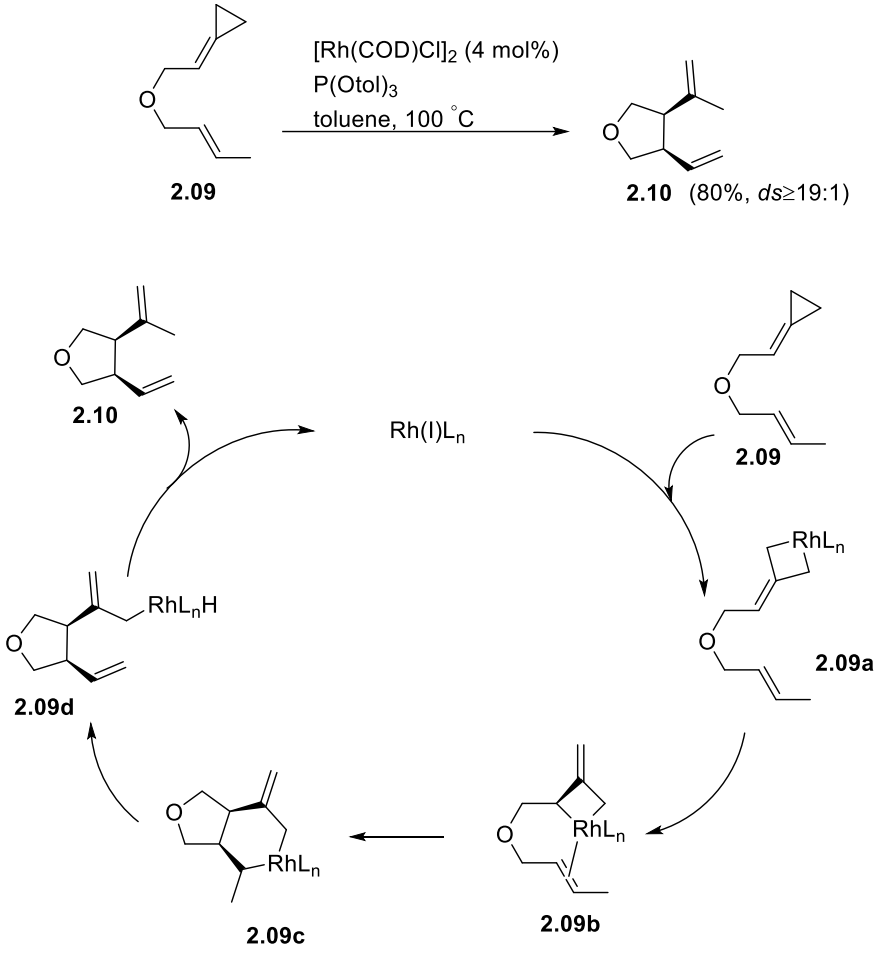

Scheme 2.1: Evans's diastereoselective Rhodium-catalysed ene-cycloisomerisation.

More recently, in 2018, Giri *et al.* described a cyclisation/cross-coupling reaction of olefin-tethered alkyl halydes with arylzinc compounds catalysed by Ni-complex for the synthesis of heterocyclic scaffolds (Scheme 2.2). This approach proved to tolerate different functional groups (CN, COMe, CO_2Me) affording the desired products with moderates to good diastereoselectivity. Based on their proposed mechanism, the $NiBr_2$ combining with the terpyridine (terpy) generates the actual catalyst that undergoes transmetalation with the arylzinc reagent; the alkyl halide is reduced by single electron transfer (SET) and then cyclise to a primary alkyl radical which after recombination and reductive elimination generate the desired product.[117]

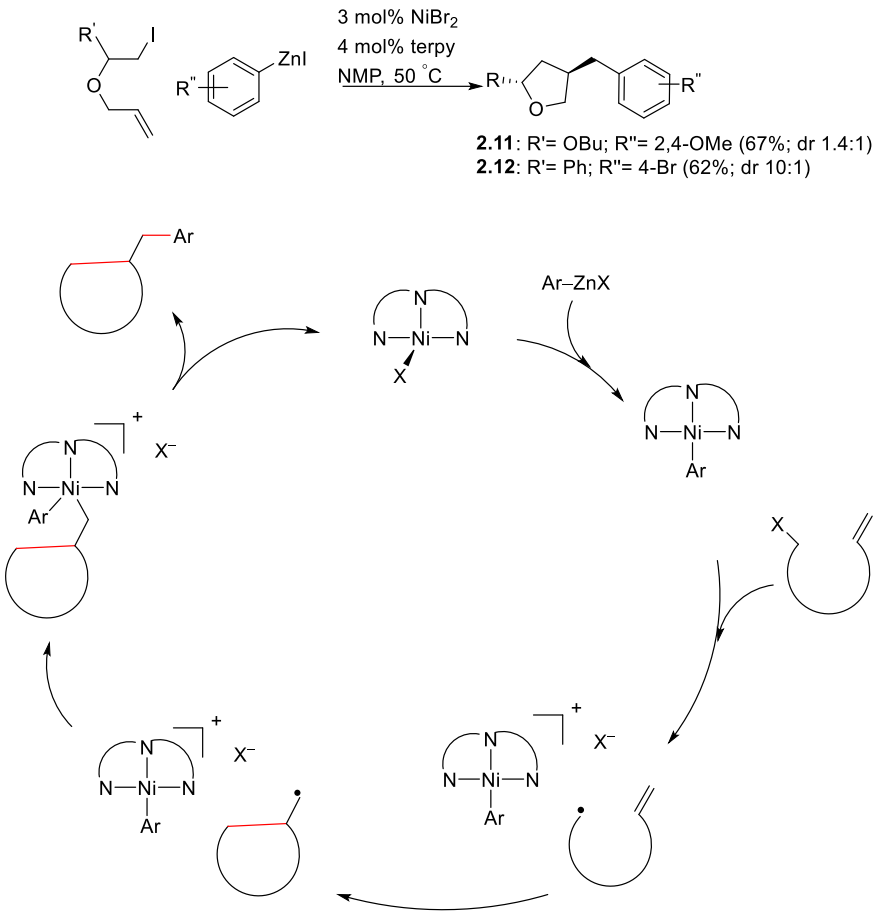

Scheme 2.2: Giri's Ni-complex catalysed cyclisation/cross-coupling reaction.

In 2000, Zhang and Lu developed a method for enantioselective carbocyclisation of enyne esters involving Pd^{II} catalysis (Scheme 2.3) The use of nitrogen containing ligands (**2.13**, **2.14**) not only allowed to get the desired products with really high enantioselectivity (up to 92%ee) but their use also inhibited the beta-hydride elimination and made the intramolecular olefin insertion into the vinyl palladium bond more preferable to its protolysis. The proposed mechanism of the reaction involves *trans*-acetoxypalladation of the triple bond, followed by intramolecular olefinic insertion; the final product is finally afforded by deacetoxypalladation.[118]

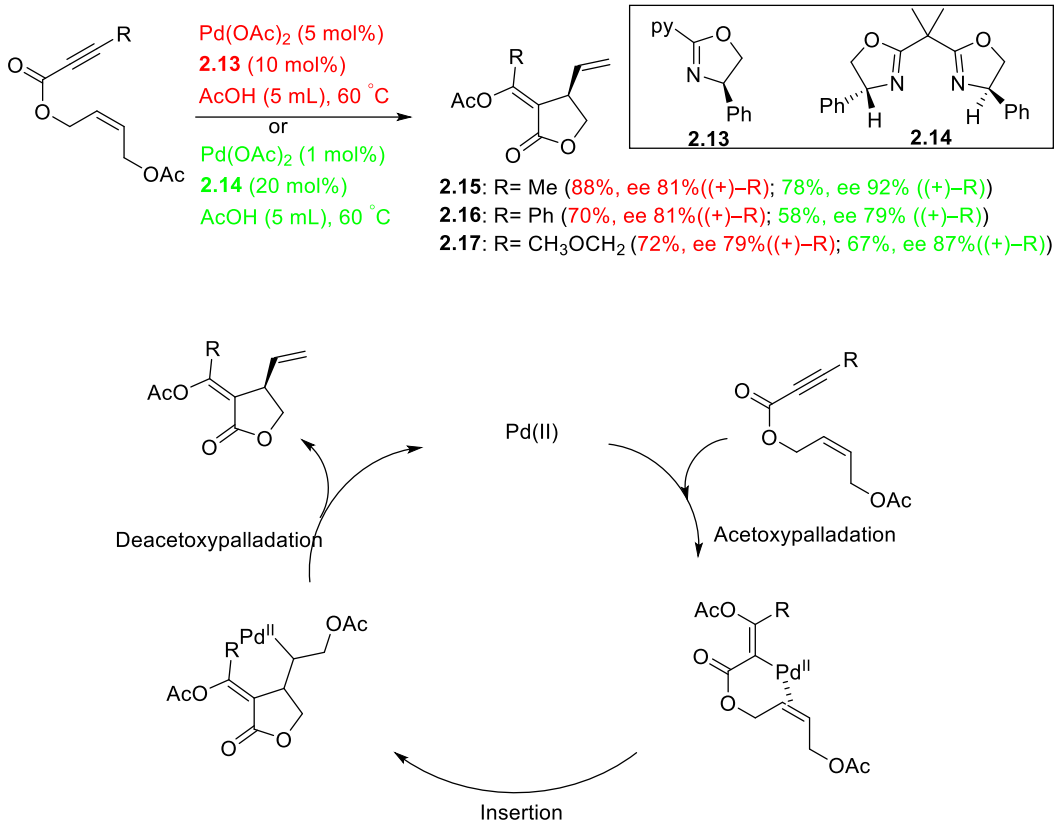

Scheme 2.3: Zang and Lu's enantioselective carbocyclisation of enyne esters.

Another example is the application of ring close metathesis using second generation Hoveyda-Grubbs catalyst for the synthesis of chiral γ-butenolides reported in 2011 by Feringa and co-workers (Scheme 2.4).[119]

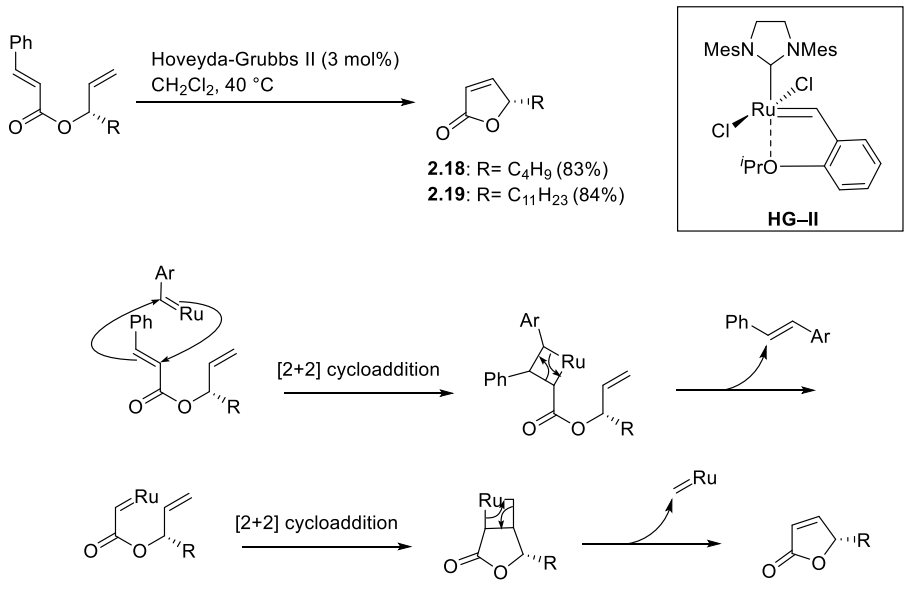

Scheme 2.4: Hoveyda-Grubbs metathesis.

Oxidative cyclisation of alcohols and carboxylic acids with pendant unsaturated chains constitutes a major tactics for the synthesis of substituted THFs and lactones. One method is the oxidation of

the alkene to a reactive intermediate prior to cyclisation.[117,120–125] In the literature many methods are reported utilising a variety of metal catalysts like Pd (II), as shown in the general Scheme 2.5a. For instance Pd(II) can coordinate to an alkene double bond hence facilitating inter or intra-molecular nucleophilic attack; the nucleopalladation intermediate can then undergo different reactions.[126] The work from Dong and co-worker is an example to that extent (Scheme 2.5a) .[125] They developed a method for the deoxygenation of alkenes using a combination of a Pd(II) catalyst bearing an electron-rich diphosphine ligand and hypervalent-iodine. In accord with their proposed mechanism, the palladium complex undergoes *trans*-acetoxypalladation with the olefin to give the organopalladium intermediate which is then oxidised by the hyper-valent iodine. Intramolecular cyclisation regenerates the catalyst and leads to an acetoxonium intermediate and then the desired product.

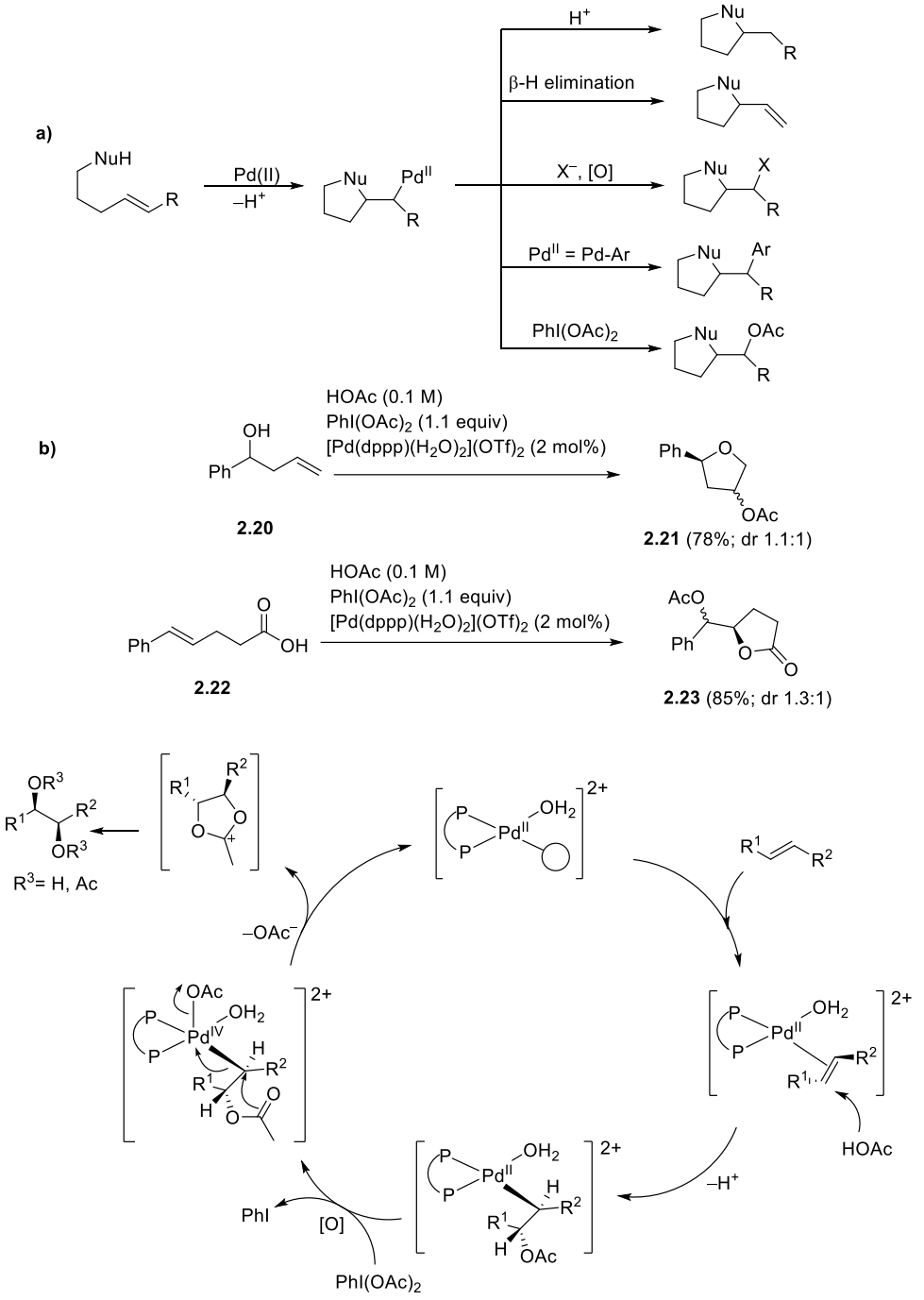

Scheme 2.5: a) General scheme of Pd catalised oxidative cyclisation; b) Dong's deoxygenation of alkenes.

Oxidative cyclisation of 1,5-dienes catalysed by transition metal-oxo species, such as OsO_4, RuO_4 and MnO_4^- is another approach for the synthesis of THFs, in particular THF-diols.[127–130] This approach, as described by Baldwin,[131] is based on a [3+2] cycloaddition of the metal-oxo species across the first alkene, followed by *syn* addition of the two oxygen atoms across the original double bond; this intermediate is oxidised before an intramolecular [3+2] cycloaddition onto the second double bond and another *syn* addition. Examples of oxidative cyclisation of 1,5-dienes for the synthesis of THF-diols have been reported by Piccialli using RuO_4,[132] Piccialli[133] and Donohoe[134] using OsO_4, and Brown and co-workers[135] using MnO_4^- (Scheme 2.6).

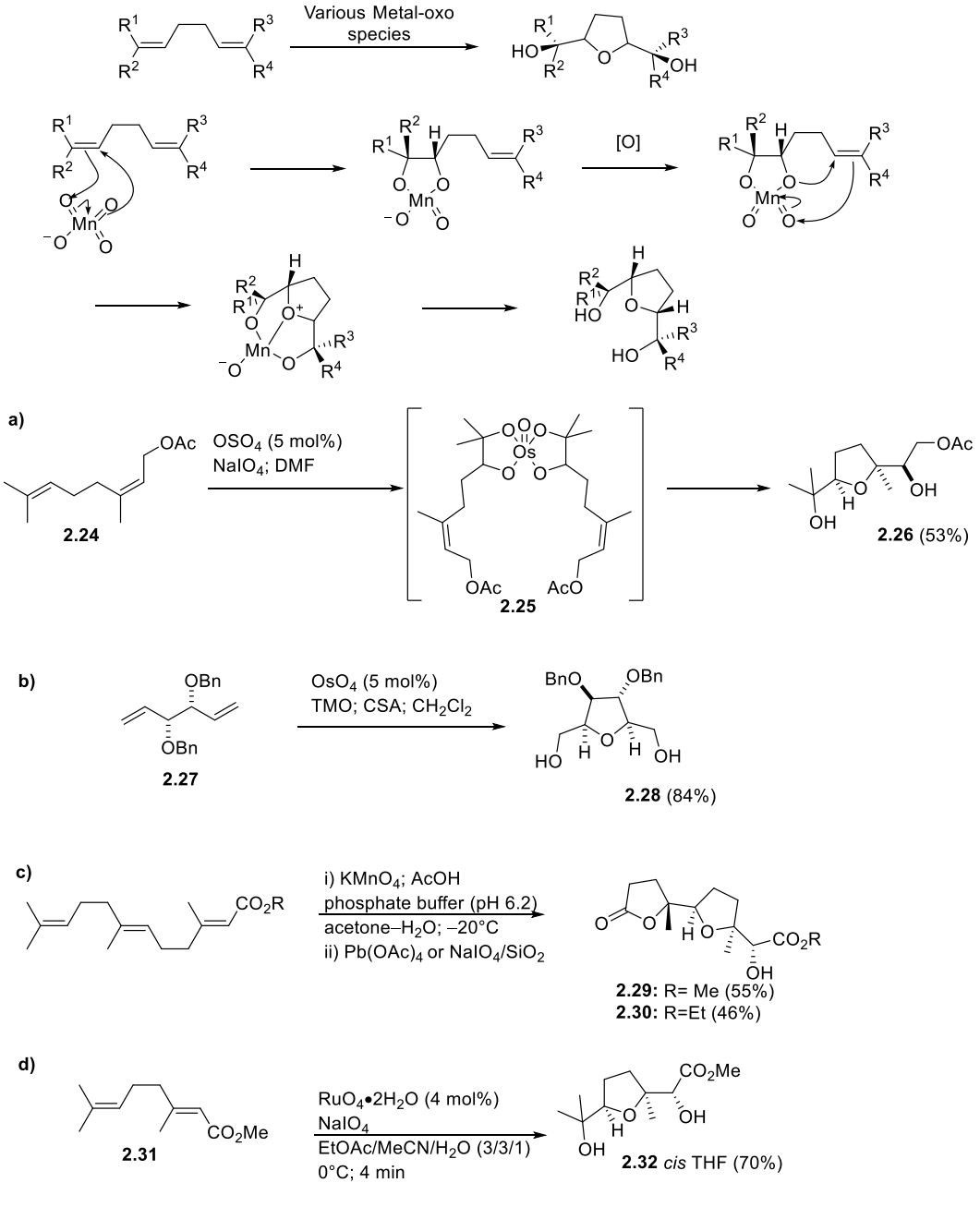

Scheme 2.6: Examples of oxidative cyclisation of hydroxyalkenes and dienes.

Intramolecular oxidative cyclisation of hydroxyalkenes can be also accomplished by using metal oxo-species complexed to the carbinol (Scheme 2.7).[98,113,126,136–138] Examples of this type of approach were reported by He and co-workers (Scheme 2.3a),[123] and Dzudza and Marks (Scheme 2.3b),[124,139] where Silver and lanthanides triflates respectively, are used for an intramolecular hydroalkoxylation of double bonds. In their work, He and co-workers, present a Silver(I)-catalysed intramolecular addition of hydroxyl or carbonyl groups to unactivated olefins. Different substrates gave good to excellent yields; for terminal alkenes only 5-exo cyclisation porducts were observed, while terminal monosubstitued alkenes gave a mixture of 5-exo and 6-endo porducts. Based on their proposed mechanism, the silver(I) activates the double bond that is then attacked by the oxygen nucleophile from the opposite face; proton transfer leads to the formation of the product

and the regeneration of the silver catalyst. Dzudza and Marks approach require instead the use of lanthanides triflates in imidazolium-based ionic liquids to mediate the hydroxylation/cyclisation of alkenols; from what they proposed the use of ionic liquids instead of common solvents, enhance the Lewis acidity of the lanthanide ion amking also easier the product separation at the end of the reaction.

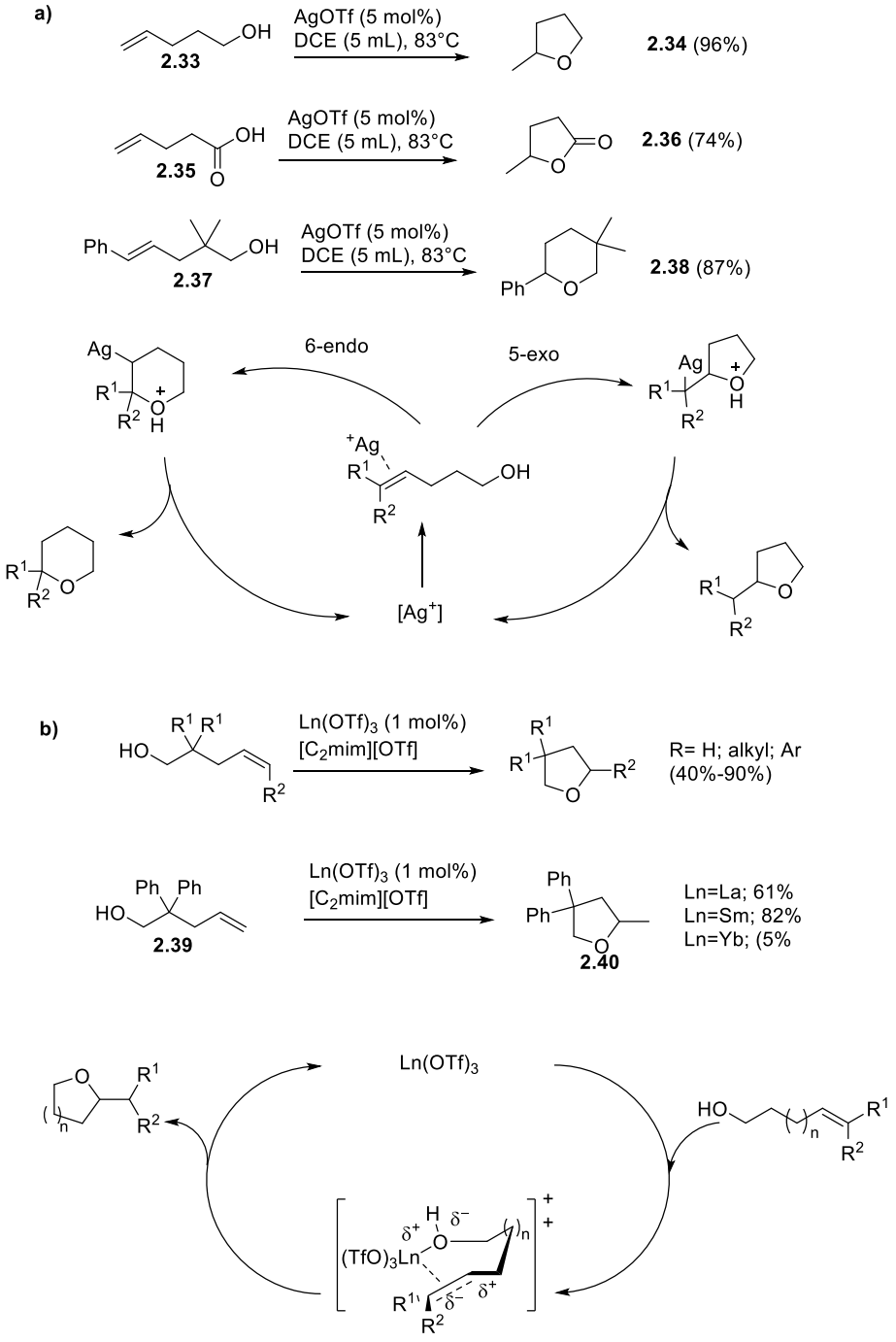

Scheme 2.7: Examples of Lewis acid-catalysed intramolecular oxidative cyclisation of hydroxyalkenes.

Many oxidative cyclisation approaches employ stoichiometric amounts of oxidising agents, and/or metal reagents or catalysts that are finite resources, which, in some cases, present toxicity issues and are unattractive from a sustainability point of view. Photoredox catalysis offer an attractive

alternative approach, elegantly harnessing energy from light to avoid the requirement for conventional highly energetic oxidising agents.[140–144] In 2013, Glorius and co-workers developed a visible light-mediated method combining a Gold catalyst with a photoactive Ru-complex for the oxy- and aminoarylation of alkenes (Scheme 2.8).[144] None the less, this methodology still utilises Au and Ru species as catalysts. Based on their porposed mechanism, the Au(I) catalyst reacts by anti-selective cyclisation with the hydroxyalkene to give the intermediate alkoxygold(I) that will then react with the aryl radical to give the Au(II) intermediate. The photoactivated Ru complex has both the roles to generate the aryl radical and the highly electrophilic Au(III) intermediate that finally by reductive elimination gives the disered product.

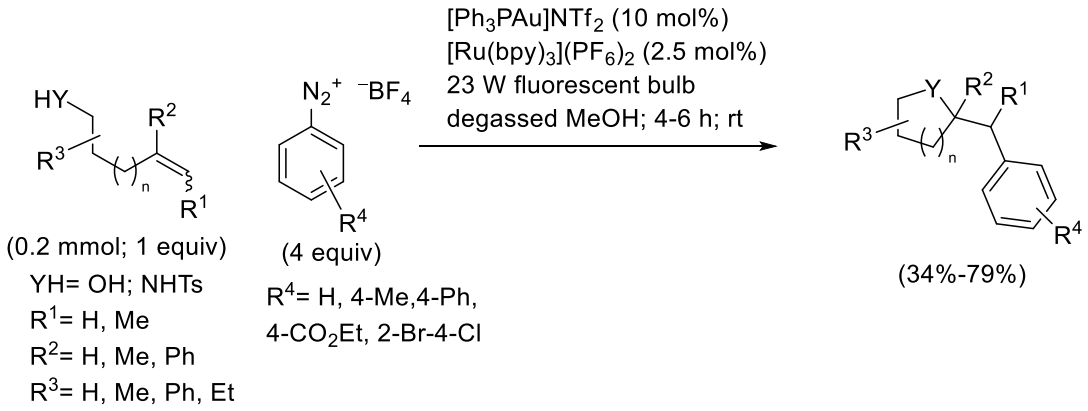

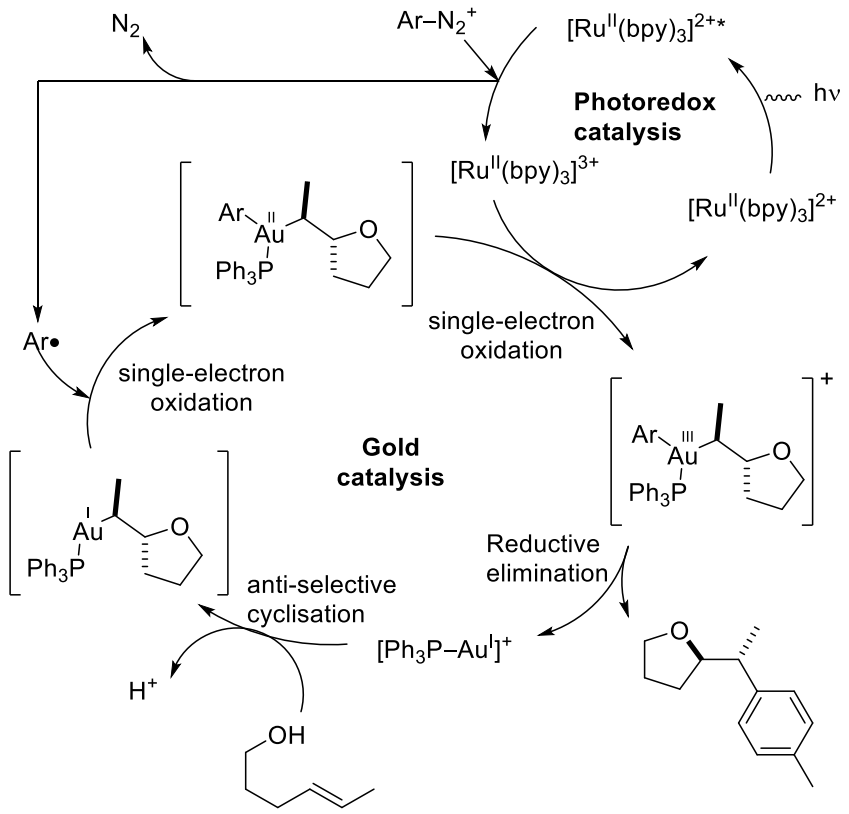

Scheme 2.8: Combined Gold and Photoredox catalysis for the oxy- and aminoarylation of alkenes by Glorius and co-workers.

In 2018, Dagousset *et al*. developed a photoredox method for the anti-Markovnikov difunctionalisation of alkenes (Scheme 2.9).[141] Their novel approach was also applied to the synthesis of substituted ethers, and is catalysed by an Ir-complex and is proposed to involve the generation of alkoxy radicals from *N*-alkoxypyridinium salt **2.41**. The advantages of this methodology are that it tolerates different functional groups (halogen, methoxy, amides), it can be performed both in batch and flow, three types of difucntionalisation can be achieved (hydroxyalkoxylation, dialkoxylation, aminoalkoxylation) with anti-Markovnikov regioslectivity. Based on their proposed mechanism, the *N*-alkoxypyridinium salt is reduced by the visible light-activated Ir catalyst, generating RO· that will then react with the alkene. The new carbon-centred radical intermediate, is oxidised by the $Ir(ppy)_3^+$ to the corresponding carbocation that is finally trapped by a nucleophile (water, alcohol or acetonitrile) to give the desired product.

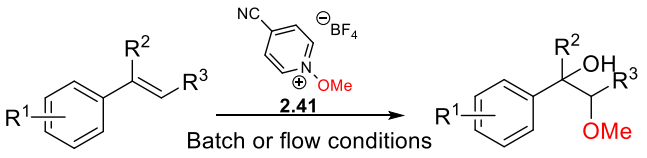

2.42: R^1= 4-Cl;R^2= H; R^3= H (65%[a]; 64%[b])
2.43:R^1= 4-Me;R^2= H;R^3= H (72%[a]; 75%[b])
2.44:R^1= 4-OMe;R^2= H;R^3= H (52%[a])
2.45:R^1= 4-OMe;R^2= H; R^3= Me (56%[a]; 60%[b])
2.46:R^1= H;R^2= Me;R^3= H (72%[a])

[a] Batch: alkene (0.2 mmol); *N*-alkoxypyridinium salt (0.1 mmol); *fac*-$Ir(ppy)_3$ (1 mol%); NaH_2PO_4•$2H_2O$ (0.1 mmol); degassed wet acetone; 3 W blue LED; rt; 36 h
[b] Flow: alkene (0.05 M; 2 equiv); *N*-alkoxypyridinium salt (1 equiv); *fac*-$Ir(ppy)_3$ (3 mol%); degassed wet acetone/CH_2Cl_2
(5/1); 450 nm blue LED; flow 0.15 mL/min; 25°C; 2 mL solution (0.1 mmol)
Flow scale up: for substrate R^1 = F; R^2 = H; R^3 = H; 80 mL solution (4 mmol)

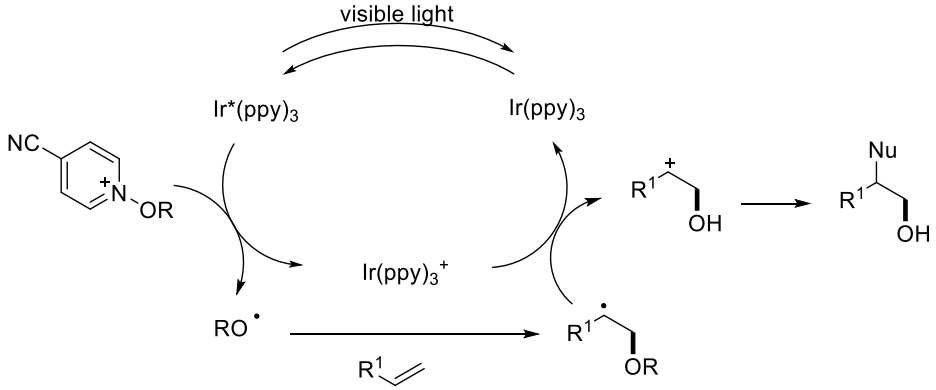

Scheme 2.9: Dagousset's Anti-Markovnikov photoredox catalysed difunctionalisation of alkenes.

More recently, in 2020, Knowles and co-workers reported a visible light-driven method for the intramolecular hydroetherification of unactivated disubstitued and trisubstitued alkenes catalysed by an Ir complex, a Brønsted base and a hydrogen atom transfer co-catalyst . This method is based on the photocatalytic activation of the hydroxyl functionality to afford the formation of C—O bond, has been applied on a broad range of substrates in terms of functional groups and alkene substitution pattern.(Scheme 2.10).[145] Their proposed mechanism involves a proton coupled

electron transfer (PCET) activation of the O—H bond by the concerted action of the Ir activated complex and the Brønsted base catalyst; the new oxygen-centred radical will then attack the alkene forming the new C—O bond and the final hydrogen atom transfer will give the final product. The catalytic cycle is closed by the reduction of the thiyl radical by the Ir(II) photocatalyst.

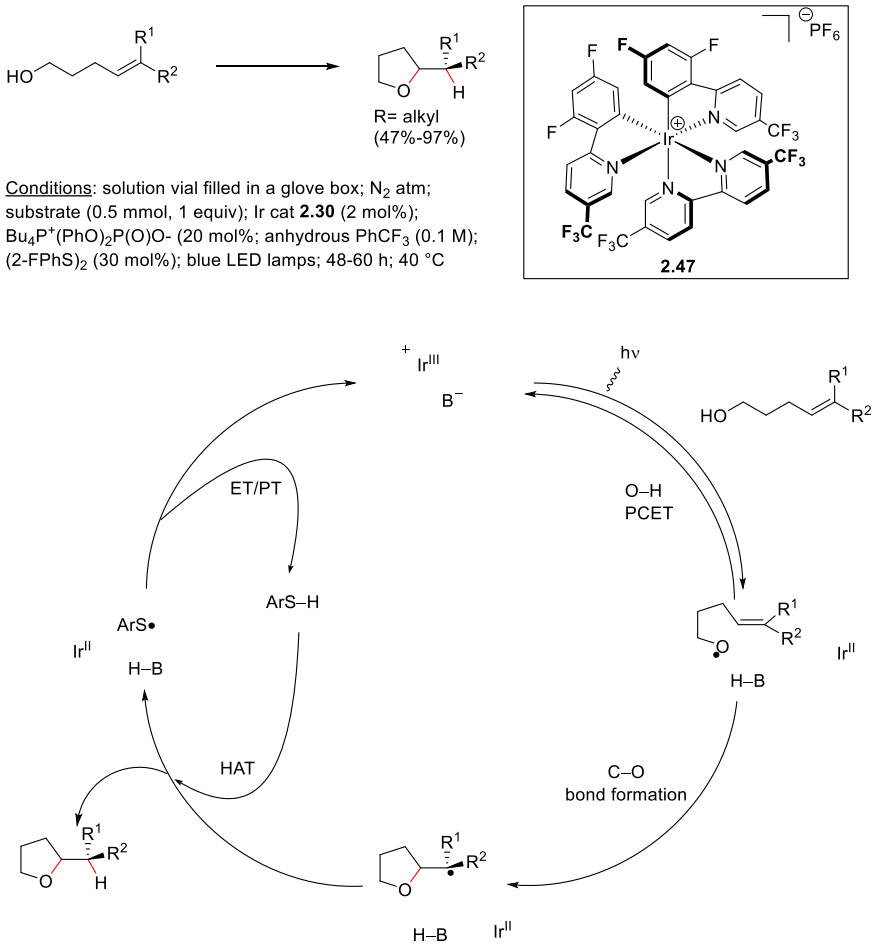

Scheme 2.10: Knowles's Ir-complex catalysed intramolecular hydroetherification.

Many of these photochemical approaches require photo-redox catalysts based on transition-metal complexes such as Ir, Ru, Au which are finite resources. But there are also some examples of organic molecules used as photocatalysts. In 2012, Nicewicz and Hamilton reported a direct *anti*-Markovnikov hydroetherification of alkenols using a combination of 9-mesityl-10-methylacridinium perchlorate **2.49** and 2-phenylmalononitrile **2.48** as photoredox catalysts (Scheme 2.11).[143]

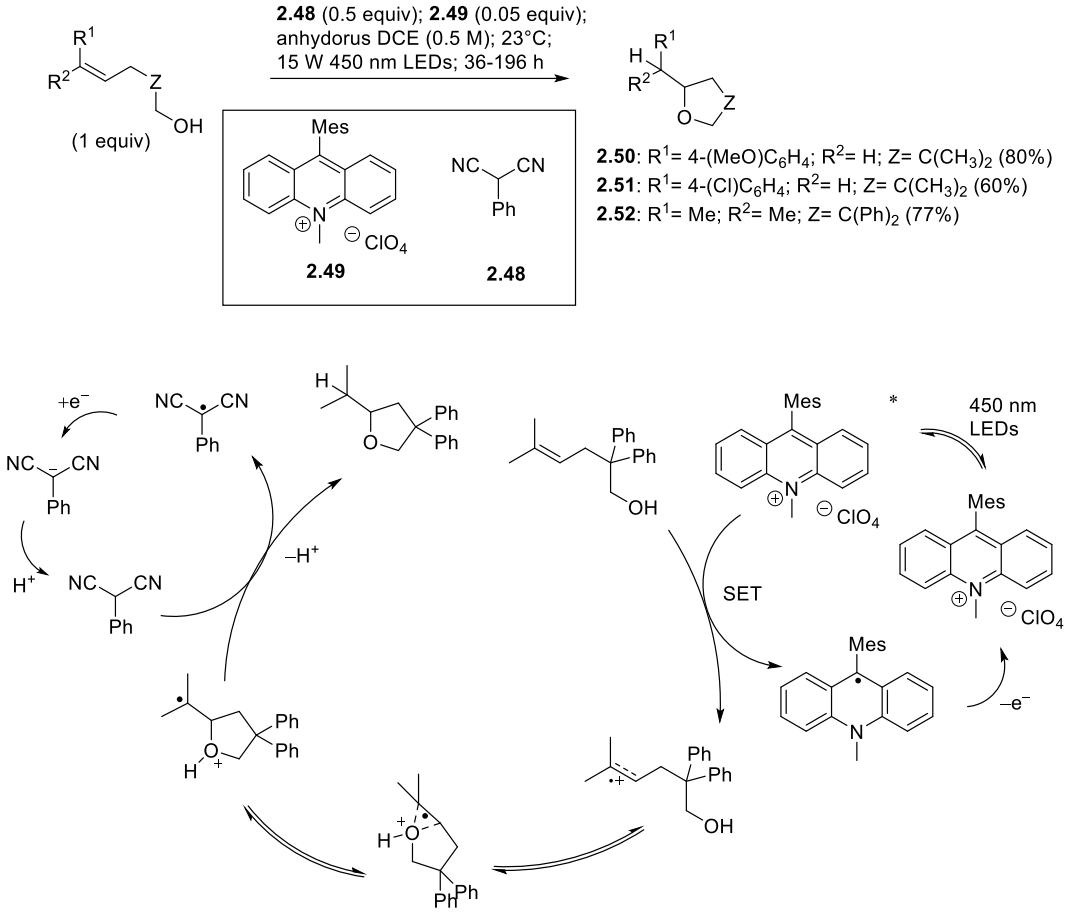

Scheme 2.11: Nicewicz and Hamilton's intramolecular anti-Markovnikov hydroetherification catalysed by **2.48** and **2.49**.

In 2015, Wagenknecht *et al*. developed two photoredox approaches, catalysed respectively by 1-(*N*,*N*-dimethylamino)pyrene (Py) **2.53** and 1,7-dicyanoperylene-3,4,9,10-tetracarboxylic acid bisimide (PDI) **2.54**, for the intra- and inter-molecular nucleophilic addition of hydroxyl functionality to styrene double bonds (Scheme 2.12).[142] The first route, catalysed by an electro-rich chromophore like Py (**2.53**), starts with a single-electron transfer onto the substrate; the intermediate radical anion is immediately protonated to the neutral benzylic radical which after electron transfer is converted to a cation that by nucleophilic attack of the alcohol at the end gives a Markovnikov-type addition product. The second approach, instead, catalysed by an electron-poor chromophore like PDI (**2.54**), starts with the oxidation of the styrene double bond to a radical cation; nucleophilic attack by the alcohol leads to the formation of a benzylic radical, by electron transfer the radical is converted to an anion intermediate that after protonation gives the final *anti*-Markovnikov-type product.

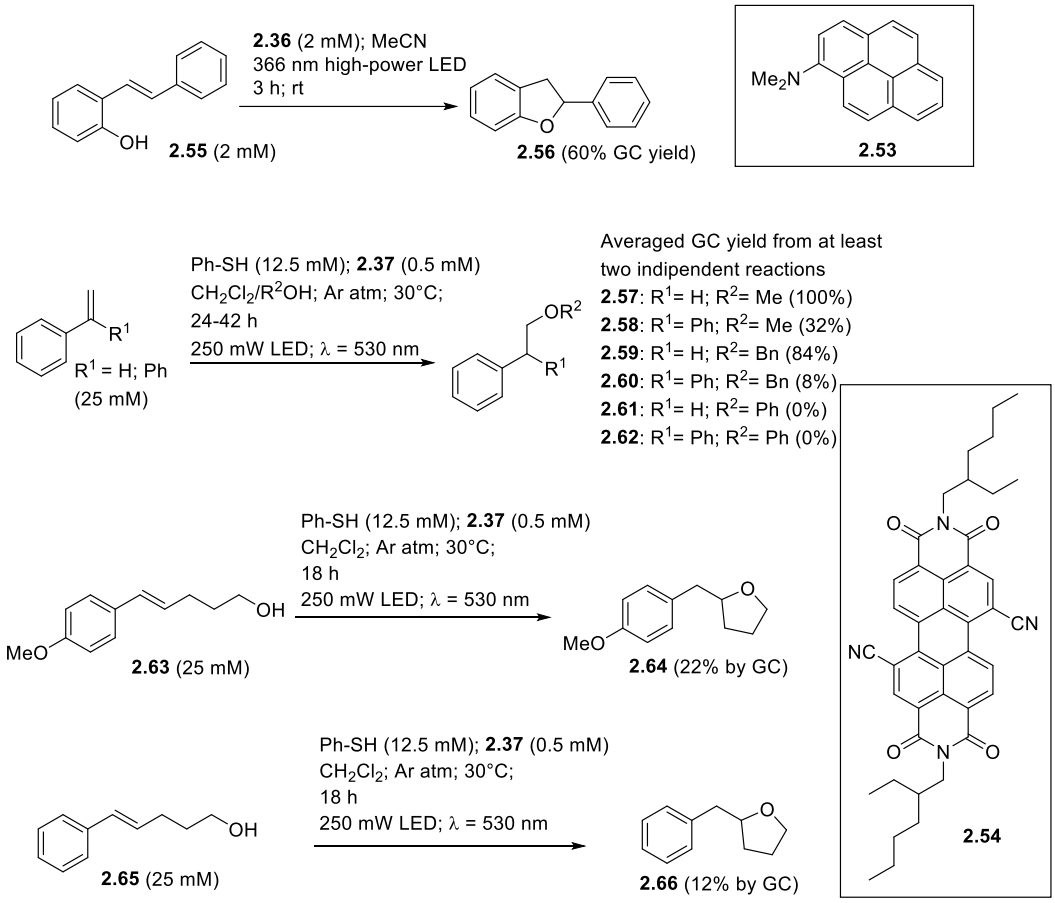

Scheme 2.12: 2.53 and **2.54** Photocatalysed Markovnikov and anti-Markovnikov intramolecular hydroetherification of styrene derivatives by Wagenknecht *et al*.

Another example of the application of an organic photocatalyst for the synthesis of cyclic ethers is the one from Laha and co-workers (Scheme 2.13).[140] They developed this photochemical method, catalysed by DCN (1,4-dicyanonaphtalene), for the intramolecular cycloetherification on the benzylic position. The reaction starts with a single-electron transfer followed by proton loss; another single-electron transfer between the DCN and the intermediate and subsequent cyclisation gives the final product.

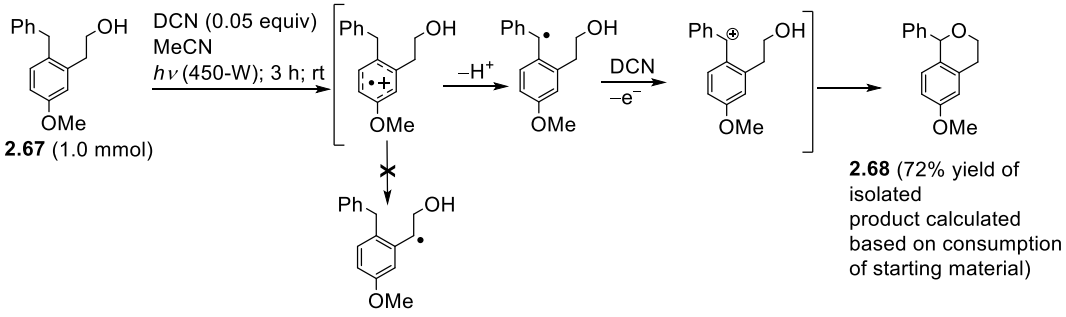

Scheme 2.13: Laha's direct benzylic C—H activation for C—O bond formation by photoredox catalysis.

2.3 Electrochemical methods for the synthesis of THFs and γ-lactones

An alternative approach for the synthesis of substituted heterocycles, and in particular cyclic ethers, and lactones is electrochemical oxidative cyclisation. The main advantage of this approach is that it reverses the polarity of electron-rich olefins that would normally serve as nucleophile by conversions to radical cations that in the end can be trapped by a pendant nucleophile such as OH or NHR (Scheme 2.10).[60,146–150]

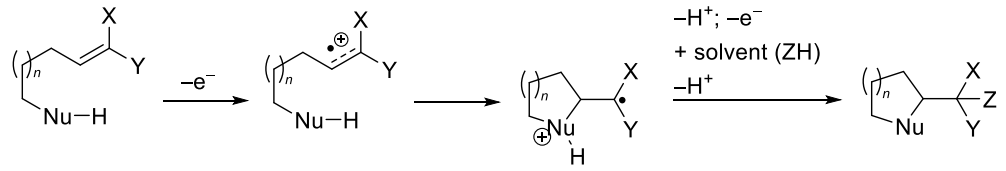

Scheme 2.14: General mechanism for the electrochemical intramolecular oxidative cyclisation.

Moeller and co-workers have pioneered these anodic oxidative cyclisations, mainly focussing upon the electrolysis of enol ethers and ketene dithioacetals, using alcohols to trap the radical cation intermediates and applying this methodology in the synthesis of natural products like (+)-nemorensic acid **2.75** (Scheme 2.15).[148,151] Starting from (*R*)–(+)–3-methylglutarate (**2.69**), it was first reduced with $BH_3{\cdot}Me_2S$ to the hydroxyester that then cyclised to lactone **2.70**. Treating the lactone with Me_3Al and 1,3–propane thiol afforded the ketene dithioacetal functionality needed for the oxidative cyclisation. The hydroxyl functionality of **2.71**, was oxidised and treated with methyl lithium, then oxidised again and treated with allyl–β–isopinocamphenyl–9–borabicyclo[3.3.1]nonane to give **2.72** as 3:1 mixture of isomers that could only be separated after the cyclisation step. Substrate **2.72** was then electrochemically oxidised and the two isomers separated by HPLC. The major isomer **2.73a** was finally converted to the final product via ozonolysis, oxidation of the aldehyde to carboxylic acid and hydrolysis of the ester functionality.

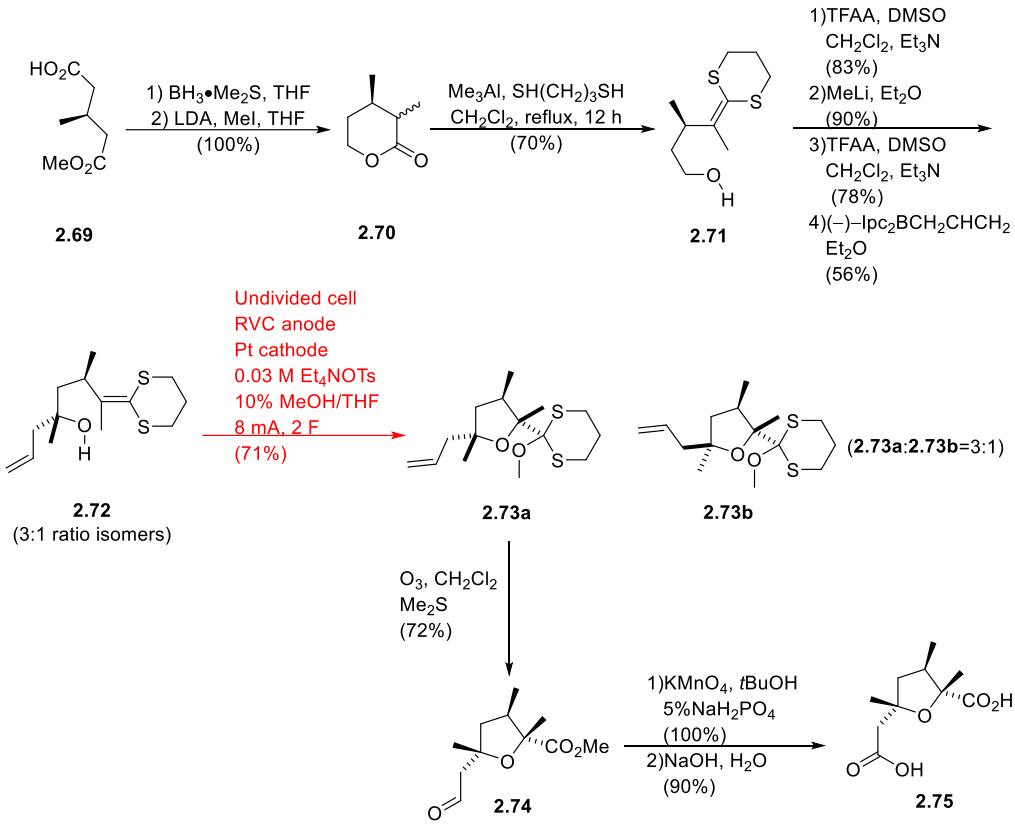

Scheme 2.15: Moeller's synthesis of (+)-nemorensic acid **2.52**.

Alcohols proved to work well as trapping agents for the radical cation intermediate generated in the oxidative process, and carboxylic acids were also demonstrated to provide effective nucleophiles in oxidative electrolysis without undergoing Koble decarboxylation.[152] In 2013, Moeller and co-workers studied the compatibility of the carboxylic acids, as nucleophiles, in anodic cyclization. First they studied the anodic oxidative coupling of ketene dithioacetals and carboxylic acids (Scheme 2.16).

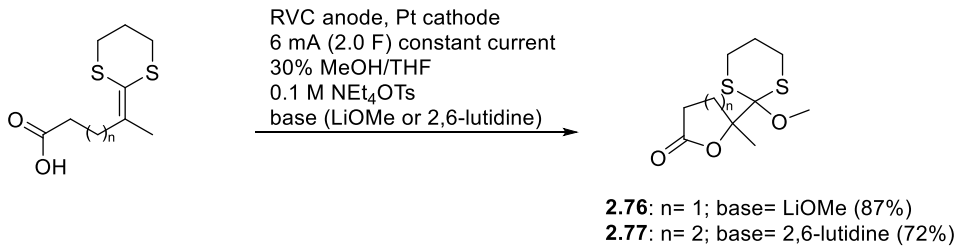

Scheme 2.16: Moeller's electrochemical intramolecular oxidative coupling of ketene dithioacetals and carboxylic acids.

Using different bases and different amount of current they discovered that Kolbe-type decarboxylation did not interfere with the oxidative coupling reaction between the carboxylic acid and the electron-rich olefin. Cyclization attempts to five and six membered rings worked well. Attempts to seven-member ring gave decomposition because the cyclization step was too slow to compete with degradation pathways. They also explored anodic coupling of carboxylic acid

groups with vinyl sulfide and enol ether functionalities (Scheme 2.17).[152] Reactions with vinyl sulfide proceeded much better than with the enol ethers, presumably due to more facile oxidation.

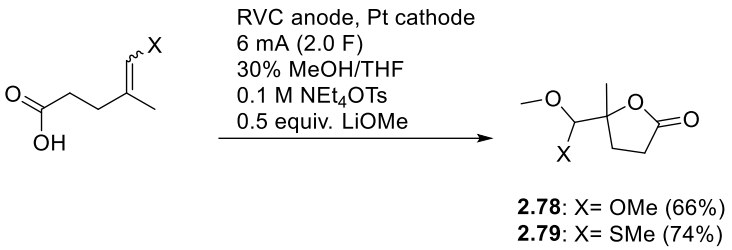

2.78: X= OMe (66%)
2.79: X= SMe (74%)

Scheme 2.17: Moeller's electrochemical intramolecular oxidative coupling of vinyl sulphides or enol ether and carboxylic acids.

Studying these examples they were able to deduce that the first oxidation occurred at the olefin rather than the carboxylate. Moeller and co-workers also investigated oxidative cyclisation of styrene derivatives to determine whether olefins with higher oxidation potential could be effective in the reaction (Table 2.1).[152] With the simple styrene derivative **2.80** they were not able to achieve a yield of better than 33% (entry 3, Table 2.1), even when increased current and the temperature were applied. None the less, they did not observe decarboxylation. They concluded that the low yield was due to a problem with the second single-electron transfer rather than the cyclization step. For this reason, their other attempts employed a methoxy-substitued styrenes, which ultimately gave the lactones with improved yield this study they were able to say that the methoxy group helped the second electron oxidation.

Table 2. 1: Moeller's Investigation of anodic lactonization of styrene derivatives

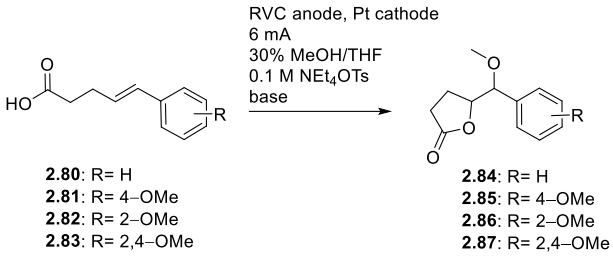

2.80: R= H
2.81: R= 4–OMe
2.82: R= 2–OMe
2.83: R= 2,4–OMe

2.84: R= H
2.85: R= 4–OMe
2.86: R= 2–OMe
2.87: R= 2,4–OMe

entry	R	Base/T	F	Yield (%)
1	H	0.5 equiv LiOMe/rt	2	15
2	H	0.5 equiv LiOMe/rt	10	27
3	H	None/40°C	10	33
4	4-OMe	0.5 equiv LiOMe/rt	2	56
5	4-OMe	None/40°C	2	76
6	2-OMe	0.5 equiv LiOMe/rt	2	48
7	2-OMe	None/40°C	2	59
8	3-OMe	0.5 equiv LiOMe/rt	2	4
9	3-OMe	0.5 equiv LiOMe/rt	10	35
10	3-OMe	None/40°C	10	23
11	2,4-OMe	0.5 equiv LiOMe/rt	2	48
12	2,4-OMe	None/40°C	2	45
13	2,4-OMe	1 equiv LiOMe/rt	2	74

From Moeller's work it was clear that carboxylic acid could be coupled to electron-rich olefins without interference from competitive decarboxylation reaction. Moreover the success of the styrene derived coupling reaction was dependent strongly on the presence and the position of the methoxy group on the aromatic ring (Scheme 2.18), being most effective when carbocation stabilisation was achieved through resonance.

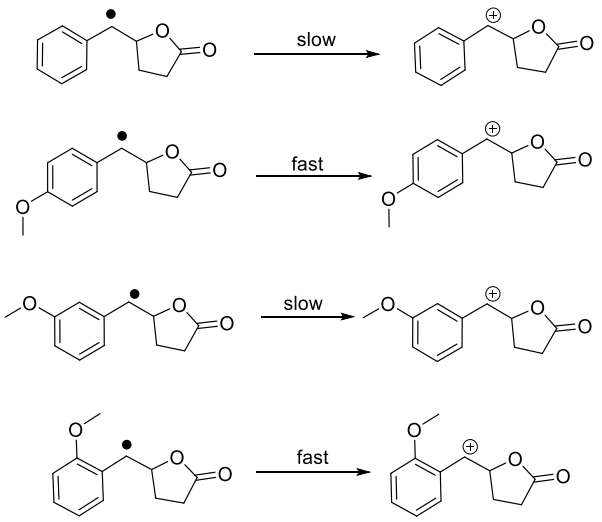

Scheme 2.18: Mechanistic insight of the electrochemical oxidative cyclisation of styrene carboxylic acid derivatives.

In recent years, some other examples of electrochemical oxidation of styrene double bond followed by nucleophilic attack have been reported. In 2018, Xu *et al*. reported the electrochemical synthesis of aromatic lactones through dehydrogenative C—O bond formation (Scheme 2.19).[153] This method proceeds under mild conditions (reactions are performed at room temperature and open air), and can tolerate different functional groups (methyl, methoxy, cyanide, nitro, ketone, halides, carboxylic acids) and proved to be scalable up to 100 g. Their cyclic voltammetry studies suggest that the oxidation of the carboxylate is easier that than the oxidation of the arene ring for both electron-rich and electron-poor compounds.

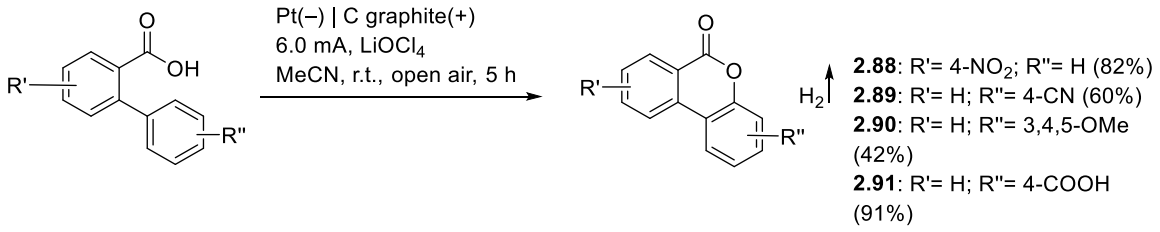

Scheme 2.19: Synthesis of aromatic lactones through electrochemical C—O bond formation.

In 2019, Xu and his group[154] reported the electrochemical dimethoxylation of olefins using platinum electrodes. Their protocol was applied on different substrates, but the majority of them containing a more readily oxidised styrenic double bond (Scheme 2.20). The outcome of their CV experiments is that the olefin is easier to oxidise than the MeOH, using the optimised reaction conditions, which exclude the possibility to generate methoxyl radicals in the presence of the olefin. So at the anode the olefin is oxidised to a radical cation that undergoes nucleophilic attack by the methanol; then the radical intermediate is oxidised to a cation that can follow two paths based on its stability: direct nucleophilic attack or semipinacol rearrangement to the acetal product.

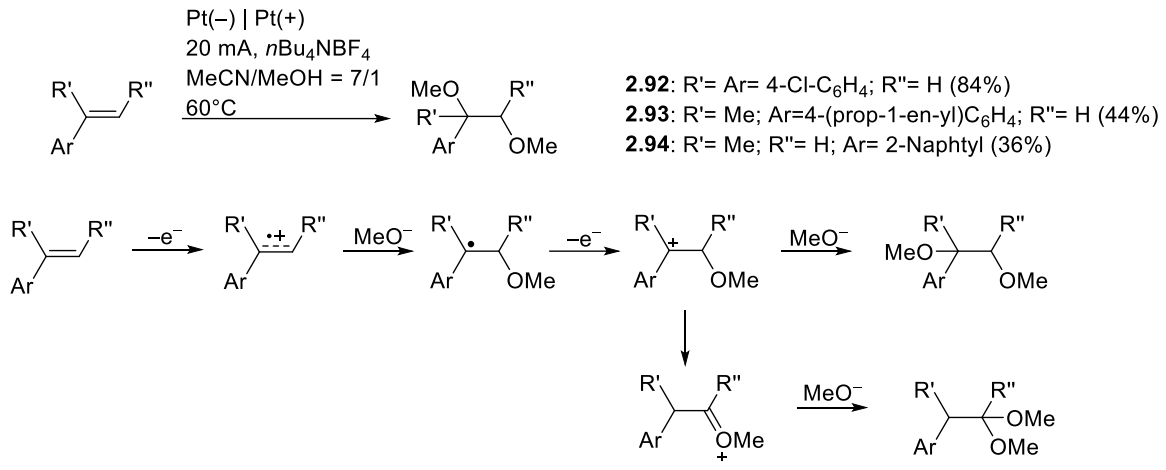

Scheme 2.20: Xu's electrochemical dimethoxylation of olefins.

In 2020, Nam *et al*. developed an electrochemical methodology for the electrochemical reductive dicarboxylation and β-hydrocarboxylation of styrene derivatives (Scheme 2.21).[155] The electrolysis requires a nickel cathode and magnesium sacrificial anode, and it is performed under an atmosphere CO_2 to give dicarboxylation and in presence of 1 equivalent of water gives β-hydrocarboxylation. It is possible that both the styrene and the CO_2 get reduced under the reduction conditions; both scenarios lead to a β–carboxylate radical intermediate that is again reduced and then can undergo protonation or carboxylation on the benzylic position.

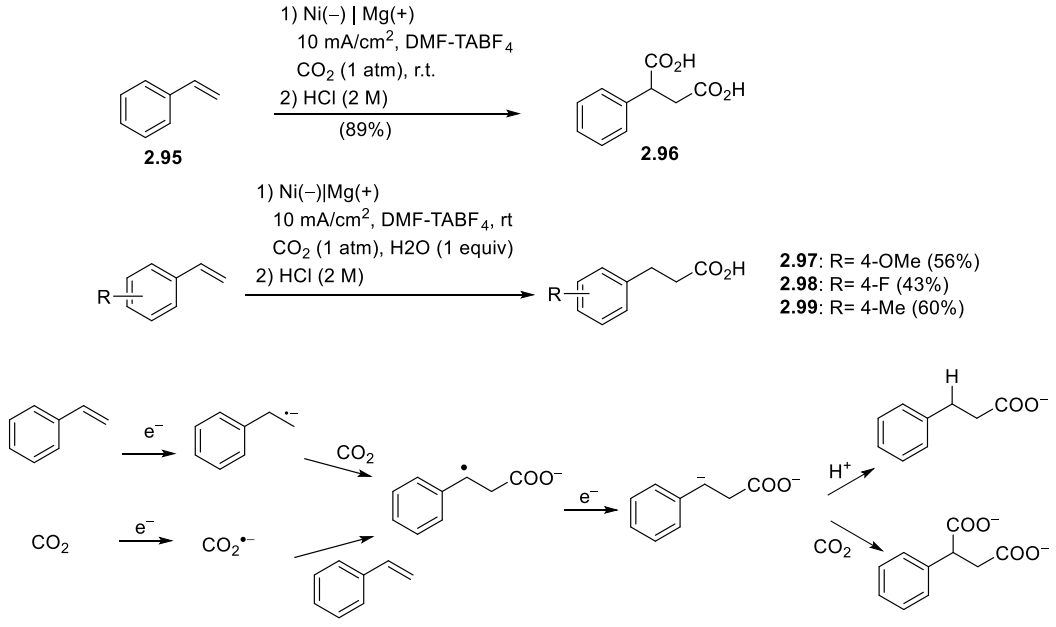

Scheme 2.21: Electrochemical reductive dicarboxylation and selective β-hydrocarboxylation of styrenes.

In 2021, Kim and co-workers[156] described the electrochemical oxidation of styrene derivatives followed by nucleophilic attack of DMF to afford formyl-protected *syn*–1,2–diols. The electrolysis is performed in an undivided cell, using Pt cathode and C anode, in the presence of trifluoroacetic acid and water (Scheme 2.18). A mechanism has been proposed, starting with the electrochemical

oxidation of the alkene to a radical cation that undergoes nucleophilic attack by the DMF. A second oxidation generates a benzylic cation that is trapped by the trifluoroacetate ion generating the *anti*-dioxyenated intermediate. Nucleophilic displacement of the trifluoroacetate group by the DMF and subsequent hydrolysis gives the syn-diformyloxylation product. Kim and co-workers also envisioned a second path where is the DMF the nucleophile that attack the benzylic cation giving the anti-diformyloxylation product; however this path is considered less likely because trifluoroacettate is a better nucleophile and also because the predominant stereoselectivity observed is *syn*.

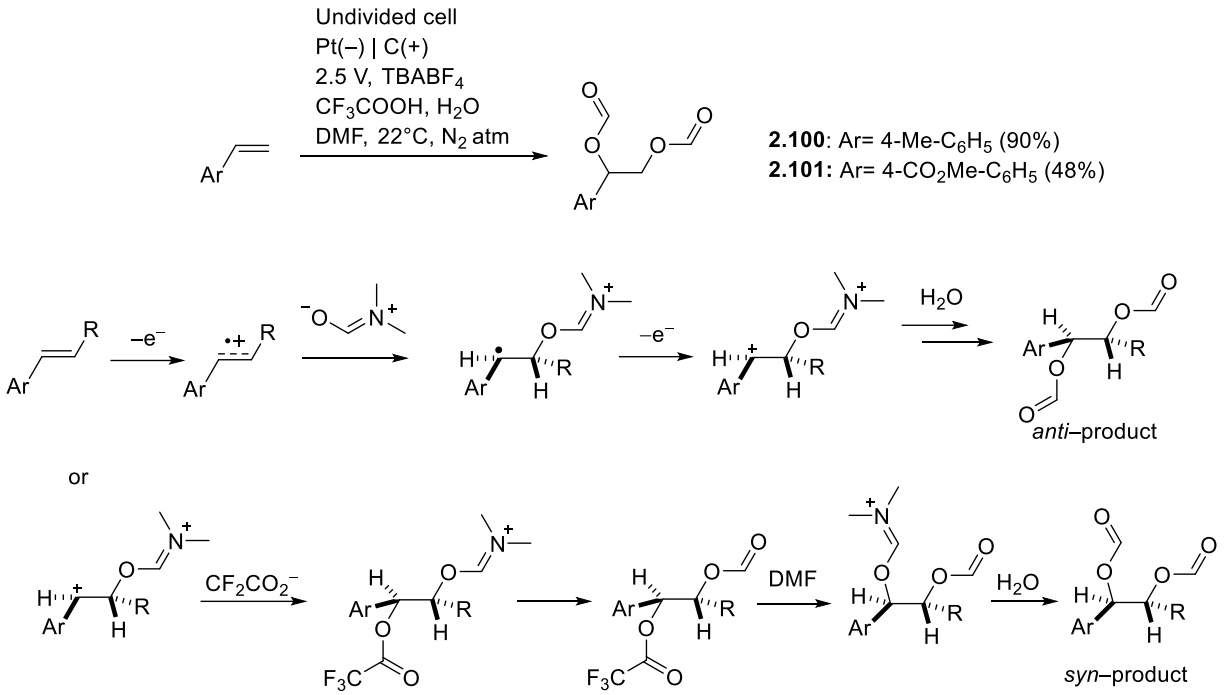

Scheme 2.22: Electrochemical dioxygenation of simple styrene derivatives.

2.4 Aims and objectives

Our ongoing interest in oxidative cyclisation approaches to oxygen heterocycles, together with our work in the field of flow electrosynthesis, prompted us to further explore anodic cyclisation of styrene derivatives based on Moeller's pioneering studies. The aim of this research was to develop the anodic oxidative cyclisation of styrene derivatives bearing pendant alcohol and acid functionalities to give THFs and lactones using a commercially available electrolysis flow cell, which possessing a narrow interelectrode gap (0.5 mm) combined with an extended path (100 cm) targeting high levels of conversion in a single pass of the reactor.

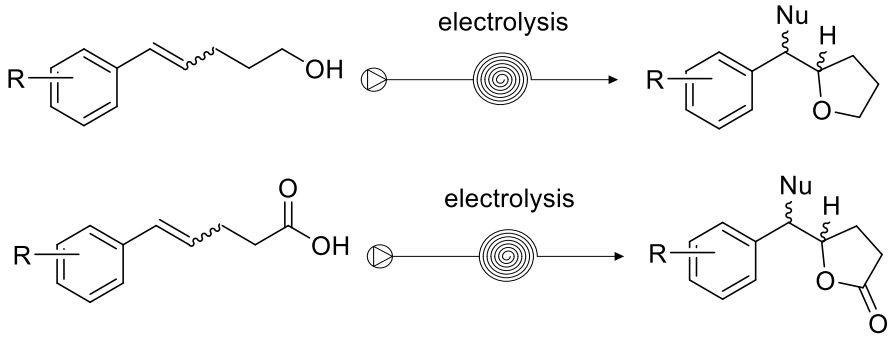

Scheme 2.22: General scheme of the proposed flow electrolysis.

2.5 Synthesis of starting materials

For the initial exploration and optimisation of the oxidative cyclisation process, (*E*)-5-phenylpent-4-en-1-ol (**2.65**) and (*E*)-5-(4-methoxyphenyl)pent-4-enoic acid (**2.81**) were selected as model substrates. For the synthesis of alkenoic acid **2.81** we relied on the protocol reported by Moeller and *co-workers* (Scheme 2.23);[152] thus, Wittig reaction of commercially available phosphonium salt **2.102** with *p*-anisaldehyde (**2.103**) afforded **2.81** with a 79% yield after recrystallisation from CH_2Cl_2 .

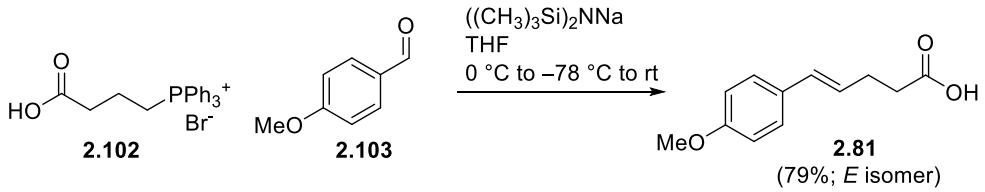

Scheme 2.23: Synthesis of alkenoic acid **2.81** by Wittig olefination of *p*-anisaldehyde.

Alcohol **2.65** could have been obtained from the corresponding carboxylic acid, made with the method described above, however, a more efficient synthesis of alkenol **2.65** was sought. The first, more direct approach, was by Wittig reaction of benzaldehyde with a phosphonium reagent **2.104** (Scheme 2.24). Phosphonium salt **2.104** is not commercially available so by adapting a

procedure reported in literature its synthesis was attempted by bromination of 1,4-butanediol **2.105** followed by reaction with PPh_3.[98,157] As reported in the literature compound **2.104a** should have been easily purified by precipitation in Et_2O. Instead, ^{1}H-NMR analysis revealed a mixture of **2.104a**, Ph_3PO, the diphosphonium salt **2.106** along with other impurities, which was obtained as a gum-like substance that was very difficult to purify**.**[158]

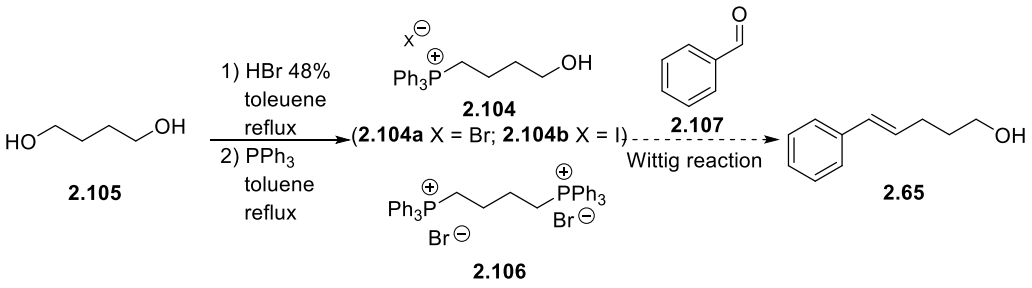

Scheme 2.24: Attempted synthetic approach to alkenol **2.65** *via* Wittig olefination.

Diphoshonium salt **2.106** was a consequence of double bromination of **2.105**; as such, one of the hydroxyl groups was protected by formation of the tetrahydropyranyl (THP) ether **2.108** to block subsequent double addition of Ph_3P to give **2.106** (Scheme 2.25). Unfortunately, a gum-like substance was obtained that proved difficult to purify.

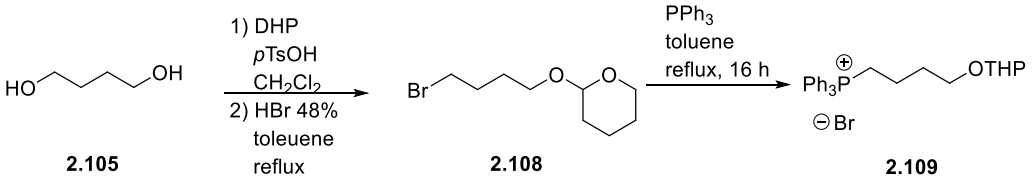

Scheme 2.25: Attempted synthesis of phosphonium salt **2.85** following protection of the hydroxyl functionality by formation of a tetrahydropyranyl ether.

A literature procedure reported for the synthesis of the phosphonium iodide salt was attempted, but the same purification issues arose again.[159] In the case of the phosphonium bromide salt **2.109**, precipitation of a semi-solid was observed, which was difficult to filter. ^{1}H-NMR spectroscopy confirmed the presence of the desired product **2.104b**, but contaminated with a lot of impurities.

Therefore, the Wittig route was abandoned in favour of a palladium-catalysed Heck cross-coupling approach towards compound **2.65** (Scheme 2.26).[160] Classical Heck reactions require a palladium(0) catalyst with phosphine ligands in presence of a base; Pd(0) can be replaced $Pd(OAc)_2$ that is reduced to the active specie Pd(0) *in situ* by the base, in this case here, with the help of TBAB that stabilises the Pd(0) in the absence of phosphine ligands.[161–163] After Heck reaction of alkene **2.110** and iodobenzene (**1.57**), purification by column chromatography gave two main fractions. One was a mixture of the desired product **2.65** and its isomer **2.111**, the other

was a mixture of the two isomeric aldehydes **2.112** and **2.113**. Palladium catalyses the migration of the alkene along the carbon chain by palladium hydride elimination and subsequent re-addition to give enols that tautomerise to the aldehydes.[164–167]

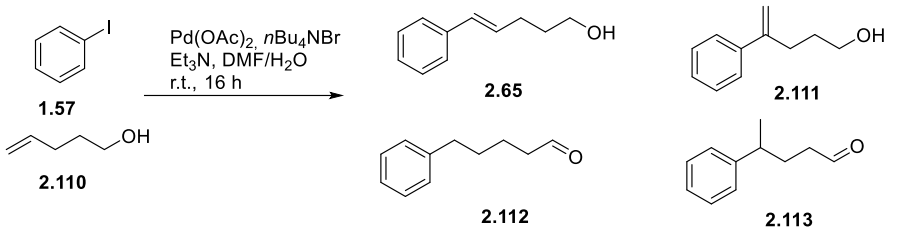

Scheme 2.26: Unsuccessful Heck coupling approach to the synthesis of alkenol **2.65**.

Another approach to obtain compound **2.65** was a two-step sequence involving a Sonogashira coupling of **2.114** and iodobenzene followed by reduction of the resulting alkyne **2.115** (Scheme 2.27).[168] This two step approach ultimately afforded the desired *E* alkenol **2.65** as a single isomer with an overall yield over the two steps of 81%.

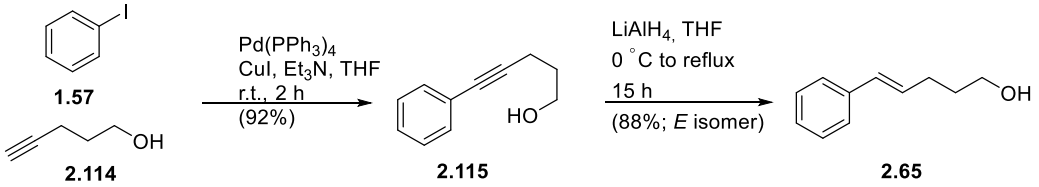

Scheme 2.27: Synthesis of alkenol **2.65** through a two step Sonogashira coupling - $LiAlH_4$ reduction sequence.

2.6 Initial exploration of the oxidative cyclisation process

With the alkenol **2.65** in hand, investigation of the crucial anodic cyclisation in the electro-flow reactor could begin (Scheme 2.28). Because the reaction was going to be performed for the first time and not knowing the reactivity of **2.65** in the Ammonite cell, a set of starting conditions was chosen. A stainless steel cathode provides a robust material for the counter electrode reaction, which will be reduction of protons here. A C/PVDF anode is a good general starting point for oxidation. The concentration of reactant was set at 0.1 M, with 0.5 equivalents of supporting electrolyte to improve conductivity. To achieve full conversion in one pass of the cell at a flow of 0.25 mL/min the required current can be calculated. Assuming that that the overall process required two electrons, the required current was determined by the formula:

$$I\,(current) = n \times F \times c \times Q = 80\,mA$$

where *n* is the number of electrons per molecule (2 electrons), *F* is the Faraday constant (96485 C/mol), *c* is the concentration (mol/mL) and *Q* is the flow (mL/min). So a current of 80 mA was needed.

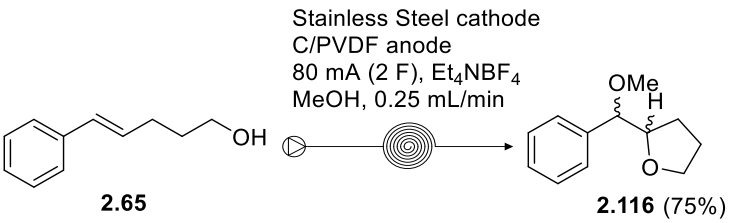

Scheme 2.28: First attempt of oxidative cyclisation of **2.65** in the Ammonite flow reactor.

During the electrolysis the formation of bubbles was observed, due to the hydrogen gas produced at the counter electrode. The cell contact voltage was between 2.9 and 3.0 V. Once the reaction was finished the solvent was evaporated and the crude dissolved in EtOAc, resulting in precipitation of the supporting electrolyte, which was then filtered off and recovered. From ^{1}H-NMR analysis of the crude no starting material remained and a major product **2.116** could be seen in the crude mixture. By HSQC NMR spectroscopy and GC-MS analysis the product was identified as the desired THF diastereoisomers **2.116**, rather than the six-member ring isomer. By GC-MS analysis, the main fragment ion peak was observed at *m/z* 121, that derived from a five-member structure and not a six-member one (Figure 2.3).

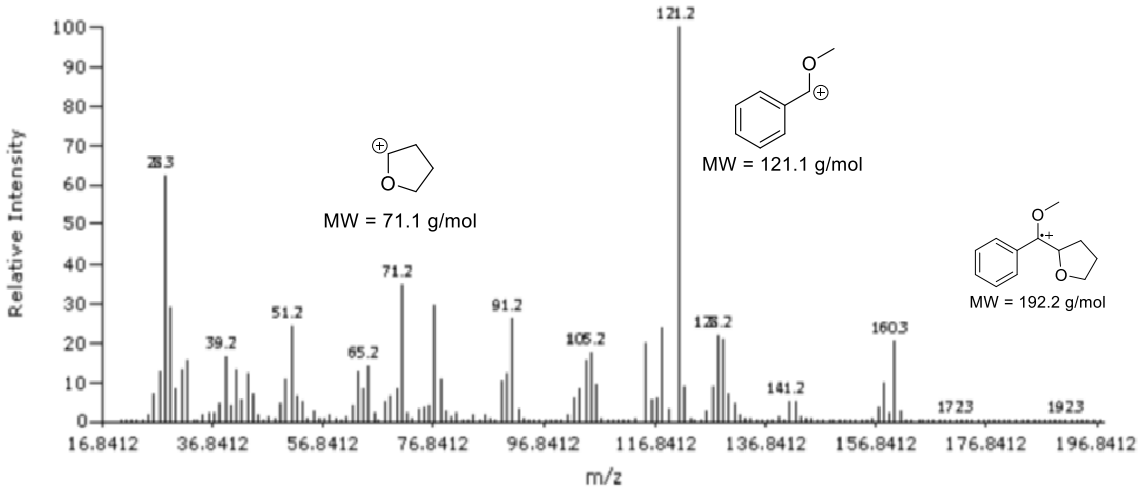

Figure 2. 3: GC-EIMS of compound **2.93** showing fragment ions

Purification afforded the desired product **2.116** as a mixture of diastereoisomers with a 75% yield. From integration of the ^{1}HNMR spectrum an 80/20 diastereoisomeric ratio favouring the *erythro* isomer was determined. The assignment of the signals for the *erythro* and *threo* isomers was based on several studies reported on substituted THFs, in particular THF-acetogenins derivatives. These studies rely on empirical rules based on ^{1}HNMR chemical shifts and comparison with

compounds of known relative stereochemistry, based on which in this case the proton on the carbon bearing the OMe group is generally more shielded in the *erythro* isomer than in the threo.[169–176] The 80/20 isomeric ratio was confirmed by chiral HPLC (Figure 2.4).

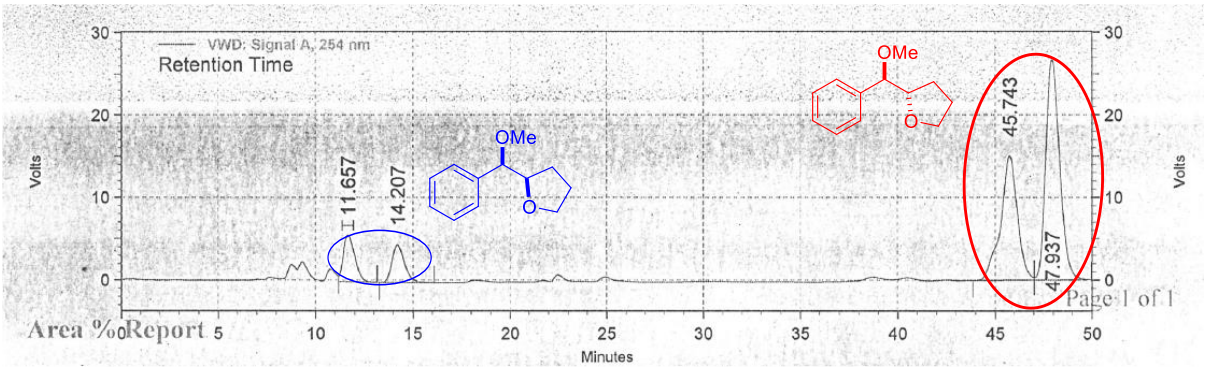

Figure 2. 4: Chiral HPLC chromatogram of compound **2.116**. (AD-H column, 0.5 mL/min, IPA/hexane 0% to 2.5% over 50 min, UV detector (254 nm)

Alkenoic acid **2.81** was subjected to the same electrolysis conditions (cell voltage registered 2.9 V) giving the lactone **2.85** with a 78% isolated yield as an 80/20 diastereoisomeric mixture favouring the *erythro* isomer (Scheme 2.29). The spectroscopic data for lactone **2.85** matched the ones reported by Moeller and co-workers.[177]

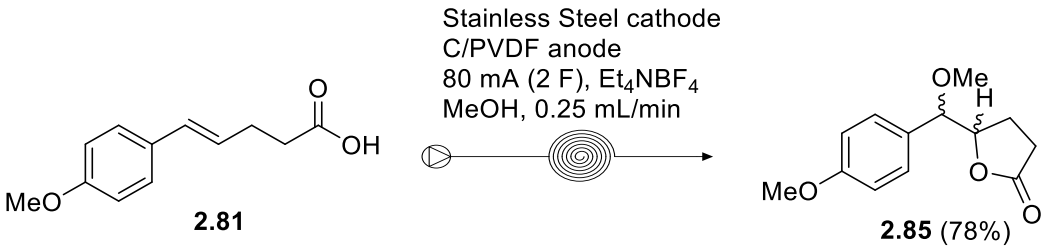

Scheme 2.29: Oxidative cyclisation of alkenoic acid **2.81** in the Ammonite flow reactor.

2.7 Optimisation of the electrolysis conditions

With the promising preliminary results, and before going on testing new substrates, optimisation of the flow electrolysis conditions was undertaken on compounds **2.65** and **2.81**, evaluating different electrodes materials, supporting electrolytes, temperature, solvents and concentration. At first, to check the yield of the different experiments, an internal standard (dimethyl terephthalate) in the ^{1}HNMR was used. Unfortunately, this method proved to be not sufficiently accurate, so a GC method has been developed for both THF **2.116** and lactone **2.85** products (figures 2.5 and 2.6). Further details concerning the development of the GC analytical method are given in the experimental section.

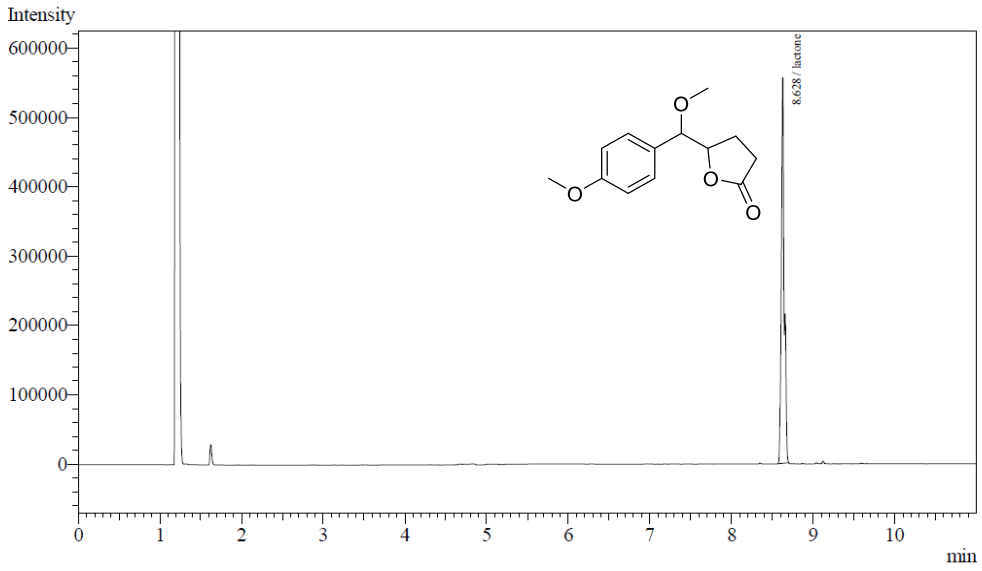

Figure 2. 5: GC chromatogram of 5-(methoxy(4-methoxyphenyl)methyl)dihydrofuran-2-3*H*-one **2.116** (retention time 8.63 min).

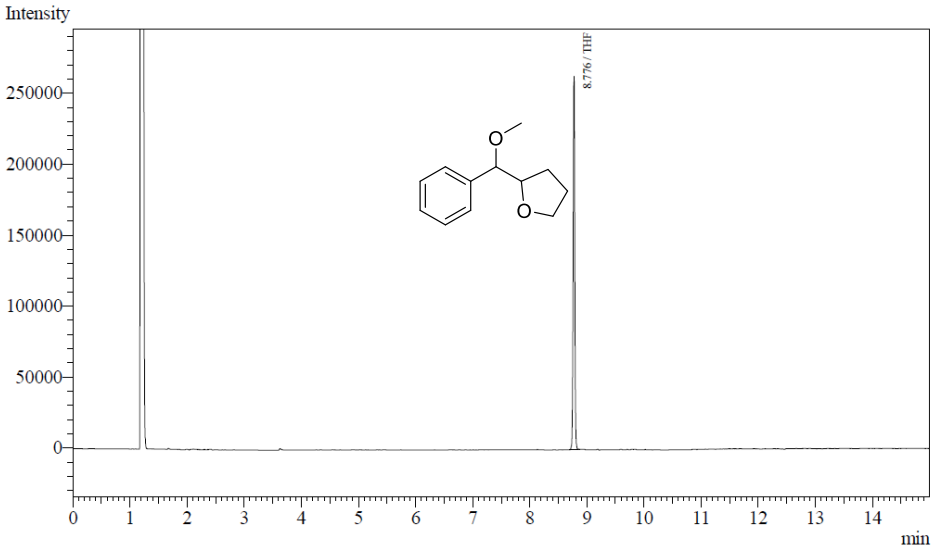

Figure 2. 6: GC chromatogram of 2-(methoxy(phenyl)methyl)tetrahydrofuran **2.85** (retention time 8.78 min).

The first parameter screened has been the anode material. The different anodes tested are shown in Figure 2.7.

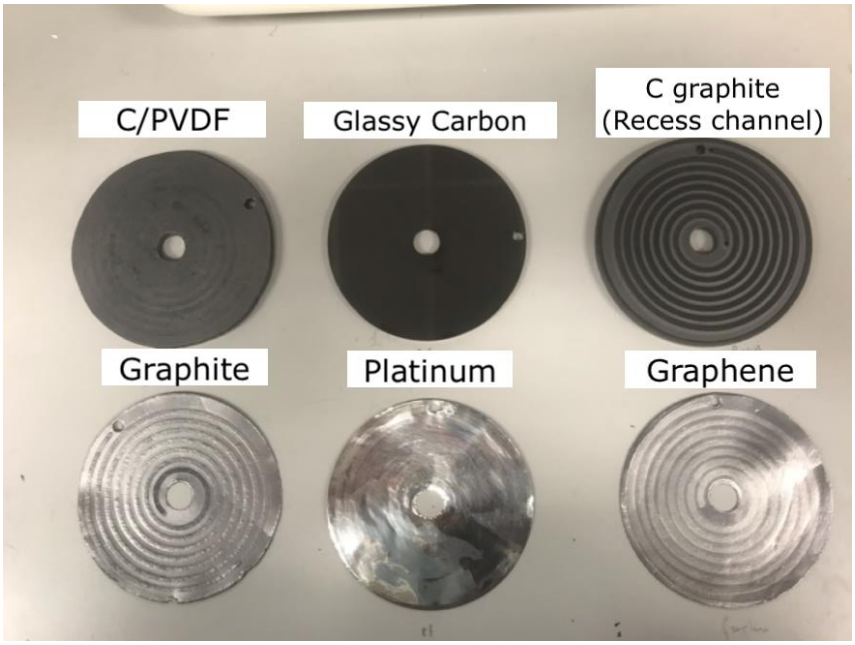

Figure 2.7: different anode materials screened in the oxidative cyclisation.

Platinum was the first anode screened; compared to C/PVF, full conversion of alkenol **2.65** and alkenoic acid **2.81** was achieved only when 2.5 times the stoichiometric current (200 mA) was applied (Table 2.2, entry 5). In addition, the yields for both THF **2.116** (44%) and lactone **2.85** (28%) inferior to those obtained with the C/PVDF anode. The very large amount of bubbles observed at the outlet of the reactor suggested that under these conditions the oxidation of the solvent (MeOH) was competing with the substrate oxidation. Other anode materials tested were Glassy carbon, Graphene and Graphite (entries 6-8), and in all cases, oxidative cyclisations to **2.116** and **2.85** gave lower yields compared to C/PVDF (Table 2.2).

Table 2. 2: Investigation of different anode materials

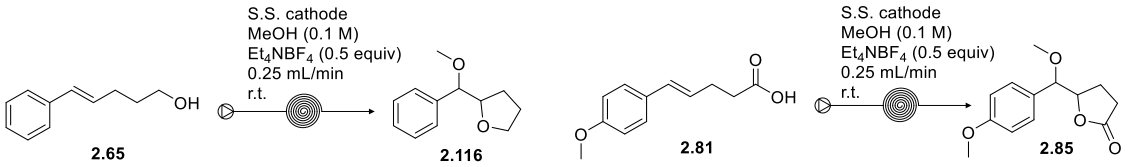

entry	Current (mA), [charge (F)]	anode	Yield 2.116 (%)[a,b]	Yield 2.85 (%)[a,b]
1	80 [2.0]	C/PVDF	68 (75 isolated)	76 (78 isolated)
2	80 [2.0]	Pt	8	12
3	120 [3.0]	Pt	18	38
4	160 [4.0]	Pt	27	33
5	200 [5.0]	Pt	44	28
6	80 [2.0]	glassy carbon	32	15
7	80 [2.0]	Graphene[c]	56	48
8	80 [2.0]	graphite	39	29

[a] Reactions performed on a scale of 0.5 mmol (substrate conc. 0.1 M). [b] Estimated using a calibrated GC. Stainless steel as cathode flow rate 0.25 mL min^{-1}, Et_4NBF_4 (0.5 equiv), rt, MeOH (0.1 M). [c] Sheet of graphene on a paper support.

Different cathode materials were also investigated including (figure 2.8). Platinum was the first cathode screened because this was the material used by Moeller and co-workers in their work,[152] then leaded bronze, copper, nickel and silver were tested but none of them improved the result obtained using a stainless steel cathode for either **2.116** and **2.85** (Table 2.3). Due to the construction of the Ammonite flow cell, one of the electrodes has a recess channel into which the gasket is located. This design feature means that one of the electrodes has to have the recess channel, and because some electrodes are only available as flat plates, not all combinations are possible. Apart from the copper where C/PVDF was used as anode, for the other trials, carbon graphite has been used because of its recess channel, in order to have a channel in the cell where the solution could pass. (Table 2.3).

Figure 2.8: different cathode materials screened.

Table 2.3: Investigation of different cathode materials.

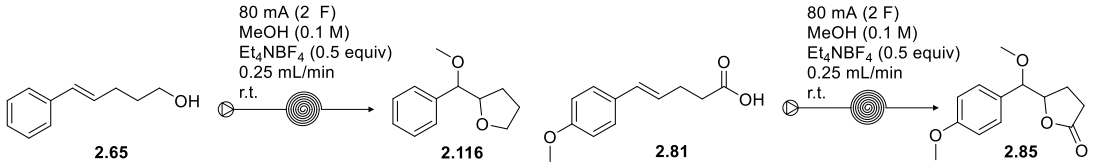

entry	cathode	anode	Yield 2.116 (%)[a,b]	Yield 2.85 (%)[a,b]
1	Pt	C graphite[c]	17	29
2	leaded bronze	C graphite[c]	8	27
3	Cu[d]	C/PVDF	35	29
4	Ni	C graphite[c]	3	47
5	Ag	C graphite[c]	40	31
6	S.S.	C/PVDF	68	76

[a] Reactions performed on a scale of 0.5 mmol (substrate conc. 0.1 M). [b] Estimated using a calibrated GC. [c] C graphite electrode with recess channel was employed. [d] Cu electrode with recess channel used.

Once confirmed that C/PVDF and stainless steel provide a suitable electrode combination for the oxidative cyclisation process, other reaction parameters were investigated, starting with the supporting electrolytes. All of them gave similar results, while in absence of electrolyte the reaction gave very low yield. Actually using Bu_4NBF_4 resulted in slightly better yields (Table 2.4, entry 2) compared to Et_4NBF_4 but we decided to stick with the Et_4NBF_4 as it can be easily recovered from the crude mixture by precipitation in EtOAc and the actual improvement in the

yield was not that big. Once decided to stick with Et_4NBF_4 as supporting electrolyte, considering the cost of it, its amount was reduced to 0.25 equivalents (entry 6) without a significant effect on the yield of the reaction. After the supporting electrolyte, another parameter checked was the concentration of the starting material; increasing the concentration in methanol from 0.1 M to 0.2 M (entry 7) did not affect the yield of **2.93**, while for lactone **2.85** a worst result, compared to the starting conditions (entry 1) was observed because of a problem of solubility of the starting material. The other parameter checked was the flow (entry 8): increasing it from 0.25 mL/min to 0.5 mL/min gave lower yields. The last parameter checked was temperature; for both alcohol **2.65** and carboxylic acid **2.81** the reaction has been run at 0° C and 50° C. Varying the temperature did not seem to heavily affect the results for the alcohol oxidative cyclization while for the cyclization of carboxylic acid **2.81** a massive drop in the yield was observed (entry 9 and 10).

Table 2.4: Investigation of flow rate, concentration, temperature, supporting electrolyte.

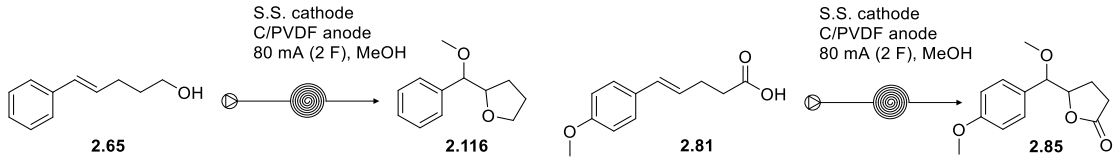

entry	Temp (° C)	flow rate (mL min^{-1})	Supporting electrolyte	Yield 2.116 (%)[a,b]	Yield 2.85 (%)[a,b]
1	rt	0.25	Et_4NBF_4 (0.5 equiv)	68 (75 isolated)	76 (78 isolated)
2	rt	0.25	Bu_4NBF_4 (0.5 equiv)	71	83
3	rt	0.25	Et_4NO*p*Ts (0.5 equiv)	69	78
4	rt	0.25	$NaClO_4$ (0.5 equiv)	66	81
5	rt	0.25	no electrolyte	17	29
6	rt	0.25	Et_4NBF_4 (0.25 equiv)	66	77
7[c]	rt	0.25	Et_4NBF_4 (0.25 equiv)	68	65
8	rt	0.50	Et_4NBF_4 (0.5 equiv)	51	55
9	50	0.25	Et_4NBF_4 (0.5 equiv)	58	38
10	0	0.25	Et_4NBF_4 (0.5 equiv)	59	18

[a] Reactions performed on a scale of 0.5 mmol (substrate conc. 0.1 M). [b] Estimated using a calibrated GC. [c] 0.2 M solution of starting material in MeOH.

At the end of this reaction parameter screening process, we observed that the best results were the ones obtained using Stainless steel as cathode, C/PVDF as anode, a flow of 0.25 mL/min, a 0.1 M concentration of starting material in methanol, the stoichiometric amount of current (80 mA,

2.0 F), room temperature and Et_4NBF_4 as supporting electrolyte (table 2.4 entries 1 and 6), whose amount we decided to reduce from 0.5 equivalents (entry 1) to 0.25 equivalents (entry 6).

2.8 Substrate scope

With the optimised conditions in hand, the substrate scope was investigated under the same conditions. As previously stated, for the synthesis of the starting carboxylic acids we relied on the protocol reported by Moeller and co-workers;[152] so starting from the commercially available phosphonium salt **2.102**, by Wittig reaction with a set of aldehydes, different carboxylic acids were synthesised and then subjected to the optimised electrolysis conditions. The carboxylic acids were reduced with $LiAlH_4$ to their corresponding alcohols in almost quantitative yield,[178] and the resulting alkenols were also subjected to the electrochemical oxidative cyclisation (Scheme 2.30).

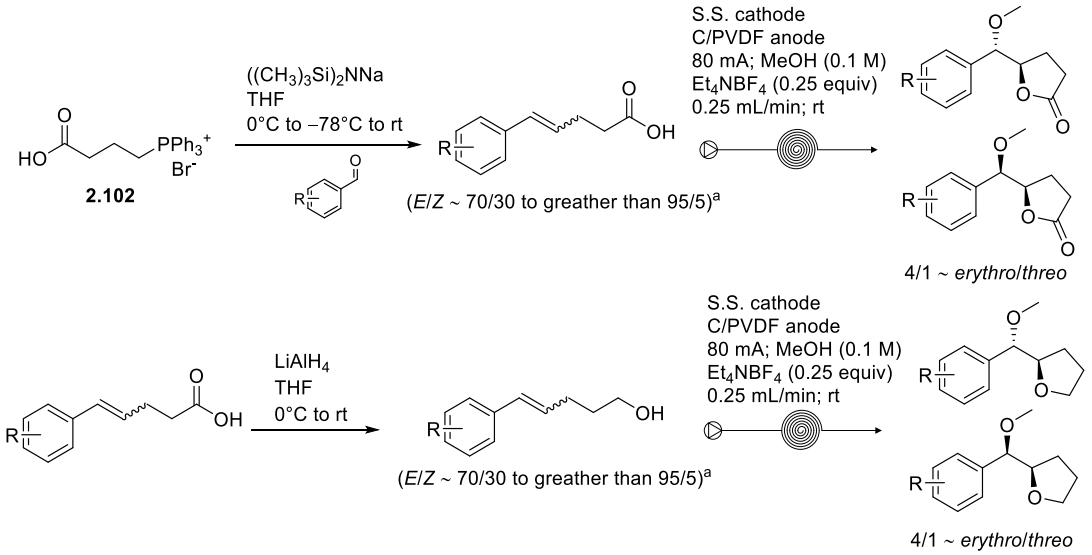

Scheme 2.30: Synthesis of substituted THFs and lactones through electrochemical flow oxidative cyclisation.[a]For ratios of alkenes isomers see experimental section.

All yields of cyclised products are for isolated pure compounds obtained from a range of carboxylic acids and alcohols (Figure 2.9). Good to moderate isolated yields were achieved and all the target compounds were obtained as approximately 4/1 (^{1}H NMR) *erythro*/*threo* diastereoisomeric mixtures.

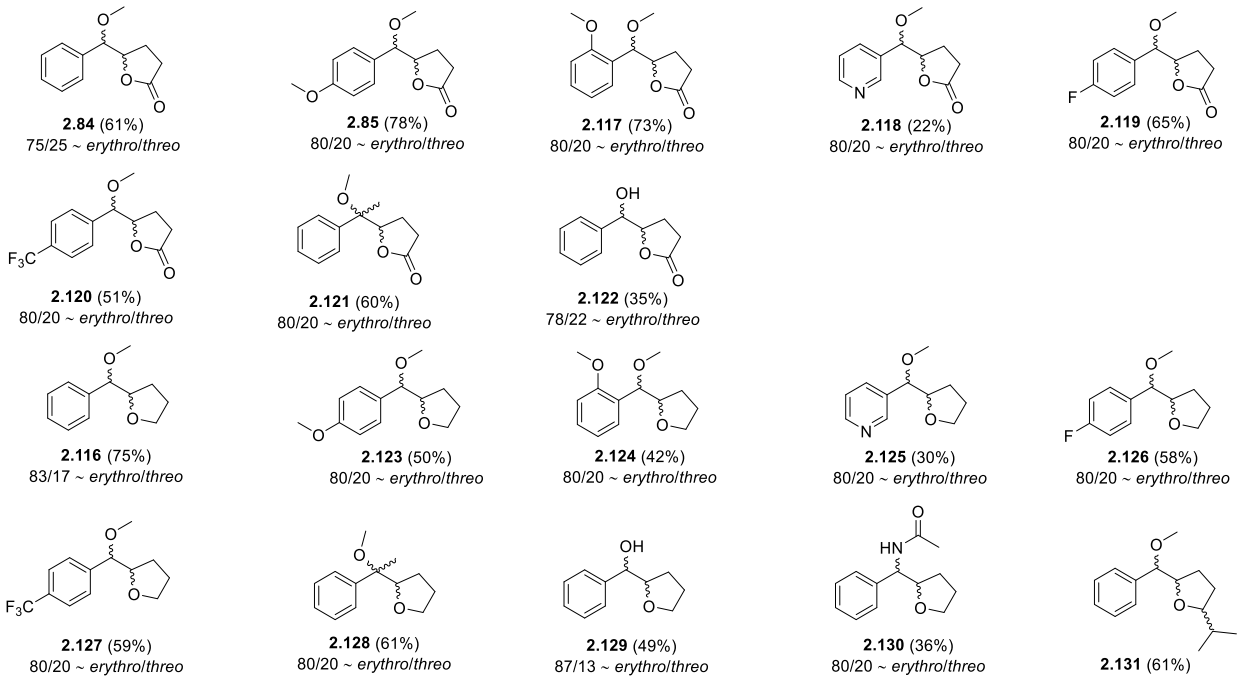

Figure 2.9: Substrate scope.

We were delighted to observe γ-lactone **2.84** in a decent 61% yield, as a 4:1 mixture of diastereoisomers *erythro*:*threo* (by ^{1}H-NMR) (scheme 2.31a), while Moeller and co-workers reported a modest 33% yield using an excess of charge and elevated temperature (scheme 31b).[152] Carboxylic acid **2.81** containing an electron-releasing group at the 4-position gave the desired γ-lactone **2.85** with a higher 78% yield, again as 4:1 *erythro*:*threo* mixture (scheme 2.31a). Moeller and co-workers reported a similar yield (76%) for the same substrate (scheme 2.31b), reinforcing the hypothesis that the presence of electron-donating group on the aromatic system is capable of stabilising the benzylic carbocation intermediate, and that this is important for efficient anodic cyclisation. It should also be noted that Moeller's electrolysis was performed with a 0.03 M solution of carboxylic acid, at 40° C, using 3.3 equivalents of supporting electrolyte and in the case of carboxylic acid **2.80** using and excess of current, while the method we developed was applied on a more concentrated solution of starting material (0.1 M), was performed at room temperature, required only 0.25 equivalents of supporting electrolytes and for all the substrates, included carboxylic acids **2.80** and **2.81**, only the stoichiometric amount of current (2.0 F) was needed to achieve full conversion.

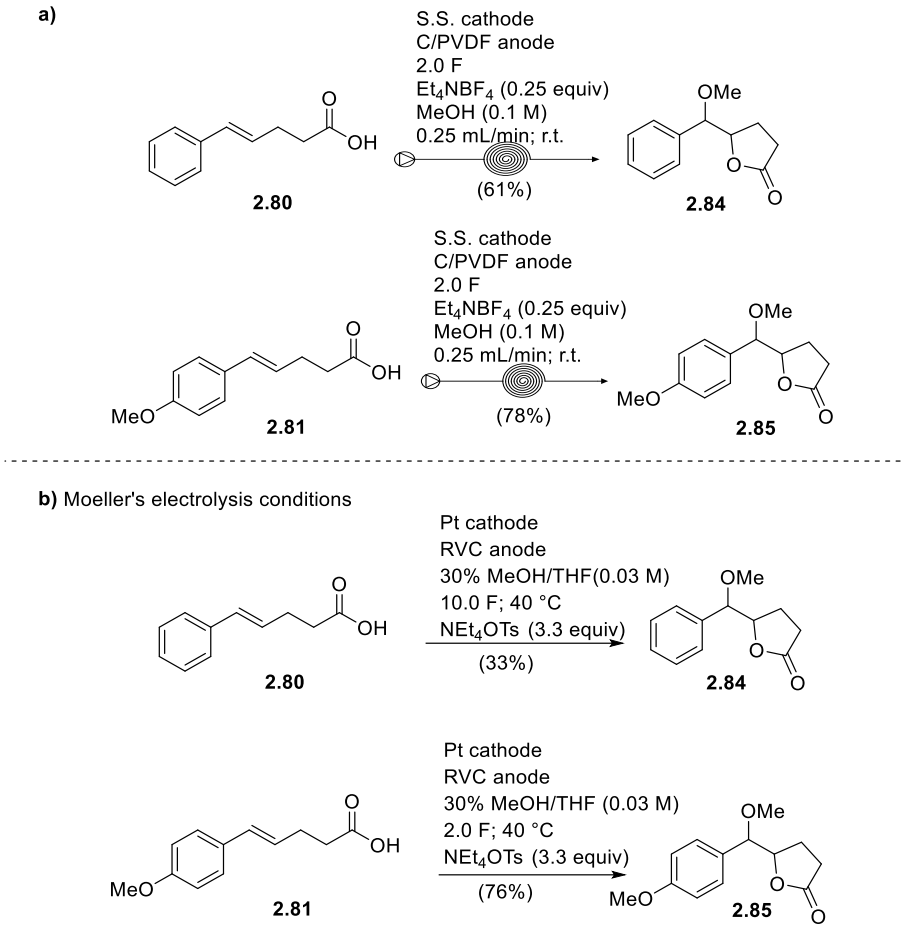

Scheme 2.31: a) Flow electrochemical oxidative cyclisation of acid **2.80** and alcohol **2.81** (this work); b) Moeller's batch oxidative cyclisation of **2.80** and **2.81**.

By contrast, oxidative cyclisation of the alcohols bearing methoxy groups at 2-, or 4-positions afforded THFs **2.123** and **2.124** in reduced yields (50% and 42%, respectively). The presence of the —OMe group on the aromatic ring would stabilise the carbocation intermediate, leading to the anticipation of a higher yield of the THFs. However, it is believed that the lower yields were due to over-oxidation of the product. [More details on this over-oxidation reaction are reported later in the CV study section]. In the case of the lactone, the stronger electron-withdrawing O—COR group may help to supress the over-oxidation of the product.

An advantage of the developed flow conditions is that it is also possible to oxidatively cyclise substrates bearing an electron-withdrawing groups on the aromatic ring. Lactones **2.119**, **2.120** and THFs **2.126** and **2.127** were obtained with yields of 65%, 51%, 58% and 59% respectively. Moreover, products **2.118** and **2.125** with a pyridine ring instead of a benzene ring were synthesised with a 22% and 30% yield without full conversion; in order to achieve full conversion, a 2.5 fold excess of current was needed, but the desired products were obtained with yields lower than 10% due to degradation. The oxidative cyclisation proved to work even for substrates with a substituent on the double bond and on the alkyl chain; THFs **2.128** and **2.131** were both obtained with a 61% yield and lactone **2.121** with 60%. Using water instead of methanol as solvent, gave

hydroxyalkyl THF **2.129** with a 49% yield. In this case, to ensure solubility of the substrate a 1/1 mixture of water and acetonitrile was used, resulting in simultaneous formation of the Ritter reaction product **2.130** in 36% yield (Scheme 2.32).

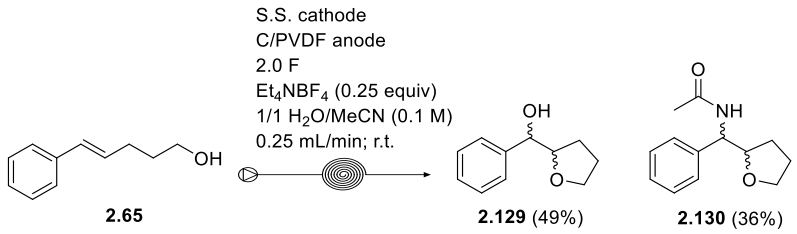

Scheme 2.32: flow electrochemical oxidative cyclisation using water as nucleophile and Ritter side-reaction.

While working on the substrate scope, oxidative cyclisation of alcohol **2.111** containing a 1-substituted styrene was investigated (Scheme 2.33).

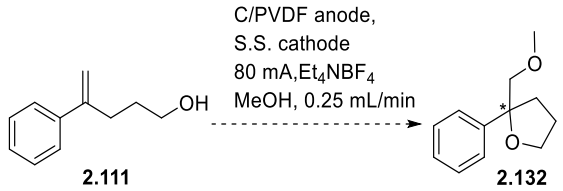

Scheme 2.33: flow electrochemical oxidative cyclisation of **2.111.**

The strategy adopted for the synthesis of compound **2.111** aimed to prepare the styrene starting from γ-butyrolactone **2.134** via the hydroxyketone **2.133** (Scheme 2.34).

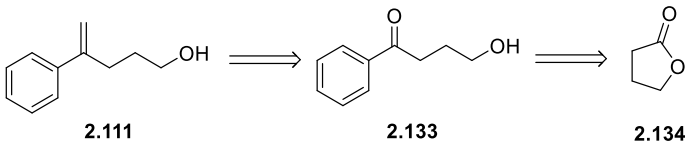

Scheme 2.34: Retrosynthetic approach for alkenol **2.111.**

The first attempt to prepare hydroxyketone **2.133** was by Friedel-Crafts reaction from benzene. Adapting a procedure reported by Feng and co-workers,[179] γ-butyrolactone **2.134** was first reacted with SO_2Cl_2 and then with benzene in the presence of $AlCl_3$. The reaction did not work; both the ^{1}H-NMR and TLC revealed a complex mixture of different products (Scheme 2.35).

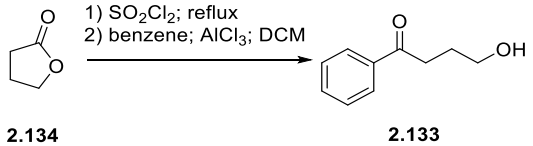

Scheme 2.35: Attempted synthesis of hydroxyketone **2.133** *via* Friedel-Crafts reaction.

A five step synthesis for compound **2.111** was then developed; it was a substantially longer route, but one that could be applied on a larger scale compared to the one previously described. Following a procedure reported in literature[180] amide **2.135** was easily obtained by reaction of γ-butyrolactone with morpholine in the presence of trimethylamine. Before conversion of the amide **2.135** to ketone **2.136** by reaction with phenyl magnesium bromide,[181] it was necessary to protect the hydroxyl group by formation of the tetrahydropyranyl acetal.[181] Ketone **2.136** was then converted to alkene by an unoptimized, low-yielding (30%) Wittig reaction[182] and finally the deprotection of the hydroxyl functionality gave the desired product **2.111** (Scheme 2.36).[181]

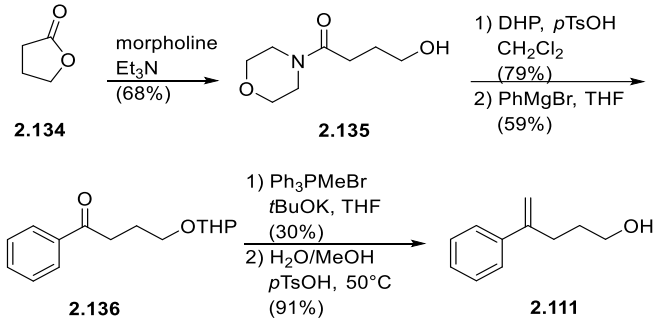

2.134 2.135 2.136 2.111

Scheme 2.36: Synthetic route to alkenol **2.111**.

With compound **2.111** in hand, the cyclization step was performed in the electro-flow reactor (Scheme 2.37).

2.111 2.132

Scheme 2.37: Attempt of flow electrochemical oxidative cyclisation of **2.111**.

The reaction was tested with the previously described conditions. Upon electrolysis in MeOH a lot of bubbles were observed and a minimum voltage of 3.2-3.3 V were registered. After the work-up, by ^{1}H-NMR the detection of the desired product **2.132** was difficult; but by GC-MS, the main peak with a retention time of 7.3 min showed an ion of (*m/z* = 192.2) corresponding to that of the methoxy THF **2.132**, with fragmentation (115 $[C_6H_{11}O_2]^{+}$, 77 $[C_6H_5]^{\cdot+}$) also consistent with the expected product. However, TLC analysis showed a multi-component mixture with little or no separation. Attempted, careful column chromatography, did not allow the desired product to be isolated. The number of different products and degradation observed in this reaction can be rationalised by considering the proposed mechanism, where, after the first oxidation an unstable

primary alkyl radical would be generated following 5-exo cyclisation (Scheme 2.38). Further oxidation would give rise to an unstable primary carbocation. Therefore, in this case, other pathways may compete, leading to the complex mixture observed. These could include 6-endo cyclisation, intermolecular reactions with MeOH and so on.

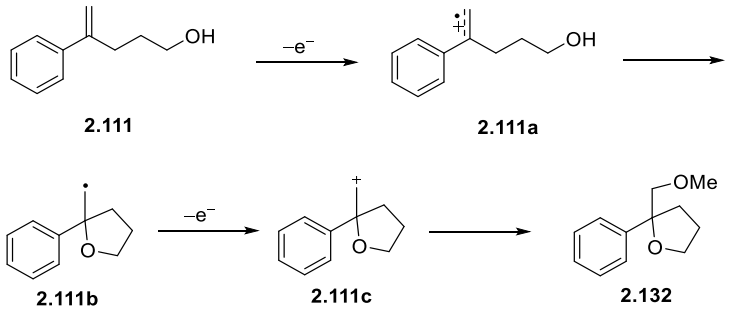

Scheme 2.38: Possible mechanism for the oxidation of hydroxystyrene **2.111**.

2.9 Mechanistic studies

During the flow electrolysis experiment, three phases can be identified: 1) when the voltage drops down from the maximum value to the lowest as the substrate enters the cell and current starts to pass, increasing from 0 mA to the set value (80 mA); 2) the steady state, when the cell is flooded with the substrate solution and the current has stabilised at the set value and the voltage remains constant; 3) when the voltage starts to increase again while the current drops down as the plug of reaction solution exits the cell. To probe the efficiency of the electrolysis at these different points, the cyclization of phenyl substituted alkenol **2.65** was performed under the optimised conditions and three fractions were collected in order to examine the reaction profile with time. As shown in Figure 11, the ^{1}HNMR spectra of the three fractions look similar, indicating that the reaction profile is fairly uniform. This validates the approach where the entire reaction sample is collected, rather than discarding the first and/or the last portion of the reaction solution (Figure 2.10).

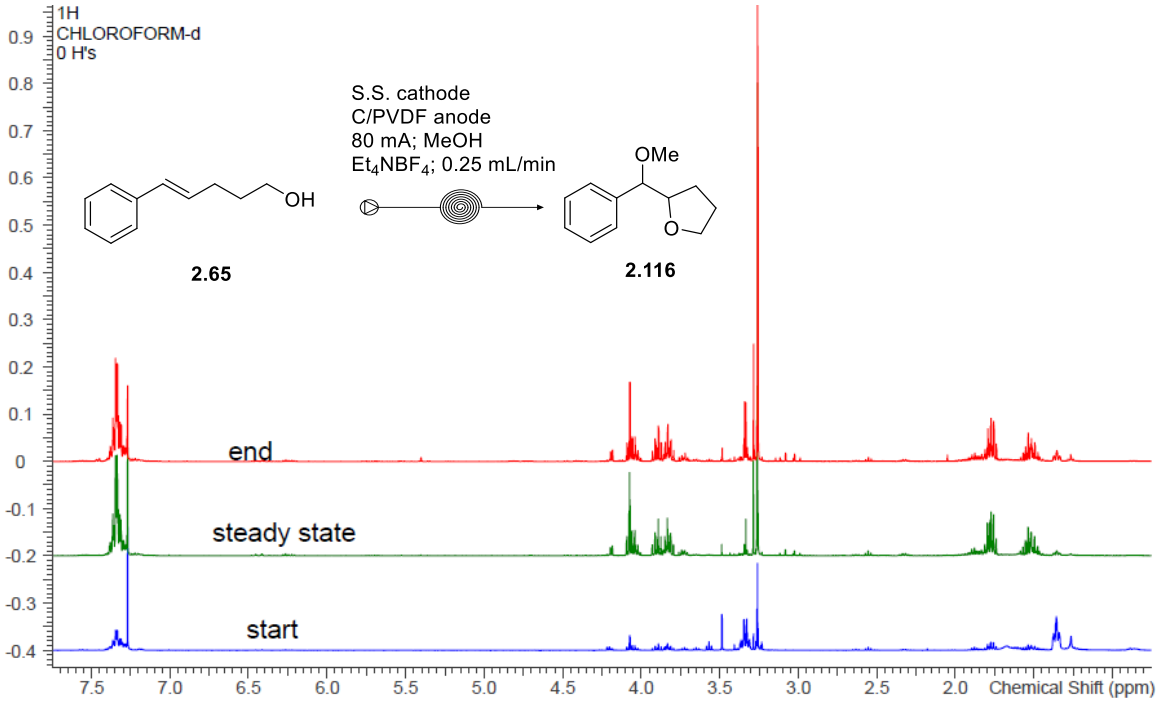

Figure 2. 10: [1]HNMR spectra taken from samples collected at three different stages of the flow electrolysis experiment.

It is believed that the anodic cyclisation proceeds *via* a two electron oxidation. The first anodic electron-transfer step leads to the formation of a radical cation that is rapidly trapped by the hydroxyl (or carboxyl) group. A second electron is abstracted, with generation of a benzylic carbocation that is trapped by a nucleophile, which is the solvent in this example (Scheme 2.39).

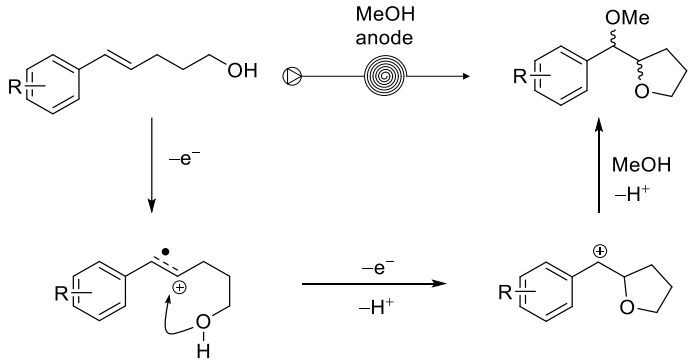

Scheme 2.39: Proposed mechanism of the oxidative cyclisation.

The proposed mechanism for this type of reaction has already been well documented.[31,60,146,147,152,183] Moeller and co-workers, as previously stated in introduction to this thesis, worked extensively on anodic cyclisation reactions towards efficient methods for the synthesis of different ring systems. The electrochemical approach allows the conversion of electron-rich olefins into radical cations that can react with nucleophiles, whilst they would normally serve as nucleophiles themselves (Scheme 2.40), giving rise to a reversal of "classical" reactivity akin to "Umpolung" of the carbonyl group.

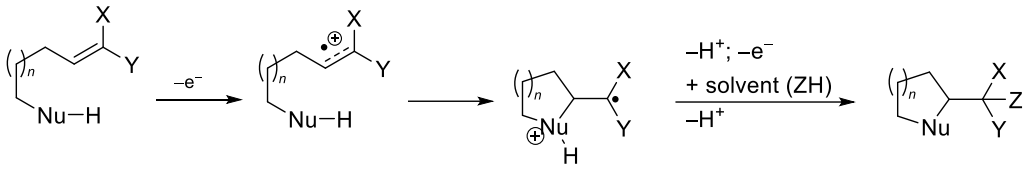

Scheme 2.40: Proposed general mechanism of the oxidative cyclisation of electron-rich alkenes reported by Moeller and co-workers.

2.10 Cyclic voltammetry

In order to explain the results of the substrate scope previously described and have a better understanding of the behaviour of the different substrates during the electrolysis we undertook some cyclic voltammetry experiments. We decided to analyse four substrates: alkenol **2.65** and its corresponding carboxylic acid **2.80**, carboxylic acid **2.81** bearing an electron-donating group on the aromatic ring and and alkenol **2.135** bearing an electron-withdrawing group on the aromatic ring (Scheme 2.41).

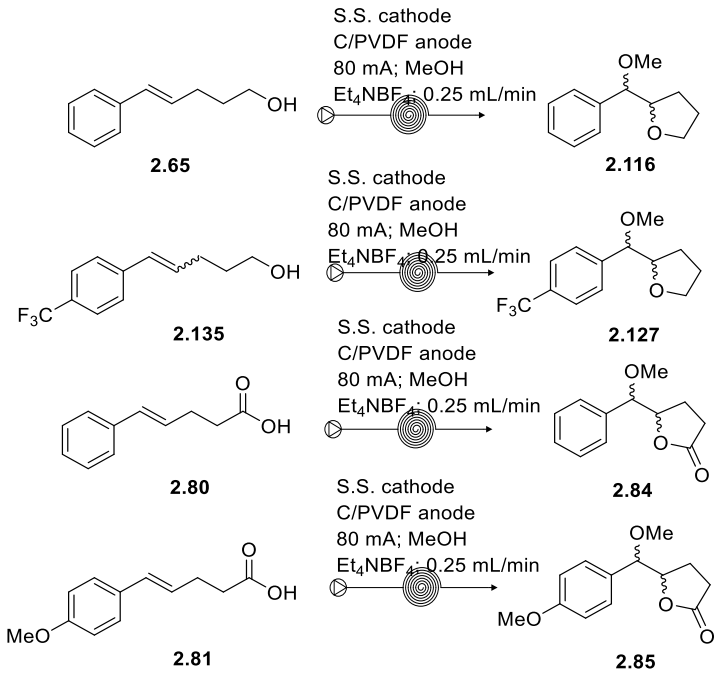

Scheme 2.41: Electrolysis reactions analysed by CV.

Cyclic voltammetry (CV) experiments were carried out in a two compartments cell using a vitreous carbon disc (diameter 3 mm) working electrode, a Pt wire counter electrode and an aqueous SCE reference electrode mounted in a Luggin capillary. An Autolab PGStat204 potentiostat with Nova 1.9 software was used and responses were analysed using Nova 1.9 software. All voltammetry run with a 5.0 mM concentration of substrate, using 100 mM supporting electrolyte.

As shown in Figure 2.11, the CV of methoxy-substituted styrene carboxylic acid **2.81** shows a lower oxidation potential (1.16 V) compared to **2.80** (1.39 V), due to the presence of the +M (electron-releasing) group on the aromatic ring, which stabilises the radical cation intermediate. This would be consistent with the observation of a higher yield for the electrolysis substrates bearing and electron-donating group on the aromatic due their oxidation under milder conditions.

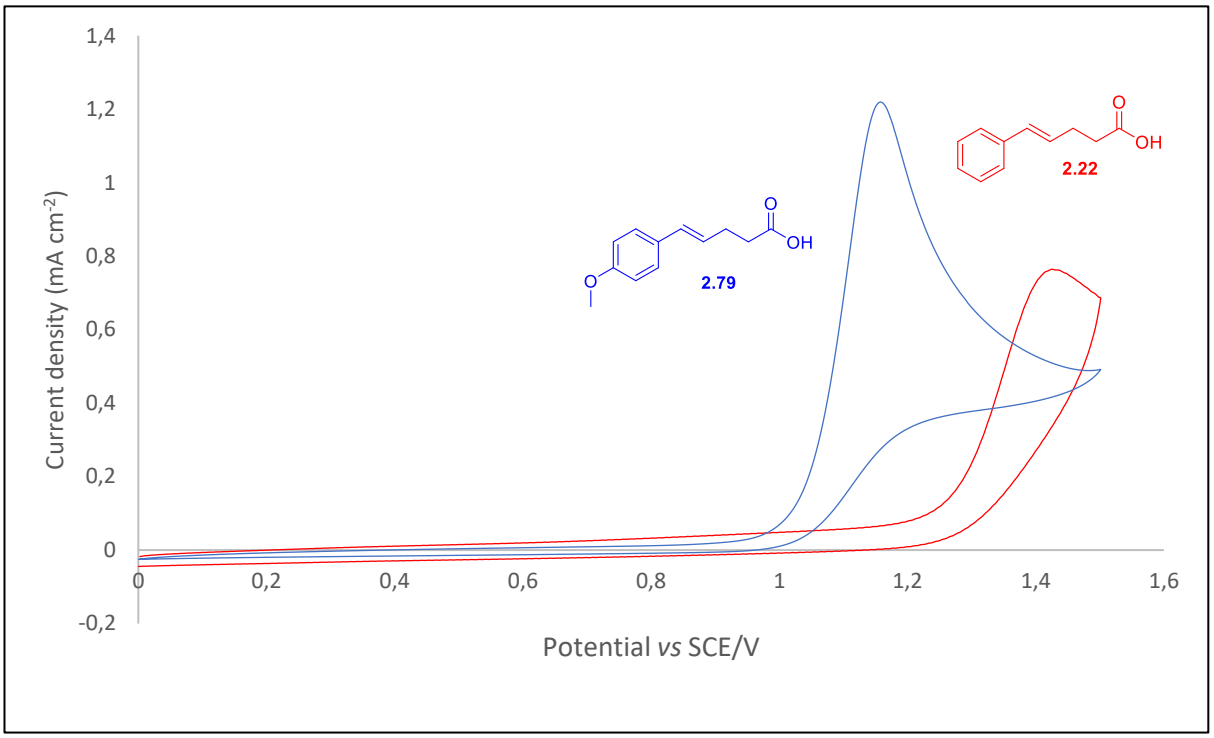

Figure 2. 11: Cyclic voltammogram for carboxylic acid **2.81** and **2.80**; potential scan rate 25 mV s^{-1}; scan range 0 to 1.5 V

From the preparative electrolyses, the 4-methoxyphenyl and 2-methoxyphenyl lactones **2.85** and **2.117** were obtained with good yields of 78% and 73%, respectively. On the other hand, the corresponding THFs **2.123** and **2.1124** were obtained in lower yields of 50% and 42%, respectively. A possible explanation, that the presence of an electron-donating group, the THFs were more liable to over-oxidation with consequent consumption of the THF product.

In order to provide evidence for this proposal, THF **2.123** was passed through the Ammonite 8 reactor under the oxidative cyclisation reaction conditions. Analysis of the outlet solution showed almost full consumption of the starting THF to give *p*-methoxy benzaldehyde and the corresponding dimethyl acetal (Scheme 2.36).

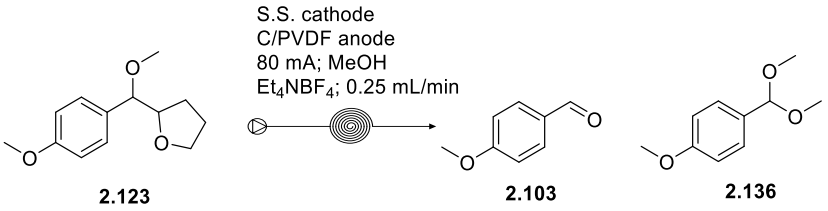

Scheme 2.42: Flow electrochemical oxidation of THF **2.123**. Evidence for over-oxidation of electron-rich styrene derivatives.

Once aware of this outcome, the crude ^{1}HNMR spectra of the reaction mixtures from anodic oxidation of different alcohol substrates were carefully re-checked and in all cases the corresponding dimethyl acetals were observed, except for substrates bearing an electron-withdrawing group (—F; —CF_3). Dimethyl acetals were most prominent in the crude ^{1}H-NMR spectra of 4-methoxyphenyl and 2-methoxyphenyl THFs **2.123** and **2.124,** but traces were also evident in the spectra of lactones **2.85**, **2.117**, **2.84** and THF **2.116**. Probably the presence of the carbonyl group for lactones **2.85** and **2.117** makes the products more electron-poor than their corresponding THFs, with consequent inhibition of the over-oxidation process.

A proposed mechanism for over-oxidation is presented in Scheme 2.43, based on the studies reported by Obigin and co-workers on the investigation of the electrochemical cleavage of benzylic C—C π and σ bonds.[184]

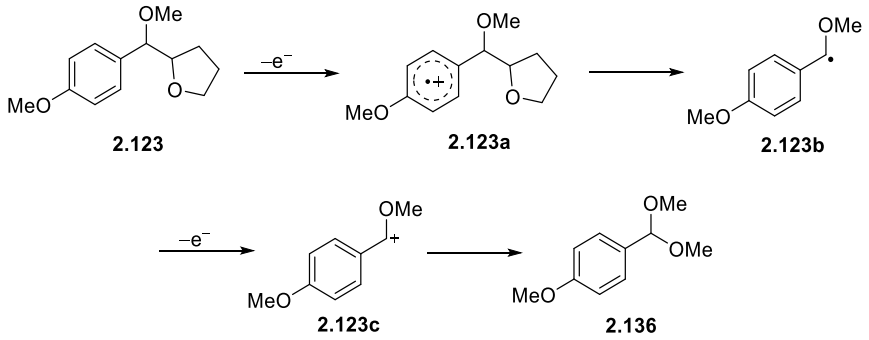

Scheme 2.43: Obigin's proposed mechanism for electrochemical over-oxidation of substrate **2.123**.

Increasing the scan range to 2.2 V for the CV of alkenoic acid **2.81** showed additional two peaks, which could be due to the over-oxidation reaction (Figure 2.12).

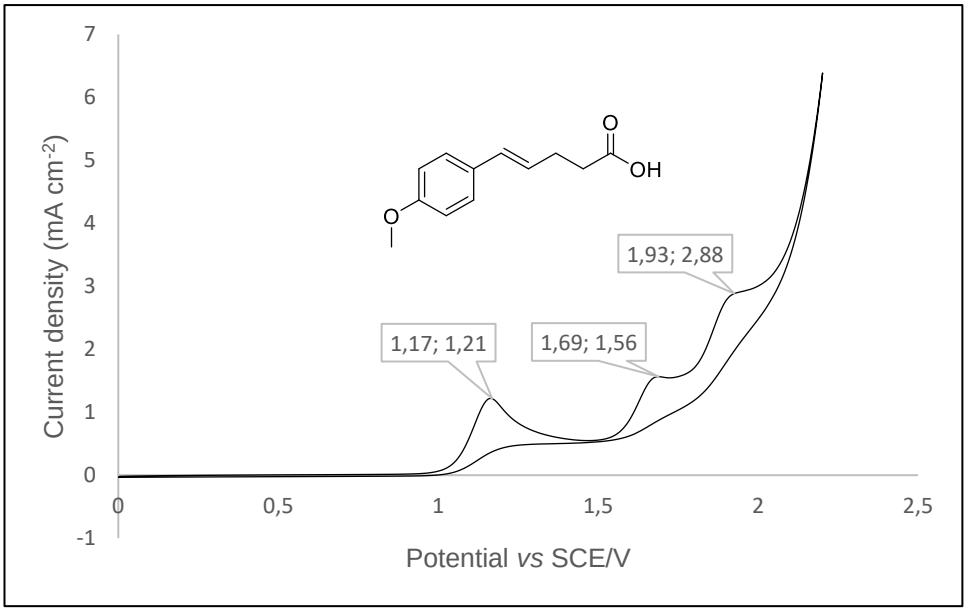

Figure 2. 12: Cyclic voltammogram for carboxylic acid **2.81**; potential scan rate 25 mV s^{-1}; scan range 0 to 2.2 V.

CV experiments have been also run on substrate **2.135** bearing an electron-withdrawing group (—CF_3) on the aromatic ring for comparison with hydroxyalkene **2.65.** As anticipated, a higher oxidation potential was registered for the alcohol with the —CF_3 electron-withdrawing group (1.74 V). This result is consistent with preparative electrolysis experiments where oxidation of alcohol **2.135** containing a CF_3 group on the aryl ring gave a lower yield (59%) of the THF product compared the unsubstituted phenyl derivative **2.65** (75%) (Figure 2.13).

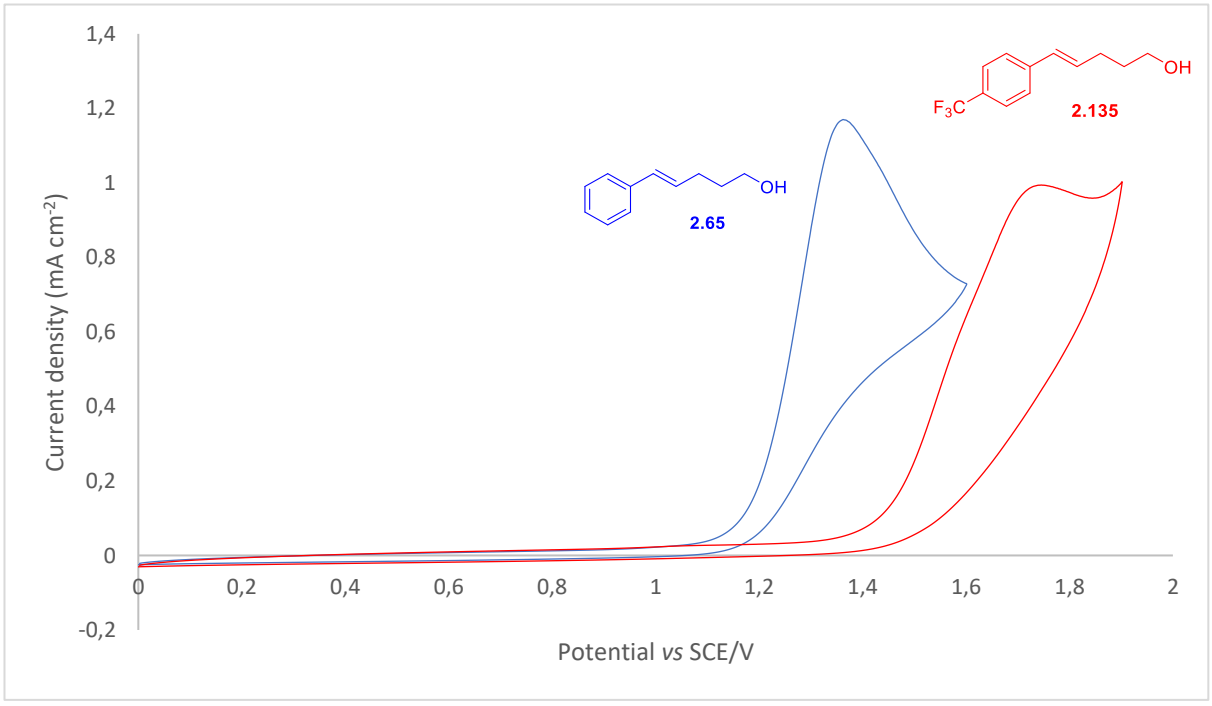

Figure 2. 13: Cyclic voltammograms for alcohols **2.65** and **2.135**; potential scan rate 25 mV s^{-1}; scan range 0 to 1.9 V

After these studies it became clear that, if the substrate is very electron-poor, the anodic cyclisation is challenging due to high oxidation potentials needed to form the radical cation. On the other hand, if the substrate is electron-rich, then the cyclised products are prone to further oxidation. This is most evident for THFs, as the lactone products are less susceptible to over-oxidation.

2.11 Scale-up and batch cell experiment

To explore whether the electrolysis developed in flow translated, we applied the same conditions in a "home-made" beaker-type cell to the synthesis of 2-hydroxybenzyl tetrahydrofuran **2.116** (Figure 2.14).

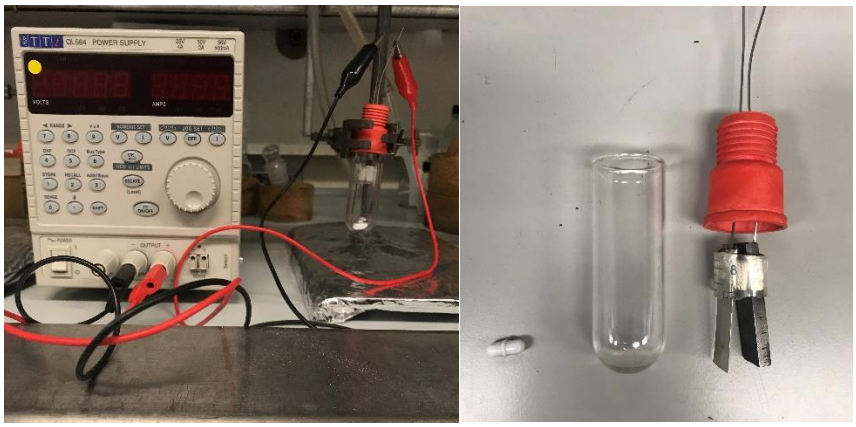

Figure 2.14: Left side: batch cell set-up; Right side: batch cell components: stirring magnet, glass vessel, stainless steel cathode and C/PVDF anode.

[Full details on the set-up of the experiment and its conditions are described in the experimental chapter]. Based on the same current density used for the reaction in the Ammonite cell, a current of 7.2 mA has been applied for 3.72 h in order to achieve full conversion of alkenol **2.65**, giving the desired THF **2.116** with a calibrated GC yield of 49%. Extension of the flow conditions to batch was demonstrated, albeit with lower performance compared to the flow approach (Scheme 2.44). A less clean reaction profile was evident from ^{1}H NMR analysis of the crude reaction mixture from the batch electrolysis, suggesting that the extended time needed in batch led to increased degradation with consequent impact on yield. However, it is important to recognise that no optimisation of the batch conditions have been carried out here.

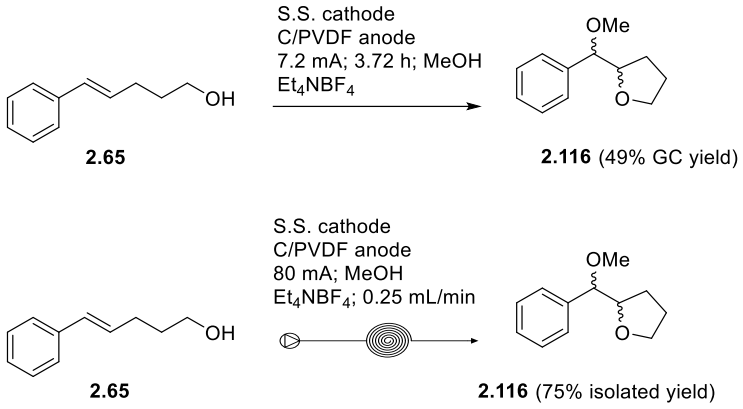

Scheme 2.44: Comparison between the batch and the flow approach for the oxidative cyclisation of alkenol **2.65**.

Another potential advantage of the flow approach is the ease of scale-up by simply running the flow electrolysis for an extended time. Under the conditions already developed, 7.4 mmol (1.2 grams) of phenylpentenol **2.65** was fully converted in 5 hours, in a single pass of the flow reactor, giving the desired product **2.116** with an isolated yield of 79% (Scheme 2.45). Thus, gram-scale amounts of oxidative cyclisation products are accessible using the same reactor and conditions within a reasonable period of time.

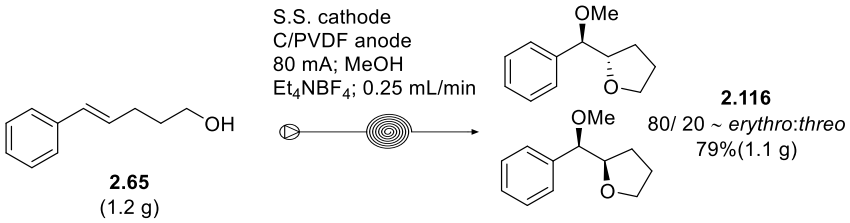

Scheme 2.45: Scale-up of the flow oxidative cyclisation of alkenol **2.65**.

2.12 Spirocycles

Spirocycles consist of two or more rings connected by one common atom. In recent years, synthetic chemistry has worked on developing efficient methods for the synthesis of these scaffolds because of their importance, especially in the field of drug discovery. Spirocycles, including spiroketal motifs, are present in many different natural molecules, and numerous bio-active, pharmaceutical and agrochemical compounds (Figure 2.15).[185–192]

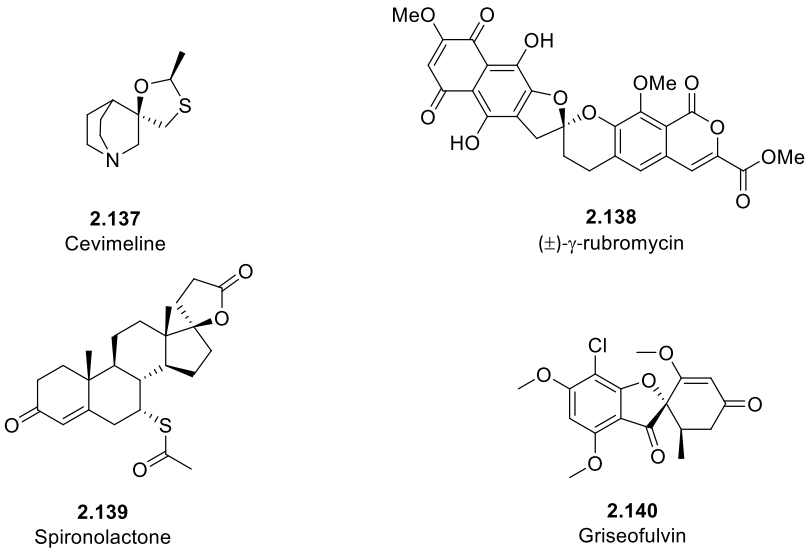

Figure 2.15: Examples of spirocycles in bio-active compounds.

Methods reported for the synthesis of spirocompounds are as diverse as the targets themselves, but common approaches include metal complex catalysis (Pd, Rh, Fe),[185,187,193,194] the use of Brønsted acids,[195] and photochemistry.[190,196,197] Most of the time these methods require the use of expensive and toxic reagents.[186] Therefore, electrochemistry has a potential application for synthesis of spirocyclic compounds as a more sustainable approach.

In 2000, Markó reported an anodic electrolysis method for the synthesis of spiroketals starting from ω-hydroxy-tetrahydropyrans (Scheme 2.46a).[186] More recently, Markó and co-workers reported the application of anodic electrochemistry for the synthesis of the spirocyclic C28-C38 fragment of okadaic acid (Scheme 2.46b);[196] while Opatz and co-workers have been working on the application of electrochemistry, in particular anodic oxidation, in the synthesis of natural products and also spirocycles (Scheme 2.46c).[198]

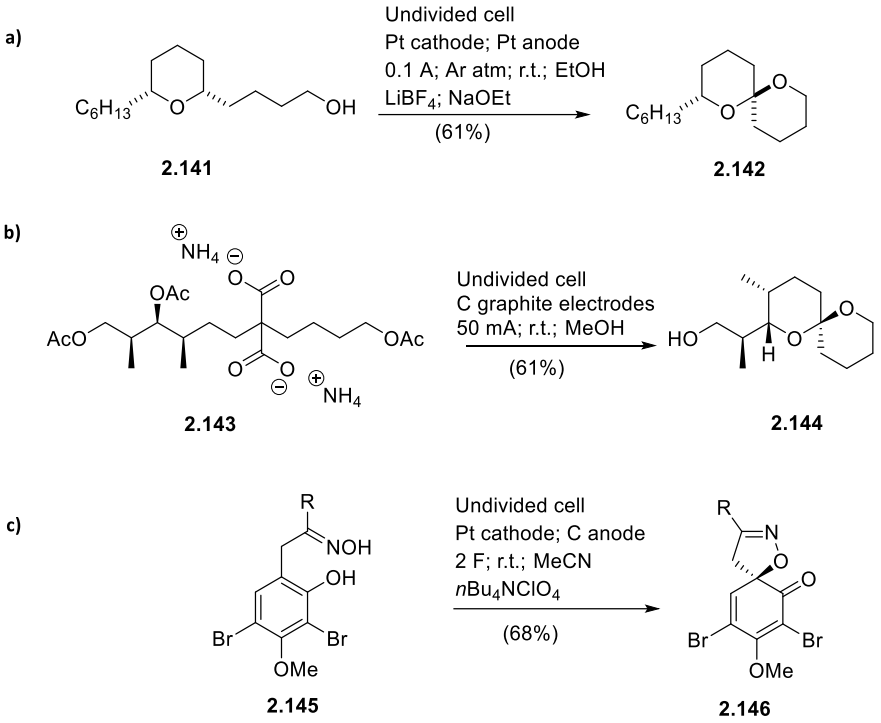

Scheme 2.46: a) Electrochemical synthesis of spiroketals by Markó; b) Electrochemical synthesis of spiricycles applied to the synthesis of okadaic acid; c) Opatz and co-workers' anodic oxidation method for the synthesis of spirocycles.

During our work on electrolysis towards the synthesis of THFs and lactones, styrene diol **2.147** was selected as a possible candidate in order to perform an intramolecular oxidative cyclisation by having a second nucleophile within the molecule (Scheme 2.47).

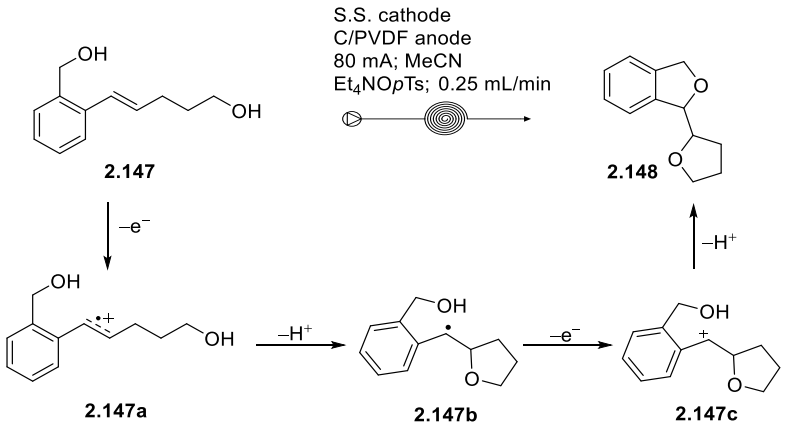

Scheme 2.47: Flow oxidative cyclisation of substrate **2.147**.

Compound **2.147** was synthesised in three steps starting from commercially available 2-iodobenzoic acid **2.129** (Scheme 2.48).[199,200] **2.149** was converted to the methoxy ester with a 95% yield before Sonogashira coupling to give compound **2.151** with a 60% yield; with $LiAlH_4$ we then manage to reduce both the ester to alcohol and the alkyne to alkene. It proved to be

necessary to convert the carboxylic acid to the methyl ester prior to the Sonogashira coupling; attempted direct coupling of the acid with the alkyne gave a mixture of products.

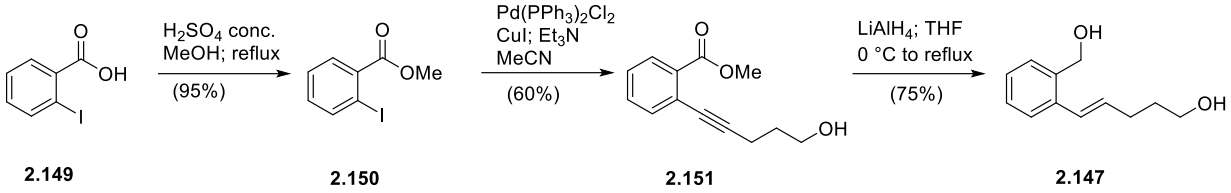

Scheme 2.48: Three step sequence for the synthesis of **2.147**.

With compound **2.147** in hand, the electrolysis step was investigated, swapping the solvent from MeOH to avoid methoxylation. MeCN was chosen as a suitable solvent and for a matter of solubility, and Et_4NOpTs was used as supporting electrolyte. The crude ^{1}HNMR spectrum of the electrolysis reaction showed starting material left (≈ 30%) and one main product, which was not the expected bis THF **2.148**. The structure of the electrolysis product was determined to be spiroketal **2.152**, isolated in 15% yield (Scheme 2.49).

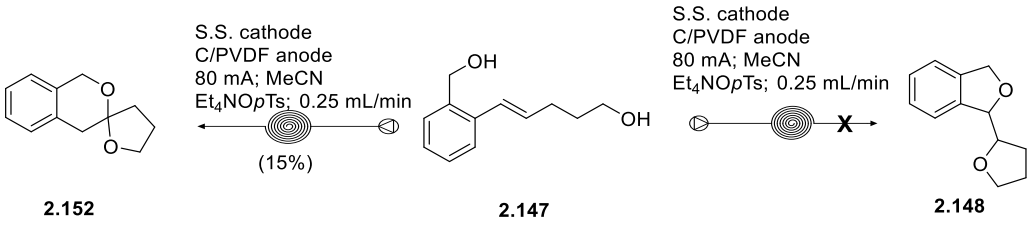

Scheme 2.49: Flow electrochemical oxidative cyclisation of **2.147** leading spiroacetal **2.152**.

This unexpected result gave some interesting information about the mechanism of the oxidative cyclisation, supporting the involvement of a carbocation intermediate. It supported initial oxidation and cyclisation with formation of a five-membered ring. In this particular case, after the second electron-transfer, a hydride migration occurs with formation of an oxacarbenium ion **2.147d**, followed by ring closing to the spirocycle **2.152** (Scheme 2.50). It maybe that cyclisation of the hydroxymethyl group onto the benzylic cation is slow relative to the hydride migration, or even reversible at the anode, where acidic conditions are present.

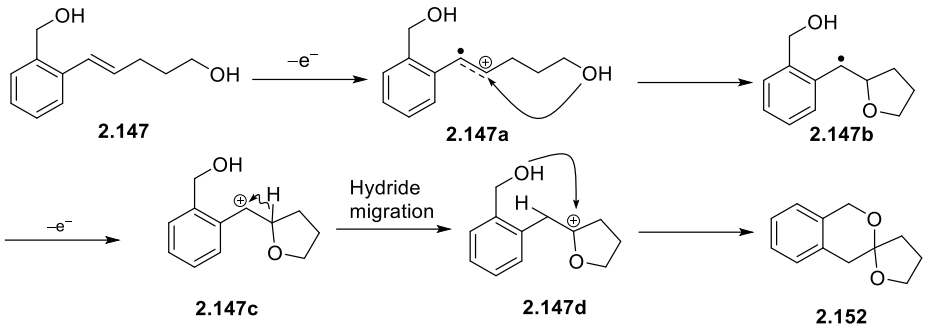

Scheme 2.50: Proposed mechanism to explain the formation of spirocycle **2.152** by anodic oxidation of **147**.

In the previous reactions, the hydride migration was not observed, probably because when working with methanol as solvent in a large excess, the cation formed after the second oxidation was rapidly trapped. In order to support this hypothesis, electrolysis of alcohol **2.65** was performed by using just five equivalents of methanol and MeCN as solvent. The crude ^{1}H-NMR supported the presence of the acetal product **2.153** in a 1/4 ratio with THF **2.116**, showing characteristic doublets at 3.03 ppm and 3.12 ppm Unfortunately, due to its volatility, most of the product tentatively assigned as **2.153** was lost on solvent removal. However, the small amount of purified material recovered was enough to obtain an ^{1}HNMR spectrum that matched data reported in literature,[201] and a GC-MS showing molecular ion $[C_5H_9O_2]^{+\cdot}$ and $[C_7H_7]^{+\cdot}$ with a mass respectively of 101.06 and 91.05 confirmed the positive outcome of the reaction (Scheme 2.51).

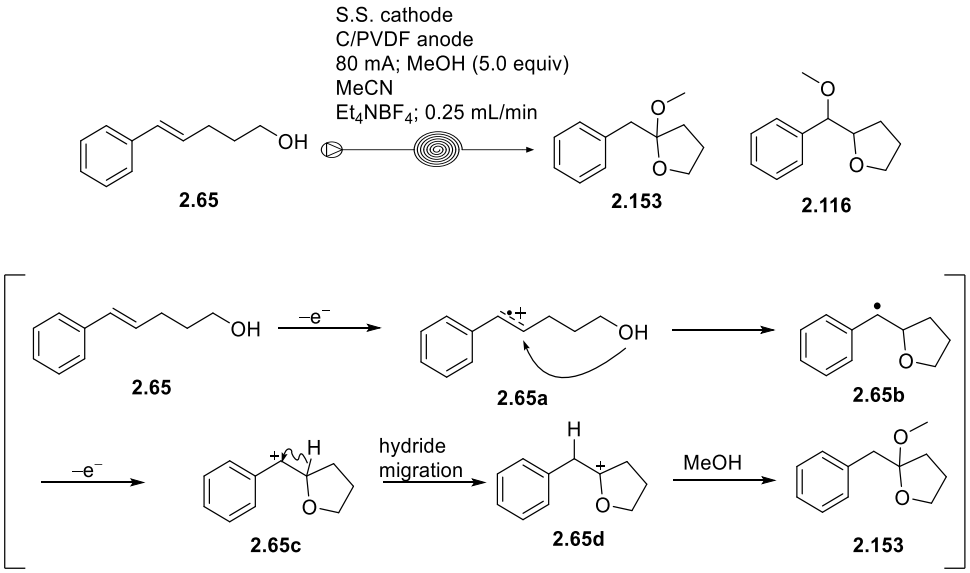

Scheme 2.51: flow electrochemical oxidative synthesis of **2.153**.

2.13 Investigation of the influence of chiral supporting electrolyte

Having developed a flow approach to anodic oxidative cyclisation, all the products were obtained as aproximately 4/1 = *erythro*/*threo* diastereoisomeric mixtures (scheme 2.52).

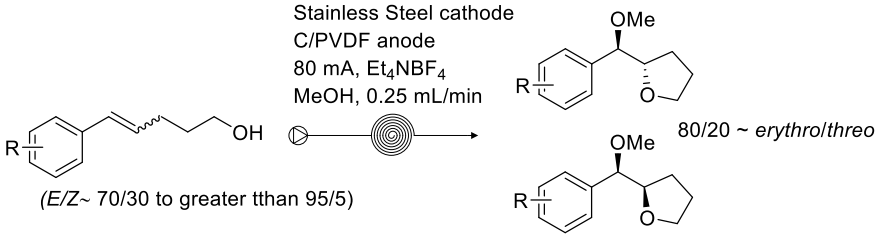

Scheme 2.52: General scheme of the flow electrochemical oxidative cyclisation method developed.

It was highly desirable to be able to improve the ratio further in favour of the *erythro* isomer or reverse it in favour of the *threo* diastereoisomer. One approach to achieving stereoselectivity could be by performing the reaction in the presence of a chiral additive, such as an enantiomerically pure chiral supporting electrolyte. In electrochemical reactions, both in batch and flow, the role of the supporting electrolyte is to act as a charge carrier by migration from one electrode to the other through the electrolyte solution. Asymmetric synthesis by electrochemical methods has been one of the most challenging subjects in organic electrochemistry;[202] some good results have been obtained using chiral modified electrodes, that normally consist of a carbon electrode modified by a film consisting of a metal complex with chiral ligands.[203–205] These electrodes unfortunately are mostly selective for a specific reactions, sometimes lack reproducibility and are difficult to prepare and to re-use.[202] Maekawa *et al*.[202] tried to perform electro-oxidative enantioselective oxidation of enol acetates using chiral supporting electrolyte TEACS (tetraethylammonium camphorsulfonate) (Figure 2.16), and their best result was an enantioselectivity of 44%. Although 44% would be considered mediocre in general asymmetric synthesis, achieving this using a chiral electrolyte remains and impressive result.

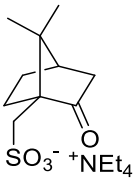

2.154

Figure 2. 16: Structure of tetraethylammonium camphorsulfonate: a chiral supporting electrolyte.

Due to the practical challenges of chiral modification of electrodes, it was decided to test TEACS as a chiral supporting electrolyte in an attempt to improve the diastereoselectivity. For the synthesis of TEACS **2.154**, a procedure reported by Maekawa and co-workers was followed (Scheme 2.53): reaction of 1*S*-(+)-camphorsulfonyl chloride **2.155** with ethanol in the presence of

a base (pyridine) to give 1*S*-(+)-ethyl camphorsulfonate **2.156** followed by treatment with trimethylamine in ethanol under reflux to finally afford the tetraethyl ammonium salt **2.154**. The reaction step between **2.155** and ethanol did not work; after the work-up compound **2.156** was not recovered. Instead compound **2.156** was synthesised by reaction of 1*S*-(+)-camphorsulfonic acid (**2.157**) with triethyl phosphite with a 67% yield.[206] The second step, the conversion of ethyl camphorsulfonate **2.156** to the tetraethyl ammonium salt **2.154** by reaction in dry EtOH with triethyl amine under reflux, finally afforded the desired product with 58% yield (Scheme 2.53).

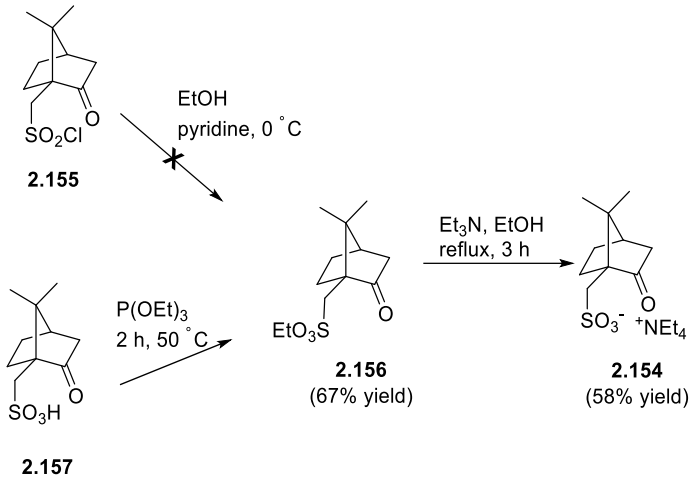

Scheme 2.53: Synthesis of chiral ammonium salt **2.154**.

Once prepared, compound **2.154** was tested as chiral supporting electrolyte for the anodic cyclisation in the flow reactor. The conditions previously described were used: a 0.1 M solution of reactant, a stoichiometric equivalent of current (80 mA, 2.0 F) and a flow rate of 0.25 mL/min. The chiral supporting electrolyte **2.154** (0.05 M) was used in place of Et_4NBF_4. During the reaction, the formation of bubbles exiting the reactor and a voltage of 3.4-3.3 V, comparable to the previous experiments run using Et_4NBF_4. Full conversion was achieved but analysis of the crude reaction mixture by ^{1}H-NMR and by TLC revealed that it had proceeded less cleanly with a small decrease in diastereoselectivity (70/30= *erythro*/*threo* instead of 80/20). (Scheme 2.54). The use of chiral supporting electrolyte was an ambitious project and it did not gave the expected outcome.

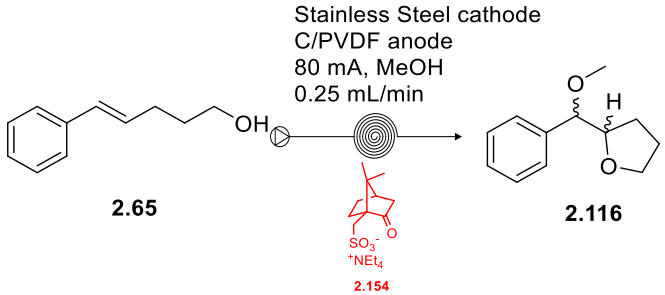

Scheme 2.54: Flow electrochemical oxidative cyclisation of **2.48** using a chiral supporting electrolyte.

2.14 Attempted trapping of cyclised carbocation intermediates as alkylsulfonium ions

Electrochemical oxidations often involve the formation of a carbocation under mild conditions. Subsequently, the carbocation undergoes typical chemical reactions such as attack by a nucleophile present in the reaction mixture, which in many cases is the solvent. In 2011, Yoshida and co-workers published electrochemical-chemical oxidation processes with trapping of carbocation intermediates as alkoxysulfonium ions,[207] where they managed to generate, accumulate and even characterize this cation intermediate. The alkoxysulfonium ion derived from the reaction between DMSO and the oxidised substrate was ultimately reacted with an amine base to give a carbonyl product following a Swern-type process (Scheme 2.55).

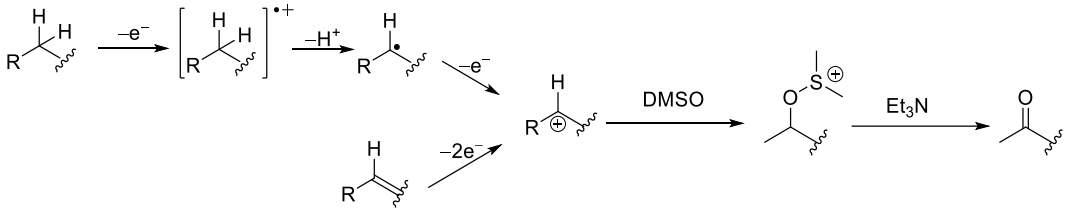

Scheme 2.55: Yoshida's integrated electrochemical-chemical oxidation mediated by alkoxysulfonium ions.

Their work started using easily oxidisable substrates such as diarylmethane **2.158**; the reaction was performed in a divided cell, applying a constant current of 8.0 mA until 2.5 F of electricity were consumed, at –78°C, in CD_2Cl_2 and using 5 equivalents of DMSO (Scheme 2.56a). They were able to characterise the alkoxysulfonium intermediate **2.159** by ^{1}HNMR analysis at –78°C. The alkoxysulfonium intermediate **2.159** was then reacted with Et_3N to give the corresponding ketone **2.160** in 91% yield. With this promising result in hand they expanded the substrate scope applying this method to aryl-substituted alkenes like **2.161** (Scheme 2.56b) and also to alkenes bearing a nucleophile group in order to enable cyclisation (Scheme 2.56c). A key advantage of Yoshida's approach is that the intermediate sulfonium ions are less prone to oxidation than methyl ethers, and thus, electrochemical degradation of the product was observed.

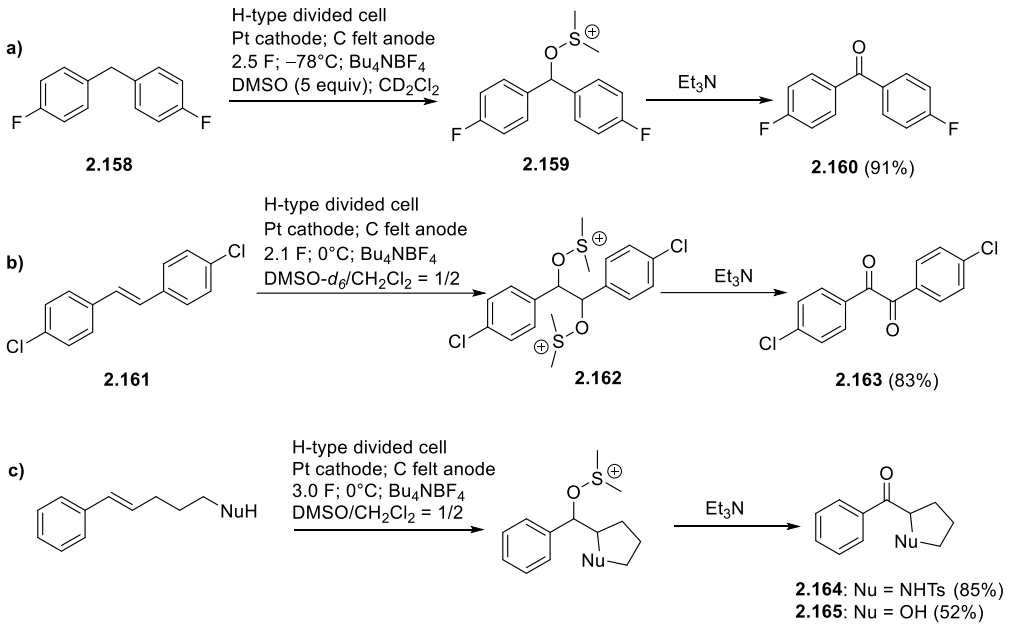

Scheme 2.56: Examples of Yoshida's integrated electrochemical-chemical oxidation mediated by alkoxysulfonium ions.

As the extension of the oxidative cyclisation to produce ketones offered interesting possibilities, the flow electrolysis method was investigated in presence of DMSO. In contrast to Yoshida's electrolysis though, our reaction would have been run in an undivided cell, open air, using a stainless steel cathode and a C/PVDF anode, Et_4NBF_4 as supporting electrolyte, a flow of 0.25 mL/min and applying the stoichiometric amount of current (80 mA, 2.0 F). Following Yoshida's conditions, the reaction was carried out at 0°C in a 3/2 mixture of CH_2Cl_2/DMSO as solvent and triflic acid to provide a counter electrode reaction (evolution of H_2). As previously stated, Yoshida ran the reaction at low temperature to slow decomposition of the intermediate alkoxysulfonium ion, and then Et_3N was added to the reaction solution to complete transformation to the ketone **2.165**. For the flow set up, the outlet of the electrolysis cell allowed the reaction mixture to flow directly into a solution of Et_3N in CH_2Cl_2 (Scheme 2.57).

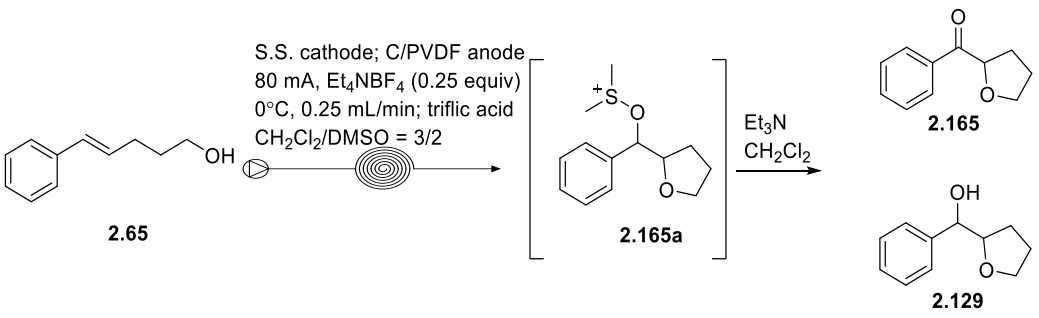

Scheme 2.57: Attempt to combine flow elctrochemical oxidative cyclisation with Yoshida's cation trapping approach for the synthesis of **2.165**.

For the first attempt (entry 1, Table 2.5), we used unpurified bench solvents to run the reaction and analysis of the crude mixture indicated the main product to be **2.129** with a significant amount of unreacted starting material present. It was encouraging to see the desired keto THF **2.165** as a minor product. This indicated that water present in the solvents or reactants could be competing with DMSO, although successful formation of the sulfonium intermediate followed hydrolysis after electrolysis could not be excluded. The proton source, required for the counter electrode reaction, was changed from triflic acid to MeOH and *t*-BuOH (entry 2 and 3); these attempts mainly gave unreacted starting material back, and also some compound hydroxy THF **2.129**. The recovery of starting material using MeOH and *t*-BuOH led to the use of a stronger acid TFA, to try to facilitate the counter electrode reaction; using TFA, almost full conversion was achieved but again in favour of product **2.129**, and in this case none of the desired ketone **2.165** was observed in the crude mixture. As previously stated, Yoshida and co-workers ran their experiments under an Argon atmosphere and using dry solvents so we switched from bench solvents to dry ones (entry 5). Unfortunately, the major product was still the hydroxyketone **2.129** although the relative amount of the desired ketone **2.165** was increased with an isolated yield of 11%. Due to the instability of the alkoxysulfonium ion intermediate, it was believed that the issue could be arising before the flow entered the Et_3N solution. Therefore, Et_3N was added directly in the reaction solution at the inlet of the reactor (entry 7); unfortunately just starting material was recovered at the outlet. The amine would have formed a salt with the added acid, protecting it from oxidation, but the amine should have been regenerated by the counter electrode reaction. Using other acids that are weaker than triflic acid (e.g. MsOH) did not lead to any improvements in the reaction, resulting in messier crude mixtures.

Table 2. 5: Investigation of Yoshida oxidation in flow[a].

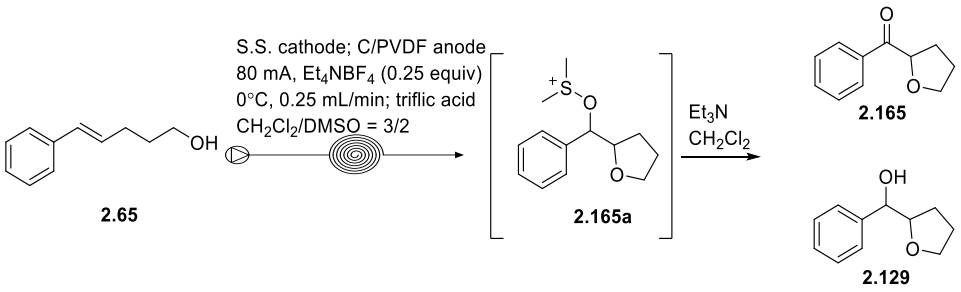

entry	Counter reagent	Flow (mL/min)	solvent	Ratio(%) 2.65/2.165/2.129[c]
1	CF_3SO_3H	0.25	DMSO/CH_2Cl_2 = 2/3	27/8/65
2	*t*-BuOH	0.25	DMSO/CH_2Cl_2 = 2/3	71/0/29
3	MeOH	0.25	DMSO/CH_2Cl_2 = 2/3	82/0/18
4	TFA	0.25	DMSO/CH_2Cl_2 = 2/3	18/0/82
5	CF_3SO_3H	0.25	Dry DMSO/CH_2Cl_2 = 2/3	18/16/66
6	Dry MeOH	0.25	Dry DMSO/CH_2Cl_2 = 2/3	77/0/23
7[b]	CF_3SO_3H	0.25	Dry DMSO/CH_2Cl_2 = 2/3	Sm 100%
8	CH_3SO_3H	0.25	Dry DMSO/CH_2Cl_2 = 2/3	28/7/65
9	CH_3SO_3H	0.5	Dry DMSO/CH_2Cl_2 = 2/3	30/6/64

[a]Reaction run using Stainless Steel cathode, C/PVDF anode, Et_4NBF_4 (0.25 equiv) as electrolyte, stoichiometric amount of current (80 mA, 2.0 F/mol), 0°C. [b] Et_3N added directly in the inlet solution. [c] Ratio between compound's proton signals in crude ^{1}H-NMR.

Unfortunately, we were not able to explore this interesting carbocation trapping / chemical oxidation approach further. The best result obtained was the formation of the keto THF **2.165** in 11% isolated yield (alcohol **2.129** obtained with a 44% isolated yield) (Scheme 2.59), which was obtained by running the reaction at 0°C, at a flow rate of 0.25 mL/min, using stainless steel cathode, C/PVDF anode, and Et_4NBF_4 as supporting electrolyte, the stoichiometric amount of current (80 mA), a 3/2 mixture DMSO/CH_2Cl_2 as solvent and triflic acid for the counter reaction (entry 5). It is possible that with further optimisation and more rigorously anhydrous conditions a higher yield for the ketone product **2.165** could be achieved, and this could be a topic for future investigation.

2.15 Conclusions and future work

In summary, we have developed a flow method for the synthesis of substituted cyclic ethers and lactones through oxidative cyclisation of styrene-derivatives. The cyclisation is performed in an Ammonite flow electrochemical cell without any oxidant or reducing agent apart from the application of electric current; the reaction proceeds under ambient conditions, in absence of added base to give lactones and THF products, including even aryl groups bearing electron deficient substituents, in moderate to good yields. Initial investigation indicated that the flow method showed higher efficiency compared to a batch process, and scale-up to ~1 g was proven to be straightforward without affecting the productivity or reduction in yield.

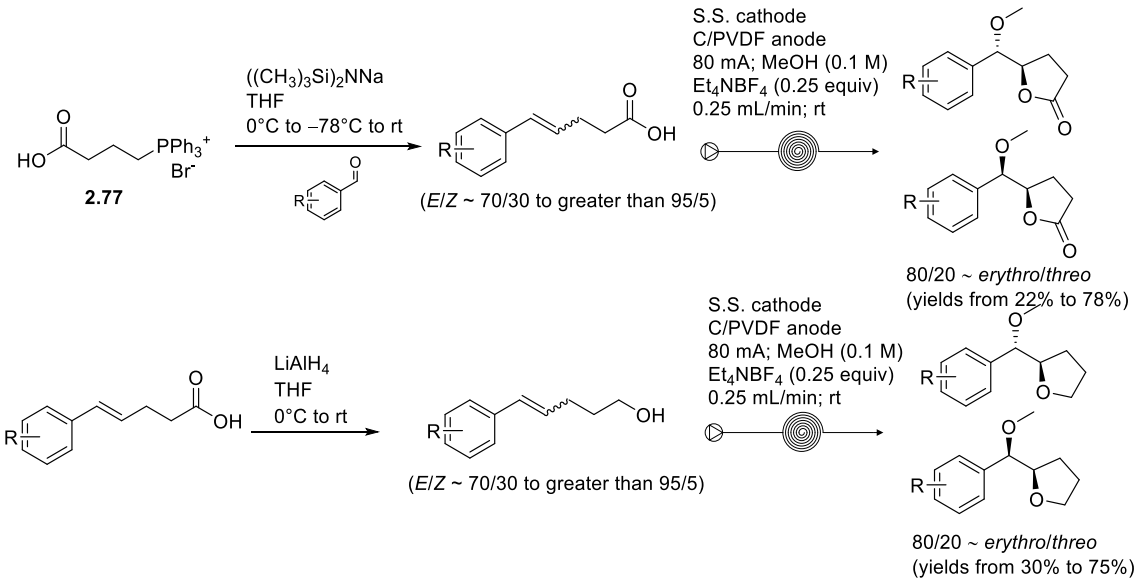

Scheme 2.58: General scheme of the flow electrochemical oxidative cyclisation of alcohol and carboxylic acids.

Adaptation of the flow oxidative cyclisation to the formation of keto THFs **2.165** following a strategy introduced by Yoshida's was also explored. Although the desired ketone **2.165** was obtained, the yield was low, and the main product was that from hydrolysis (i.e. hydroxy THF **2.129**). An interesting hydride shift-spirocyclisation of **2.147** to give **2.152** was also discovered. Future work could focus on developing these method for the synthesis of keto THFs and spirocycles.

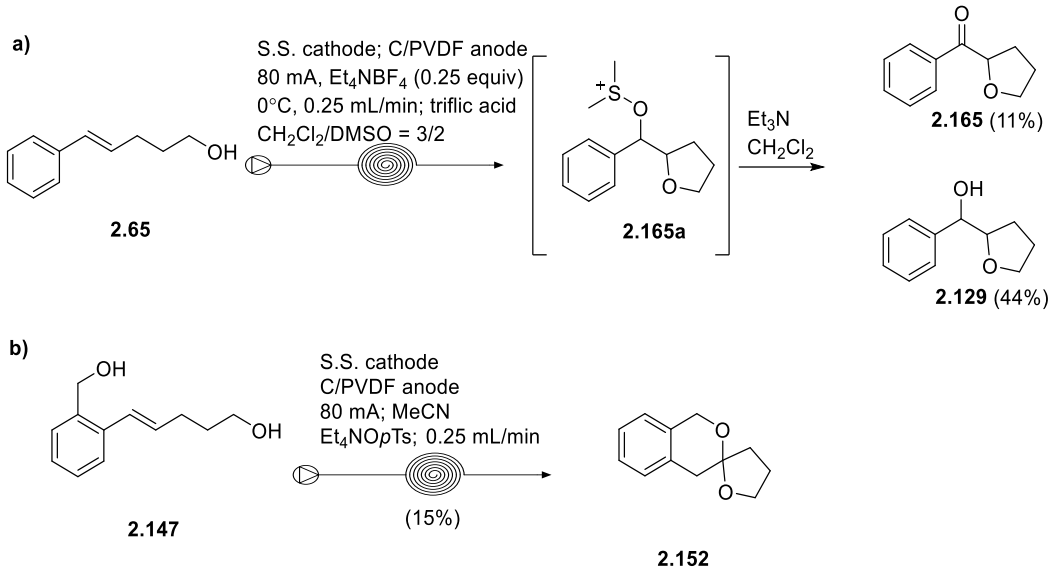

Scheme 2.59: a) Attempted trapping of cyclised carbocation intermediates as alkylsulfonium ions; b) Flow electrolysis of **2.147** to give the spirocycle **2.152**.

Chapter 3 ELECTROCHEMICAL REDUCTION OF DOUBLE BONDS

3.1 Common methods for hydrogenation of alkenes

The most commonly used method for the hydrogenation of alkenes is catalytic hydrogenation. It is one of the most important reactions in organic chemistry, especially because of its many different applications in industry, from pharmaceutical to the petrochemical materials.[208,209] It requires the use of hydrogen gas and a transition metal catalyst (Rh, Pd, Au, Ir, Ru, Ni); the catalyst can be heterogeneous (e.g. a metal such as Pd supported on a solid material like carbon) or a homogeneous soluble catalyst (e.g. Wilkinson's catalyst). Heterogeneous catalysts are more stable, easy to separate and to re-use and easier to handle; they have higher catalytic ability and their use helps to reduce the process costs. Homogeneous catalysts are mostly used for enantioselective transformations, provide better selectivity, have a higher turnover and require milder conditions, but they are frequently more expensive and difficult to reuse.[208–210] The use of metal catalysts for hydrogenation started in 1910 with Sabatier using Ni oxide and currently there are many methods based on different metals; the most widely used are Pd and Pt, like palladium on carbon and Adam's catalyst (PtO_2).[210]

In 1966 Wilkinson and co-workers reported the synthesis of a chlorotris(triphenylphosphine)rhodium(I) complex, known as Wilkinson's catalyst, for the homogeneous hydrogenation of unsaturated compounds.[211–214] It can be used for selective hydrogenation, and displays useful chemoselectivities such as not affecting functional groups like C=O, CN and aryl. Less substituted and exocyclic double bonds are preferentially hydrogenated using Wilkinson's catalyst (Scheme 3.1).

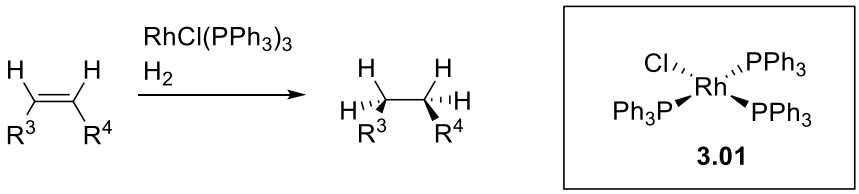

Scheme 3.1: Hydrogenation catalysed by Wilkinson's catalyst.

In 1979 Crabtree and co-workers developed an iridium based complex **3.02** for the homogeneous catalytic hydrogenation of olefins. This catalyst proved to be more active than the Wilkinson catalyst and it is also capable of catalysing hydrogenation of tri- and tetrasubstitued olefins (Scheme 3.2).[215,216]

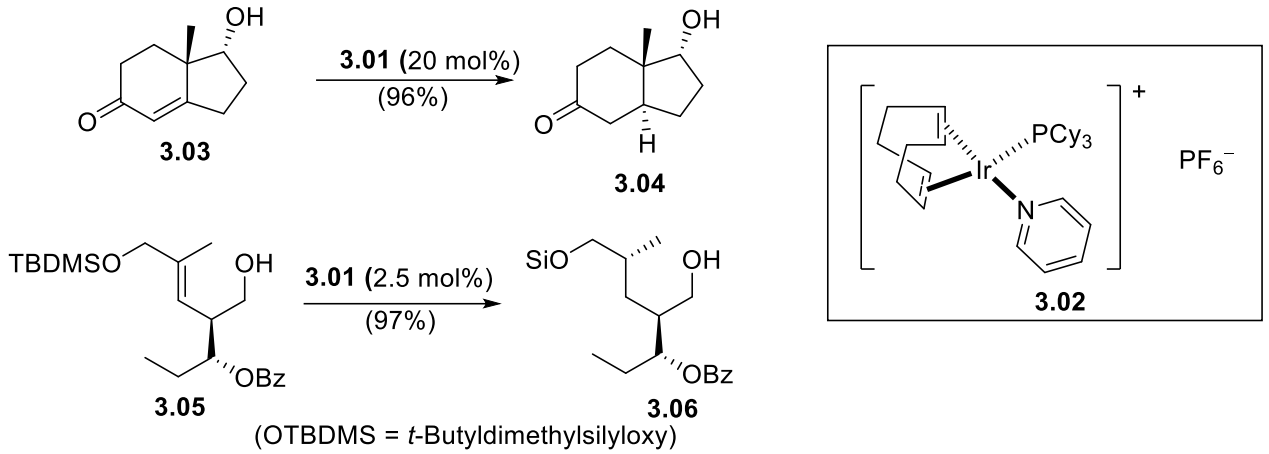

Scheme 3.2: Examples of hydrogenation using Crabtree's catalyst.

In 1980, Noyori and co-workers, reported the synthesis of a BINAP-Rh(I) complex and its use as catalyst for the asymmetric hydrogenation of α-(acylamino)acrylic acids or esters to the corresponding amino acid derivatives with high enantioselectivity.[217,218] Later, in 1986, Noyori *et al.* developed another BINAP catalyst, this time a Ru(II) based catalyst which proved to work with a wider range of olefins (Scheme 3.3).[219] Nowadays, most of the new methods of catalytic hydrogenation are focused on performing the process asymmetrically by adding chiral ligands to the metal.[220]

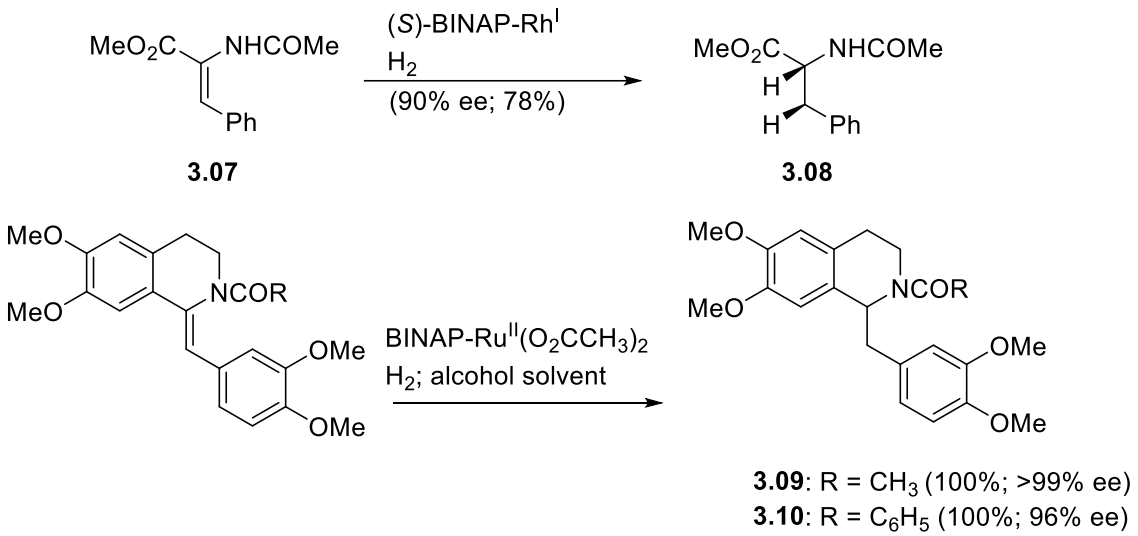

Scheme 3.3: Asymmetric hydrogenation developed by Noyori an co-workers.

Despite the predominance of catalytic hydrogenation, there are other useful methods to reduce C—C double bonds. Around 1960, it was discovered that diimide (HN=NH) could reduce double bonds (Scheme 3.4).[221] Diimide promoted reduction does not need hydrogen gas or a catalyst, and has the advantage that it can be run under mild conditions, and tolerates different functional groups like esters, amines, halides. However, the need of an excess of diimide makes selective

reduction of a specific double bond difficult in presence of different alkenes; however symmetrical and less sterically hindered ones are preferentially hydrogenated. Diimide reduction can be exploited to reduce certain alkynes to alkenes, in particular alkyl-substitued alkynes undergo reduction to *cis*-alkenes. 1-Iodoalkynes instead, have a reduced reactivity so their reduction will stop at the *cis*-alkene, as shown in Scheme 3.4.[221]

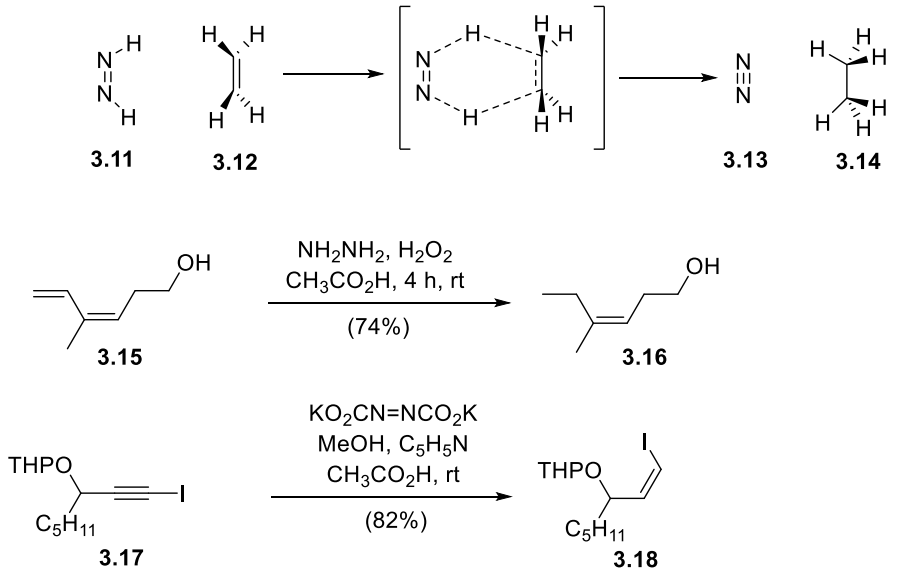

Scheme 3.4: Diimide promoted hydrogenation of alkenes.

Another method to achieve formal hydrogenation of alkene double bonds is *via* hydroboration followed by protonation (Scheme 3.5).[222] This can be advantageous when the substrate is incompatible with metal catalysts; for example, the presence of thiols may lead to deactivation of Pd-catalysts.

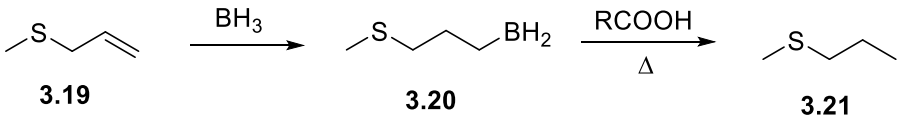

Scheme 3.5: Formal hydrogenation of alkenes promoted *via* hydroboration.

3.2 Electrochemical methods for the hydrogenation of alkenes

In the recent past electrochemistry started to be considered as a valid, more sustainable and safer method to perform hydrogenation/reduction of olefins mostly because it can avoid the use of highly flammable hydrogen gas and of expensive transition-metal catalysts that are also finite resources.[223] An early example from Kashimura and co-workers, reported in 2003,[224] is an electrochemical version of the Birch reduction of aromatics (Scheme 3.6). The reaction was

performed in an undivided cell, using magnesium electrodes, using $LiClO_4$ as supporting electrolyte, THF as solvent and *t*-BuOH as proton donor, under constant current at room temperature. No mechanistic insight was provided, although it may be expected to follow an electron-transfer pathway similar to the classical Birch reduction.

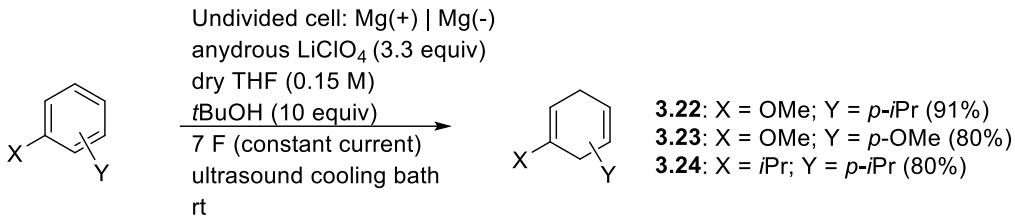

Scheme 3.6: Kashimura electrochemical hydrogenation.

In 2019, Baran *et al.*[225] repored a Birch-type electroreduction. This methodology requires a sacrificial anode (Mg or Al), dimethylurea as proton source; it proved to be scalable and to be compatible with a broad range of substrates (Scheme 3.7).

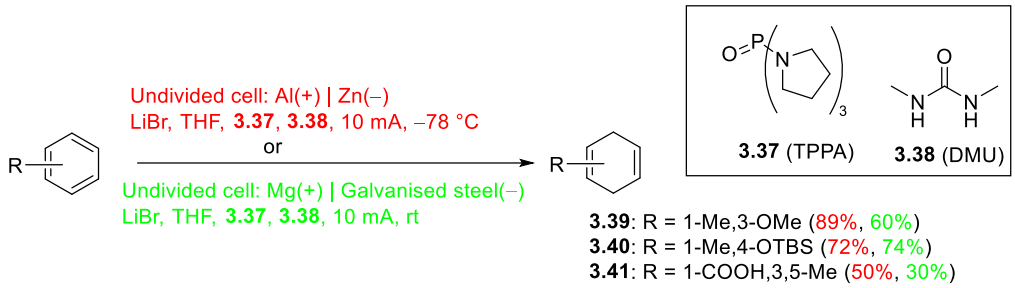

Scheme 3.7: Baran's electroreduction inspired by Li-ion battery chemistry.

In 2006, Navarro *et al.*[226] reported the homogeneous electro-mediated reduction (HEMR) of different unsaturated organic compounds, including cyclohexene, cyclohexanone, benzaldehyde, and styrene (Scheme 3.8). The reaction was performed in DMF as solvent in an undivided cell equipped with Ni^0 foam as cathode and a Ni or Fe sacrificial anode, under inert atmosphere, with NaI as supporting electrolyte and a $Nickel^{II}$-bipyridine complex **3.29** as mediator. The proposed mechanism involves the oxidation of the sacrificial anode and the reduction of the mediator at the cathode, reduction of the substrate by the reduced mediator and protonation of the reduced substrate by the residual water.

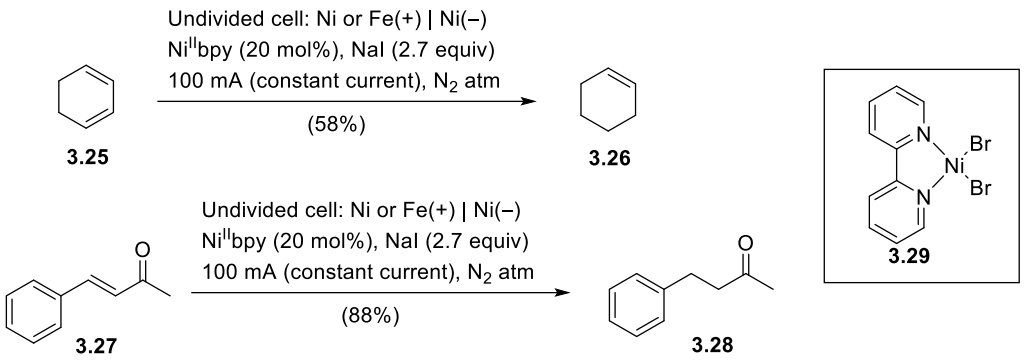

Scheme 3.8: Navarro homogeneous electro-mediated reduction.

In 2016 Tajima *et al.*[227] reported the electro-chemical reduction of activated olefins promoted by silica–gel supported sulfonic acid (Si—SO_3H). The reaction is performed in an undivided cell, in MeCN, using Pt anode, glassy carbon (GC) cathode, Bu_4NBF_4 as supporting electrolyte and Si—SO_3H as promoter (Scheme 3.9). The role of the silica-gel supported sulfonic acid is to favour the protonation step minimising the elimination and polymerisation side-reactions.

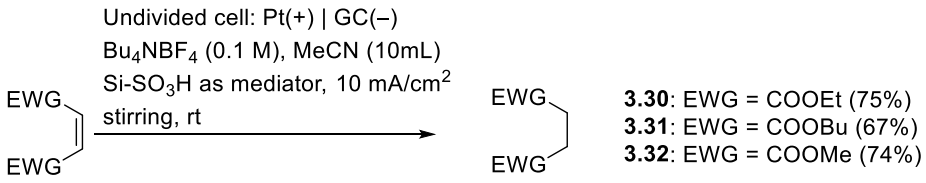

Scheme 3.9: Si—SO_3H promoted electrochemical reduction of activated olefins.

In 2019 Xia and co-workers reported the electrochemical 1,4-reduction of α,β-unsaturated ketones (Scheme 3.10).[228] The electrolysis is performed at room temperature and open air, in an undivided cell, using Pt electrodes and inexpensive and safe reagents. Ammonium chloride and methanol by the proposed mechanism are considered the hydrogen donors, while oxidation of DMSO is the proposed counter reaction. This methodology proved to be scalable and to be compatible with ketones bearing different functional groups.

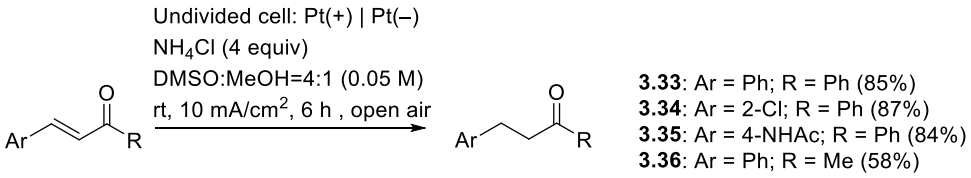

Scheme 3.10: Xia's electrochemical 1,4-reduction of α,β-unsaturated ketones.

In 2019, Ge and Li[229] reported the electrochemical hydrogenation of alkynes to *Z*-alkenes and alkanes with good yields and chemo and stereoselectivity. The reaction is performed in an undivided cell using a graphite anode and a platinum cathode in presence of $PdCl_2$ to catalyse the

hydrogenation. Based on their proposed mechanism the solvent MeOH is the hydrogen source that gets adsorbed on the palladium catalyst; then the hydrogen transfer happens between the Pd and the alkyne to generate the desired alkene. According to their proposal, the supporting electrolyte nBu$_4$NI is reduced at the cathode to tributylamine which is then oxidised at the anode forming an amine radical cation that can also act as hydrogen source (Scheme 3.11).

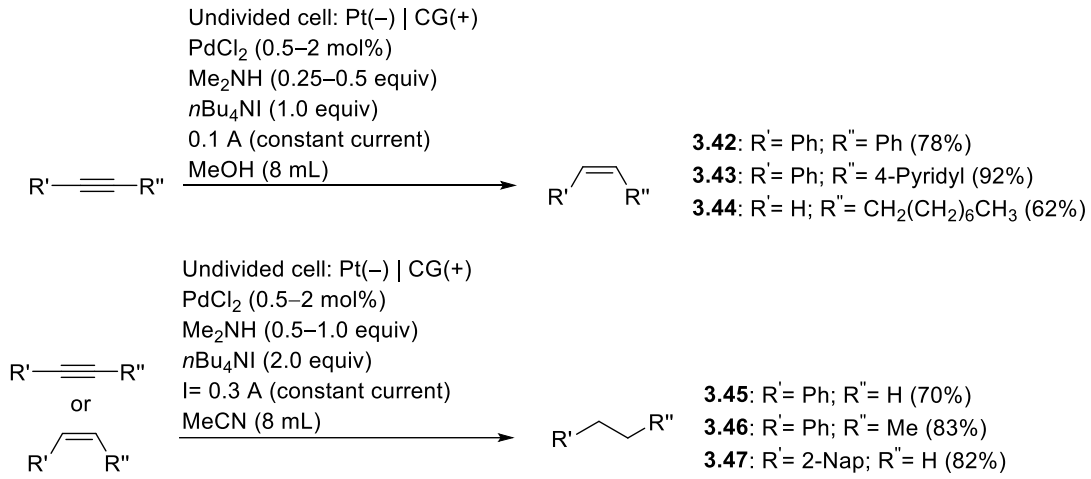

Scheme 3.11: Ge and Li's electrochemical hydrogenation of alkynes.

Also in 2019, Li *et al.*[230] reported the electrochemical hydrogenation of alkynes and alkenes using ammonia gas as hydrogen source. The reaction is carried out in an undivided cell, using graphite felt electrodes, at room temperature, under ammonia atmosphere. This protocol is compatible with different functional group (unconjugated alkenes, benzyl, Boc, Cbz, heterocycles, sulfide, silyl group). Based on the proposed mechanism the substrate is reduced at the cathode before the proton transfer with the ammonia (Scheme 3.12). With the requirement of so many additives and electrolyte, and a Pd catalyst, the advantage of such a process over classical methods is unclear.

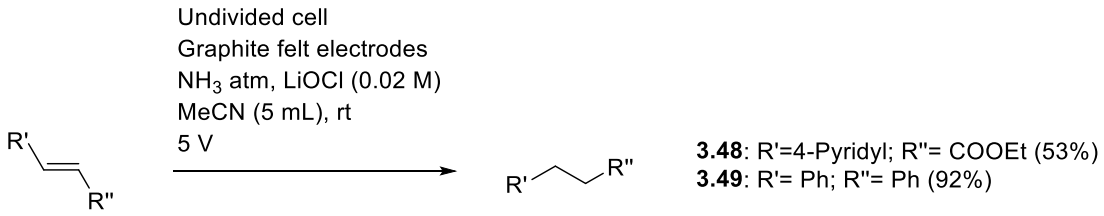

Scheme 3.12: Li's electrochemical reduction using gaseous ammonia.

In 2019, Atobe's group published their work on the hydrogenation of alkynes to *Z*-alkenes and to alkanes using a flow reactor equipped with a proton-exchange membrane.[231] In this process, the electrode acts also as catalyst: at the Pt anode hydrogen is oxidised to protons which pass through the membrane and get reduced to monoatomic hydrogen and deposit on the cathode "catalyst" where the hydrogenation of the substrate takes place (Scheme 3.13).

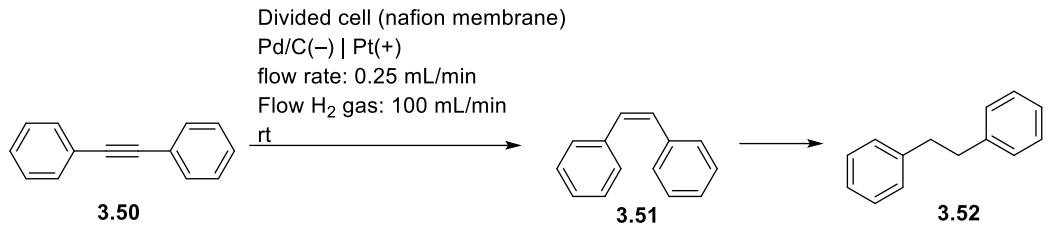

Scheme 3.13: Electrocatalytic hydrogenation of alkynes in a proton-exchange membrane (PEM) reactor.

In 2020 Li *et al*.[232] reported the electrochemical deuteration of α,β-unsaturated carbonyl compounds. The reaction is performed in an undivided cell equipped with graphite felt electrodes, D_2O is used as deuterium source, no metal catalyst or stoichiometric reductant is needed; it is performed at room temperature and this method can be applied to a wide range of α,β-unsaturated compounds with moderate to good yields. Based on their proposed mechanism the substrate is reduced at the cathode and the oxidation of D_2O to generate oxygen provides the counter reaction (Scheme 3.14).

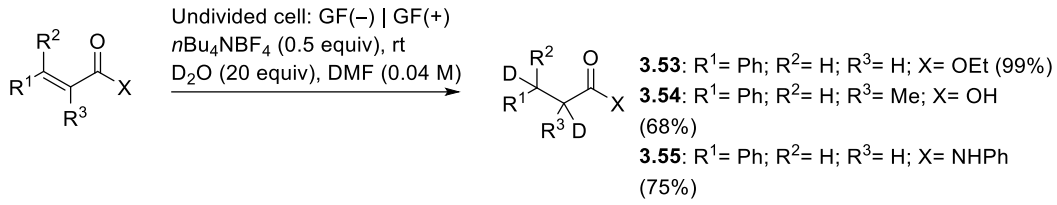

Scheme 3.14: Electrochemical deuteration of α,β-unsaturated carbonyl compounds.

In 2020 Huang and co-workers reported this metal-free cathodic hydrogenation of unsaturated carbon-carbon bonds.[233] The reaction is performed open air, at room temperature, in an undivided cell, using carbon electrodes and nBu$_4$NHSO$_4$ as supporting electrolyte (Scheme 3.15). The solvents, DMSO and water, are the hydrogen source in this reaction as confirmed by deuterium-labelling experiments.

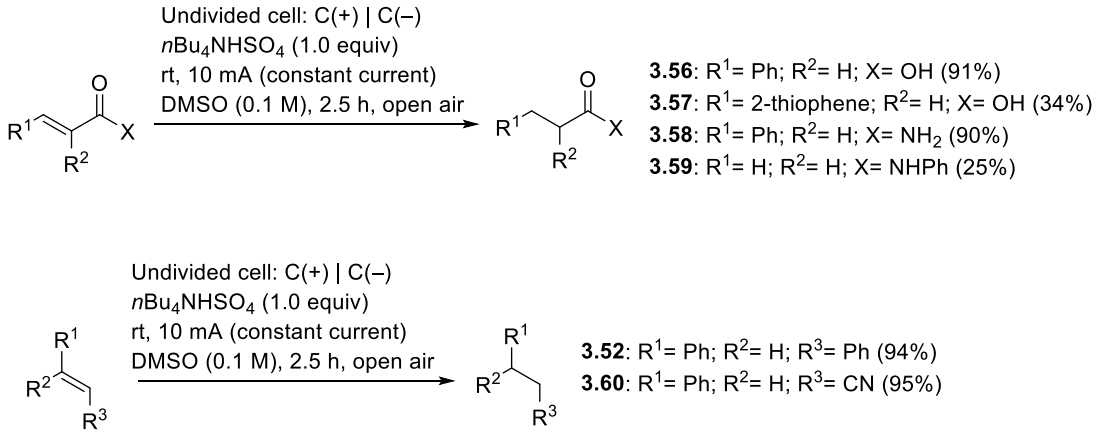

Scheme 3.15: Metal-free cathodic hydrogenation of unsaturated carbon-carbon bonds.

3.3 Aims and objectives

As previously discussed, the hydrogenation of unsaturated C—C bonds is one of the most important reactions in organic chemistry, especially because of its many different applications in industry. Most of the current methods require the use of transition metal catalysts and highly flammable hydrogen gas. In the recent past, some efforts to make this type of reactions safer and more sustainable has been made by the use of electrochemistry.

After a surprising result obtained during our studies on the flow electrochemical cyclisation previously described in chapter 2 and after a review of the literature regarding electrochemical reduction of double bonds we decided to focus our efforts on the development of the electrochemical reduction of styrene double bonds using the Ammonite 8 flow reactor. Our aim was to first optimise the electrolysis conditions, then attempt to expand the substrate scope and we also felt that it would have been of interest to investigate whether the same substrates could be oxidised or reduced, selectively, by simply changing the electrolysis conditions.

3.4 Discovery of electrochemical reduction of hydroxyalkene 2.48's double bond

While working on the oxidative cyclisation of hydroxyalkene **2.65**, reported in Chapter 2, we applied fluoride as nucleophile instead of methanol in an effort to make fluorinated products (Scheme 3.16). To do so, the same electrolysis conditions were applied but using TBAF both as supporting electrolyte and as source of fluoride anion and ethyl acetate, instead of methanol, as solvent in order to have just one nucleophile in the reaction environment. After removal of solvent, the crude mixture was analysed by ^{1}HNMR and massspectrometry, but the desired product **3.61** was not detected. By careful column chromatography a couple of fractions were isolated, surprisingly resulting in identification of ester **3.62** and alcohol **3.63**. Although the yields of these unexpected products was low, there isolation clearly indicated the styrene alkene was susceptible toward reduction/hydrogenation under the electrolysis conditions. Full conversion was achieved; it should be noted that 80% of the mass balance was unaccounted for, so it is probable that some oxidation was also taking place with some degradation too as shown by the a complex TLC and crude ^{1}HNMR.

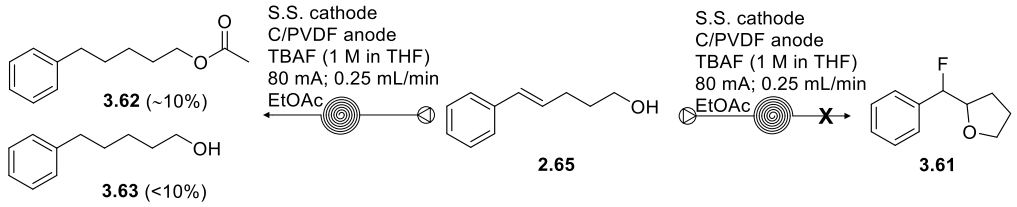

Scheme 3.16: Attempted fluorinative oxidative cyclisation of **2.48**, with observed alkene hydrogenation.

3.5 Optimisation of the electrolysis conditions

Our first focus was to develop the reductive method in order to increase the yield of the reduction product(s), and allow selective transformation. Using the conditions described above (see Scheme 3.16) the desired alcohol **3.63** was obtained with a yield less than 10%, while ester **3.62** was isolated with a yield of around 10%. For the optimisation we decided to use calibrated gas chromatography as the analytical method, and to use *E*-stilbene **3.64** as substrate instead of hydroxyalkene **2.65**. This was to avoid any issues due to side reactions of the alcohol functional groups and because both, **3.64** and its hydrogenated product bibenzene **3.52** are readily available commercially and inexpensive.

As first attempt, we replicated the conditions previously described, using a 0.1 M solution of *E*-stilbene in EtOAc, containing 1.2 equivalents of TBAF (Table 3.1). The electrolyte solution was passed through the Ammonite 8 reactor, using a stainless steel cathode and a C/PVDF anode and applying the stoichiometric theoretical current of 80 mA (Table 1 entry 1). With these conditions the desired reduction product **3.52** was obtained with a 40% GC yield but the overall mass recovery was very low considering that only 7% of *E*-stilbene was unreacted. Switching solvent from EtOAc to THF was carried out to identify whether the solvent actually played a role in the electrolysis process, and also because the TBAF was already in THF solution (Table 1 entry 2). The result was similar to the one in EtOAc, with 42% of bibenzyl **3.52** and low mass recovery. We then investigated TBAI as a sacrificial supporting electrolyte that is readily oxidised (0.54 V vs SCE for $I_2+2e^- \rightarrow 2I^-$). Because TBAI is insoluble in THF, a 9/1 mixture THF/MeCN was used. This attempt gave just a 12% of bibenzyl but less degradation compared to the previous trials, with the major part of *E*-stilbene (81%) left unreacted (Table 1 entry 3). On the basis of the "cleaner" reaction profile, further work on the optimisation used TBAI as supporting electrolyte. Increasing the current to 3 F and 4 F increased the GC yield for bibenzyl to 32% in both cases (Table 1 entries 4 and 6). Passing the solution twice through the reactor while applying the stoichiometric amount of current both times gave 28% of bibenzyl with a 63% of starting material left (Table 1 entry 5). Applying 5 F of current increased the yield for bibenzyl to 46% but with such an excess of current there was still 36% of starting material left (Table 3.1 entry 7), indicating surprisingly high selectivity when large excess of charge was applied.

Table 3.1: Initial screening of different conditions for the electrochemical reduction of stilbene.

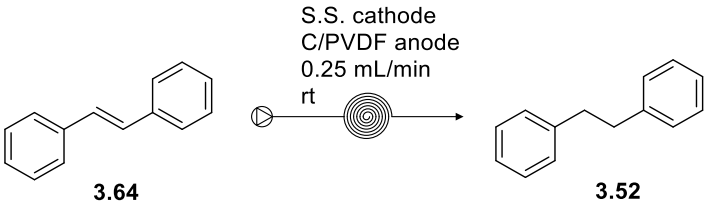

entry	current (mA), [charge (F)]	supporting electrolyte (1.2 equiv)	solvent	RSM 3.64(%)[a, b]	yield 3.52(%)[a, b]
1	80 [2.0]	TBAF	EtOAc	7	40
2	80 [2.0]	TBAF	THF	6	42
3	80 [2.0]	TBAI	THF/MeCN (9/1)[d]	81	12
4	120 [3.0]	TBAI	THF/MeCN (9/1)[d]	57	32
5	80 [2.0][c]	TBAI	THF/MeCN (9/1)[d]	63	28
6	160 [4.0]	TBAI	THF/MeCN (9/1)[d]	54	32
7	200 [5.0]	TBAI	THF/MeCN (9/1)[d]	34	46

[a] Reactions performed on a scale of 0.5 mmol (substrate conc. 0.1 M). [b] Estimated using calibrated GC analysis. [c] Performed over two passes at 80 mA (outlet solution collected and passed again through the electrolysis cell). [d] MeCN needed to dissolve the supporting electrolyte which is insoluble in neat THF.

After these results, and before further increasing the current applied, different electrodes were tested. Using carbon electrodes (Table 3.2 entry 1), poor conversion was realised compared to the result using a ss cathode (Table 1 entry 3). A combination of Pt cathode and C graphite anode gave a 38% of bibenzyl leaving a 54% of *E*-stilbene (Table 3.2 entry 2). The conversion was improved using Ag as cathode and C graphite anode, giving 46% of bibenzyl and 39% of *E*-stilbene (Table 3.2 entry 3) using a stoichiometric equivalent of charge. Retaining the combination of an Ag cathode and C graphite anode, doubling the charge to 4 F, a full conversion was finally achieved with an 88% GC yield of bibenzyl (Table 3.2 entry 4). With the optimised combination of electrodes (Ag cathode and C graphite anode) and current (160 mA, 4 F), alternative solvents (MeCN and MeOH) were tested leading to poorer results (Table 3.2 entries 5 and 6).

Table 3. 2: Screening of cathodes and solvents.

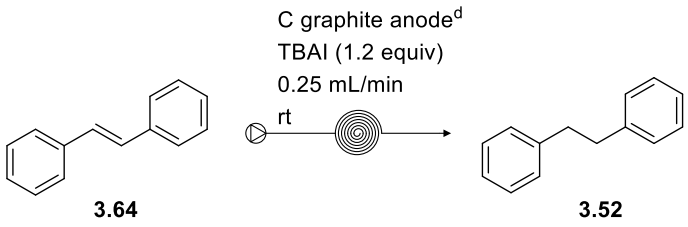

entry	cathode	current (mA), [charge (F)]	solvent	RSM 3.64(%)[a, b]	Yield 3.52(%)[a, b]
1	C/PVDF	80 [2.0]	THF/MeCN (9/1)[c]	83	5
2	Pt	80 [2.0]	THF/MeCN (9/1)[c]	54	38
3	Ag	80 [2.0]	THF/MeCN (9/1)[c]	39	46
4	Ag	160 [4.0]	THF/MeCN (9/1)[c]	0	88
5	Ag	160 [4.0]	MeCN	50	40
6	Ag	160 [4.0]	MeOH	73	21

[a] Reactions performed on a scale of 0.5 mmol (substrate conc. 0.1 M). [b] Estimated using a calibrated GC. [c] MeCN needed to dissolve the supporting electrolyte, which is insoluble in neat THF.[d] To opperate the Ammonite cell, one of the electrodes needs to have a recess channel, and an Ag electrode with a recess was not available at the time of the work.

Once established that Ag cathode and C graphite anode were the preferred electrodes for this process and that an excess of charge was needed (4 F), a series of different supporting electrolytes were also tested (Table 3.3). Most of them were tetrabutylammonium salts; TBAF was tested again with these new conditions giving full conversion and a 75% GC yield for the product (Table 3.3 entry 2), but the best result was achieved using TBABr giving full conversion and 93% GC yield (Table 3.3 entry 3). Supporting electrolytes that were not ammonium salts gave degradation (Table 3.3 entry 1), or no reaction at all (Table 3.3 entries 7 and 8).

Table 3. 3: Screening of electrolytes.

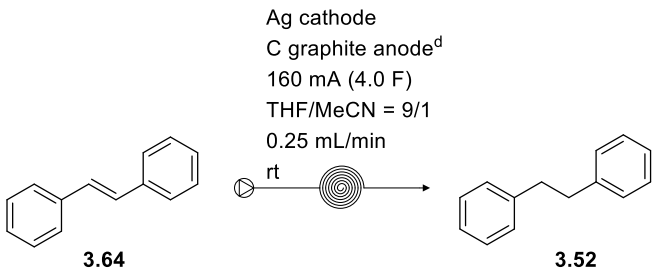

entry	supporting electrolyte (1.2 equiv)	RSM 3.64(%)[a, b]	Yield 3.52(%)[a, b]
1	$NaClO_4$	37	6.5
2	TBAF	0	74.5 (55% isolated)
3	**TBABr**	**0**	**93**
4	TBACl	0	89
5	$TBAClO_4$	0	51
6	$TBABF_4$	0	56
7	Me_3SI	99	0
8	NaI	100	0

[a] Reactions performed on a scale of 0.5 mmol (substrate conc. 0.1 M). [b] Estimated using a calibrated GC. [c] MeCN needed to dissolve the electrolyte otherwise insoluble in neat THF. [d] To opperate the Ammonite cell, one of the electrodes needs to have a recess channel, and an Ag electrode with a recess was not available at the time of the work.

After screening conditions, the conditions for this electrolysis process were established: Ag cathode, C graphite anode, 1.2 equivalents of TBABr as supporting electrolyte, THF/MeCN = 9/1 as solvent, a flow rate of 0.25 mL/min and a current of 160 mA (4 F). However, for completion some other variations from these conditions have been investigated (Table 4): with a lower amount of applied charge (3 F) full conversion wasn't achieved, with 17% of starting material remaining (Table 3.4 entry 1). By increasing the concentration of the substrate from 0.1 M to 0.5 M full conversion was still achieved with a 75% GC yield for bibenzyl. Although the yield was lower, it was considered to still be acceptable, and promising for higher rates of production (Table 3.4 entry 2). The process was proved to work at a range of temperatures from 0 °C and 50 °C (Table 3.4 entries 3 and 4). In addition, increasing the flow to 0.5 mL/min still allowed a high conversion, with just 5% of starting material unreacted and returning 75% of product (Table 3.4 entry 5). The amount of electrolyte could be decreased to 0.8 equivalents with full conversion and a 80% GC yield for bibenzyl (Table 3.4 entry 6).

Table 3. 4: Investigation of flow rate, concentration and temperature.

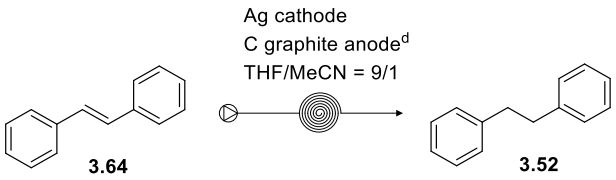

entry	substrate conc.	T (°C)	current (mA), [charge (F)]	supporting electrolyte	flow (mL/min)	RSM 3.64(%)[a, b]	Yield 3.52(%)[a, b]
1	0.1 M	rt	120 [3.0]	TBABr (1.2 equiv)	0.25	17	63
2	0.5 M	rt	804 [4.0]	TBABr (1.2 equiv)	0.25	0	75
3	0.1 M	0	160 [4.0]	TBABr (1.2 equiv)	0.25	2	82
4	0.1 M	50	160 [4.0]	TBABr (1.2 equiv)	0.25	2	79
5	0.1 M	rt	320 [4.0]	TBABr (1.2 equiv)	0.50	5	75
6	0.1 M	rt	160 [4.0]	TBABr (0.8 equiv)	0.25	0	80

[a] Reactions performed on a scale of 0.5 mmol (substrate conc. 0.1 M). [b] Estimated using a calibrated GC. [d] To opperate the Ammonite cell, one of the electrodes needs to have a recess channel, and an Ag electrode with a recess was not available at the time of the work.

In conclusion, the highest yielding conditions to perform the electrochemical reduction of stilbene were identified as: Ag as cathode, C graphite as anode, with a flow of 0.25 mL/min, a 0.1 M concentration of starting material in THF/MeCN = 9/1, 160 mA of current (4.0 F), room temperature and 1.2 equivalents of TBABr as supporting electrolyte.

3.6 Gigantol

Gigantol is a substituted bibenzyl that is found in nature, together with other bibenzyl derivatives, in particular is extracted from the stem of *Dendrobium* Orchidaceae species (figure 3.1). These plants are commonly used in traditional Chinese medicine for the treatment of different health conditions: gastritis, inflammations, cardiovascular diseases.[234–237] Interest in these compounds has grown over the years as a result of these bioactivities, and recent studies seem to confirm their bioactivity not only for the treatment of the previously cited health conditions, but adding anti-oxidant, anti-coagulating, anti-mutagenic and anti-cancer activity.[238] In particular Gigantol shows cytotoxic activity against lung cancer, overcoming its metastasis[239] and against the proliferation of liver cancer.[240]

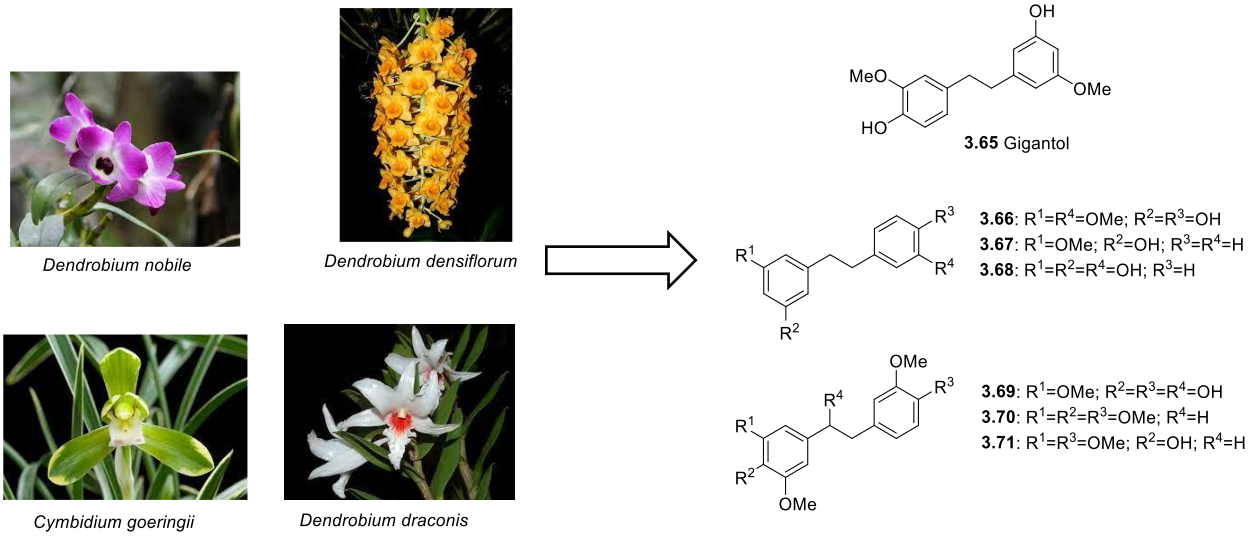

Figure 3.1: examples of Orchidaceae species and the substituted bibenzyls extracted from their stems.

Several of these bibenzyl compounds can be extracted from the stems of the plant using EtOH and the extract can then be columned or purified by HPLC in order to isolate the different components.[235] In 1982, Crombie and Jamieson[241] described a synthetic approach for Canniprene (Scheme 3.17), a member of the bibenzyl(dihydrostilbene)-spiran-dihydrophenantrene group of metabolites of *Cannabis sativa*. This approach starts with a Wittig olefination between phosphonium salt **3.72** and aldehyde **3.73** and subsequent protection of the phenol functionality with a benzoyl group. Then, by hydrogenation over palladium on carbon, they simultaneously hydrogenated the stilbene double bond and removed the benzyl group. Compound **3.76** was obtained by etherification using 3-chloro-3-methylbutyne; the triple bond was selectively reduced to double bond by hydrogenation over Lindlar catalyst and finally the desired product **3.78** was obtained by Claisen rearrangement and deprotection of the benzoyl group.

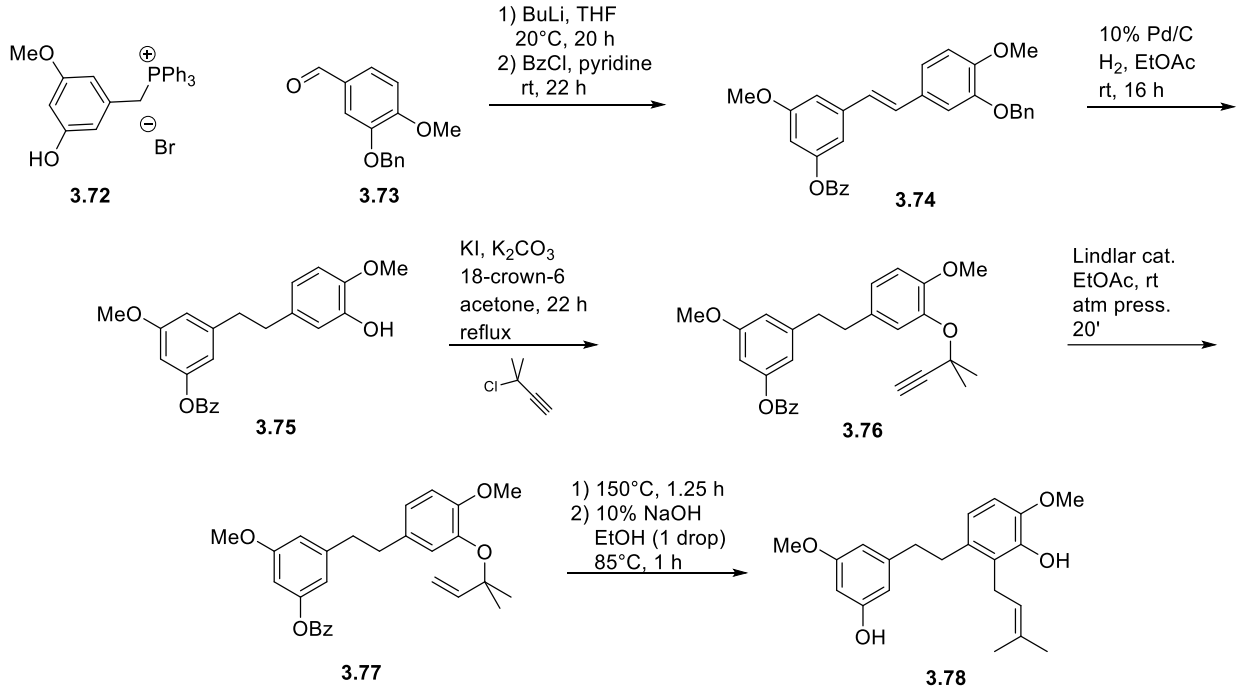

Scheme 3.17: Crombie and Jamiesons' synthesis of canniprene (**3.78**).

In 2015, Wei and co-workers reported syntheses of gigantol and other analogues (Scheme 3.18),[238] adapting and modifying the synthetic path previously described by Crombie. Analogues **3.79** and **3.80** were synthesised starting from aldehyde **3.81** by $NaBH_4$ reduction to alcohol followed by conversion to the phosphonate **3.82** by reaction with PBr_3 to form the corresponding bromide and then with $P(OEt)_3$ (Scheme 3.18a). Wittig olefination, alkene hydrogenation over Palladium on carbon and demethylation using BBr_3 afforded **3.79**. Similarly, compound **3.80** was prepared starting from the same aldehyde, by mono-demethylation using sodium ethanethiolate in DMF, followed again by Wittig olefination and palladium on carbon hydrogenation (Scheme 3.18a).

The synthesis of Gigantol also followed a similar overall process, based again on Wittig olefination and subsequent hydrogenation of the double bond (Scheme 3.18b).

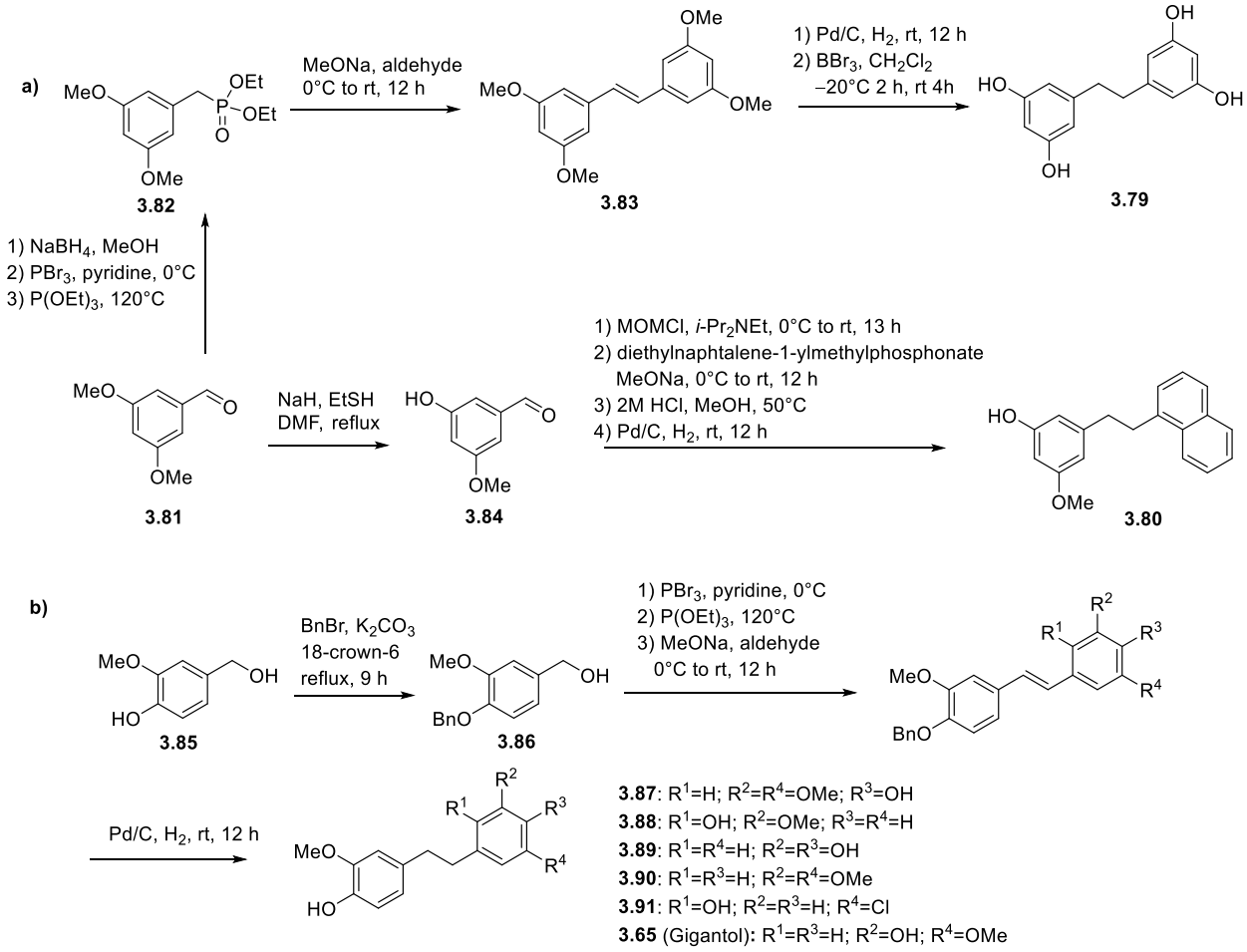

Scheme 3.18: Synthetic approach to gigantol (**3.65**) and its analogues by Wei and co-workers.

In light of our promising results for the reduction of stilbene to bibenzyl, we decided to apply our electrolysis approach for the hydrogenation of a gigantol precursor **3.96**, replacing the use of a metal catalyst and avoiding the need for hydrogen gas. For the synthesis of the stilbene precursor **3.96**, the procedure reported by Wei and co-workers was followed, but modifying some steps due to issues encountered during the synthesis (Scheme 3.19). First , selective mono-demethylation of 3,5-dimethoxybenzaldehyde (**3.81**) was performed using the procedure described by Castedo and co-workers,[242] giving phenol **3.84** in 87% yield. Then the phenolic group was protected using MOMCl in 76% yield.[243]

For the other fragment, the hydroxyl group of vanillin (**3.92**) was first protected using MOMCl and then the aldehyde functionality was reduced with $NaBH_4$.[243] The benzyl group was replaced by MOM as a protecting group for both phenolic hydroxyl groups to avoid an additional deprotection step. Benzyl alcohol **3.94** was transformed to phosphonate **3.95**. The literature procedure, using PBr_3 afforded the bromide,[238] although the reaction was very messy and the final compound was prone to degradation. Instead, the corresponding benzyl iodide was prepared by Appel reaction with PPh_3, imidazole and iodine.[243] By the literature procedure, the next step was performed using

triethyl phosphite as solvent, but with approach the purification of the crude mixture proved to be difficult; by column chromatography was impossible to separate the product from the phosphite. So the method was adapted performing the reaction in toluene under reflux using only 0.9 equivalents of triethyl phosphite.[243] Phosphonate **3.95** was obtained with a low 30% yield due to partial degradation of the starting material and also to the formation of MOM deprotected phosphonate (≈35%). The deprotected side product was resubjected to reaction with MOMCl and used in the next step. Finally the Horner–Emmons olefination between **3.93** and **3.95** was performed,[243] affording the substituted stilbene **3.96** in 40% yield. With compound **3.96** in hand, the electrolysis step was performed under the optimised conditions. Thus, a solution of stilbene **3.96** in a 9/1 THF/MeCN mixture, with TBABr as supporting electrolyte, was passed through the Ammonite 8 reactor using Ag cathode and C graphite anode, at a flow of 0.25 mL/min and applying a charge of 4.0 F. Gratifyingly, the desired product **3.97** was obtained in 55% yield after purification by column chromatography (Scheme 3.19)., representing a formal synthesis of the natural product with introduction of an electrochemical hydrogenation step.

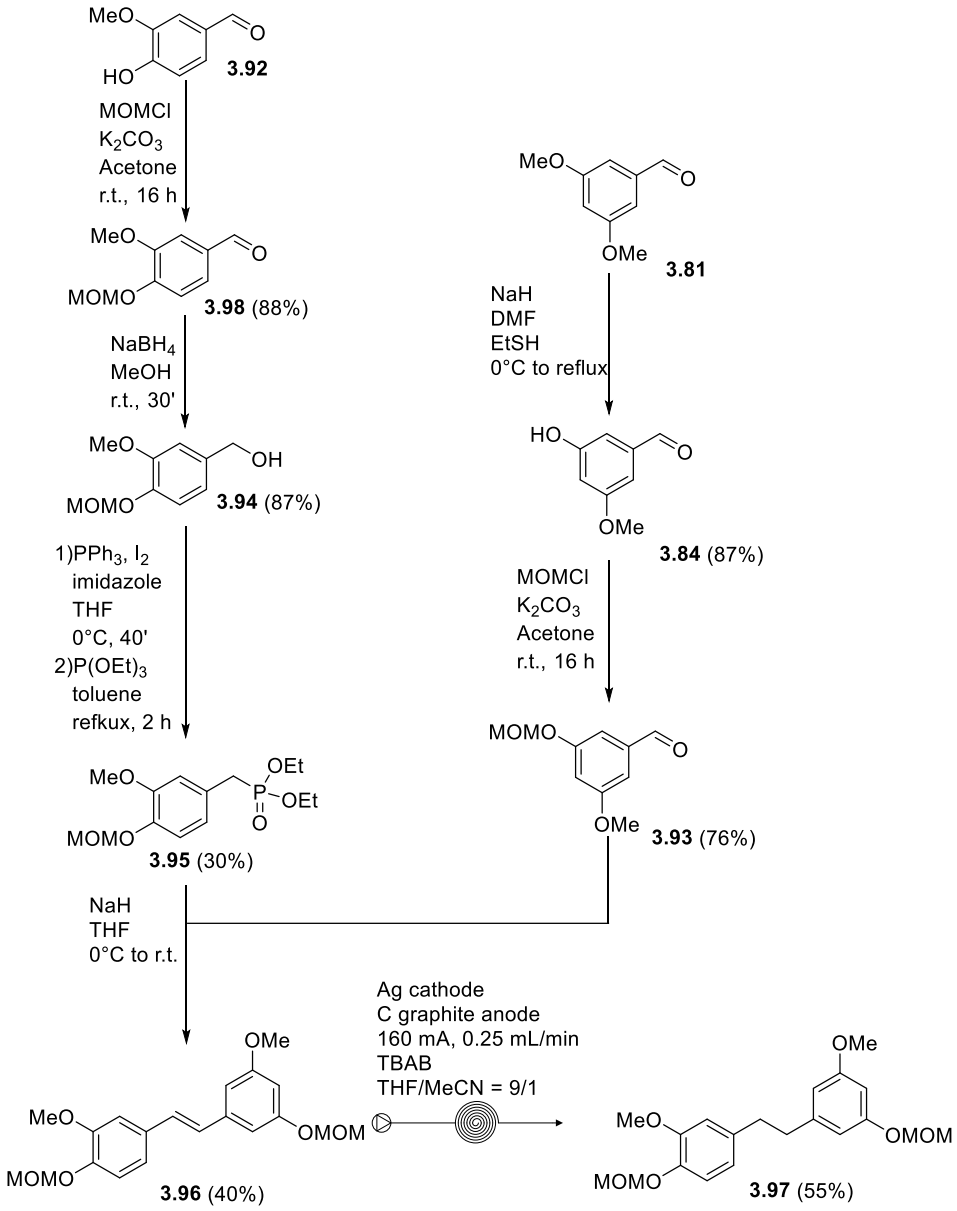

Scheme 3.19: synthesis of MOM-protected gigantol **3.97** through our electrolysis method in the Ammonite flow reactor.

To summarise, our developed electrolysis method was applied to the synthesis of a pharmaceutical intermediate, achieving an acceptable 55% yield for the hydrogenation of stilbene derivative **3.96**. Cathodic electrolysis was used in place of the classical hydrogenation over a Pd on carbon catalyst, avoiding the use of hydrogen gas and a transition metal catalyst. The electrolysis carried out on a 0.5 mmol scale required 30 min, relatively mild conditions, without the need for hydrogen gas, which was replaced with electrons from electricity and protons from the reaction solvent MeCN.

3.7 Investigation of the substrate scope for the cathodic alkene reduction

With the optimised conditions in hand, the substrate scope was investigated under the optimised conditions described above. All the reported yields are for isolated pure compounds. As previously described, *E*-stilbene (**3.64**) was reduced to bibenzyl (**3.52**) in 80% yield, and the gigantol intermediate **3.96** gave the hydrogenation product **3.97** in 55% yield. Different substrates that were already available in our laboratory bearing a styrenic double bond were then tested; cathodic reduction of tri-substituted alkenes *trans*–α–methylstylbene **3.98** and triphenylethylene 3.**101** afforded **3.99** (81%), and **3.100** (77%), respectively. 1,1-Diphenylethylene also underwent reduction using the electrochemical method to give 1,1-diphenylethane (**3.102**). Two further simple styrene derivatives, 1-phenylcyclohexene and 1,2-dihydronaphthalene, were reduced to afford **3.104** in 62% and **3.106** in 76%, respectively.

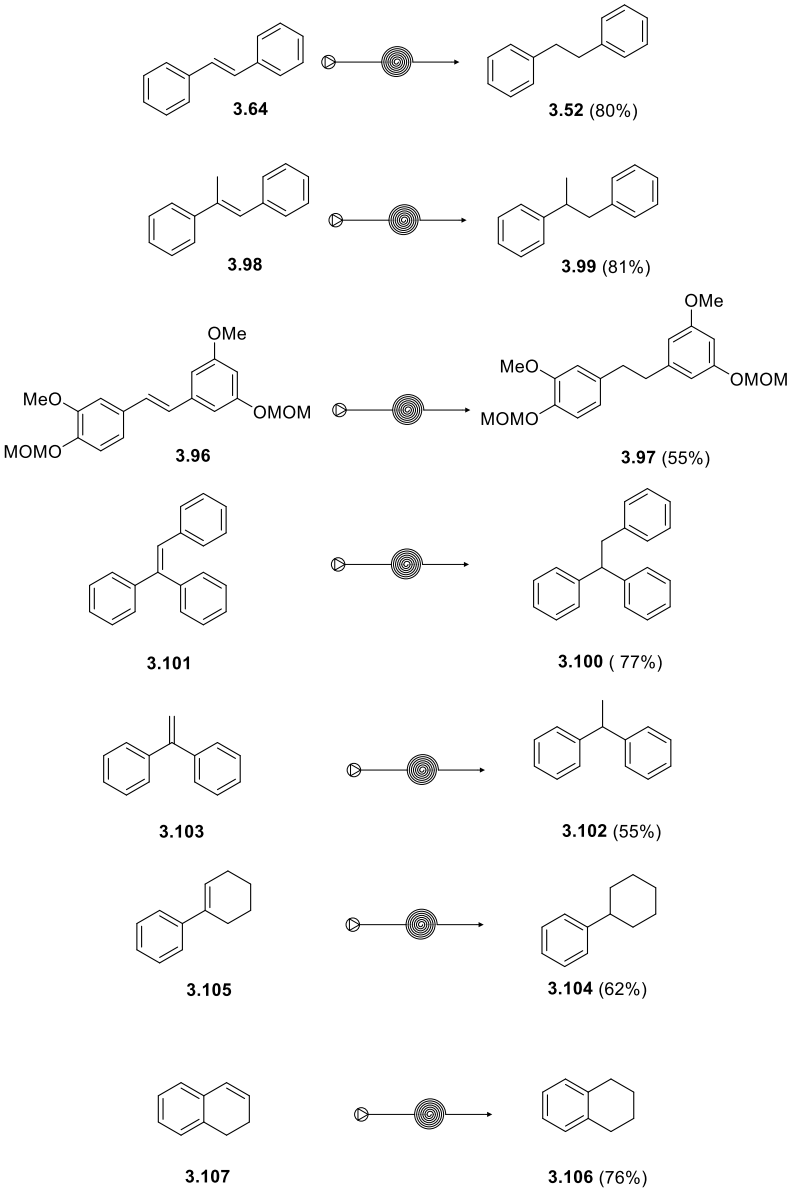

Electrolysis conditions: Ag cathode; C graphite anode; 0.1 M substrate; 160 mA; 0.25 mL/min; TBAB (1.2 equiv); THF/MeCN = 9/1

Scheme 3.20: Substrate scope for electrochemical reduction.

In order to establish whether a styrene-type double bond is required for the cathodic reduction process, we decided to investigate prenylated phenol ether **3.107**, which was easily synthesised by reaction of phenol **3.108** with 3,3-dimethylallylbromide (**3.109**).[244] In this case the electrolysis just returned starting material was recovered, indicating that double bonds containing conjugation are required for electrochemical reduction (Scheme 3.21). Indeed, initial single electron-transfer in the case of phenol ether **3.107** would likely involve the aryl system, making further electron-transfer to the alkene even more challenging to achieve.

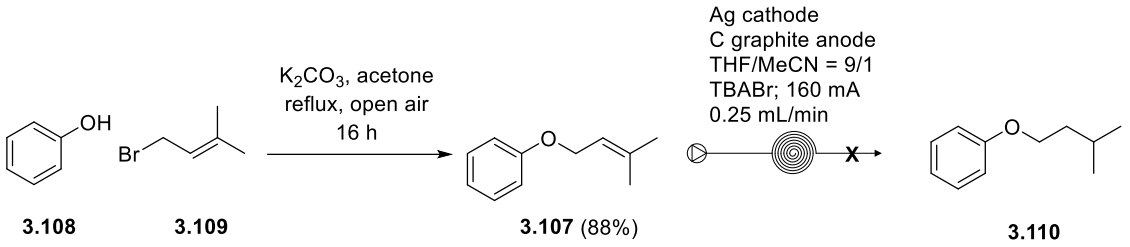

Scheme 3.21: Synthesis of prenylated phenol **3.104** and attempted electrochemical reduction.

Substrate **3.111** containing a vinylogous carbamate functionality was also tested, as its reduction would lead to amino-acid derivatives (Scheme 3.22). Synthesis of the enamine was achieved in 46% following the simple condensation procedure reported by Hebbache and co-workers.[245] Unfortunately, electrolysis of the enamine **3.111** did not afford any of the desired product **3.112**, and instead degradation was observed.

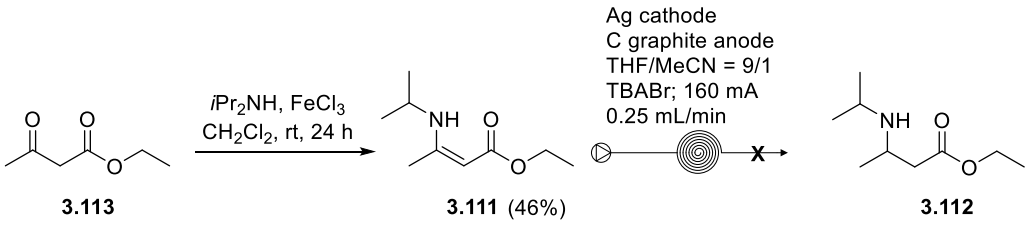

Scheme 3.22: Synthesis of **3.111** and attempted electrochemical reduction to give β-amino ester **3.112**.

In order to further investigate the substrate scope, we decided to test some of the same substrates that underwent the oxidative cyclisation reported in chapter 2. This way, we could demonstrate the possibility that by electrolysis, by simply changing the conditions, the same substrate can give different products. For the same reason *E*-stilbene was subject to the oxidative electrolysis conditions described in chapter 2. Surprisingly we did not obtain exclusively the expected product **3.113**, but acetal **3.114** was also obtained (Scheme 3.23). Formation of the acetal can be accounted for by a semipinacol rearrangement. These two products were obtained respectively in 41% and 33% isolated yield.

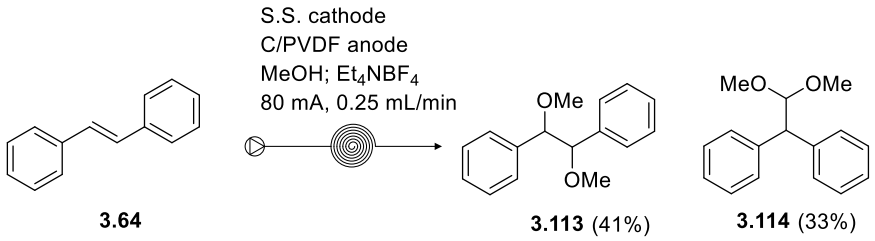

Scheme 3.23: Electrochemical oxidation of stilbene (**3.64**) in the Ammonite flow reactor using the conditions previously described for oxidative cyclisation (chapter 2).

After this interesting result, investigation of the carboxylic acids and hydroxyalkenes used in the electrochemical oxidative cyclisation began under the reduction conditions (Scheme 3.24). Pleasingly, alcohols **2.65** and **3.114** were reduced to the corresponding alkanes **3.63** and **3.115** in isolated yields of 60% and 51%, respectively. However, subjecting alkenol **3.116**, bearing a fluorine in the *para* position, to the reductive conditions gave substantial degradation. Fortunately, it was possible to isolate a small fraction containing three main components. These three compounds were identified from the ^{1}H-NMR and the mass spectra of the mixture as starting material **3.116**, the desired reduction product **3.117** and a compound **3.63** that had undergone defluorination and double bond-reduction (combined yield <10%). In addition, alkenol **2.135** with a CF_3 group in the *para* position was electrolysed under the reductive procedure, with none of the desired product observed. As observed for the fluorobenzene above, some hydrodefluorination was also evident in this case although no pure products were isolated.

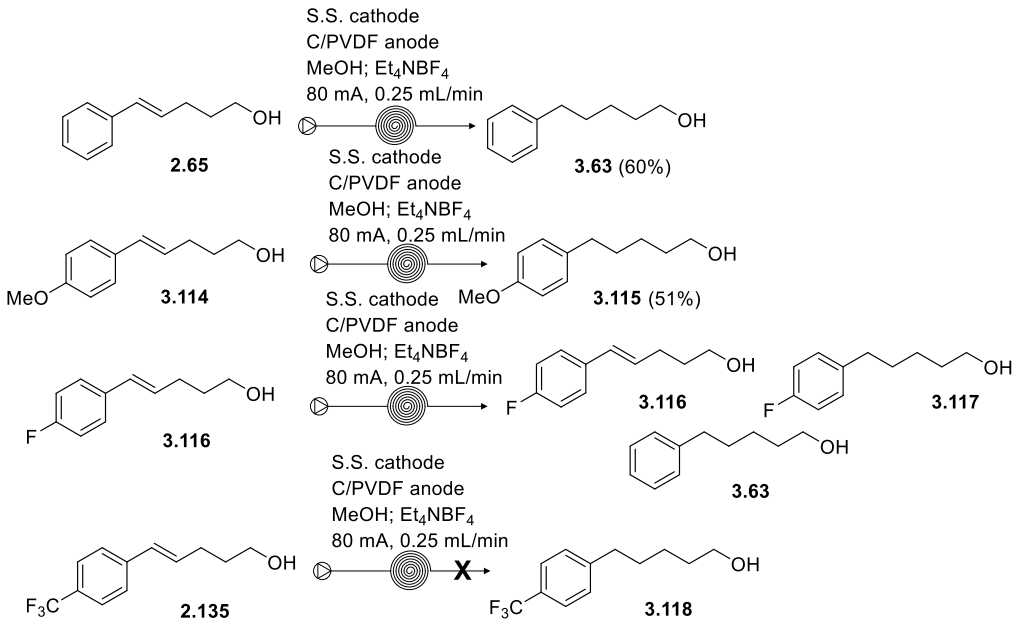

Scheme 3.24: attempts of electrochemical reduction of double bonds in the Ammonite flow reactor.

Furher electrolysis of some of the alkenoic acids under the reductive electrolysis conditions was carried out, but the results were disappointing, with just degradation being observed. Protection of the acid functionality as the corresponding methyl esters[246] had little effect and mainly degradation was observed. However, some traces of the desired reduced products could be observed for the *ortho* and *para*-methoxystryrenes, but only ester **3.124** was isolated in 10% yield (Scheme 3.25).

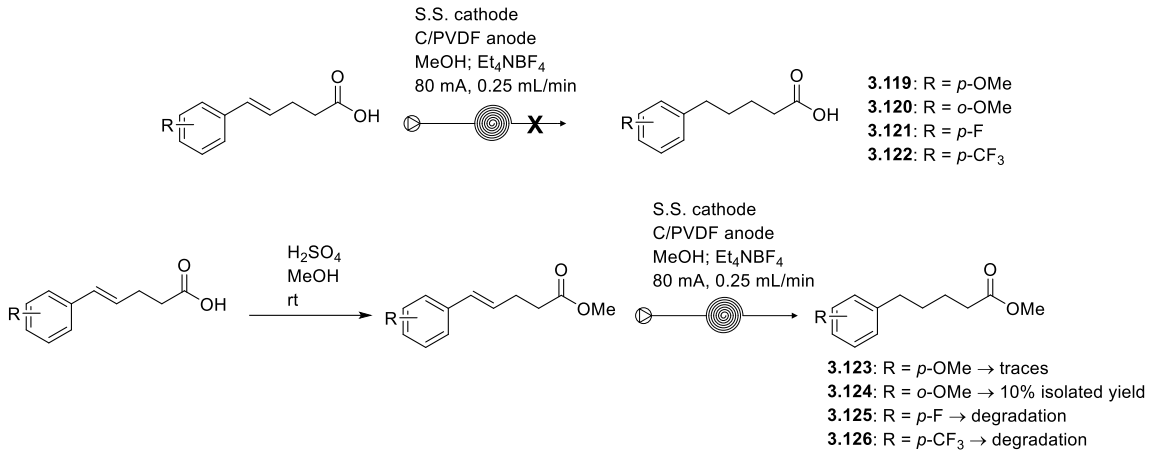

Scheme 3.25: Attempted of electrochemical reduction of alkenoic acids and esters in the Ammonite flow reactor.

Unfortunately, due to the disappointing results obtained the substrate scope appeared to be more limited and the decision was made not to explore the reaction further. As just described, the electrolysis method developed proved to work efficiently with styrene double bond without the presence on the molecule of other group that could possibly undergo reduction, like carbonyl group; instead the presence of a hydroxyl functionality seemed to not affect the reduction (see product **3.63** and **3.115**). Unactivated double bonds seemed to resist to this hydrogenation conditions (see Scheme 3.21) and that could possibly mean that this approach can selectively reduce certain double bonds in the presence of others on the same molecule. Substrates carrying a fluorine atom on the aromatic ring apparently undergoes defluorination and this will be the topic of the next section 3.9.

3.8 Mechanistic studies for the reduction of stilbene

In order to develop an understanding of the mechanism of the electrochemical reduction of stilbene, selected experiments and CV studies were conducted. These are described in this section.

Cyclic voltammetry experiments were carried out in a two compartment cell using a vitreous carbon disc (diameter 3 mm) working electrode, a Pt wire counter electrode and an aqueous saturated calomel electrode (SCE) reference electrode mounted in a Luggin capillary. An Autolab PGStat204 potentiostat with Nova 1.9 software was used and responses were analysed using Nova 1.9 software. All cyclovoltammetry was performed with a 5.0 mM concentration of substrate, using 100 mM supporting electrolyte.

As shown in Figure 3.2, from the cyclic voltammogram of *E*-stilbene, three reduction peaks are observed, two of them reversible. The first one at –1.15 V is related to oxygen reduction to its

radical anion (this signal is known in literature),[247] probably the solution has not been degassed for enough time. The other two peaks are due to the reduction of €-stilbene, and are consistent with its cyclic voltammogram and reduction potentials reported in literature.[248] A reversible peak at –2.29 V corresponds to the first reduction of stilbene to its radical anion, while the second irreversible peak at –2.69 V is relative to the second reduction to the dianions that immediately react with two protons to give the bibenzyl product. This last peak is not reversible.

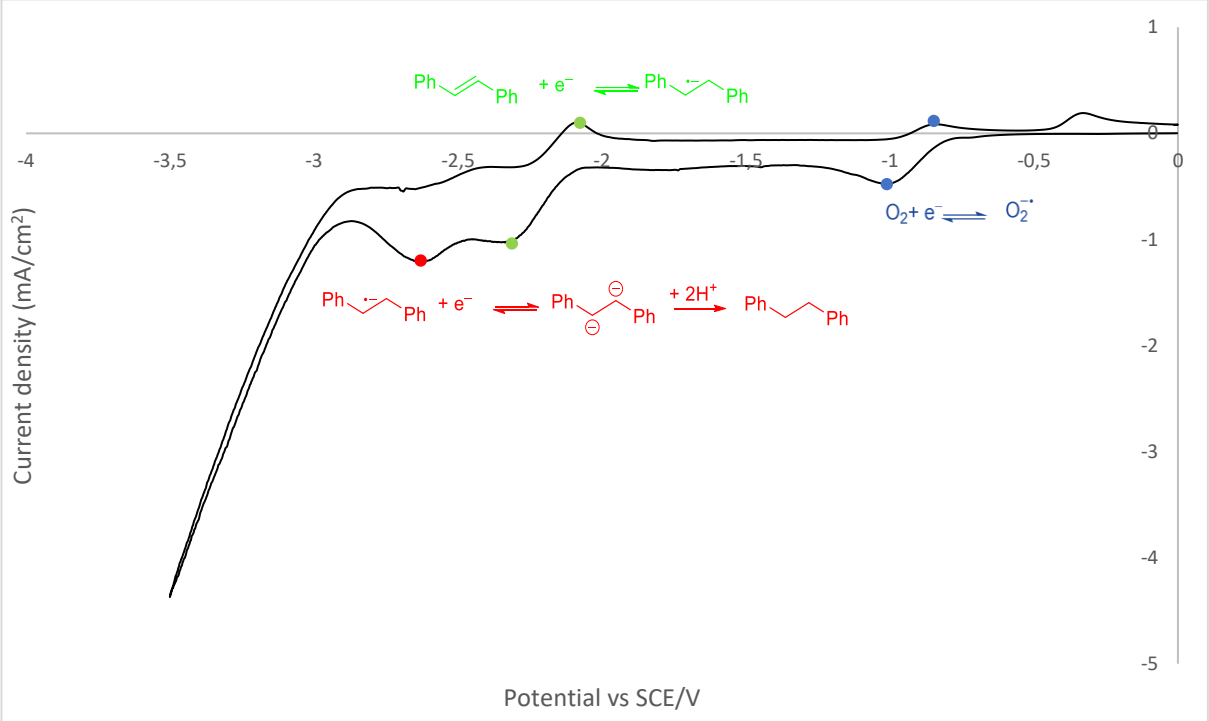

Figure 3.2: Cyclic voltammogram of *E*-stilbene **3.65** potential scan rate 25 mV s^{-1};THF/MeCN; scan range 0 to –3.5 V

In all electrochemical processes, there has to be a counter reaction; in this case, to balance the reduction of the *E*-stilbene, a compound that readily undergoes oxidation is required in the system. This compound is TBABr, which does not only serve as supporting electrolyte but also as counter-reagent, giving a source of bromide ion to be oxidised at the anode (Figure 3.3).

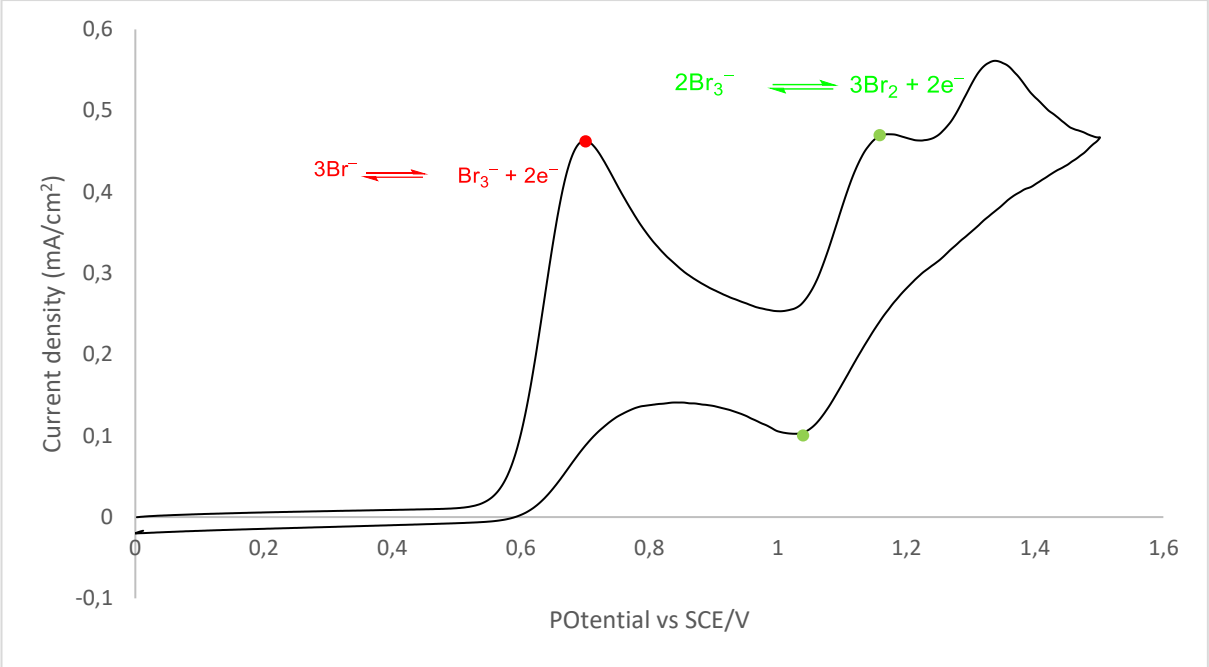

Figure 3.3: Cyclic voltammogram of TBABr potential scan rate 25 mV s^{-1}; THF/MeCN; scan range 0 to 1.5 V.

The cyclovoltammetry for the oxidation of the bromide anion is already known and reported in literature.[249] Br^- can be first oxidised to Br_3^- that can then be oxidised to Br_2. Both step are reversible based on Bard and co-workers[249] but apparently, using a glassy carbon electrode, Br_3^- oxidation looks less reversible on carbon and this apparent change in kinetics is believed to be due to nonelectroactive adsorbed species interfering with the $Br^-/Br_3^-/Br_2$ reaction. This seems to be also the case as shown in Figure 3.3, where two peaks appear at 0.69 V and 1.16 V, respectively. The other oxidative peak at 1.3 V is due to some moisture in the solution.

After the cyclic voltammetry experiments,some deuterium labelling experiments were tried in order to understand if the mechanism was based on a H atom or H^+ abstraction and identify the source of that. At first, the reaction was run using deuterated THF considered a possible source of $H^{\cdot}$ but no deuterated bibenzyl was observed (Scheme 3.26).

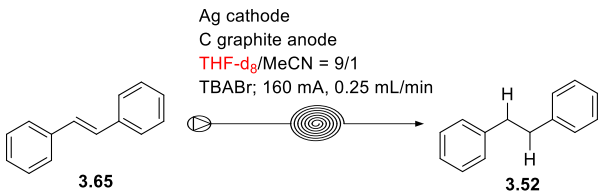

Scheme 3.26: deuterium-labelling experiment using THF-d_8.

On the basis of the initial experiment in deuterated solvent, the hydrogen source would have been a proton donor rather than H atom abstraction, so despite the mechanistic insights reported by Ge and Li in their work on electrochemical reduction of olefins[229] were not very clear, it seemed plausible that the supporting electrolyte tetraalkylammonium ion may have acted as a proton source. To try to substantiate this hypothesis, an attempt was made to synthesise a

deuterium-labelled TBAB (tetrabutyammonium bromide) (**3.119**) starting from commercially available deuterated butanol **3.120** (Scheme 3.27).

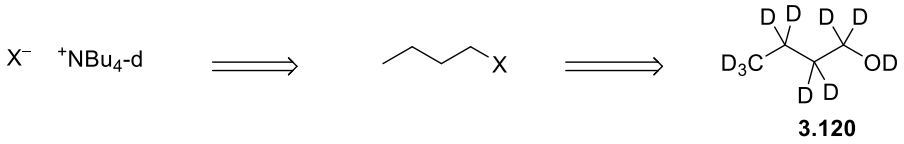

3.120

Scheme 3.27: General approach to the synthesis of X^{-} $^{+}NBu_4$-d.

Before using the more costly labelled starting material, the right reaction conditions were investigated using unlabelled material (Scheme 3.28). Starting from 1-bromobutane (**3.121**), reaction with a solution of ammonia in methanol was attempted to form tributylamine adapting a procedure reported by Maekewa and co-workers.[202] After 1 h at room temperature, only starting material was observed, so the reaction was heated under reflux. After 2 h under reflux formation of some dibutylamine was observed, and after 16 h a mixture of dibutylamine, tributylamine and also TBABr was obtained. Modification of the reaction conditions to avoid losing both the ammonia and the bromo-butane involved lowering the temperature to 40°C, and addition of K_2CO_3 to neutralise excess HBr gave improved results. The reaction solvent was changed from MeOH to MeCN, as TBABr remained in solution whereas the inorganic salts were insoluble. Under the modified conditions, with an excess (8 equiv) of alkyl bromide, a yield of 58% was achieved. To avoid the issue of volatility of ammonia, a parallel reaction between 1-bromobutane and dibutylamine was carried out, giving the tetraalkylammonium bromide in 86% yield. Ultimately, even the presence of two deuterated chains would be expected to provide some deuteration in the electrochemical process and useful data on the reaction mechanism.

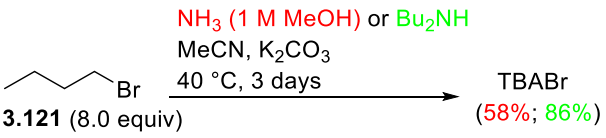

Scheme 3.28: alkylation of NH_3 and Bu_2NH with bromobutane **3.121** to give TBABr.

Once the formation of the quaternary ammonium salt was optimised, the method for synthesis of bromobutane starting from butanol **3.122** was investigated. First butanol was reacted with Ph_3PBr_2 following a procedure reported in the literature,[250] but the desired alkyl bromide product was produced in a very low yield (less than 20%). It is believed that the low yield obtained in our hands was due to the quality of the Ph_3PBr_2. An alternative procedure reported in the same paper,[250] reacting butanol with PBr_3 also proved unsuccessful with no trace of the desired product. From the optimisation process we knew that TBAI also worked as supporting electrolyte, so attention turned to the conditions reported by Wang and co-workers[243] to make iodobutane as a less volatile alkylating agent, again starting from butanol by reaction with triphenylphosphine,

imidazole and iodine (Scheme 3.29). After just 40 minutes full conversion was achieved and the crude product was of sufficient purity to be used directly in the reaction with dibutylamine, which yielded the desired ammonium salt.

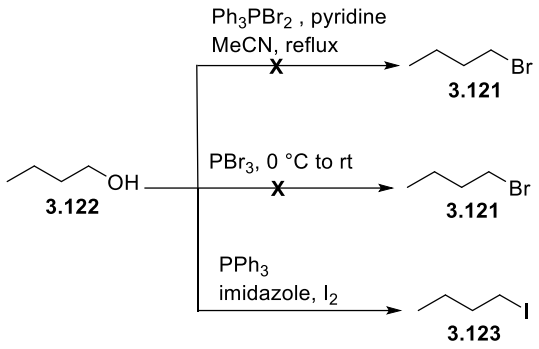

Scheme 3.29: Attempted preparations of *n*-butyl halides from *n*-butanol.

With the reaction conditions in hand we went on to apply them to the synthesis of the deuterated butanol, and the desired ammonium salt **3.124** was obtained in 40% yield (Scheme 3.30).

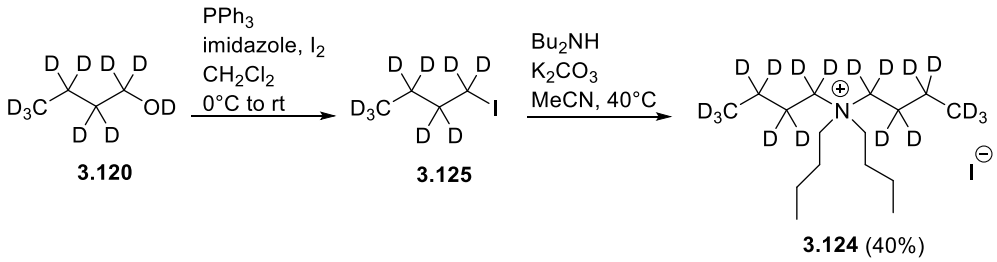

Scheme 3.30: Synthesis of the deuterated supporting electrolyte **3.124**

With the deuterium-enriched tetraalkylammonium electrolyte **3.124** in hand, the electrolysis reaction was repeated (Scheme 3.31). However, no observable deuterium incorporation into the bibenzyl product **3.52** was observed by ^{1}H-NMR and GC-MS.

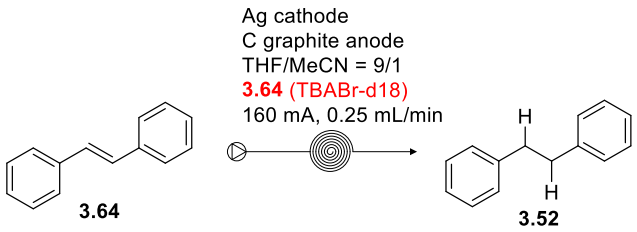

Scheme 3.31: Attempted deuterium-labelling experiment using deuterated supporting electrolyte **3.124**

As, even with only partial deuteration of the supporting electrolyte, some deuterium incorporation would be expected if that was the source of deuterium, at this point the most reasonable sources of protons in the electrolysis medium would be any trace water present in the solvents and the MeCN itself, which was added in order to dissolve the supporting electrolyte.

Not considering the MeCN previously was an oversight, as it is the most acidic component of the reaction mixture (pK_a = 31.3), and an electrolysis carried out using MeCN-d_3 showed full deuteration in the bibenzyl product **3.52-d_2**; by ^{1}HNMR the singlet at 2.95 ppm for the four aliphatic protons integrated only for two protons because of the successful deuteration (Scheme 3.32). In addition, another experiment conducted by adding a couple of drops of D_2O gave also gave a high level of deuteration of the reduced product; this time a 65% of deuterated product **3.52-d_2** was observed in the ^{1}H-NMR compared to a 35% of non-deuterated bibenzyl **3.52**.

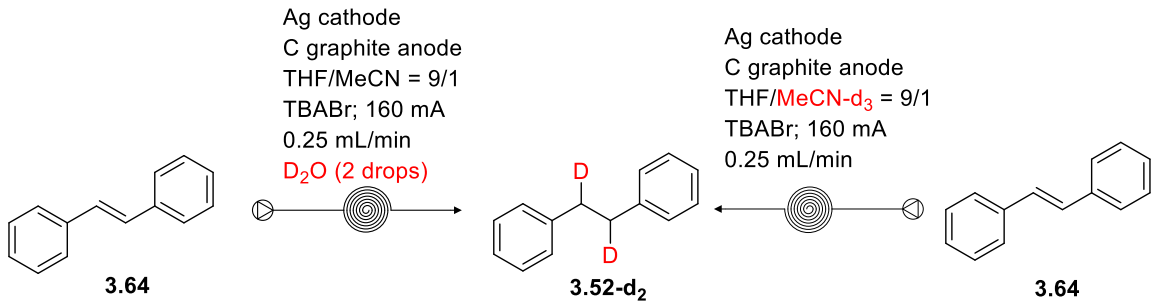

Scheme 3.32: Deuterium-labelling experiments using D_2O and MeCN-d_3.

The labelling result was confirmed by GC-MS (Figure 3.4).

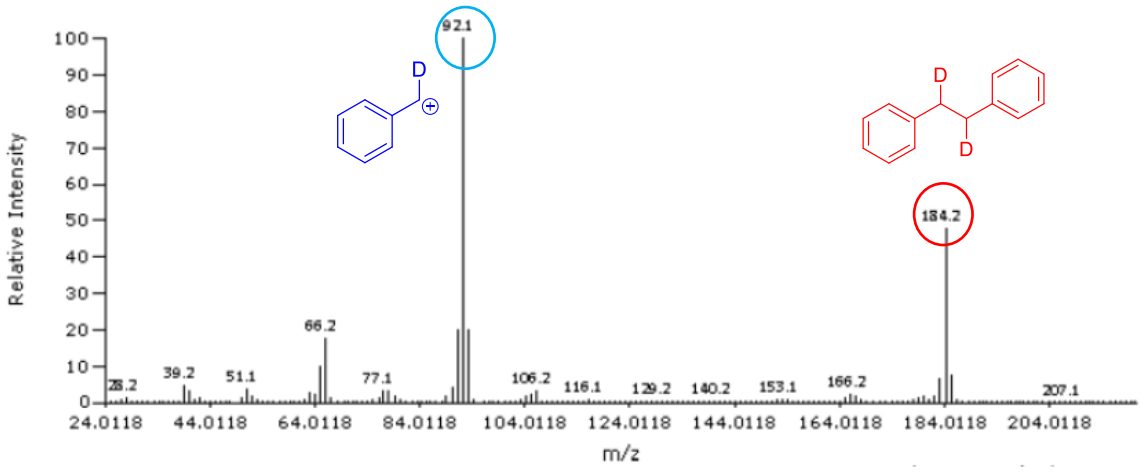

Figure 3.4: GC-MS spectrum (EI) of deuterated bibenzyl **3.52-d_2** showing high level of incorporation.

Ultimately, the source of the "hydrogen" in the electrolysis product was confirmed to originate from acid protons, either in the CH_3CN co-solvent or water present in bench solvent. This seems to be consistent with an EEC type mechanism, as shown in the cyclic voltamogram in Figure 3.1, where two sequential electron-transfers lead to the formation of dianion that is protonated by an acidic component of the reaction medium (CH_3CN co-solvent or water).

3.9 Defluorination side-reaction

The hydrodefluorination observed when the fluoroaryl and trifluoromethyl compounds were subjected to the cathodic electrolysis conditions was an unexpected result, and was investigated further. Fluorine is the most electronegative element on the periodic table (χ = 4) and its bond with carbon is the strongest in organic chemistry (105 Kcal/mol).[251,252] Fluorinated fragments are present in many molecules, from drugs to agrochemical compounds and polymers. The presence of fluorine atoms in a molecule can indeed influence significantly its physical, chemical and biological properties.[251,253–255] Over the years, different approaches have been used for the activation of the C—F bond and in particular for the selective activation of one of them in trifluoromethyl derivatives. The most common methods require the use of Lewis acids, in particular silicon, due to its affinity for the fluorine atom or metal catalysts. Some attempts of using electrochemistry are reported in literature but the most recent examples exploit visible light and photocatalysis.

In 1997, Thiebault and co-workers, reported the cyclic voltammetry studies of the reductive cleavage of the C—F bond in fluoromethylarenes[256] (Scheme 32). To study the effect of the solvent and the temperature on the reduction process, the experiments were run:

- In liquid ammonia at –38 °C using KBr as supporting electrolyte, a gold working electrode, a platinum counter electrode and an Ag^+/Ag reference electrode.
- In DMF at 20 °C using nBu$_4$NBF$_4$ as supporting electrolyte, a carbon working electrode, a platinum counter electrode and an aqueous SCE reference electrode.

The experiments, run on a series of different fluorinated arenes, demonstrated that the process, unlike chlorinated and brominated compounds, does not go through a carbene intermediate but instead involves a first electron-transfer, fluoride expulsion, a second reduction and a final protonation (Scheme 3.33). The rate of defluorination increases from the trifluoro to the difluoro to the monofluoro compound.

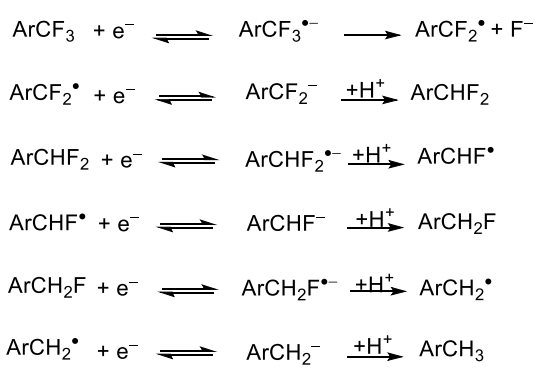

Scheme 3.33: Electrochemical defluorination mechanism described by Thiebault.

In 1999, Uneyama *et al*.[257] reported the synthesis of enol ethers *via* reductive hydrodefluorination using a lead cathode and a carbon anode in MeCN, in presence of TMSCl, Et_3N and nBu_4NBr as supporting electrolyte (Scheme 3.34).

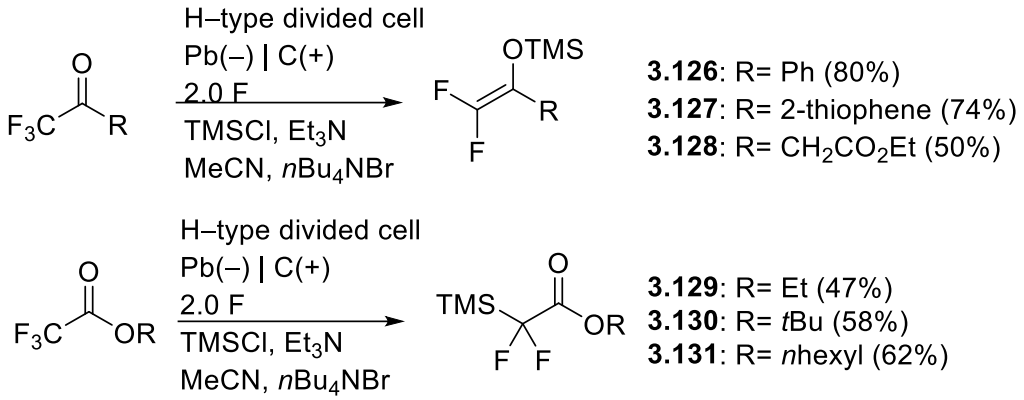

Scheme 3.34: Electrochemical hydrodefluorination by Uneyama.

In 2008, Senboku and co-workers[258] reported the electrochemical carboxylation of difluorotoluenes in presence of CO_2, using a platinum cathode and magnesium anode (scheme 3.35).

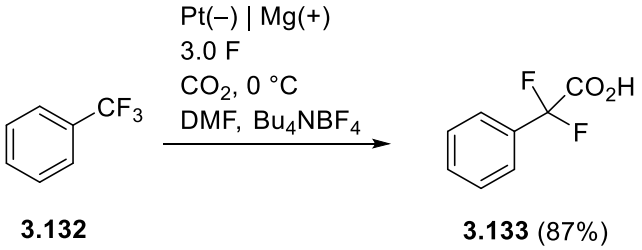

Scheme 3.35: Electrochemical carboxylation of difluorotoluenes by Senboku.

In 2011, Cao and Wu reported a Nickel catalysed hydrodefluorination of fluoroarenes and substituted benzotrifluorides with lithium triethylborohydride as reducing agent.[259] The nickel catalyst is reduced by the superhydride to Ni^0 that then undergoes oxidative addition to the fluorinated substrate. Superhydride then attacks this intermediate replacing the fluorine and finally reductive elimination affords the desired product (Scheme 3.36).

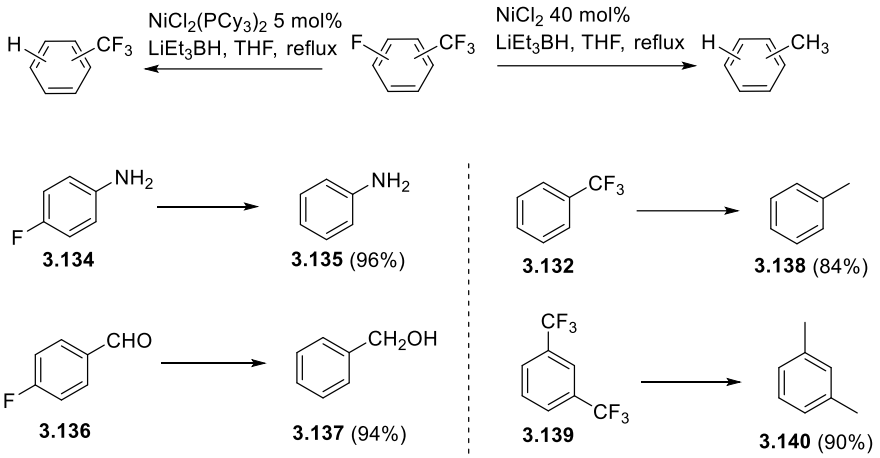

Scheme 3.36: Nickel-catalysed hydrodefluorination of fluoroarenes and trifluorotoluenes with superhydride.

In 2013, Oestreich and co-workers reported in their review a series of methods catalysed by Lewis acids for the hydrodefluorination of C—F bonds.[251] Most of these examples use Silicon compounds as Lewis acids, as the highly fluoridophilic silicon cation is able to cleave the C—F bond forming a carbenium ion and a fluorosilane.

An example is the work of Ozerov and co-workers.[260] They reported a C—F activation method based on the abstraction of a F^- by a strong Lewis acid tricoordinate silicon cation followed by hydride transfer from the Et_3SiH.

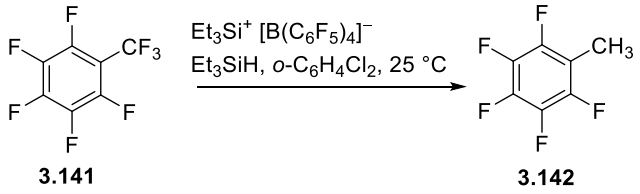

Scheme 3.37: Ozerov's defluorination by silicon Lewis acid derivatives.

Müller and co-workers in 2006 also provided a method where the silycium cation serves both as Lewis acid and hydride source. A key role is apparently played by the counter ion and its weak coordinating nature.[261]

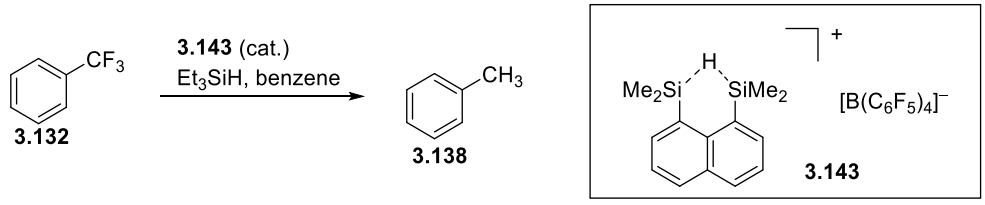

Scheme 3.38: Müller's defluorination by silicon Lewis acid derivatives.

Vol'pin *et al*. showed another approach that instead of using a silicon cation as Lewis acid, a combination of $AlCl_3$ and Et_3SiH can be used. Hypotheses for the mechanism involve $AlCl_3$ leading to a fluorine chlorine exchange and subsequent hydrogenolysis; $AlCl_3$ activate the hydrosilane with subsequent generation of the fluoro-silicon species that gives rise C—F bond cleavage.[262]

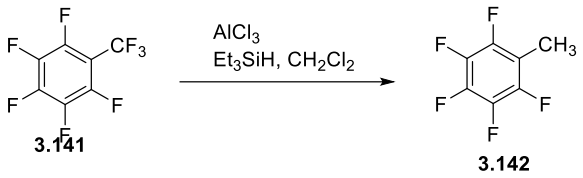

Scheme 3.39: Vol'pin's defluorination approach based on acombination of $AlCl_3$ and Et_3SiH.

In 2013 Oestreich *et al*. developed a method for hydrodefluorination where a Ruthenium complex salt is used to activate the organosilane, abstracting a hydride and generating the silicon cation that is able to defluorinate the molecule.[263]

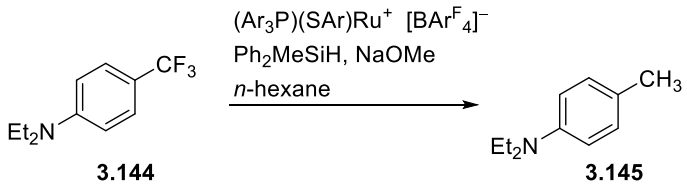

Scheme 3.40: Oestreich's hydrodefluorination *via* Ru complex.

In the review[251] are reported also some example where instead of the silicon, elements of the third group, like aluminium and boron, are used as Lewis acid.

An example to that extent, is the work by Nicolaou *et al*. where AlH_3 is used to hydrodefluorinate a glycosyl fluoride. The role of AlH_3 is to serve both as hydride source and Lewis acid.[264]

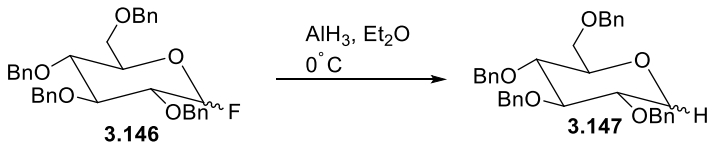

Scheme 3.41: Nicolaou's hydrodefluorination of a glycosil fluoride.

Alcarazo and co-workers reported instead in 2010 a method where a combination of hexaphenylcarbodiphosphorane and $B(C_6F_5)_3$ is used to activate the carbon-fluorine bond.[265]

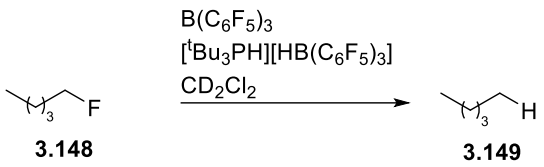

Scheme 3.42: Alcarazo's method for the activation of C—F bonds.

In 2016, Lalic and co-workers[254] reported the metal-catalysed activation of C—F bond to selectively hydrodefluorinate $ArCF_3$ to $ArCHF_2$ (Scheme 3.43). Their method requires a combination of Palladium acetate and copper fluoride to activate the C—F bond, Ph_3SiH to stabilise the intermediate and *t*BuOH as source of proton.

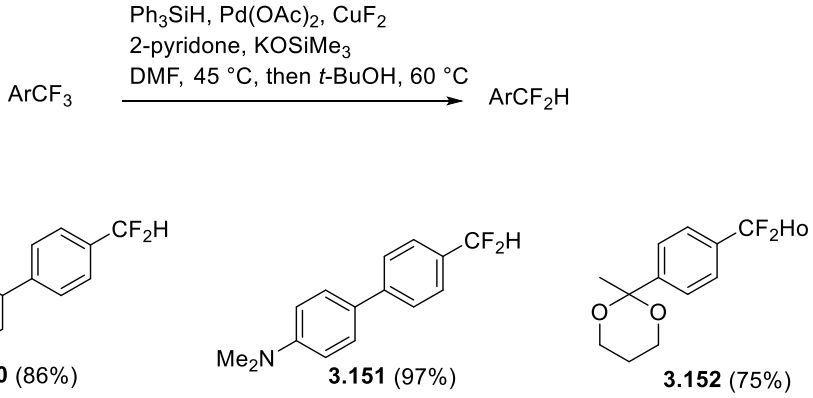

Scheme 3.43: Lalic's catalytic activation of a single C—F bond in trifluoromethyl arenes.

In 2017, König *et al*.[266] described their visible light- catalytic method for the activation of C—F bond in trifluoromethylarene and the selective cleavage of just one fluorine. This method requires a combination of TMP and HBpin as Lewis acid to activate the C—F bond and an Ir photocatalyst; once generated the $Ar—CF_2^{\cdot}$ radical, it can be trapped by methacrylamide that can also act as proton source (Scheme 3.44).

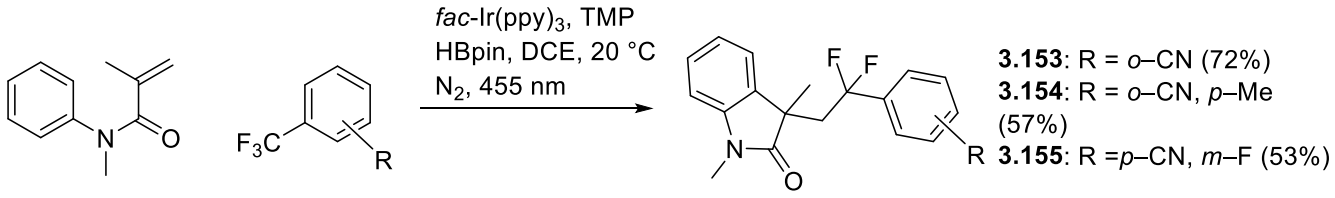

Scheme 3.44: König's selective single C—F bond cleavage in trifuoromethylarenes *via* visible-light catalysis and Lewis acid activation.

Another example of defluoroalkylation and hydrodefluorination of trifluoromethylarenes by photocatalysis was reported by Jui *et al.* (Scheme 3.45).[253] Their method does not need any metals but a combination of Miyake's phenoxazine and thiophenol as catalysts, formate salts and

visible light. They exploit the formation of a difluorobenzylic radical to access a different set of $ArCF_2R$ and $ArCF_2H$ substrates.

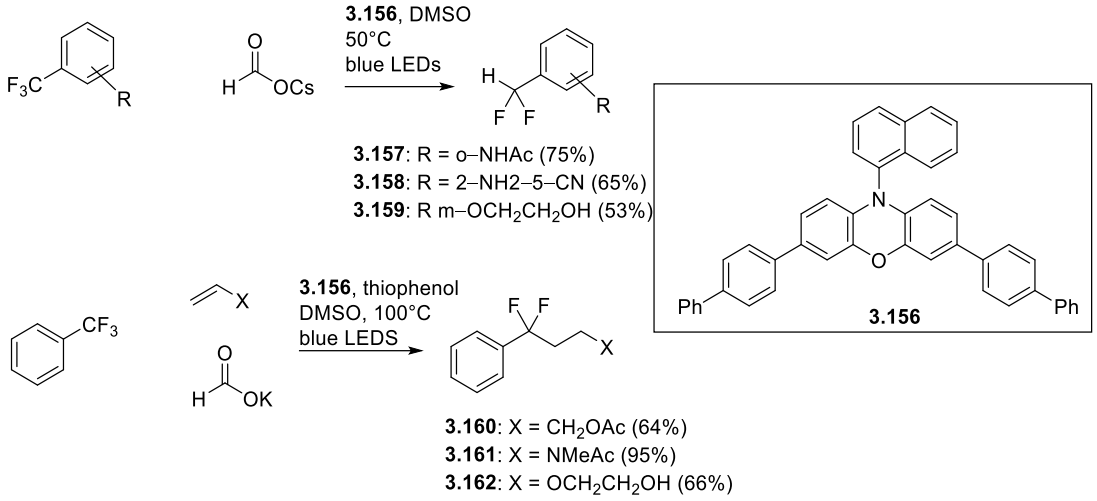

Scheme 3.45: Photo-redox catalysed defluroalkylation of trifluoromethylarenes with unactivated alkenes.

As previously described, while working on the substrate scope, we observed the hyrodefluorination of compounds **3.115** and **2.117**. The reaction gave a lot of degradation so a clean fraction of the products could not be isolated for full characterisation. None the less, these results were considered interesting in terms of a future possible work on electrochemical hydrodefluorination. For this reason, we decided to test these conditions on benzotrifluoride **3.132**. The electrolysis reaction gave full conversion of the starting material and a voltage of 4.41 V was registered. The crude was analysed by GC–MS and two peaks were observed with *m/z* values consistent with the hydrodefluorination products **3.163** and **3.164**. The crude mixture was purified by distillation but because of the small scale of the reaction and the close boiling points of the two, it was not possible to isolate the two compounds, but a fraction corresponding to the mixture of the two was isolated. For both **3.163** and **3.164** the characteristic peaks relative to the aliphatic protons, with a ratio 1:2=**3.164**:**3.163**, and the fluorine peaks matched the data reported in literature: in the ^{1}H-NMR a triplet at 6.67 ppm with a *J* value of 56 Hz for **3.163** and a doublet at 5.40 ppm with a *J* value of 48 Hz for **3.164**; in F-NMR a doublet at –110 ppm with a *J* value of 56 Hz for **3.163** and a triplet at –207 ppm with a *J* value of 48 Hz for **3.164**.[267,268]

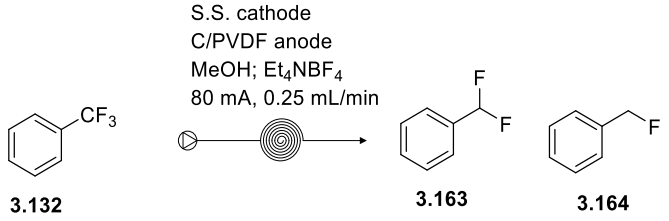

Scheme 3.46: Electrochemical hydrodefluorination of benzotrifluoride using the Ammonite flow reactor.

Unfortunately, insufficient time was available to investigate this interesting preliminary result further, but considering the literature on this subject, especially regarding electrochemistry, this topic could be interesting for future development.

3.10 Conclusions and future work

In summary, we have developed a method for the selective reduction of styrene-double bonds. The reduction is performed in an Ammonite flow electrochemical cell without any oxidant or reducing agent apart from electric current; the reaction proceeds under ambient conditions, in absence of added metal catalyst and especially without the need of H_2 gas. We applied this method to the synthesis of an intermediate of Gigantol, a natural compound use to treat several health conditions. Cyclic voltammetry experiments and some deuterium-labbeling experiments have been run in order to have a better understanding of the process. Unfortunately this method couldn't be applied to molecules bearing a carbonyl group so further studies should be done.

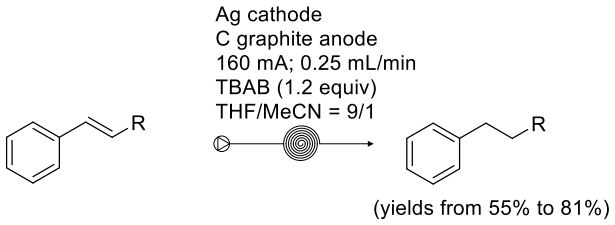

Scheme 3.47: General scheme of our flow electrolysis method for the reduction of styrene double bonds.

While working on the substrate scope a defluorination side-reaction was discovered and considering the literature on this subject, especially electrochemistry related, this reaction should be investigated and developed in the future, especially because of its possible application in the synthesis of fluorinated pharmaceutical intermediates.

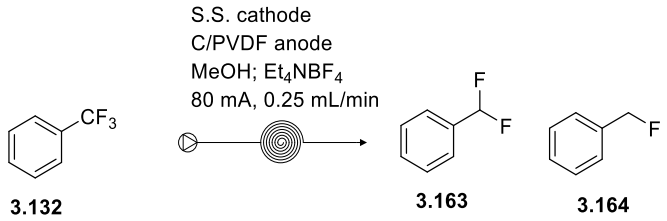

Scheme 3.48: Defluorination side reaction scheme.

Chapter 4 EXPERIMENTAL

4.1 General experimental

Chemicals were purchased from Sigma–Aldrich, Fisher Scientific, Alfa Aesar and Fluorchem. All air/moisture sensitive reactions were carried out under an inert atmosphere, in oven–dried or flame–dried glassware.

Tetraethylammonium tetrafluoroborate (Alfa Aesar, 99%) was recrystallised from hot methanol and dried at 60 ºC under reduced pressure (~10 mbar) for 24 h.

CH_2Cl_2 (from CaH_2) was distilled before use, and where appropriate, other reagents and solvents were purified using standard techniques.

TLC was performed on aluminium plates precoated with silica gel 60 with an F_{254} indicator; visualised under UV light (254 nm) and/or by staining with potassium permanganate.

Flash column chromatography was performed using high purity silica gel, pore size 60 Å, 230–400 mesh particle size, purchased from Merck.

^1H NMR and ^{13}C NMR spectra were recorded in $CDCl_3$ (purchased from Cambridge Isotope Laboratories) at 298 K using Bruker DPX400 (400 and 101 MHz respectively) spectrometers. Chemical shifts are reported on the δ scale in ppm and were referenced to residual solvent ($CDCl_3$: 7.27 ppm for ^1H-NMR spectra and 77.0 ppm for ^{13}C-NMR spectra). All spectra were reprocessed using ACD/Labs software version 2015 or ACD/Spectrus. Coupling constants (*J*) were recorded in Hz and matched where possible. The following abbreviations for the multiplicity of the peaks are s (singlet), d (doublet), t (triplet), q (quartet), quin (quintet), br (broad), and m (multiplet).

Samples were analysed using a Waters (Manchester, UK) Acquity TQD mass tandem quadrupole mass spectrometer. Samples were introduced to the mass spectrometer *via* an Acquity H-Class quaternary solvent manager (with TUV detector at 254 nm, sample and column manager). Ultrahigh performance liquid chromatography was undertaken using Waters BEH C18* column (50 mm x 2.1 mm 1.7 µm). Samples were analysed using a Thermo (Hemel Hempstead, UK) Trace GC-MS single quadrupole mass spectrometer. Low resolution positive ion electron ionisation (or chemical ionisation using ammonia as a reagent gas) mass spectra were recorded over a mass range of *m/z* 40–500 at 70 eV.

Gas chromatography was performed using a Shimadzu GC 2014 equipped with an autosampler, FID detector and Agilent technologies HP5 column (Phenomenex ZB5-MS 30 m x 0.25 mm 0.25 µm thickness non-polar column). The results were processed using GC Solution Lite software.

Fourier-transform infrared (FT-IR) spectra are reported in wavenumbers (cm^{-1}) and were recorded using a diamond ATR accessory, as solids or neat liquids.

Syntheses were carried out in an Ammonite 8 flow cell (Cambridge Reactor Design) with C/PVDF (carbon/ polyvinylidene fluoride composite) anode, 316L stainless steel cathode and recess carbon graphite anode and silver cathode. Full details of the Ammonite 8 have been published elsewhere[269], and the reactor is available commercially from Cambridge Reactor Design Ltd. (www.cambridgereactordesign.com). The cell current was controlled with a Rapid Electronics switching mode power supply (85-1903). A peristaltic pump (Ismatec® REGLO Digital Ms-2/6) was used to flow the solutions through the electrochemical cell. This cell has a spiral electrolyte channel, 1 m in length and 2 mm in width and the interelectrode gap is 0.5 mm.

4.2 Ammonite 8 reactor set-up

To set-up the Ammonite 8 reactor we followed the guide lines reported in the AMMONITE SPIRAL ELECTROCHEMICAL CELLS-User Guide by Cambridge Reactor Design.[89]

The Ammonite 8 reactor is an undivided cell developed by Prof. Brown Group at the University of Southampton and manufactured by the company Cambridge Reactor Design. It is an undivided cell made of: Perspex top plate with bolts; a copper plate electrical contact; a Carbon/PVDF (polyvinylidene fluoride) working electrode; a polymer gasket (FFKM); a stainless steel counter electrode with a recessed channel and an aluminium base plate (insulating spacer not shown).

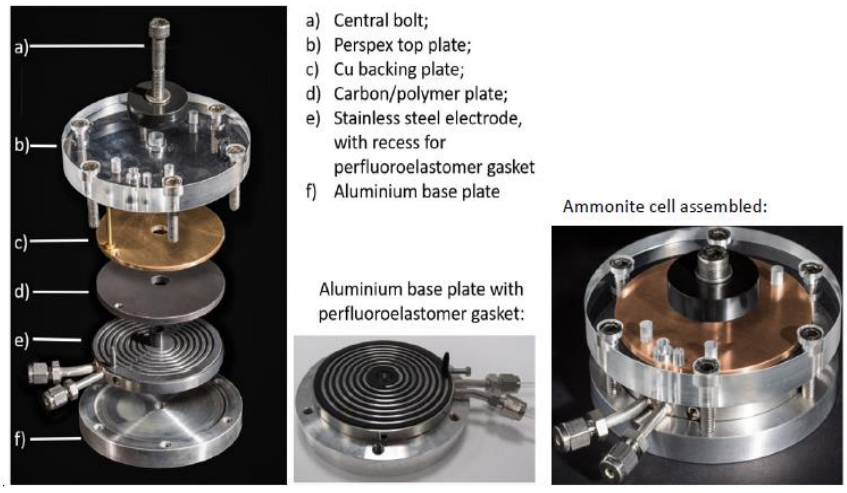

Figure 4. 1: Images of the Ammonite 8 electrochemical flow reactor.

Before each experiment both the working and the counter electrodes need to be cleaned and polished; to remove any organic contaminant from previous reactions they are normally washed with MeOH, then polished with some cotton wool, in circular motion, to remove any unwanted residues. In particular the C/PVDF is polished using a polishing cloth stacked on a flat support and

some silica (99.8%, pore size 60 Å, 230–400 mesh particle size, purchased from Merck): the C/PVDF is first wet with some MeOH; with a spatula some silica is added on the surface of the polishing cloth; the surface of the electrode is polished with the polishing cloth in circular motion in order to remove the top layer of the electrode and finally the electrode is rinsed with MeOH to remove the residue of carbon and silica and let it dry. (Figure 4.2)

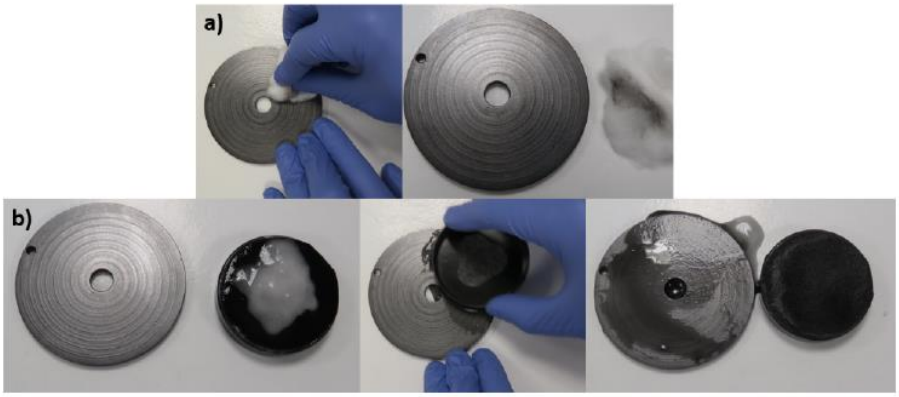

Figure 4. 2: how to polish the C/PVDF electrode.

Once the electrodes have been polished, to assemble the reactor, the stainless steel is put on top of the base plate; the polymer gasket is put in position into the recessed groove being careful not to block the inlet and outlet holes; the C/PVDF electrode is put on top of the gasket and then are put the copper contact plate and the Perspex plate respectively. Everything is finally tighten with the screws using an allen key. It is important to follow the right order to avoid to break the Perspex top plate: first is put in position the central screw avoiding to tighten too much; the external screws are slightly tighten proceeding by couples of opposite screws; once everything is in position, following the same order, all the screws are tightened to seal the system. (Figure 4.3)

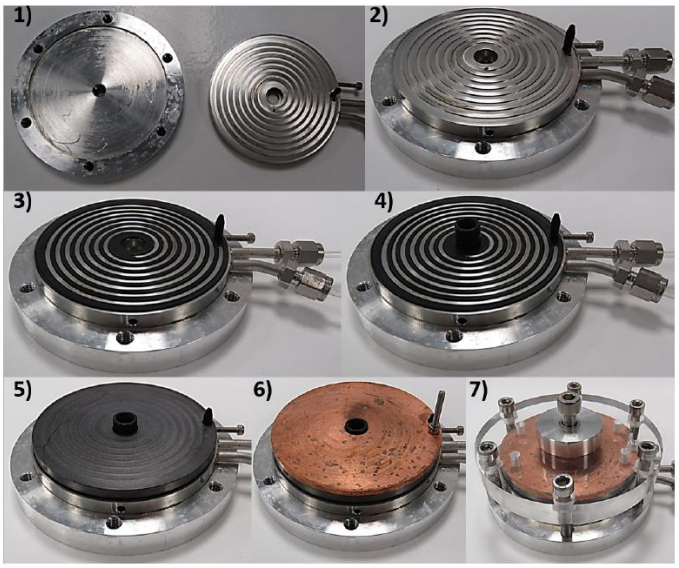

Figure 4. 3: how to assemble the cell.

The Ammonite reactor is connected to the pump and the reaction solvent is pumped through it in order to check the presence of any leakages and to ensure that the pump is performing the correct flow rate. Once done that the Ammonite cell is connected to the power supply via crocodile clips (red = anode, black = cathode) and at this point everything is ready to run the experiment; just turn on the power supply and start pumping the reaction solution through the cell. On completion of the reaction, remember to dismantle the reactor and clean all the components: if everything is left connected, due to the organic residues, some parts could get stuck together with consequent risk of breaking them while trying to separate them.

4.3 Gas chromatography

4.3.1 General procedure

Gas chromatography was performed using a Shimadzu GC 2014 equipped with an autosampler, FID detector and Agilent technologies HP5 column (Phenomenex ZB5-MS 30 m x 0.25 mm 0.25 µm thickness non-polar column). The results were processed using GC Solution Lite software.

For the development of the GC methods, once found the right elution conditions, standard solutions at different known concentration have been prepared and injected in the GC. The calibration curves were built integrating the area under the peak of each solution; once done that, the straight-line plot generated was used to calculate the concentration of unknown solutions.

4.3.2 Expermental procedure for GC yield calculation

5 mL of a 0.1 M solution of the appropriate substrate and supporting electrolyte in the appropriate solvent were pumped through the reactor using the specified conditions and collected in a 10 mL volumetric flask, which was made up to 10 mL by addition of the appropriate solvent (theoretical dilution, C_{max} = 0.05 M). The amount of product was estimated injecting the outlet solution in the GC with the calibration method previously developed.

4.3.3 GC method for oxidative cyclisation

For the analysis of both the lactone and the tetrahydrofuran, separation was carried out using He as a carrier gas at 1.2 mL/ min. The injector temperature was set at 240 °C and 1 µL of sample was injected in splitless mode. The oven temperature was initially held at 70 °C and for the lactone then programmed to increase at 20 °C min^{-1} to 250 °C, where was held for 2 min and for the tetrahydrofuran programmed to increase at 10 °C min^{-1} to 200°C where was held for 2 min. (Figure 4.4)

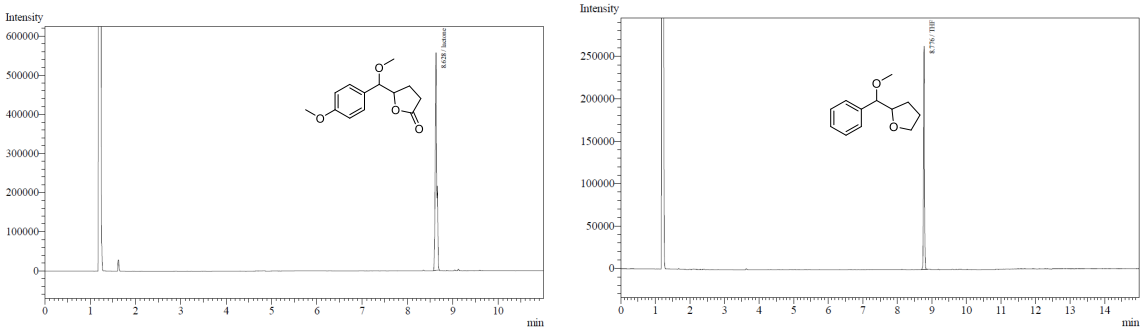

Figure 4.4: GC chromatograms of lactone (ret. t. = 8.628 min) and THF (ret. t. = 8.776 min). Conditions: Agilent technologies HP5 column (Phenomenex ZB5-MS 30 m x 0.25 mm 0.25 µm thickness non-polar column); He as carrier gas at 1.2 mL min^{-1}; injector T 240 °C; 1 µL of sample injected in splitless mode; oven T increased at 20 °C min^{-1} from 70 °C to 250 °C, hold for 2 min for **2.116** and oven T increased at 10 °C min^{-1} from 70 °C to 200 °C, hold for 2 min for **2.85**.

4.3.4 GC method for the elctrochemical reduction of alkenes

For the analysis of both (*E*)-stilbene (starting material) and bibenzene (product), separation was carried out using He as a carrier gas at 1.2 mL/ min. The injector temperature was set at 280 °C and 1 µL of sample was injected in split mode. The oven temperature was initially held at 70 °C and programmed to increase at 35 °C min^{-1} to 200 °C, where was held for 3 min and then increased at 35 °C min^{-1} to 250°C where was held for 2 min. (Figure 4.5).

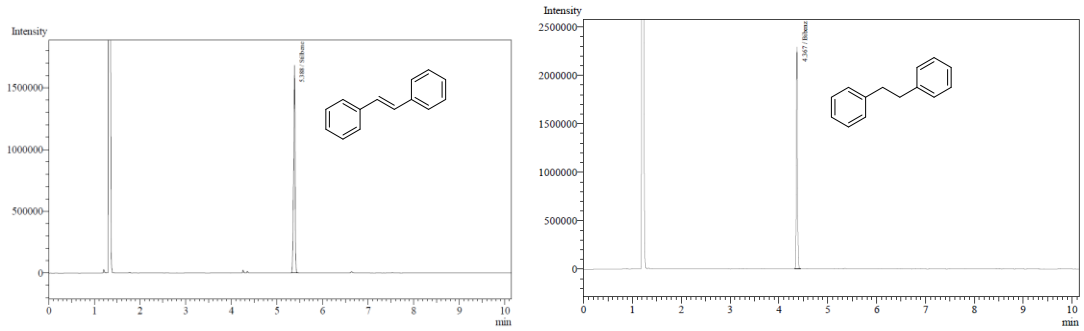

Figure 4.5: GC chromatograms of (*E*)-stilbene (ret. t. = 5.388 min) and bibenzyl (ret. t. = 4.367 min). Conditions: Agilent technologies HP5 column (Phenomenex ZB5-MS 30 m x 0.25 mm 0.25 µm thickness non-polar column); He as carrier gas at 1.2 mL min^{-1}; injector T 280 °C; 1 µL of sample injected in split mode; oven T increased at 35 °C min^{-1} from 70 °C to 20 °C, hold for 3 min and then increased at 35 °C min^{-1} to 250 °C, hold for 2 min

4.4 Experimental procedures and characterisation data

4.4.1 Batch electrolysis set-up

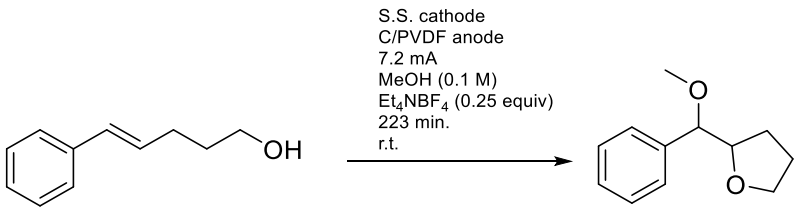

- **Surface Area**: The surface area of the batch electrode used was 1.8 cm^2
- **Current Density**: The cell averaged current density used was the same as for the reaction in the Ammonite 8: (80 mA)/(20 cm^2) = 4 mA/cm^2
- **Current Applied**: (4 mA/cm^2) x (1.8 cm^2) = 7.2 mA

The theoretical electrolysis time (t_{theo}) for the electrochemical oxidative cyclisation of alkenol **1** in the batch electrochemical process was calculated using the following equation, based on a 2-electrons process:

$$t_{theo}=\frac{n \times m \times F}{I}$$

- **n**: number of electrons involved in the process (2)
- **m**: moles of substrate (0.5 x 10^{-3} mol)
- **F**: Faraday's constant (96485 s A mol^{-1})
- **I**: current applied (7.2 x 10^{-3} A)

The theoretical electrolysis time is 223 min.

(*E*)-5-Phenyl-4-penten-1-ol (0.080 g, 0.500 mmol, 1.00 equiv), Et_4NBF_4 (0.027 g, 0.125 mmol, 0.250 equiv) were dissolved in MeOH (5 mL) in a 5 mL vial. A C/PVDF anode and a stainless steel cathode were submerged in the solution. The mixture was stirred at rt for 223 minutes while applying a current of 7.2 mA. When electrolysis was complete, the reaction mixture was diluted in a 10 mL volumetric flask and an aliquot of this solution was analysed by GC. Full consumption of starting material was achieved and the desired product was obtained with a GC yield of 49%.

4.4.2 5-Phenyl-pent-4-yn-1-ol

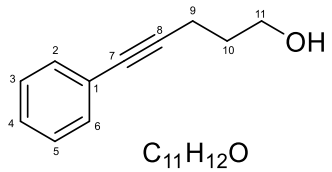

$C_{11}H_{12}O$
Mol Wt: 160.22 g/mol

5-Phenyl-4-pentyn-1-ol was prepared following the procedure of Lu *et al*.[168]

Iodobenzene (9.70 g, 47.6 mmol, 2.00 equiv) and 4-Pentyn-1-ol (2.00 g, 23.8 mmol, 1.00 equiv) were dissolved in a mixture of THF (10 mL) and Et_3N (66 mL). $Pd(PPh_3)_4$ (0.300 g, 0.240 mmol, 1.00 mol %) and CuI (0.100 g, 0.480 mmol, 2.00 mol %) were added in one portion and the mixture was stirred at rt for 2 h. The yellow suspension was filtered and the solvent removed under reduced pressure. The resulting brown oil was purified by column chromatography (SiO_2, toluene/EtOAc = 8/2) to give the title alkyne as a red oil (3.50 g, 21.9 mmol, 92%).

Physical and spectroscopic data are consistent with reported literature values.[168]

^{1}H-NMR: (400 MHz, $CDCl_3$) δ ppm = 7.38-7.41 (m, 2H, **$H_{2,6}$**), 7.26-7.30 (m, 3H, **H_{3-5}**), 3.83 (t, *J* = 5.5 Hz, 2H, **H_{11}**), 2.55 (t, *J* = 6.9 Hz, 2H, **H_9**), 1.87 (tt, *J* = 6.9, 5.5 Hz, 2H, **H_{10}**)

^{13}C-NMR: (101 MHz, $CDCl_3$) δ ppm = 131.5 (**$C_{2,6}$**), 128.2 (**$C_{3,5\ or\ 4}$**), 127.7(**$C_{3,5\ or\ 4}$**), 123.7 (**C_1**), 89.3 (**C_7**), 81.1 (**C_8**), 61.8 (**C_{11}**), 31.4 (**C_{10}**), 16.0 (**C_9**)

LRMS: (ESI^+) 161.1 $[M+H]^+$

4.4.3 (*E*)-5-Phenyl-pent-4-en-1-ol

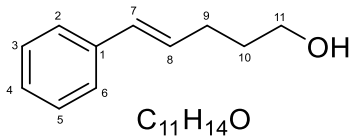

$C_{11}H_{14}O$

Mol Wt: 162.23 g/mol

(*E*)-5-Phenyl pent-4-en-1-ol was prepared following the procedure of Seiders *et al.*[270]

A solution of 5-Phenyl-4-pentyn-1-ol (1.80 g, 11.2 mmol, 1.00 equiv) in anhydrous THF (45 mL) was added dropwise at 0 °C to a solution of $LiAlH_4$ (45.0 mL of 1.00 M in THF, 45.0 mmol). The resulting solution was stirred under reflux for 15 h. After cooling to rt, the mixture was transferred by cannula into an ice-cooled saturated solution of Rochelle's salt (150 mL). EtOAc (100 mL) was added and the solution was stirred for 3 h, during which time it warmed to rt. The phases were separated and the aqueous phase was extracted with EtOAc (2 x 80 mL). The combined organic phases were washed with water (80 mL), brine (80 mL), then dried ($MgSO_4$) filtered and the solvent removed under reduced pressure. The resulting yellow oil was purified by column chromatography (SiO_2, toluene/EtOAc = 8/2) to give the title (*E*)-hydroxyalkene as a colourless oil (1.60 g, 9.80 mmol, 88%).

Physical and spectroscopic data are consistent with reported literature values.[270]

^{1}H-NMR: (400 MHz, $CDCl_3$) δ ppm = 7.20-7.38 (m, 5H, $\mathbf{H_{Ar}}$), 6.45 (d, *J* = 15.8 Hz, 1H, $\mathbf{H_7}$), 6.25 (dt, *J* = 15.8, 6.9 Hz, 1H, $\mathbf{H_8}$), 3.74 (t, *J* = 7.2 Hz, 2H, $\mathbf{H_{11}}$), 2.36 (m, 2H, $\mathbf{H_9}$), 1.78 (m, 2H, $\mathbf{H_{10}}$)

^{13}C-NMR: (101 MHz, $CDCl_3$) δ ppm = 137.3 ($\mathbf{C_1}$), 130.1 ($\mathbf{C_7}$), 129.7 ($\mathbf{C_8}$), 128.2 ($\mathbf{C_{ArH}}$), 126.6 ($\mathbf{C_{2/6}}$), 125.6 ($\mathbf{C_{2\text{-}6}}$), 62.1 ($\mathbf{C_{11}}$), 31.9 ($\mathbf{C_{10}}$), 29.0 ($\mathbf{C_9}$)

LRMS: (ESI^+) 163.1 $[M+H]^+$

4.4.4 2-(Methoxy(phenyl)methyl)tetrahydrofuran

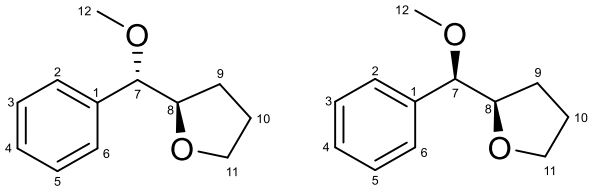

erythro:*threo* ~ 83:17 (^{1}H-NMR)

$C_{12}H_{16}O_2$

Mol Wt: 192.26 g/mol

A solution of (*E*)-5-Phenyl-4-penten-1-ol (0.400 g, 2.50 mmol, 1.00 equiv), Et_4NBF_4 (0.270 g, 1.20 mmol, 0.500 equiv) in MeOH (25 mL) was passed through the Ammonite 8 reactor (ss cathode, C/PVDF anode) with a flow of 0.25 mL/min and a current of 80 mA (steady state V = 2.9 V). The effluent was collected and the solvent evaporated under reduced pressure. The electrolyte was recovered by precipitation from EtOAc and recovered by filtration. Solvent was removed under reduced pressure. The resulting clear oil was purified by column chromatography (SiO_2, toluene/EtOAc = 8/2) to give the title product as a clear oil (0.360 g, 1.87 mmol, 75%), as a 83:17 mixture of *erythro* and *threo* diasteroisomers, respectively. By careful column chromatography, samples of each diastereoisomer were obtained for characterisation.

NMR data for *erythro* diastereoisomer (major; more polar)

^{1}H-NMR: (400 MHz, $CDCl_3$) δ ppm = 7.29-7.40 (m, 5H, $\mathbf{H_{Ar}}$), 4.02-4.09 (m, 2H, $\mathbf{H_7}$, $\mathbf{H_8}$), 3.79-3.93 (m, 2H, $\mathbf{H_{11}}$), 3.26 (s, 3H, $\mathbf{H_{12}}$), 1.78-1.82 (m, 2H, $\mathbf{H_{10}}$), 1.44-1.60 (m, 2H, $\mathbf{H_9}$)

^{13}C-NMR: (101 MHz, $CDCl_3$) 138.9 ($\mathbf{C_1}$), 128.3($\mathbf{C_{ArH}}$), 128.0 ($\mathbf{C_{ArH}}$), 127.6 ($\mathbf{C_{ArH}}$), 86.8 ($\mathbf{C_7}$), 82.3 ($\mathbf{C_8}$), 68.6 ($\mathbf{C_{11}}$), 56.8 ($\mathbf{C_{12}}$), 28.3 ($\mathbf{C_9}$), 25.5 ($\mathbf{C_{10}}$)

NMR data for *threo* diastereoisomer (minor; less polar)

^{1}H-NMR: (400 MHz, $CDCl_3$) δ ppm = 7.39-7.28 (m, 5H, $\mathbf{H_{Ar}}$), 4.19 (d, *J* = 4.9 Hz, 1H, $\mathbf{H_7}$), 4.03 (m, 1H, $\mathbf{H_8}$), 3.85 (m, 1H, $\mathbf{H_{11}}$), 3.73 (m, 1H, $\mathbf{H_{11}}$), 3.29 (s, 3H, $\mathbf{H_{12}}$), 1.75-1.95 (m, 4H, $\mathbf{H_9}$, $\mathbf{H_{10}}$)

^{13}C-NMR: (101 MHz, $CDCl_3$) 139.3($\mathbf{C_1}$), 128.3($\mathbf{C_{ArH}}$), 127.7 ($\mathbf{C_{ArH}}$), 127.4 ($\mathbf{C_{ArH}}$), 85.6 ($\mathbf{C_7}$), 82.4 ($\mathbf{C_8}$), 68.6 ($\mathbf{C_{11}}$), 57.2 ($\mathbf{C_{12}}$), 26.9 ($\mathbf{C_9}$), 25.7 ($\mathbf{C_{10}}$)

Data collected on the mixture of diastereoisomers

LRMS: (ESI$^+$) 193.3 $[M+H]^+$

LRMS: (EI) *m/z* 192 (1%, $[M]^+$), 121 (100%, $[C_8H_9O]^\bullet$), 71 (35%, $[C_4H_7O]^{\bullet+}$)

HRMS: (EI) *m/z* for $[C_{12}H_{16}O_2]^{\bullet+}$ calcd: 192.11448 found: 192.11443

FT-IR: ν_{max} (neat) 2923, 1084, 1067 cm^{-1}

4.4.5 Phenyl(tetrahydrofuran-2-yl)methanol

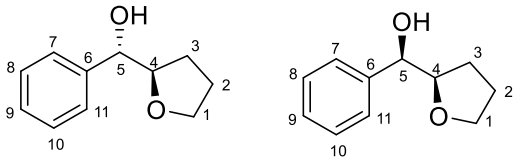

erythro:*threo* ~ *87:13* (^{1}H-NMR)
$C_{11}H_{14}O_2$
Mol Wt: 178,01 g/mol

A solution of (*E*)-5-Phenyl-4-penten-1-ol (0.240 g, 1.50 mmol, 1.00 equiv), Et_4NBF_4 (0.080 g, 0.370 mmol, 0.250 equiv) in MeCN/H_2O = 1/1 (15 mL) was passed through the Ammonite 8 reactor (ss cathode, C/PVDF anode) at a flow rate of 0.25 mL min^{-1} and a current of 80 mA (steady state V= 2.9 V). The effluent was collected and the solvent evaporated under reduced pressure. The electrolyte was recovered by filtration after precipitation from EtOAc. The solution was concentrated under reduced pressure, and the resulting colourless oil was purified by column chromatography (SiO_2, toluene/EtOAc = 1/1) to give the desired product as a colourless oil (0.120 g, 0.670 mmol, 45%), as an 87:13 mixture of *erythro* and *threo* diasteroisomers, respectively. By careful column chromatography, samples of each diastereoisomer were obtained for characterisation. Obtained also *N*-(Phenyl(tetrahydrofuran-2-yl)methyl)acetamide with a ratio of 6/4 by ^{1}H-NMR for the desired product Phenyl-(tetrahydrofuran-2-yl)methanol.

Physical and spectroscopic data are consistent with reported literature values.[141]

NMR data for *erythro* diastereoisomer (major; more polar)

^{1}H-NMR: (400 MHz, $CDCl_3$) δ ppm = 7.28-7.42 (m, 5H, **H_{Ar}**), 4.45 (dd, *J* = 7.5, 2.5 Hz, 1H, **H_5**), 4.02 (q, *J* = 7.5 Hz, 1H, **H_4**), 3.84-3.97 (m, 2H, **H_1**), 2.97 (d, *J* = 2.5 Hz, 1H, **OH**), 1.82-2.00 (m, 2H, **H_2**), 1.59-1.78 (m, 2H, **H_3**)

^{13}C-NMR: (101 MHz, $CDCl_3$) δ ppm = 140.6 (**C_6**), 128.4 (**$C_{8,10}$**), 127.9 (**C_9**), 126.9 (**$C_{7,11}$**), 83.4 (**C_4**), 77.3 (**C_5**), 68.4 (**C_1**), 27.9 (**C_3**), 26.0 (**C_2**)

NMR data for *threo* diastereoisomer (minor; less polar)

^{1}H-NMR: (400 MHz, $CDCl_3$) δ ppm = 7.28-7.42 (m, 5H, **H_{Ar}**); 4.95 (m, 1H, **H_5**); 4.10 (m, 1H, **H_4**); 3.84-3.97 (m, 2H, **H_1**); 2.48 (d, *J* = 2.3 Hz, 1H, **OH**); 1.82-2.00 (m, 2H, **H_2**); 1.59-1.78 (m, 2H, **H_3**)

^{13}C-NMR: (101 MHz, $CDCl_3$) δ ppm = 140.5 (**C_6**), 128.2 (**$C_{8,10}$**), 127.4 (**C_9**), 126.0 (**$C_{7,11}$**), 83.1 (**C_4**), 74.0 (**C_5**), 69.0 (**C_1**), 26.0 (**C_3**), 24.7 (**C_2**)

Data collected on the mixture of diastereoisomers

LRMS: (ESI$^+$) 201.3 $[M+Na]^+$, 179.3 $[M+H]^+$

4.4.6 *N*-(Phenyl(tetrahydrofuran-2-yl)methyl)acetamide

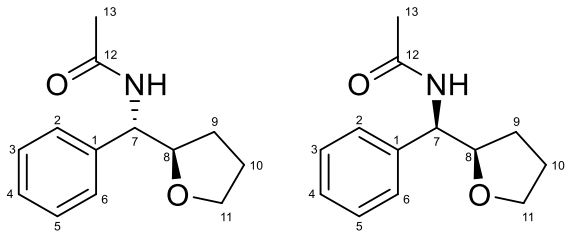

erythro:*threo* ~ 80:20 (^{1}H-NMR)

$C_{13}H_{17}NO_2$

Mol Wt: 219.1 g/mol

A solution of (*E*)-5-Phenyl-4-penten-1-ol (0.400 g, 2.50 mmol, 1.00 equiv), Et_4NBF_4 (0.080 g, 0.370 mmol, 0.250 equiv) in a 9/1 mixture MeCN/H_2O (15.0 mL) was passed through the Ammonite 8 reactor (ss cathode, C/PVDF anode) at a flow rate of 0.25 mL min^{-1} and a current of 80 mA (steady state V = 3.4 V). The effluent was collected and the solvent evaporated under reduced pressure. The electrolyte was recovered by filtration after precipitation from EtOAc. The solvent removed under reduced pressure and the resulting clear oil was purified by column chromatography (SiO_2, toluene/EtOAc = 1/1 to 100% EtOAc) to give the title product as a colourless oil (0.120 g, 0.550 mmol, 36%), as an 80:20 mixture of *erythro* and *threo* diasteroisomers, respectively. By careful column chromatography, samples of each diastereoisomer were obtained for characterisation. Obtained also Phenyl-(tetrahydrofuran-2-yl)methanol with a ratio of 8/2 by ^{1}H-NMR for the desired product *N*-(Phenyl(tetrahydrofuran-2-yl)methyl)acetamide.

NMR data for *erythro* diastereoisomer (major; more polar)

^{1}H-NMR: (400 MHz, $CDCl_3$) δ ppm = 7.35-7.24 (m, 5H, $\mathbf{H_{Ar}}$), 6.24 (bd, *J* = 8.5 Hz, 1H, **NH**), 5.05 (dd, *J* = 3.8, 8.5 Hz, 1H, $\mathbf{H_7}$), 4.14 (m, 1H, $\mathbf{H_8}$), 3.94 (m, 1H, $\mathbf{H_{11}}$), 3.79 (m, 1H, $\mathbf{H_{11}}$), 2.04 (s, 3H, $\mathbf{H_{13}}$), 1.87-1.98 (m, 2H, $\mathbf{H_{10}}$), 1.68-1.77 (m, 2H, $\mathbf{H_9}$)

^{13}C-NMR: (101 MHz, $CDCl_3$) δ ppm = 169.7 ($\mathbf{C_{12}}$), 141.1 ($\mathbf{C_1}$), 128.5 ($\mathbf{C_{ArH}}$), 127.4 ($\mathbf{C_{ArH}}$), 127.0 ($\mathbf{C_{ArH}}$), 81.3 ($\mathbf{C_8}$), 68.8 ($\mathbf{C_{11}}$), 55.4 ($\mathbf{C_7}$), 29.1 ($\mathbf{C_9}$), 25.7 ($\mathbf{C_{10}}$), 23.4 ($\mathbf{C_{13}}$)

NMR data for *threo* diastereoisomer (minor; less polar)

^{1}H-NMR: (400 MHz, $CDCl_3$) δ ppm = 7.24-7.35 (m, 5H, $\mathbf{H_{Ar}}$), 6.38 (bd, *J* = 8.5 Hz, 1H, **NH**), 4.98 (dd, *J* = 3.8, 8.5 Hz, 1H, $\mathbf{H_7}$), 4.26 (m, 1H, $\mathbf{H_8}$), 3.68-3.72 (m, 2H, $\mathbf{H_{11}}$), 1.99 (s, 3H, $\mathbf{H_{13}}$), 1.87-1.98 (m, 2H, $\mathbf{H_{10}}$), 1.42-1.56 (m, 2H, $\mathbf{H_9}$)

^{13}C-NMR: (101 MHz, $CDCl_3$) δ ppm = 169.2 ($\mathbf{C_{12}}$), 138.7 ($\mathbf{C_1}$), 128.4 ($\mathbf{C_{ArH}}$), 128.3 ($\mathbf{C_{ArH}}$), 127.6 ($\mathbf{C_{ArH}}$), 80.9 ($\mathbf{C_8}$), 68.7 ($\mathbf{C_{11}}$), 56.3 ($\mathbf{C_7}$), 28.1 ($\mathbf{C_9}$), 25.6 ($\mathbf{C_{10}}$), 23.4 ($\mathbf{C_{13}}$)

Data collected on the mixture of diastereoisomers

LRMS: (ESI^+) 242.3 $[M+Na]^+$

HRMS: (ESI^+) *m/z* for $[C_{13}H_{17}NO_2Na]^+$ $[M+Na]^+$ calcd: 242.1152 found: 242.1151

FT-IR: ν_{max} (neat) 3296, 1648, 1540, 1063, 724 cm^{-1}

4.4.7 (*E*)-5-Phenylpent-4-enoic acid

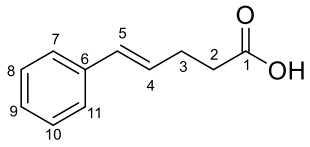

$C_{11}H_{12}O_2$

Mol Wt: 176.2 g/mol

(*E*)-5-phenylpent-4-enoic acid was prepared following the procedure of Perkins *et al.*[177]

To a suspension of (3-Carboxypropyl)triphenylphosphonium bromide (4.45 g, 10.4 mmol, 1.10 equiv) in THF (50 mL) was added a 2 M solution of Sodium *bis*(Trimethylsilyl)amide in THF (10.4 mL, 20.7 mmol, 2.20 equiv) at 0 °C. The solution was stirred for 30 minutes and then cooled down to -78 °C. Benzaldehyde (1.00 g, 9.42 mmol, 1.00 equiv) was added dropwise and then the reaction mixture was allowed to warm up to rt over-night. Water (20 mL) and Et_2O (20 mL) were added. Phases were separated and the organic phase was discharted; the aqueous phase was acidified to pH = 1 with a 2 M HCl solution and then extracted with EtOAc (3 x 20 mL). The combined organic phases were dried ($MgSO_4$), filtered and solvent removed under reduced pressure. The resulting pale oil was purified by column chromatography (SiO_2, Toluene/EtOAc = 6/4 to 1/1) to give the title carboxylic acid as a white solid (1.00 g, 5.67 mmol, 60%).

Physical and spectroscopic data are consistent with reported literature values.[177]

^{1}H-NMR: (400 MHz, $CDCl_3$) δ ppm = 7.17-7.37 (m, 5H, **H_{Ar}**), 6.39 (d, *J* = 15.9 Hz, 1H, **H_5**), 6.15 (m, 1H, **H_4**), 2.40-2.52 (m, 4H, **H_3**, **H_2**)

^{13}C-NMR: (101 MHz, $CDCl_3$) δ ppm = 177.5 (**C_1**), 137.3 (**C_6**), 131.2 (**C_5**), 128.5 (**C_{ArH}**), 128 (**C_4**), 127.2(**C_{ArH}**), 126.1 (**C_{ArH}**), 33.5 (**C_2**), 27.9 (**C_3**)

LRMS: (ESI^+) 177.3 $[M+H]^+$

4.4.8 5-(Methoxy(phenyl)methyl)dihydrofuran-2-3*H*-one

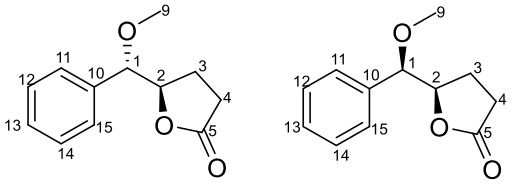

erythro:*threo* ~ 75:20 (^{1}H-NMR)

$C_{12}H_{14}O_3$

Mol Wt: 206.2 g/mol

A solution of (*E*)-5-Phenylpent-4-enoic acid (0.270 g, 1.50 mmol, 1.00 equiv), Et_4NBF_4 (0.160 g, 0.750 mmol, 0.500 equiv) in MeOH (15 mL) was passed through the Ammonite 8 reactor (ss cathode, C/PVDF anode) with a flow of 0.25 mL/min and a current of 96 mA (steady state V= 3.1 V). The effluent was collected and the solvent evaporated under reduced pressure. The electrolyte was recovered by precipitation in EtOAc and filtered away. The solution was concentrated under reduced pressure. The resulting clear oil was purified by column chromatography (SiO_2, toluene/EtOAc = 9/1 to 8/2) to give the desired product as a clear oil (0.190 g, 0.920 mmol, 61%) as a 75:25 mixture of *erythro* and *threo* diasteroisomers, respectively. By careful column chromatography, samples of each diastereoisomer were obtained for characterisation.

Physical and spectroscopic data are consistent with reported literature values.[177]

Data for *erythro* diastereoisomer (major; more polar)

^{1}H-NMR: (400 MHz, $CDCl_3$) δ ppm = 7.31-7.41 (m, 5H, $\mathbf{H_{Ar}}$), 4.69 (td, *J* = 7.0, 5.6 Hz, 1H, $\mathbf{H_2}$), 4.25 (d, *J* = 5.6 Hz, 1H, $\mathbf{H_1}$), 3.31 (s, 3H, $\mathbf{H_9}$), 2.22-2.41 (m, 2H, $\mathbf{H_4}$), 2.02 (td, *J* = 7.0, 8.8 Hz, 2H, $\mathbf{H_3}$)

^{13}C-NMR: (101 MHz, $CDCl_3$) δ ppm = 177.0 ($\mathbf{C_5}$), 136.4 ($\mathbf{C_{10}}$), 128.7 ($\mathbf{C_{ArH}}$), 128.6 ($\mathbf{C_{ArH}}$), 127.6 ($\mathbf{C_{ArH}}$), 85.0 ($\mathbf{C_1}$), 81.9 ($\mathbf{C_2}$), 57.1 ($\mathbf{C_9}$), 28.1 ($\mathbf{C_4}$), 24.0 ($\mathbf{C_3}$)

LRMS: (ESI$^+$) 207.1 $[M+H]^+$

Data for *threo* diastereoisomer (minor; less polar)

^{1}H-NMR: (400 MHz, $CDCl_3$) δ ppm = 7.31-7.38 (m, 5H, $\mathbf{H_{Ar}}$), 4.58 (td, *J* = 5.4, 3.4 Hz, 1H, $\mathbf{H_2}$), 4.48 (d, *J* = 3.4 Hz, 1H, $\mathbf{H_1}$), 3.34 (s, 3H, $\mathbf{H_9}$), 2.56 (m, 1H, $\mathbf{H_4}$), 2.40 (m, 1H, $\mathbf{H_4}$), 2.30 (m, 1H, $\mathbf{H_3}$), 2.02 (m, 1H, $\mathbf{H_3}$)

^{13}C-NMR: (101 MHz, $CDCl_3$) δ ppm = 177.6 ($\mathbf{C_5}$), 136.7 ($\mathbf{C_{10}}$), 128.7 ($\mathbf{C_{ArH}}$), 128.3 ($\mathbf{C_{ArH}}$), 126.9($\mathbf{C_{ArH}}$), 84.1($\mathbf{C_1}$), 82.7($\mathbf{C_2}$), 57.7 ($\mathbf{C_9}$), 28.3 ($\mathbf{C_4}$), 21.4($\mathbf{C_3}$)

LRMS: (ESI$^+$) 207.1 $[M+H]^+$

4.4.9 Dihydro-5-(hydroxyl(phenyl)methyl)furan-2(3*H*)-one

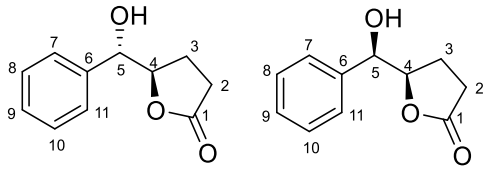

erythro:*threo* ~ 78:22 (^{1}H-NMR)

$C_{11}H_{12}O_3$

Mol Wt: 192.1 g/mol

A solution of (*E*)-5-Phenylpent-4-enoic acid (0.260 g, 1.50 mmol, 1.00 equiv), Et_4NBF_4 (0.080 g, 0.370 mmol, 0.250 equiv) in MeCN/H_2O = 1/1 (15 mL) was passed through the Ammonite 8 reactor (ss cathode, C/PVDF anode) with a flow of 0.25 mL/min and a current of 80 mA (steady state V= 2.6 V). The effluent was collected and the solvent evaporated under reduced pressure. The electrolyte was recovered by precipitation in EtOAc and filtered away. The solution was concentrated under reduced pressure. The resulting clear oil was purified by column chromatography (SiO_2, toluene/EtOAc = 6/4 to 1/1) to give the desired product as a colourless oil (0.100 g, 0.520 mmol, 35%) as a 78:22 mixture of *erythro* and *threo* diasteroisomers, respectively. By careful column chromatography, samples of each diastereoisomer were obtained for characterisation.

Physical and spectroscopic data are consistent with reported literature values.[271]

NMR data for *erythro* diastereoisomer (major; more polar)

^{1}H-NMR: (400 MHz, $CDCl_3$) δ ppm = 7.29-7.42 (m, 5H, **H_{Ar}**), 5.11 (s, 1H, **H_5**), 4.70 (m, 1H, **H_4**), 2.89 (s, 1H, **OH**), 2.57 (m, 1H, **H_2**), 2.44 (m, 1H, **H_2**), 2.30 (m, 1H, **H_3**), 1.93 (m, 1H, **H_3**)

^{13}C-NMR: (101 MHz, $CDCl_3$) δ ppm = 177.9 (**C_1**), 138.5 (**C_6**), 128.6 (**C_{ArH}**), 128.1 (**C_{ArH}**), 126.0 (**C_{ArH}**), 83.4 (**C_4**), 73.4 (**C_5**), 28.6 (**C_2**), 20.64 (**C_3**)

NMR data for *threo* diastereoisomer (minor; less polar)

^{1}H-NMR: (400 MHz, $CDCl_3$) δ ppm = 7.31-7.47 (m, 5H, **H_{Ar}**), 4.72 (dd, *J* = 2.6, 6.5 Hz, 1H, **H_5**), 4.65 (td, *J* = 6.5, 7.2 Hz, 1H, **H_4**), 2.75 (d, *J* = 2.6 Hz, 1H, **OH**), 2.41-2.50 (m, 2H, **H_2**), 1.99-2.10 (m, 2H, **H_3**)

^{13}C-NMR: (101 MHz, $CDCl_3$) δ ppm = 176.9 (**C_1**), 138.4 (**C_6**), 128.73 (**C_{ArH}**), 128.70 (**C_{ArH}**), 126.9 (**C_{ArH}**), 83.4 (**C_4**), 76.4 (**C_5**), 28.4 (**C_2**), 23.9 (**C_3**)

Data collected on the mixture of diastereoisomers

LRMS: (ESI^+) 193.2 $[M+H]^+$

4.4.10 (*E*)-5-(4-Methoxyphenyl)pent-4-enoic acid

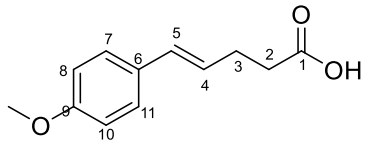

$C_{12}H_{14}O_3$

Mol Wt: 206.2 g/mol

(*E*)-5-(4-Methoxyphenyl)pent-4-enoic acid was prepared following the procedure of Perkins *et al.*[177]

To a suspension of (3-Carboxypropyl)triphenylphosphonium bromide (5.70 g, 13.2 mmol, 1.20 equiv) in THF (60 mL) was added a 2 M solution of Sodium *bis*(Trimethylsilyl)amide in THF (13.2 mL, 26.4 mmol, 2.40 equiv) at 0 °C. The solution was stirred for 30 minutes and then cooled down to -78 °C. *p*-Anisaldehyde (1.50 g, 11.0 mmol, 1.00 equiv) was added dropwise and then the reaction mixture was allowed to warm up to rt over-night. Water (20 mL) and Et_2O (20 mL) were added. Phases were separated and the organic phase was discharted; the aqueous phase was acidified to pH = 1 with a 2 M HCl solution and then extracted with EtOAc (3 x 20 mL). The combined organic phases were dried ($MgSO_4$), filtered and solvent removed under reduced pressure. The resulting brown solid was purified by recrystallization in dichloromethane at 0°C to give the title carboxylic acid as a white solid (1.80 g, 8.73 mmol, 79%).

Physical and spectroscopic data are consistent with reported literature values.[177]

^{1}H-NMR: (400 MHz, $CDCl_3$) δ ppm = 7.29 (m, 2H, **$H_{7,11}$**), 6.85 (m, 2H, **$H_{8,10}$**), 6.40 (d, *J* = 16.0 Hz, 1H, **H_5**), 6.08 (m, 1H, **H_4**), 3.82 (s, 3H, **H_{12}**), 2.50-2.57 (m, 4H, **$H_{2,3}$**)

^{13}C-NMR: (101 MHz, $CDCl_3$) δ ppm = 178.0 (**C_1**), 158.9 (**C_9**), 130.6 (**C_5**), 130.1 (**C_6**), 127.2 (**$C_{7,\ 11}$**), 125.8 (**C_4**), 113.9 (**$C_{8,\ 10}$**), 55.3 (**C_{12}**), 33.7 (**C_3**), 27.9 (**C_2**)

LRMS: (ESI$^+$) 207.3 $[M+H]^+$

Mp: 144°-147°C

4.4.11 5-(Methoxy(4-methoxyphenyl)methyl)dihydrofuran-2-3*H*-one

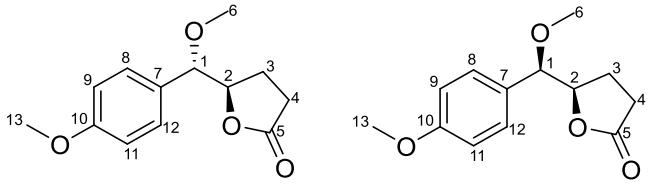

erythro:*threo* ~ 80:20 (^{1}H-NMR)
$C_{13}H_{16}O_4$
Mol Wt: 236,1 g/mol

A solution of (*E*)-5-(4-Methoxyphenyl)pent-4-enoic acid (0.300 g, 1.50 mmol, 1.00 equiv), Et_4NBF_4 (0.160 g, 0.750 mmol, 0.500 equiv) in MeOH (15 mL) was passed through the Ammonite 8 reactor (ss cathode, C/PVDF anode) with a flow of 0.25 mL/min and a current of 80 mA (steady state V= 2.9 V). The effluent was collected and the solvent evaporated under reduced pressure. The electrolyte was recovered by precipitation in EtOAc and filtered away. The solution was concentrated under reduced pressure. The resulting clear oil was purified by column chromatography (SiO_2, toluene/EtOAc = 9/1 to 8/2) to give the desired product as a white solid (0.280 g, 1.17 mmol, 78%) as a 80:20 mixture of *erythro* and *threo* diasteroisomers, respectively.

Physical and spectroscopic data are consistent with reported literature values.[177]

Data for *erythro* diastereoisomer (major; more polar)

^{1}H-NMR: (400 MHz, $CDCl_3$) δ ppm = 7.22-7.27 (m, 2H, **$H_{8,12}$**), 6.90-6.95 (m, 2H, **$H_{9,11}$**), 4.66 (td, *J* = 6.9, 5.8 Hz, 1H, **H_2**), 4,20 (d, *J* = 5.8 Hz, 1H, **H_1**), 3.83 (s, 3H, **H_{13}**), 3.29 (s, 3H, **H_6**), 2.22-2.43 (m, 2H, **H_4**), 1.98-2.02 (m, 2H, **H_3**)

^{13}C-NMR: (101 MHz, $CDCl_3$) δ ppm = 177.1 (**C_5**), 159.9 (**C_{10}**), 128.8 (**$C_{8,12}$**), 128.2 (**C_7**), 114.1 (**$C_{9,11}$**), 84.6 (**H_1**), 82.0 (**C_2**), 56.9 (**C_6**), 55.3 (**C_{13}**), 28.2 (**C_4**), 24.0 (**C_3**)

LRMS: (ESI$^+$) 237.3 $[M+H]^+$

Data for *threo* diastereoisomer (minor; less polar)

^{1}H-NMR: (400 MHz, $CDCl_3$) δ ppm = 7.22-7.27 (m, 2H, **$H_{8,12}$**), 6.90-6.95 (m, 2H, **$H_{9,11}$**), 4.58 (td, *J* = 5.3, 3.4 Hz, 1H, **H_2**), 4.41 (d, *J* = 3.4 Hz, 1H, **H_1**), 3.83 (s, 3H, **H_{13}**), 3.31 (s, 3H, **H_6**), 2.53 (m, 1H, **H_4**), 2.22-2.43 (m, 2H, **H_4**, **H_3**), 2.06 (m, 1H, **H_3**)

^{13}C-NMR: (101 MHz, $CDCl_3$) δ ppm = 177.1 (**C_5**), 159.9 (**C_{10}**), 128.27 (**$C_{8,12}$**), 128.2 (**C_7**), 114.1 (**$C_{9,11}$**), 83.7 (**H_1**), 82.7 (**C_2**), 57.4 (**C_6**), 55.3 (**C_{13}**), 28.3 (**C_4**), 21.6 (**C_3**)

LRMS: (ESI$^+$) 237.2 $[M+H]^+$

Data collected on the mixture of diastereoisomers

Mp: 75°-79°C

4.4.12 (*E*)-5-(4-Methoxyphenyl)pent-4-en-1-ol

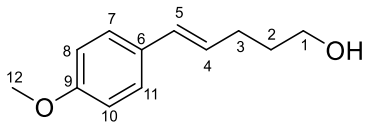

$C_{12}H_{16}O_2$

Mol Wt: 192.3 g/mol

(*E*)-5-(4-Methoxyphenyl)pent-4-en-1-ol was prepared following the procedure of Farndon *et al.*[178]

To a solution of (*E*)-5-(4-Methoxyphenyl)pent-4-enoic acid (0.300 g, 1.45 mmol, 1.00 equiv), in anhydrous THF (10 mL), at 0°C, was added dropwise a 1M solution of $LiAlH_4$ in THF (2.90 mL, 2.90 mmol, 2.00 equiv). The suspension was stirred for 1 h at rt. Then it was cooled down to 0°C and water (0.400 mL) and a 10% aqueous solution of NaOH (0.300 mL) were slowly added. The mixture was filtered through celite and washed with dichloromethane. Phases were separated and the aqueous phase was extracted with dichloromethane (2 x 5 mL). The combined organic phases were dried ($MgSO_4$), filtered and solvent removed under reduced pressure. The desired product was obtained as a white solid without further purification (0.290 g, 1.45 mmol, 100%).

Physical and spectroscopic data are consistent with reported literature values.[178]

^{1}H-NMR: (400 MHz, $CDCl_3$) δ ppm = 7.32-7.27 (m, 2H, **$H_{7,11}$**), 6.88-6.83 (m, 2H, **$H_{8,10}$**), 6.38 (d, *J* = 16.0 Hz, 1H, **H_5**), 6.1 (dt, *J* = 16.0, 7.4 Hz, 1H, **H_4**), 3.81 (s, 3H, **H_{12}**), 3.72 (t, *J* = 6.2 Hz, 2H, **H_1**), 2.30 (m, 2H, **H_3**), 1.75 (q, *J* = 6.6 Hz, 2H, **H_2**)

^{13}C-NMR: (101 MHz, $CDCl_3$) δ ppm = 158.7(**C_9**), 130.4 (**C_6**), 129.7 (**C_5**), 127.9 (**C_4**), 127.0 (**$C_{7,11}$**), 113.9 (**$C_{8,10}$**), 62.5 (**C_1**), 55.3 (**C_{12}**), 32.4 (**C_2**), 29.3 (**C_3**)

LRMS: (ESI^+) 193.3 $[M+H]^+$

Mp: 74°-79°C

4.4.13 2-(Methoxy(4-methoxyphenyl)methyl)tetrahydrofuran

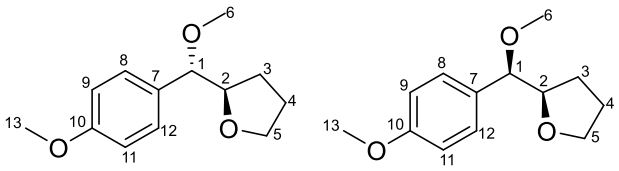

erythro:*threo* ~ 80:20 (^{1}H-NMR)
$C_{13}H_{18}O_3$
Mol Wt: 222.3 g/mol

A solution of (*E*)-5-(4-Methoxyphenyl)pent-4-en-1-ol (0.190 g, 1.00 mmol, 1.00 equiv), Et_4NBF_4 (0.110 g, 0.500 mmol, 0.500 equiv) in MeOH (10 mL) was passed through the Ammonite 8 reactor (ss cathode, C/PVDF anode) with a flow of 0.25 mL/min and a current of 80 mA (steady state V = 2.6 V). The effluent was collected and the solvent evaporated under reduced pressure. The electrolyte was recovered by precipitation in EtOAc and filtered away. The solution was concentrated under reduced pressure. The resulting clear oil was purified by column chromatography (SiO_2, toluene/EtOAc = 9/1 to 8/2) to give the desired product as a colourless oil (0.110 g, 0.490 mmol, 50%) as a 80:20 mixture of *erythro* and *threo* diasteroisomers, respectively. By careful column chromatography, samples of each diastereoisomer were obtained for characterisation.

Data for *erythro* diastereoisomer (major; more polar)

^{1}H-NMR: (400 MHz, $CDCl_3$) δ ppm = 7.23-7.26 (m, 2H, **$H_{8,12}$**), 6.88-6.93 (m, 2H, **$H_{9,11}$**), 3.98-4.06 (m, 2H, **H_1**, **H_2**), 3.90 (m, 1H, **H_5**), 3.78-3.85 (m, 4H, **H_5**, **H_{13}**), 3.23 (s, 3H, **H_6**), 1.73-1.83 (m, 2H, **H_4**), 1.41-1.58 (m, 2H, **H_3**)

^{13}C-NMR: (101 MHz, $CDCl_3$) δ ppm = 159.4 (**C_{13}**), 131.0 (**C_{10}**), 128.8 (**$C_{11,15}$**), 113.8 (**$C_{12,14}$**), 86.3 (**C_2**), 82.4 (**C_1**), 68.6 (**C_5**), 56.6 (**C_9**), 55.2 (**C_{16}**), 28.4 (**C_3**), 25.6(**C_4**)

LRMS: (ESI$^+$) 245.3 $[M+Na]^+$

Data for *threo* diastereoisomer (minor; less polar)

^{1}H-NMR: (400 MHz, $CDCl_3$) δ ppm = 7.23-7.29 (m, 2H, **$H_{8,12}$**), 6.87-6.93 (m, 2H, **$H_{9,11}$**), 4.10 (d, *J* = 5.4 Hz, 1H, **H_1**), 3.99 (m, 1H, **H_2**), 3.79-3.87 (m, 4H, **$H_{13,5}$**), 3.71 (m, 1H, **H_5**), 3.25 (s, 1H, **H_6**), 1.76-1.95 (m, 4H, **$H_{3,4}$**)

^{13}C-NMR: (101 MHz, $CDCl_3$) δ ppm = 159.1 (**C_{13}**), 131.3 (**C_{10}**), 128.6 (**$C_{11,15}$**), 113.7 (**$C_{12,14}$**), 85.2 (**C_2**), 82.3 (**C_1**), 68.6 (**C_5**), 56.9 (**C_9**), 55.2 (**C_{16}**), 27.2 (**C_3**), 25.7 (**C_4**)

LRMS: (ESI$^+$) 245.3 $[M+Na]^+$

Data collected on the mixture of diastereoisomers

HRMS: (ESI$^+$) m/z for $[C_{13}H_{18}O_3Na]^+$ $[M+Na]^+$ calcd: 245.1154 found: 245.1148

FT-IR: ν_{max} (neat) 2850, 1095, 1065 cm^{-1}

4.4.14 (*E*)-5-(2-Methoxyphenyl)pent-4-enoic acid

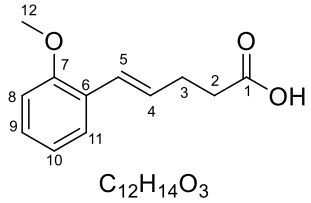

$C_{12}H_{14}O_3$

Mol Wt: 206.2 g/mol

(*E*)-5-(2-Methoxyphenyl)pent-4-enoic acid was prepared following the procedure of Perkins *et al.*[177]

To a suspension of (3-Carboxypropyl)triphenylphosphonium bromide (4.00 g, 9.32 mmol, 1.10 equiv) in THF (50 mL) was added a 2 M solution of Sodium *bis*(Trimethylsilyl)amide in THF (9.30 mL, 18.6 mmol, 2.20 equiv) at 0 °C. The solution was stirred for 30 minutes and then cooled down to -78 °C. *o*-Anisaldehyde (1.15 g, 8.47 mmol, 1.00 equiv) was added dropwise and then the reaction mixture was allowed to warm up to rt over-night. Water (20 mL) and Et_2O (20 mL) were added. Phases were separated and the organic phase was discharted; the aqueous phase was acidified to pH = 1 with a 2 M HCl solution and then extracted with EtOAc (3 x 20 mL). The combined organic phases were dried ($MgSO_4$), filtered and solvent removed under reduced pressure. The resulting brown solid was purified by recrystallization in dichloromethane at 0°C to give the title carboxylic acid as a white solid (0.580 g, 2.81 mmol, 33%).

Physical and spectroscopic data are consistent with reported literature values.[177]

^{1}H-NMR: (400 MHz, $CDCl_3$) δ ppm = 7.41 (dd, *J* = 1.7, 7.7 Hz, 1H, **H_{11}**), 7.21 (td, *J* = 1.7, 7.7 Hz, 1H, **H_9**), 6.92 (td, *J* = 1.7, 7.7 Hz, 1H, **H_{10}**), 6.86 (dd, *J* = 1.7, 7.7 Hz, 1H, **H_8**), 6.77 (d, *J* = 15.8 Hz, 1H, **H_5**), 6.22 (m, 1H, **H_4**), 3.85 (s, 3H, **H_{12}**), 2.54-2.62 (m, 4H, **$H_{2,3}$**)

^{13}C-NMR: (101 MHz, $CDCl_3$) δ ppm = 179.1 (**C_1**), 156.7 (**C_7**), 128.7 (**C_4**), 128.3 (**C_9**), 126.6 (**C_{11}**), 126.3 (**C_6**), 125.8 (**C_5**), 120.6 (**C_{10}**), 110.8 (**C_8**), 55.4 (**C_{12}**), 33.8 (**C_3**), 28.4 (**C_2**)

LRMS: (ESI^+) 207.3 $[M+H]^+$

Mp: 88°-91° C

4.4.15 5-(Methoxy(2-methoxyphenyl)methyl)dihydrofuran-2(3*H*)-one

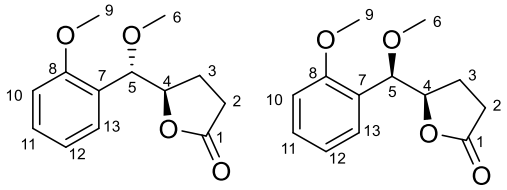

erythro:*threo* ~ 80:20 (^{1}H-NMR)
$C_{13}H_{16}O_4$
Mol Wt: 236.1 g/mol

A solution of (*E*)-5-(2-Methoxyphenyl)pent-4-enoic acid (0.310 g, 1.50 mmol, 1.00 equiv), Et_4NBF_4 (0.080 g, 0.370 mmol, 0.250 equiv) in MeOH (15 mL) was passed through the Ammonite 8 reactor (ss cathode, C/PVDF anode) with a flow of 0.25 mL/min and a current of 80 mA (steady state V= 3.0 V). The effluent was collected and the solvent evaporated under reduced pressure. The electrolyte was recovered by precipitation in EtOAc and filtered away. The solution was concentrated under reduced pressure. The resulting clear oil was purified by column chromatography (SiO_2, toluene/EtOAc = 8/2) to give the desired product as a colourless oil (0.260 g, 1.10 mmol, 73%) as a 80:20 mixture of *erythro* and *threo* diasteroisomers, respectively. By careful column chromatography, samples of each diastereoisomer were obtained for characterisation.

Physical and spectroscopic data are consistent with reported literature values.[177]

NMR data for *erythro* diastereoisomer (major; more polar)

^{1}H-NMR: (400 MHz, $CDCl_3$) δ ppm = 7.32 (dd, *J* = 1.6, 7.3 Hz, 1H, **H_{13}**), 7.22 (ddd, *J* = 1.6, 7.6, 8.2 Hz, 1H, **H_{11}**), 6.94 (ddd, *J* = 1.0, 7.3, 7.6 Hz, 1H, **H_{12}**), 6.83 (dd, *J* = 1.0, 8.2 Hz, 1H, **H_{10}**), 4.66 (d, *J* = 5.4 Hz, 1H, **H_5**), 4.60 (m, 1H, **H_4**), 3.77 (s, 3H, **H_9**), 3.21 (s, 3H, **H_6**), 2.50 (m, 1H, **H_2**), 2.35 (m, 1H, **H_2**), 1.95-2.10 (m, 2H, **H_3**)

^{13}C-NMR: (101 MHz, $CDCl_3$) δ ppm = 177.5 (**C_1**), 157.2 (**C_7**), 129.2 (**C_{11}**), 128.0 (**C_{13}**), 125.0 (**C_8**), 121.0 (**C_{12}**), 110.4 (**C_{10}**), 82.2 (**C_4**), 78.7 (**C_5**), 57.3 (**C_6**), 55.4 (**C_9**), 28.5 (**C_2**), 24.1 (**C_3**)

NMR data for *threo* diastereoisomer (minor; less polar)

^{1}H-NMR: (400 MHz, $CDCl_3$) δ ppm = 7.41 (dd, *J* = 1.5, 7.5 Hz, 1H, **H_{13}**), 7.33 (ddd, *J* = 1.5, 7.3, 8.7 Hz, 1H, **H_{11}**), 7.03 (ddd, *J* = 0.7, 7.3, 7.5 Hz, 1H, **H_{12}**), 6.91 (dd, *J* = 0.7, 8.7 Hz, 1H, **H_{10}**), 4.96 (d, *J* = 2.4 Hz, 1H, **H_5**), 4.73 (m, 1H, **H_4**), 3.87 (s, 3H, **H_9**), 3.35 (s, 3H, **H_6**), 2.66 (m, 1H, **H_2**), 2.39 (m, 1H, **H_2**), 2.26 (m, 1H, **H_3**), 1.91 (m, 1H, **H_3**)

^{13}C-NMR: (101 MHz, $CDCl_3$) δ ppm = 178.2 (**C_1**), 156.8 (**C_7**), 129.0 (**C_{11}**), 126.9 (**C_{13}**), 124.6 (**C_8**), 120.7 (**C_{12}**), 110.3 (**C_{10}**), 80.8 (**C_4**), 78.6 (**C_5**), 57.9 (**C_6**), 55.2 (**C_9**), 28.6 (**C_2**), 20.8 (**C_3**)

Data collected on the mixture of diastereoisomers

LRMS: (ESI^+) 237.2$[M+H]^+$

4.4.16 (*E,Z*)-5-(2-Methoxyphenyl)pent-4-en-1-ol

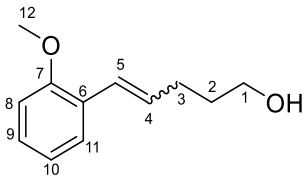

$C_{12}H_{16}O_2$

Mol Wt: 192.1 g/mol

(*E,Z*)-5-(2-Methoxyphenyl) pent-4-en-1-ol was prepared following the procedure of Farndon *et al.*[178]

To a solution of (*E,Z*)-5-(2-Methoxyphenyl)pent-4-enoic acid (0.600 g, 2.90 mmol, 1.00 equiv), in anhydrous THF (15 mL), at 0 °C, was added dropwise a 1M solution of $LiAlH_4$ in THF (5.80 mL, 5.80 mmol, 2.00 equiv). The suspension was stirred for 1 h at rt. Then it was cooled down to 0 °C and water (0.800 mL) and a 10% aqueous solution of NaOH (0.600 mL) were slowly added. The mixture was filtered through celite and washed with dichloromethane. Phases were separated and the aqueous phase was extracted with dichloromethane (2 x 5 mL). The combined organic phases were dried ($MgSO_4$), filtered and solvent removed under reduced pressure. The desired product was obtained as a colourless oil without further purification (0.450 g, 2.30 mmol, 82%, 70/30 *E*/*Z*).

Physical and spectroscopic data are consistent with reported literature values.[178]

NMR data for *E* isomer

^{1}H-NMR: (400 MHz, $CDCl_3$) δ ppm = 7.42 (dd, *J* = 1.6, 8.4 Hz, 1H, **H_9**), 7.21 (m, 1H, **H_{11}**), 6.84-6.98 (m, 2H, **$H_{8,10}$**), 6.76 (d, *J* = 16.0 Hz, 1H, **H_5**), 6.23 (dt, *J* = 7.0, 16.0 Hz, 1H, **H_4**), 3.85 (s, 3H, **H_{12}**), 3.72 (t, *J* = 6.5 Hz, 2H, **H_1**), 2.35 (m, 2H, **H_3**), 1.75 (m, 2H, **H_2**)

^{13}C-NMR: (101 MHz, $CDCl_3$) δ ppm = 156.3 (**C_6**), 130.8 (**C_4**), 127.9 (**C_{11}**), 126.7 (**C_7**), 126.4 (**C_9**), 125.0 (**C_5**), 120.6 (**C_8**), 110.8 (**C_{10}**), 62.5 (**C_1**), 55.4 (**C_{12}**), 32.3 (**C_2**), 29.8 (**C_3**)

NMR data for *Z* isomer

^{1}H-NMR: (400 MHz, $CDCl_3$) δ ppm = 7.16-7.26 (m, 2H, **$H_{9,11}$**), 6.84-6.98 (m, 2H, **$H_{8,10}$**), 6.56 (d, *J* = 11.5 Hz, 1H, **H_5**), 5.74 (dt, *J* = 7.3, 11.5 Hz, 1H, **H_4**), 3.84 (s, 3H, **H_{12}**), 3.66 (t, *J* = 6.3 Hz, 2H, **H_1**), 2.30-2.40 (m, 2H, **H_3**), 1.68-1.82 (m, 2H, **H_2**)

^{13}C-NMR: (101 MHz, $CDCl_3$) δ ppm = 156.9 (**C_6**), 132.1 (**C_4**), 130.0 (**C_9**), 128.2 (**C_{11}**), 126.3 (**C_7**), 124.9 (**C_5**), 120.1 (**C_8**), 110.4 (**C_{10}**), 62.5 (**C_1**), 55.4 (**C_{12}**), 32.7 (**C_2**), 25.0 (**C_3**)

Data collected on the mixture

LRMS: (ESI^+) 193.2 $[M+H]^+$

4.4.17 2-(Methoxy(2-methoxyphenyl)methyl)tetrahydrofuran

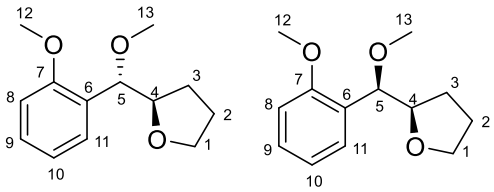

erythro:*threo* ~ 80:20 (^{1}H-NMR)

$C_{13}H_{18}O_3$
Mol Wt: 222.1 g/mol

A solution of (*E,Z*)-5-(2-Methoxyphenyl)pent-4-en-1-ol (0.280 g, 1.50 mmol, 1.00 equiv), Et_4NBF_4 (0.080 g, 0.370 mmol, 0.250 equiv) in MeOH (15 mL) was passed through the Ammonite 8 reactor (ss cathode, C/PVDF anode) with a flow of 0.25 mL/min and a current of 80 mA (steady state V = 3.0 V). The effluent was collected and the solvent evaporated under reduced pressure. The electrolyte was recovered by precipitation in EtOAc and filtered away. The solution was concentrated under reduced pressure. The resulting clear oil was purified by column chromatography (SiO_2, toluene/EtOAc = 8/2) to give the desired product as a colourless oil (0.140 g, 0.630 mmol, 42%) as a 80:20 mixture of *erythro* and *threo* diasteroisomers, respectively. By careful column chromatography, samples of each diastereoisomer were obtained for characterisation.

NMR data for *erythro* diastereoisomer (major; more polar)

^{1}H-NMR: (400 MHz, $CDCl_3$) δ ppm = 7.39 (dd, *J* = 1.7, 7.8 Hz, 1H, **H_{11}**), 7.27 (td, *J* = 1.7, 8.7 Hz, 1H, **H_9**), 6.99 (td, *J* = 0.8, 7.8 Hz, 1H, **H_{10}**), 6.89 (dd, *J* = 0.8, 8.7 Hz, 1H, **H_8**), 4.65 (d, *J* = 7.3 Hz, 1H, **H_5**), 4.04 (td, *J* = 7.3 Hz, 1H, **H_4**), 3.96 (m, 1H, **H_1**), 3.78-3.88 (m, 4H, **H_1**, **H_{12}**), 3.24 (s, 3H, **H_{13}**), 1.73-1.96 (m, 2H, **H_2**), 1.51-168 (m, 2H, **H_3**)

^{13}C-NMR: (101 MHz, $CDCl_3$) δ ppm = 157.5 (**C_6**), 128.7 (**C_9**), 127.9 (**C_{11}**), 127.5 (**C_7**), 120.8 (**C_{10}**), 110.4 (**C_8**), 82.6 (**C_4**), 79.0 (**C_5**), 68.5 (**C_1**), 56.7 (**C_{13}**), 55.4 (**C_{12}**), 27.6 (**C_3**), 25.6 (**C_2**)

NMR data for *threo* diastereoisomer (minor; less polar)

^{1}H-NMR: (400 MHz, $CDCl_3$) δ ppm = 7.40 (dd, *J* = 1.8, 7.6 Hz, 1H, **H_{11}**), 7.26 (td, *J* = 1.8, 8.0 Hz, 1H, **H_9**), 6.98 (td, *J* = 0.8, 7.6 Hz, 1H, **H_{10}**), 6.88 (dd, *J* = 0.8, 8.0 Hz, 1H, **H_8**), 4.84 (d, *J* = 3.7 Hz, 1H, **H_5**), 4.10 (td, *J* = 3.7, 7.9 Hz, 1H, **H_4**), 3.89 (m, 1H, **H_1**), 3.83 (s, 3H, **H_{12}**), 3.76 (m, 1H, **H_1**), 3.31 (s, 3H, **H_{13}**), 1.83-1.99 (m, 2H, **H_3**, **H_2**)**,** 1.77 (m, 1H, **H_2**), 1.67 (m, 1H, **H_3**)**

^{13}C-NMR: (101 MHz, $CDCl_3$) δ ppm = 157.3 (**C_7**), 128.3 (**C_9**), 127.4 (**C_6**), 127.3 (**C_{11}**), 120.6 (**C_{10}**), 110.2 (**C_8**), 81.0 (**C_4**), 78.6 (**C_5**), 68.7 (**C_1**), 57.4 (**C_{13}**), 55.3 (**C_{12}**), 25.9 (**C_2**), 25.5 (**C_3**)

Data collected on the mixture of diastereoisomers

LRMS: (ESI^+) 245.2 $[M+Na]^+$

HRMS: (ESI^+) *m/z* for $[C_{13}H_{18}O_3Na]^+$ $[M+Na]^+$ calcd: 245.1148 found: 245.1150

FT-IR: ν_{max} (neat) 2934, 1104, 1065, 753 cm^{-1}

4.4.18 (*E*)-5-(4-Fluorophenyl)pent-4-enoic acid

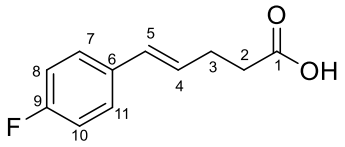

$C_{11}H_{11}FO_2$

Mol Wt: 194.2 g/mol

(*E*)-5-(4-Fluorophenyl)pent-4-enoic acid was prepared adapting the procedure of Perkins *et al.*[177]

To a suspension of (3-Carboxypropyl)triphenylphosphonium bromide (3.80 g, 8.86 mmol, 1.10 equiv) in THF (50 mL) was added a 2 M solution of Sodium *bis*(Trimethylsilyl)amide in THF (8.90 mL, 17.7 mmol, 2.20 equiv) at 0 °C. The solution was stirred for 30 minutes and then cooled down to -78 °C. 4-Fluorobenzaldehyde (1.00 g, 8.06 mmol, 1.00 equiv) was added dropwise and then the reaction mixture was allowed to warm up to rt over-night. Water (20 mL) and Et_2O (20 mL) were added. Phases were separated and the organic phase was discharted; the aqueous phase was acidified to pH = 1 with a 2 M HCl solution and then extracted with EtOAc (3 x 20 mL). The combined organic phases were dried ($MgSO_4$), filtered and solvent removed under reduced pressure. The resulting brown solid was purified by recrystallization in dichloromethane at 0°C to give the title carboxylic acid as a white solid (0.600 g, 3.09 mmol, 38%).

Physical and spectroscopic data are consistent with reported literature values.[178]

^{1}H-NMR: (400 MHz, $CDCl_3$) δ ppm = 7.28-7.33 (m, 2H, $\mathbf{H_{7,11}}$), 6.96-7.03 (m, 2H, $\mathbf{H_{8,10}}$), 6.41 (d, *J* = 15.9 Hz, 1H, $\mathbf{H_5}$), 6.15 (m, 1H, $\mathbf{H_4}$), 2.50-2.60 (m, 4H, $\mathbf{H_{2,3}}$)

^{13}C-NMR: (101 MHz, $CDCl_3$) δ ppm = 177.9 ($\mathbf{C_1}$), 162.1 (d, *J* = 245.7 Hz, $\mathbf{C_9}$), 133.4 (d, *J* = 2.9 Hz, $\mathbf{C_6}$), 130.1 ($\mathbf{C_5}$), 127.7 ($\mathbf{C_4}$), 127.5 ($\mathbf{C_{7,11}}$, *J* = 8.1 Hz), 115.3 (d, *J* = 22.0 Hz, $\mathbf{C_{8,10}}$), 33.5 ($\mathbf{C_2}$), 27.8 ($\mathbf{C_3}$)

LRMS: (ESI^+) 195.2 $[M+H]^+$

Mp: 90°-95° C

4.4.19 5-((4-Fluorophenyl)(methoxy)methyl)dihydrofuran-2(3*H*)-one

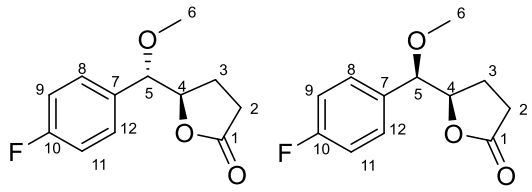

erythro:*threo* ~ 80:20 (^{1}H-NMR)

$C_{12}H_{13}FO_3$
Mol Wt: 224.1 g/mol

A solution of (*E*)-5-(4-Fluorophenyl)pent-4-enoic acid (0.290 g, 1.50 mmol, 1.00 equiv), Et_4NBF_4 (0.080 g, 0.370 mmol, 0.250 equiv) in MeOH (15 mL) was passed through the Ammonite 8 reactor (ss cathode, C/PVDF anode) with a flow of 0.25 mL/min and a current of 80 mA (steady state V= 3.0 V). The effluent was collected and the solvent evaporated under reduced pressure. The electrolyte was recovered by precipitation in EtOAc and filtered away. The solution was concentrated under reduced pressure. The resulting clear oil was purified by column chromatography (SiO_2, toluene/EtOAc = 9/1 to 8/2) to give the desired product as a white solid (0.220 g, 0.980 mmol, 65%) as a 80:20 mixture of *erythro* and *threo* diasteroisomers, respectively. By careful column chromatography, samples of each diastereoisomer were obtained for characterisation.

NMR data for *erythro* diastereoisomer (major; more polar)

^{1}H-NMR: (400 MHz, $CDCl_3$) δ ppm = 7.29-7.35 (m, 2H, **H_8**, **H_{12}**), 7.05-7.14 (m, 2H, **H_9**, **H_{11}**), 4.65 (m, 1H, **H_4**), 4.24 (d, *J* = 5.3 Hz, 1H, **H_5**), 3.30 (s, 3H, **H_6**), 2.26-2.44 (m, 2H, **H_2**), 1.96-2.11 (m, 2H, **H_3**)

^{13}C-NMR: (101 MHz, $CDCl_3$) δ ppm = 176.9 (**C_1**), 164.4 (d, *J* = 246.5 Hz, **C_{10}**), 132.1 (d, *J* = 2.9 Hz, **C_7**), 129.2 (d, *J* = 8.1 Hz, **$C_{8,\,12}$**), 115.7 (d, *J* = 21.3 Hz, **$C_{9,\,11}$**), 84.2 (**C_5**), 81.7 (**C_4**), 57.2 (**C_6**), 28.1 (**C_2**), 23.9 (**C_3**)

NMR data for *threo* diastereoisomer (minor; less polar)

^{1}H-NMR: (400 MHz, $CDCl_3$) δ ppm = 7.29-7.35 (m, 2H, **H_8**, **H_{12}**), 7.05-7.14 (m, 2H, **H_9**, **H_{11}**), 4.56 (m, 1H, **H_4**), 4.43 (d, *J* = 3.3 Hz, 1H, **H_5**), 3.32 (s, 3H, **H_6**), 2.55 (m, 1H, **H_2**), 2.41 (m, 1H, **H_2**), 2.25 (m, 1H, **H_3**), 2.06 (m, 1H, **H_3**)

^{13}C-NMR: (101 MHz, $CDCl_3$) δ ppm = 177.3 (**C_1**), 163.6 (d, *J* = 246.5 Hz, **C_{10}**), 132.4 (d, *J* = 2.9 Hz, **C_7**), 128.5 (d, *J* = 8.1 Hz, **$C_{8,\,12}$**), 115.7 (d, *J* = 21.3 Hz, **$C_{9,\,11}$**), 83.6 (**C_5**), 82.4 (**C_4**), 57.6 (**C_6**), 28.3 (**C_2**), 21.6 (**C_3**)

Data collected on the mixture of diastereoisomers

LRMS: (ESI$^+$) 225.2 $[M+H]^+$

HRMS: (ESI$^+$) *m/z* for $[C_{12}H_{13}FO_3Na]^+$ $[M+Na]^+$ calcd: 247.0738 found: 247.0736

FT-IR: ν_{max} (neat) 2938, 1769, 1154, 1109 cm^{-1}

4.4.20 (*E*)-5-(4-Fluorophenyl)pent-4-en-1-ol

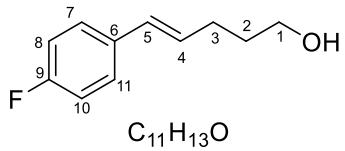

$C_{11}H_{13}O$

Mol Wt: 180.1 g/mol

(*E*)-5-(4-Fluorophenyl)pent-4-en-1-ol was prepared adapting the procedure of Farndon *et al.*[178]

To a solution of (*E*)-5-(4-Fluorophenyl)pent-4-enoic acid (0.500 g, 2.60 mmol, 1.00 equiv), in anhydrous THF (10 mL), at 0 °C, was added dropwise a 1M solution of $LiAlH_4$ in THF (5.20 mL, 5.20 mmol, 2.00 equiv). The suspension was stirred for 1 h at rt. Then it was cooled down to 0 °C and water (0.800 mL) and a 10% aqueous solution of NaOH (0.600 mL) were slowly added. The mixture was filtered through celite and washed with dichloromethane. Phases were separated and the aqueous phase was extracted with dichloromethane (2 x 5 mL). The combined organic phases were dried ($MgSO_4$), filtered and solvent removed under reduced pressure. The resulting oil was purified by column chromatography (SiO_2, toluene/EtOAc = 6/4) to give the desired product as a colourless oil (0.400 g, 2.20 mmol, 85%).

Physical and spectroscopic data are consistent with reported literature values.[178]

^{1}H-NMR: (400 MHz, $CDCl_3$) δ ppm = 7.28-7.34 (m, 2H, $\mathbf{H_{7,\,11}}$), 6.95-7.02 (m, 2H, $\mathbf{H_{8,\,10}}$), 6.40 (d, *J* = 16.1 Hz, 1H, $\mathbf{H_5}$), 6.15 (dt, *J* = 6.8, 16,1 Hz, 1H, $\mathbf{H_4}$), 3.72 (t, *J* = 6.8 Hz, 2H, $\mathbf{H_1}$), 2.30 (dt, *J* = 6.8, 7.2 Hz, 2H, $\mathbf{H_3}$), 1.76 (quin, *J* = 6.8, 7.2 Hz, 2H, $\mathbf{H_2}$)

^{13}C-NMR: (101 MHz, $CDCl_3$) δ ppm = 161.9 (d, *J* = 246.5 Hz, $\mathbf{C_9}$), 133.8 (d, *J* = 3.7 Hz, $\mathbf{C_6}$), 129.8 ($\mathbf{C_4}$), 129.2 ($\mathbf{C_5}$), 127.4-127.3 (d, *J* = 8.1 Hz, $\mathbf{C_{7,\,11}}$), 115.4-115.2 (d, *J* = 22.7 Hz, $\mathbf{C_{8,\,10}}$), 62.4 ($\mathbf{C_1}$), 32.2 ($\mathbf{C_2}$), 29.3 ($\mathbf{C_3}$)

LRMS: 181.3 $[M+H]^+$

4.4.21 2-((4-Fluorophenyl)(methoxy)methyl)tetrahydrofuran

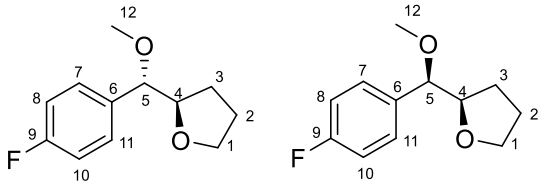

erythro:*threo* ~ 80:20 (^{1}H-NMR)

$C_{12}H_{15}FO_2$
Mol Wt: 210.1 g/mol

A solution of (*E*)-5-(4-Fluorophenyl)pent-4-en-1-ol (0.2700 g, 1.50 mmol, 1.00 equiv), Et_4NBF_4 (0.080 g, 0.370 mmol, 0.250 equiv) in MeOH (15 mL) was passed through the Ammonite 8 reactor (ss cathode, C/PVDF anode) with a flow of 0.25 mL/min and a current of 80 mA (steady state V = 3.4 V). The effluent was collected and the solvent evaporated under reduced pressure. The electrolyte was recovered by precipitation in EtOAc and filtered away. The solution was concentrated under reduced pressure. The resulting clear oil was purified by column chromatography (SiO_2, toluene/EtOAc = 9/1) to give the desired product as a colourless oil (0.180 g, 0.870 mmol, 58%) as a 80:20 mixture of *erythro* and *threo* diasteroisomers, respectively. By careful column chromatography, samples of each diastereoisomer were obtained for characterisation.

NMR data for *erythro* diastereoisomer (major; more polar)

^{1}H-NMR: (400 MHz, $CDCl_3$) δ ppm = 7.28-7.34 (m, 2H, **$H_{7,11}$**), 7.02-7.09 (m, 2H, **$H_{8,10}$**), 4.08 (d, *J* = 7.2 Hz, 1H, **H_5**), 4.03 (dt, *J* = 7.2, 7.5 Hz, 1H, **H_4**), 3.77-3.92 (m, 2H, **H_1**), 3.25 (s, 3H, **H_{12}**), 1.73-1.81 (m, 2H, **H_2**), 1.43-1.59 (m, 2H, **H_3**)

^{13}C-NMR: (101 MHz, $CDCl_3$) δ ppm = 162.5 (d, *J* = 246.5 Hz, **C_9**), 134.6 (d, *J* = 3.7 Hz, **C_6**), 129.2-129.1 (d, *J* = 8.8 Hz, **$C_{7,11}$**), 115.4-115.2 (d, *J* = 21.3 Hz, **$C_{8,10}$**), 85.9 (**C_5**), 82.1 (**C_4**), 68.6 (**C_1**), 56.8 (**C_{12}**), 28.2 (**C_3**), 25.5 (**C_2**)

NMR data for *threo* diastereoisomer (minor; less polar)

^{1}H-NMR: (400 MHz, $CDCl_3$) δ ppm = 7.28-7.34 (m, 2H, **$H_{7,11}$**), 7.02-7.09 (m, 2H, **$H_{8,10}$**), 4.13 (d, *J* = 6.2 Hz, 1H, **H_5**), 4.00 (m, 1H, **H_4**), 3.84 (m, 1H, **H_1**), 3.74 (m, 1H, **H_1**), 3.27 (s, 3H, **H_{12}**), 1.80-1.95 (m, 4H, **$H_{2,3}$**)

^{13}C-NMR: (101 MHz, $CDCl_3$) δ ppm = 162.4 (d, *J* = 245.0 Hz, **C_9**), 135.0 (d, *J* = 2.9 Hz, **C_6**), 129.1 (*J* = 8.1 Hz, **$C_{7,11}$**), 115.1 (d, *J* = 21.3 Hz, **$C_{8,10}$**), 85.1 (**C_5**), 82.1 (**C_4**), 68.6 (**C_1**), 57.1 (**C_{12}**), 27.3 (**$C_{2\text{ or }3}$**), 25.7 (**$C_{2\text{ or }3}$**)

Data collected on the mixture of diastereoisomers

LRMS: (ESI^+) 233.2 $[M+Na]^+$

HRMS: (ESI^+) *m/z* for $[C_{12}H_{15}FO_2Na]^+$ $[M+Na]^+$ calcd: 233.0945 found: 233.0949

FT-IR: ν_{max} (neat) 2870, 1507, 1067 cm^{-1}

4.4.22 (*E*,*Z*)-5-(4-Trifluoromethylphenyl)pent-4-enoic acid

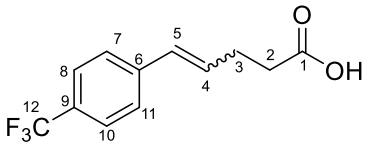

$C_{12}H_{11}F_3O_2$

Mol Wt: 244.1 g/mol

(*E*,*Z*)-5-(4-Trifluoromethylphenyl)pent-4-enoic acid was prepared adapting the procedure of Perkins *et al.*[177]

To a suspension of (3-Carboxypropyl)triphenylphosphonium bromide (4.40 g, 10.2 mmol, 1.10 equiv) in THF (50 mL) was added a 1 M solution of Lithium *bis*(Trimethylsilyl)amide in THF/ethylbenzene (20.5 mL, 20.5 mmol, 2.20 equiv) at 0 °C. The solution was stirred for 30 minutes and then cooled down to -78 °C. 4-(Trifluoromethyl)benzaldehyde (1.60 g, 9.31 mmol, 1.00 equiv) was added dropwise and then the reaction mixture was allowed to warm up to rt over-night. Water (20 mL) and Et_2O (20 mL) were added. Phases were separated and the organic phase was discharted; the aqueous phase was acidified to pH = 1 with a 2 M HCl solution and then extracted with EtOAc (3 x 20 mL). The combined organic phases were dried ($MgSO_4$), filtered and solvent removed under reduced pressure. The resulting brown solid was purified by column chromatography (SiO_2, Toluene/EtOAc = 6/4 to 1/1) to give the title carboxylic acid as a white solid (0.600 g, 2.46 mmol, 26%, 70/30 *E*/*Z*).

Physical and spectroscopic data are consistent with reported literature values.[272, 273]

NMR data for *E* isomer

^{1}H-NMR: (400 MHz, $CDCl_3$) δ ppm = 11.04 (bs, 1H, **OH**), 7.55 (d, *J* = 8.5 Hz, 2H, **H_8**, **H_{10}**), 7.44 (d, *J*= 8.5 Hz, 2H, **H_7**, **H_{11}**), 6.48 (d, *J* = 15, 5 Hz, 1H, **H_5**), 6.33 (m, 1H, **H_4**), 2.55-2.61 (m, 4H, **H_3**, **H_2**)

^{13}C-NMR: (101 MHz, $CDCl_3$) δ ppm = 178.2 (**C_1**), 140.7 (**C_6**), 130.8(**C_4**), 130.1(**C_5**), 126.2(**C_8**, 10), 125.5(q, *J* = 3.8 Hz, **$C_{7,11}$**), 125.3 (q, *J* = 271.5 Hz, **C_{12}**), 33.0 (**C_2**), 27.5 (**C_3**)

NMR data for *Z* isomer

^{1}H-NMR: (400 MHz, $CDCl_3$) δ ppm = 11.04 (bs, 1H, **OH**), 7.60 (d, *J* = 8.0 Hz, 2H, **H_8**, **H_{10}**), 7.37 (d, *J*= 8.0 Hz, 2H, **H_7**, **H_{11}**), 6.48 (d, *J* = 11.5 Hz, 1H, **H_5**), 5.76 (m, 1H, **H_4**), 2.63-2.70 (m, 2H, **H_3**), 2.48-2.53 (m, 2H, **H_2**)

^{13}C-NMR: (101 MHz, $CDCl_3$) δ ppm = 178.2 (**C_1**), 140.4 (**C_6**), 131.9(**C_4**), 129.3(**C_5**), 128.9(**$C_{7,11}$**), 125.2 (q, *J* = 271.5 Hz, **C_{12}**), 125.2(q, *J* = 3.8 Hz, **$C_{7,11}$**), 33.4 (**C_2**), 23.4 (**C_3**)

Data collected on the mixture

LRMS: (ESI^+) 245.1 $[M+H]^+$

4.4.23 5-(methoxy(4-(Trifluoromethyl)phenyl)methyl)dihydrofuran-2(3*H*)-one

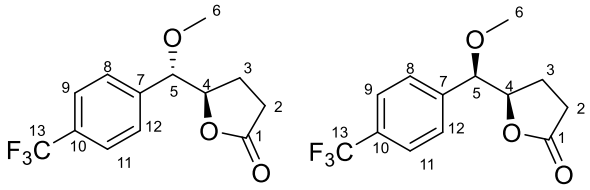

erythro:*threo* ~ 80:20 (^{1}H-NMR)
$C_{13}H_{13}F_3O_3$
Mol Wt: 274.1 g/mol

A solution of (*E*,*Z*)-5-(4-trifluoromethylphenyl)pent-4-enoic acid (0.370 g, 1.50 mmol, 1.00 equiv), Et_4NBF_4 (0.080 g, 0.370 mmol, 0.250 equiv) in MeOH (15 mL) was passed through the Ammonite 8 reactor (ss cathode, C/PVDF anode) with a flow of 0.25 mL/min and a current of 80 mA (steady state V = 3.1 V). The effluent was collected and the solvent evaporated under reduced pressure. The electrolyte was recovered by precipitation in EtOAc and filtered away. The solution was concentrated under reduced pressure. The resulting clear oil was purified by column chromatography (SiO_2, toluene/EtOAc = 9/1 to 6/4) to give the desired product as a white solid (0.210 g, 0.770 mmol, 51%) as a 80:20 mixture of *erythro* and *threo* diasteroisomers, respectively. By careful column chromatography, samples of each diastereoisomer were obtained for characterisation.

NMR data for *erythro* diastereoisomer (major; more polar)

^{1}H-NMR: (400 MHz, $CDCl_3$) δ ppm = 7.58 (d, *J* = 8.2 Hz, 2H, **H_9**, **H_{11}**), 7.40 (d, *J* = 8.2 Hz, 2H, **H_8**, **H_{12}**), 4.59 (ddd, *J* = 7.3, 6.5, 4.7 Hz, 1H, **H_4**), 4.26 (d, *J* = 4.7 Hz, 1H, **H_5**), 3.25 (s, 3H, **H_6**), 2.25-2.35 (m, 2H, **H_2**), 2.00-2.06 (m, 2H, **H_3**)

^{13}C-NMR: (101 MHz, $CDCl_3$) δ ppm = 176.9 (**C_1**), 140.9 (**C_7**), 130.9 (q, *J* = 32.9 Hz, **C_{10}**), 127.9 (**$C_{9,\,11}$**), 125.6 (q, *J* = 3.6 Hz, **$C_{8,\,12}$**), 122.9 (q, *J* = 272.0 Hz, **C_{13}**), 84.3 (**C_5**), 81.5 (**C_4**), 57.5 (**C_6**), 28.1 (**C_2**), 23.9 (**C_3**)

NMR data for *threo* diastereoisomer (minor; less polar)

^{1}H-NMR: (400 MHz, $CDCl_3$) δ ppm = 7.66 (d, *J* = 8.1 Hz, 2H, **H_9**, **H_{11}**), 7.47 (d, *J* = 8.1 Hz, 2H, **H_8**, **H_{12}**), 4.57 (ddd, *J* = 7.5, 5.5, 4.1 Hz, 1H, **H_4**), 4.53 (d, *J* = 4.1 Hz, 1H, **H_5**), 3.36 (s, 3H, **H_6**), 2.60 (m, 1H, **H_2**), 2.44 (m, 1H, **H_2**), 2.24 (m, 1H, **H_3**), 2.06 (m, 1H, **H_3**)

^{13}C-NMR: (101 MHz, $CDCl_3$) δ ppm = 177.2 (**C_1**), 141.1 (**C_7**), 130.3 (q, *J* = 32.7 Hz, **C_{10}**), 127.3 (**$C_{9,\,11}$**), 125.7 (q, *J* = 3.8 Hz, **$C_{8,\,12}$**), 83.7 (**C_5**), 82.2 (**C_4**), 57.9 (**C_6**), 28.2 (**C_2**), 21.6 (**C_3**)

Data collected on the mixture of diastereoisomers

LRMS: (ESI$^+$) 275.2 $[M+H]^+$

HRMS: (ESI$^+$) *m/z* for $[C_{13}H_{13}F_3O_3Na]^+$ $[M+Na]^+$ calcd: 297.0709 found: 297.0708

FT-IR: ν_{max} (neat) 1773, 1322, 1063 cm^{-1}

4.4.24 (*E*,*Z*)-5-(4-Trifluoromethyl)pent-4-en-1-ol

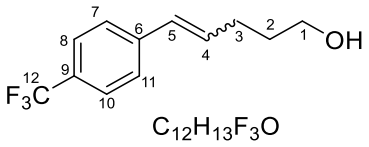

$C_{12}H_{13}F_3O$

Mol Wt: 230.1 g/mol

(*E*,*Z*)-5-(4-Trifluoromethyl)pent-4-en-1-ol was prepared adapting the procedure of Farndon *et al.*[178]

To a solution of (*E*, *Z*)-5-(4-trifluoromethylphenyl)pent-4-enoic acid (0.500 g, 2.05 mmol, 1.00 equiv), in anhydrous THF (10 mL), at 0 °C, was added dropwise a 1M solution of $LiAlH_4$ in THF (4.10 mL, 4.10 mmol, 2.00 equiv). The suspension was stirred for 1 h at rt. Then it was cooled down to 0 °C and water (0.80 mL) and a 10% aqueous solution of NaOH (0.60 mL) were slowly added. The mixture was filtered through celite and washed with dichloromethane. Phases were separated and the aqueous phase was extracted with dichloromethane (2 x 5 mL). The combined organic phases were dried ($MgSO_4$), filtered and solvent removed under reduced pressure. The resulting oil was purified by column chromatography (SiO_2, toluene/EtOAc = 6/4) to give the desired product as a colourless oil (0.400 g, 1.74 mmol, 85%, 70/30 *E*/*Z*).

Physical and spectroscopic data are consistent with reported literature values.[145]

NMR data for *E* isomer

^{1}H-NMR: (400 MHz, $CDCl_3$) δ ppm = 7.54 (d, *J* = 8.5 Hz, 2H, **$H_{8,10}$**), 7.44 (d, *J* = 8.5 Hz, 2H, **$H_{7,11}$**), 6.44 (d, *J* = 16.6 Hz, 1H, **H_5**), 6.35 (m, 1H, **H_4**), 3.73 (t, *J* = 6.6 Hz, 2H, **H_1**), 2.35 (q, *J* = 6.6 Hz, 2H, **H_3**), 1.76 (m, 2H, **H_2**)

^{13}C-NMR: (101 MHz, $CDCl_3$) δ ppm = 141.0 (**C_6**), 134.2 (**C_4**), 128.97 (q, *J* = 39.0 Hz, **C_9**), 128.9 (**$C_{7,11}$**), 126.1 (**C_5**), 125.1 (q, *J* = 3.7 Hz, **$C_{8,10}$**), 123.1 (q, *J* = 272.0 Hz, **C_{12}**), 62.3 (**C_1**), 32.6 (**C_3**), 24.9 (**C_2**)

NMR data for *Z* isomer

^{1}H-NMR: (400 MHz, $CDCl_3$) δ ppm = 7.60 (d, *J* = 8.5 Hz, 2H, **$H_{8,10}$**), 7.35 (d, *J* = 8.5 Hz, 2H, **$H_{7,11}$**), 6.46 (d, *J* = 11.6 Hz, 1H, **H_5**), 5.80 (dt, *J* = 7.5, 11.6 Hz, 1H, **H_4**), 3.68 (t, *J* = 6.6 Hz, 2H, **H_1**), 2.43 (q, *J* = 6.6 Hz, 2H, **H_3**), 1.76 (m, 2H, **H_2**)

^{13}C-NMR: (101 MHz, $CDCl_3$) δ ppm = 141.1 (**C_6**), 132.9 (**C_4**), 129.2 (**$C_{7,11}$**), 128.7 (q, *J* = 31.9 Hz, **C_9**), 128.3 (**C_5**), 125.5 (q, *J* = 3.7 Hz, **$C_{8,10}$**), 123.2 (q, *J* = 272.0 Hz, **C_{12}**), 62.3 (**C_1**), 32.0 (**C_3**), 29.3 (**C_2**)

Data collected on the mixture

LRMS: (ESI^+) 231.2 $[M+H]^+$

4.4.25 2-(Methoxy(4-trifluoromethyl)phenyl)methyl)tetrahydrofuran

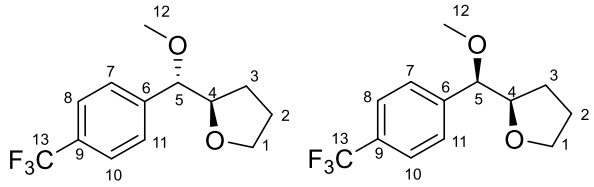

erythro:*threo* ~ 80:20 (^{1}H-NMR)

$C_{13}H_{15}F_3O_2$

Mol Wt: 260.1 g/mol

A solution of (*E*,*Z*)-5-(4-Trifluoromethyl)pent-4-en-1-ol (0.340 g, 1.50 mmol, 1.00 equiv), Et_4NBF_4 (0.080 g, 0.370 mmol, 0.250 equiv) in MeOH (15 mL) was passed through the Ammonite 8 reactor (ss cathode, C/PVDF anode) with a flow of 0.25 mL/min and a current of 80 mA (steady state V= 3.6 V). The effluent was collected and the solvent evaporated under reduced pressure. The electrolyte was recovered by precipitation in EtOAc and filtered away. The solution was concentrated under reduced pressure. The resulting clear oil was purified by column chromatography (SiO_2, toluene/EtOAc = 8/2) to give the desired product as a colourless oil (0.230 g, 0.880 mmol, 59%) as a 80:20 mixture of *erythro* and *threo* diasteroisomers, respectively. By careful column chromatography, samples of each diastereoisomer were obtained for characterisation.

NMR data for *erythro* diastereoisomer (major; more polar)

^{1}H-NMR: (400 MHz, $CDCl_3$) δ ppm = 7.62 (d, *J* = 8.2 Hz, 2H, **$H_{8,10}$**), 7.48 (d, *J* = 8.2 Hz, 2H, **H_7**, **H_{11}**), 4.20 (d, *J* = 5.5 Hz, 1H, **H_5**), 4.01 (m, 1H, **H_4**), 3.84 (m, 1H, **H_1**), 3.74 (m, 1H, **H_1**), 3.29 (s, 3H, **H_{12}**), 1.80-1.95 (m, 4H, **H_2**, **H_3**)

^{13}C-NMR: (101 MHz, $CDCl_3$) δ ppm = 143.7 (**C_6**), 130.0 (q, *J* = 32.0 Hz, **C_9**), 127.8 (**$C_{7,11}$**), 125.2 (q, *J* = 3.8 Hz, **$C_{8,10}$**), 123.1 (q, *J* = 272.5 Hz, **C_{13}**), 85.3 (**C_5**), 82.0 (**C_4**), 68.7 (**C_1**), 57.4 (**C_{12}**), 27.3 (**C_3**), 25.7 (**C_2**)

NMR data for *threo* diastereoisomer (minor; less polar)

^{1}H-NMR: (400 MHz, $CDCl_3$) δ ppm = 7.64 (d, *J* = 8.0 Hz, 2H, **$H_{8,10}$**), 7.47 (d, *J* = 8.0 Hz, 2H, **$H_{7,11}$**), 4.18 (d, *J* = 6.6 Hz, 1H, **H_5**), 4.05 (m, 1H, **H_4**), 3.77-3.89 (m, 2H, **H_1**), 3.28 (s, 3H, **H_{12}**), 1.71-1.83 (m, 2H, **H_2**), 1.49-1.65 (m, 2H, **H_3**)

^{13}C-NMR: (101 MHz, $CDCl_3$) δ ppm = 143.1 (**C_6**), 130.2 (q, *J* = 34.6 Hz, **C_9**), 127.9 (**$C_{7,11}$**), 125.3 (q, *J* = 3.6 Hz, **$C_{8,10}$**), 123.0 (q, *J* = 274.6 Hz, **C_{13}**), 85.9 (**C_5**), 81.9 (**C_4**), 68.7 (**C_1**), 57.2 (**C_{12}**), 28.0 (**C_3**), 25.6 (**C_2**)

Data collected on the mixture of diastereoisomers

LRMS: (ESI$^+$) 229.3 [M-OMe]$^+$

HRMS: (ESI$^+$) *m/z* for $[C_{13}H_{15}F_3O_2Na]^+$ [M+Na]$^+$ calcd: 283.0916 found: 283.0921

FT-IR: ν_{max} (neat) 2938, 1322, 1064 cm^{-1}

4.4.26 (*E,Z*)-5-Phenylhex-4-enoic acid

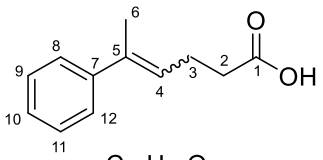

$C_{12}H_{14}O_2$

Mol Wt: 190.1 g/mol

(*E,Z*)-5-Phenylhex-4-enoic acid was prepared adapting the procedure of Perkins *et al.*[177]

To a suspension of (3-Carboxypropyl)triphenylphosphonium bromide (4.30 g, 9.99 mmol, 1.20 equiv) in THF (50 mL) was added a 2 M solution of Sodium *bis*(Trimethylsilyl)amide in THF (10.0 mL, 19.9 mmol, 2.40 equiv) at 0 °C. The solution was stirred for 30 minutes and then cooled down to -78 °C. Acetophenone (1.00 g, 8.30 mmol, 1.00 equiv) was added dropwise and then the reaction mixture was allowed to warm up to rt over-night. Water (20 mL) and Et_2O (20 mL) were added. Phases were separated and the organic phase was discharted; the aqueous phase was acidified to pH = 1 with a 2 M HCl solution and then extracted with EtOAc (3 x 20 mL). The combined organic phases were dried ($MgSO_4$), filtered and solvent removed under reduced pressure. The resulting brown oil was purified by column chromatography (SiO_2, toluene/EtOAc = 8/2) to give the desired product as a yellow oil (1.10 g, 5.81 mmol, 70%, 73/27 = *E/Z*).

Physical and spectroscopic data are consistent with reported literature.[274]

NMR data for *E* isomer

^{1}H-NMR: (400 MHz, $CDCl_3$) δ ppm = 7.40-7.15 (m, 5H, $\mathbf{H_{Ar}}$), 5.76 (m, 1H, $\mathbf{H_4}$), 2.48-2.60 (m, 4H, $\mathbf{H_{2,3}}$), 2.06-2.09 (m, 3H, $\mathbf{H_6}$)

^{13}C-NMR: (101 MHz, $CDCl_3$) δ ppm = 179.1 ($\mathbf{C_1}$), 143.5 ($\mathbf{C_5}$), 136.6 ($\mathbf{C_7}$), 128.2 ($\mathbf{C_{ArH}}$), 126.8 ($\mathbf{C_{ArH}}$), 125.7 ($\mathbf{C_{ArH}}$), 125.6 ($\mathbf{C_4}$), 33.9 ($\mathbf{C_{2\ or\ 3}}$), 23.9 ($\mathbf{C_{2\ or\ 3}}$), 15.9 ($\mathbf{C_6}$)

NMR data for *Z* isomer

^{1}H-NMR: (400 MHz, $CDCl_3$) δ ppm = 7.40-7.15 (m, 5H, $\mathbf{H_{Ar}}$), 5.46 (m, 1H, $\mathbf{H_4}$), 2.30-2.40 (m, 4H, $\mathbf{H_{2,3}}$), 2.03-2.05 (m, 3H, $\mathbf{H_6}$)

^{13}C-NMR: (101 MHz, $CDCl_3$) δ ppm = 179.1 ($\mathbf{C_1}$), 141.6 ($\mathbf{C_5}$), 138.3 ($\mathbf{C_7}$), 127.8 ($\mathbf{C_{ArH}}$), 126.7 ($\mathbf{C_{ArH}}$), 124.8 ($\mathbf{C_4}$), 34.3 ($\mathbf{C_{2\ or\ 3}}$), 25.6 ($\mathbf{C_6}$), 24.3 ($\mathbf{C_{2\ or\ 3}}$)

Data collected on the mixture

LRMS: (ESI^+) 191.3 $[M+H]^+$

4.4.27 5-(1-Methoxy-1-phenylethyl)dihydrofuran-2(3*H*)-one

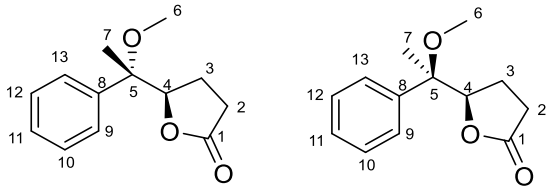

erythro:*threo* ~ 80:20 (^{1}H-NMR)

$C_{13}H_{16}O_3$

Mol Wt: 220.1 g/mol

A solution of (*E,Z*)-5-Phenylhex-4-enoic acid (0.280 g, 1.50 mmol, 1.00 equiv), Et_4NBF_4 (0.080 g, 0.370 mmol, 0.250 equiv) in MeOH (15 mL) was passed through the Ammonite 8 reactor (ss cathode, C/PVDF anode) with a flow of 0.25 mL/min and a current of 80 mA (steady state V = 2.9 V). The effluent was collected and the solvent evaporated under reduced pressure. The electrolyte was recovered by precipitation in EtOAc and filtered away. The solution was concentrated under reduced pressure. The resulting clear oil was purified by column chromatography (SiO_2, toluene/EtOAc = 9/1 to 8/2) to give the desired product as a white solid (0.200 g, 0.910 mmol, 60%) as a 80:20 mixture of *erythro* and *threo* diasteroisomers, respectively.

NMR data for *erythro* diastereoisomer (major)

^{1}H-NMR: (400 MHz, $CDCl_3$) δ ppm = 7.31-7.40 (m, 5H, $\mathbf{H_{Ar}}$), 4.53 (dd, *J* = 7.8, 5.6 Hz, 1H, $\mathbf{H_4}$), 3.22 (s, 3H, $\mathbf{H_6}$), 2.21 (m, 1H, $\mathbf{H_2}$), 1.94-2.14 (m, 2H, $\mathbf{H_3}$), 1.81 (m, 1H, $\mathbf{H_2}$), 1.67 (s, 3H, $\mathbf{H_7}$)

^{13}C-NMR: (101 MHz, $CDCl_3$) δ ppm = 177.3 ($\mathbf{C_1}$), 139.0 ($\mathbf{C_8}$), 128.4, ($\mathbf{C_{ArH}}$), 127.9 ($\mathbf{C_{ArH}}$), 127.3 ($\mathbf{C_{ArH}}$), 85.3 ($\mathbf{C_4}$), 79.9 ($\mathbf{C_5}$), 50.7 ($\mathbf{C_6}$), 27.8 ($\mathbf{C_2}$), 22.4 ($\mathbf{C_3}$), 19.1 ($\mathbf{C_7}$)

NMR data for *threo* diastereoisomer (minor)

^{1}H-NMR: (400 MHz, $CDCl_3$) δ ppm = 7.31-7.40 (m, 5H, $\mathbf{H_{Ar}}$), 4.46 (dd, *J* = 8.2, 5.4 HZ, 1H, $\mathbf{H_4}$), 3.22 (s, 3H, $\mathbf{H_6}$), 2.48 (m, 1H, $\mathbf{H_2}$), 2.33 (m, 1H, $\mathbf{H_2}$), 2.21 (m, 1H, $\mathbf{H_3}$), 1.90 (m, 1H, $\mathbf{H_3}$), 1.69 (s, 3H, $\mathbf{H_7}$)

^{13}C-NMR: (101 MHz, $CDCl_3$) δ ppm = 177.8 ($\mathbf{C_1}$), 140.5 ($\mathbf{C_8}$), 128.5 ($\mathbf{C_{ArH}}$), 127.7 ($\mathbf{C_{ArH}}$), 126.8 ($\mathbf{C_{ArH}}$), 86.4 ($\mathbf{C_4}$), 80.2 ($\mathbf{C_5}$), 50.9 ($\mathbf{C_6}$), 28.4 ($\mathbf{C_2}$), 21.8 ($\mathbf{C_3}$), 19.6 ($\mathbf{C_7}$)

Data collected on the mixture of diastereoisomers

LRMS: (ESI^+) 221.3 $[M+H]^+$

HRMS: (ESI^+) *m/z* for $[C_{13}H_{16}O_3Na]^+$ $[M+Na]^+$ calcd: 243.0992 found: 243.0990

FT-IR: ν_{max} (neat) 2982, 1759, 1119, 697 cm^{-1}

4.4.28 (*E,Z*)-5-Phenylhex-4-en-1-ol

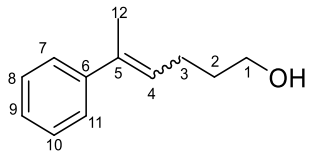

$C_{12}H_{16}O$

Mol Wt: 176.1 g/mol

(*E,Z*)-5-Phenylhex-4-en-1-ol was prepared adapting the procedure of Farndon *et al.*[178]

To a solution of (*E,Z*)-5-Phenylhex-4-enoic acid (0.550 g, 2.90 mmol, 1.00 equiv), in anhydrous THF (10 mL), at 0 °C, was added dropwise a 1M solution of $LiAlH_4$ in THF (5.80 mL, 5.80 mmol, 2.00 equiv). The suspension was stirred for 1 h at rt. Then it was cooled down to 0 °C and water (0.800 mL) and a 10% aqueous solution of NaOH (0.600 mL) were slowly added. The mixture was filtered through celite and washed with dichloromethane. Phases were separated and the aqueous phase was extracted with dichloromethane (2 x 5 mL). The combined organic phases were dried ($MgSO_4$), filtered and solvent removed under reduced pressure. The desired product was obtained as a colourless oil without further purification (0.480 g, 2.70 mmol, 94%, 70/30 *E*/*Z*).

NMR data for *E* isomer

^{1}H-NMR: (400 MHz, $CDCl_3$) δ ppm = 7.17-7.42 (m, 5H, $\mathbf{H_{Ar}}$), 5.80 (td, *J* = 1.5, 6.7 Hz, 1H, $\mathbf{H_4}$), 3.72 (t, *J* = 6.4 Hz, 2H, $\mathbf{H_1}$), 2.30 (td, *J* = 7.2 Hz, 2H, $\mathbf{H_3}$), 2.06 (s, 3H, $\mathbf{H_{12}}$), 1.75 (m, 2H, $\mathbf{H_2}$)

^{13}C-NMR: (101 MHz, $CDCl_3$) δ ppm = 143.8 ($\mathbf{C_{12}}$), 135.4 ($\mathbf{C_6}$), 128.2 ($\mathbf{C_{ArH}}$), 127.6 ($\mathbf{C_4}$), 126.6 ($\mathbf{C_{ArH}}$), 125.6 ($\mathbf{C_{ArH}}$), 62.6 ($\mathbf{C_1}$), 32.6 ($\mathbf{C_2}$), 25.0 ($\mathbf{C_3}$), 15.8 ($\mathbf{C_{12}}$)

NMR data for *Z* isomer

^{1}H-NMR: (400 MHz, $CDCl_3$) δ ppm = 7.17-7.42 (m, 5H, $\mathbf{H_{Ar}}$), 5.48 (td, (td, *J* = 1.5, 7.8 Hz, 1H, $\mathbf{H_4}$), 3.59 (t, *J* = 6.8 Hz, 2H, $\mathbf{H_1}$), 2.02-2.10 (m, 5H, $\mathbf{H_3}$, $\mathbf{H_{12}}$), 1.62 (m, 2H, $\mathbf{H_2}$)

^{13}C-NMR: (101 MHz, $CDCl_3$) δ ppm = 141.9 ($\mathbf{C_{12}}$), 137.0 ($\mathbf{C_6}$), 128.1 ($\mathbf{C_{ArH}}$), 127.9 ($\mathbf{C_{ArH}}$), 126.7 ($\mathbf{C_4}$), 126.5 ($\mathbf{C_{ArH}}$), 62.5 ($\mathbf{C_1}$), 25.6 ($\mathbf{C_3}$), 25.3 ($\mathbf{C_{12}}$)

Data collected on the mixture

LRMS: (ESI^+) 177.3 $[M+H]^+$

HRMS: (ESI^+) *m/z* for $[C_{12}H_{16}ONa]^+$ $[M+Na]^+$ calcd: 199.1093 found: 199.1098

FT-IR: ν_{max} (neat) 3327, 1053, 695 cm^{-1}

4.4.29 2-(1-Methoxy-1-phenylethyl)tetrahydrofuran

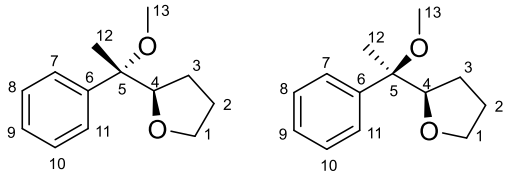

erythro:*threo* ~ 80:20 (^{1}H-NMR)
$C_{13}H_{18}O_2$
Mol Wt: 206.1 g/mol

A solution of (*E,Z*)-5-Phenylhex-4-en-1-ol (0.260 g, 1.50 mmol, 1.00 equiv), Et_4NBF_4 (0.080 g, 0.370 mmol, 0.250 equiv) in MeOH (15 mL) was passed through the Ammonite 8 reactor (ss cathode, C/PVDF anode) with a flow of 0.25 mL/min and a current of 80 mA (steady state V = 3.1 V). The effluent was collected and the solvent evaporated under reduced pressure. The electrolyte was recovered by precipitation in EtOAc and filtered away. The solution was concentrated under reduced pressure. The resulting clear oil was purified by column chromatography (SiO_2, toluene/EtOAc = 9/1) to give the desired product as a colourless oil (0.190 g, 0.920 mmol, 61%) as a 80:20 mixture of *erythro* and *threo* diasteroisomers, respectively.

NMR data for *erythro* diastereoisomer (major)

^{1}H-NMR: (400 MHz, $CDCl_3$) δ ppm = 7.25-7.44 (m, 5H, $\mathbf{H_{Ar}}$), 4.02 (t, *J* = 7.3 Hz, 1H, $\mathbf{H_4}$), 3.68-3.75 (m, 2H, $\mathbf{H_1}$), 3.15 (s, 3H, $\mathbf{H_{13}}$), 1.46-1.88 (m, 7H, $\mathbf{H_{12}}$, $\mathbf{H_2}$, $\mathbf{H_3}$)

^{13}C-NMR: (101 MHz, $CDCl_3$) δ ppm = 141.9 ($\mathbf{C_6}$), 128.0 ($\mathbf{C_{ArH}}$), 127.2 ($\mathbf{C_{ArH}}$), 127.1 ($\mathbf{C_{ArH}}$), 85.9 ($\mathbf{C_4}$), 81.2 ($\mathbf{C_5}$), 68.9 ($\mathbf{C_1}$), 50.6 ($\mathbf{C_{13}}$), 27.1 ($\mathbf{C_{3\ or\ 2}}$), 25.7 ($\mathbf{C_{3\ or\ 2}}$), 17.6 ($\mathbf{C_{12}}$)

NMR data for *threo* diastereoisomer (minor)

^{1}H-NMR: (400 MHz, $CDCl_3$) δ ppm = 7.25-7.44 (m, 5H, $\mathbf{H_{Ar}}$), 3.96 (t, *J* = 6.7 Hz, 1H, $\mathbf{H_4}$), 3.68-3.75 (m, 2H, $\mathbf{H_1}$), 3.16 (s, 3H, $\mathbf{H_{13}}$), 1.46-1.88 (m, 7H, $\mathbf{H_{12}}$, $\mathbf{H_2}$, $\mathbf{H_3}$)

^{13}C-NMR: (101 MHz, $CDCl_3$) δ ppm = 142.6 ($\mathbf{C_6}$), 127.9 ($\mathbf{C_{ArH}}$), 127.3 ($\mathbf{C_{ArH}}$), 127.0 ($\mathbf{C_{ArH}}$), 86.2 ($\mathbf{C_4}$), 80.6 ($\mathbf{C_5}$), 68.8 ($\mathbf{C_1}$), 50.6 ($\mathbf{C_{13}}$), 26.4 ($\mathbf{C_{3\ or\ 2}}$), 25.9 ($\mathbf{C_{3\ or\ 2}}$), 19.0 ($\mathbf{C_{12}}$)

Data collected on the mixture of diastereoisomers

LRMS: (ESI^+) 229.2 $[M+Na]^+$

HRMS: (ESI^+) *m/z* for $[C_{13}H_{18}O_2Na]^+$ $[M+Na]^+$ calcd: 229.1199 found: 229.1201

FT-IR: ν_{max} (neat) 2977, 1071, 701 cm^{-1}

4.4.30 (E,Z)-5-(Pyridin-3-yl)pent-4-enoic acid

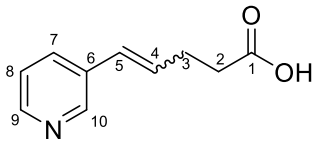

$C_{10}H_{11}NO_2$
Mol Wt: 177.1 g/mol

(*E*,*Z*)-5-(Pyridin-3-yl)pent-4-enoic acid was prepared adapting the procedure of Perkins *et al.*[177]

To a suspension of (3-Carboxypropyl)triphenylphosphonium bromide (6.60 g, 15.4 mmol, 1.10 equiv) in THF (20 mL) was added a 1 M solution of Lithium *bis*(Trimethylsilyl)amide in THF/ethylbenzene (30.8 mL, 30.8 mmol, 2.20 equiv) at 0 °C. The solution was stirred for 30 minutes and then cooled down to -78 °C. 3-Pyridine carboxyaldehyde (1.50 g, 14.0 mmol, 1.00 equiv) was added dropwise and then the reaction mixture was allowed to warm up to rt over-night. Water (20 mL) and Et_2O (20 mL) were added. Phases were separated and the organic phase was discharted; the aqueous phase was acidified to pH = 7 with a 2 M HCl solution and then extracted with EtOAc (3 x 20 mL). The combined organic phases were dried ($MgSO_4$), filtered and solvent removed under reduced pressure. The resulting brown solid was purified by column chromatography (SiO_2, DCM/MeOH = 95/5 to 90/10) to give the title carboxylic acid as a white solid (0.800 g, 4.50 mmol, 32%, 70/30 *E*/*Z*).

NMR data for *E* isomer

^{1}H-NMR: (400 MHz, $CDCl_3$) δ ppm = 11.13 (bs, 1H, **OH**), 8.59 (s, 1H, **H_{10}**), 8.43 (d, *J* = 4.4 Hz, 1H, **H_9**), 7.70 (d, *J* = 7.9 Hz, 1H, **H_7**), 7.28 (dd, *J* = 4.4, 7.9 Hz, 1H, **H_8**), 6.29-6.48 (m, 2H, **H_4**, **H_5**), 2.43-2.70 (m, 4H, **H_2**, **H_3**)

^{13}C-NMR: (101 MHz, $CDCl_3$) δ ppm = 176.5 (**C_1**), 146.6 (**C_9**), 146.5 (**C_{10}**), 133.8 (**C_6**), 133.7 (**C_7**), 132,1 (**C_4**), 126.9 (**C_5**), 123.8 (**C_8**), 28.3 (**C_3**), 24,1 (**C_2**)

NMR data for *Z* isomer

^{1}H-NMR: (400 MHz, $CDCl_3$) δ ppm = 11.13 (bs, 1H, **OH**), 8.59 (s, 1H, **H_{10}**), 8.47 (d, *J* = 4.2 Hz, 1H, **H_9**), 7.67 (d, *J* = 7.8 Hz, 1H, **H_7**), 7.35 (dd, *J* = 4.2, 7.8 Hz, 1H, **H_8**), 6.38 (m, 1H, **H_5**), 5.87 (dt, *J* = 7.2, 11.7 Hz, **H_4**), 2.43-2.70 (m, 4H, **H_2**, **H_3**)

^{13}C-NMR: (101 MHz, $CDCl_3$) δ ppm = 176.4 (**C_1**), 148.4 (**C_{10}**), 146.3 (**C_9**), 136.9 (**C_7**), 133.6 (**C_6**), 133.5 (**C_4**), 125.9 (**C_5**), 123.6 (**C_8**), 34.2 (**C_3**), 33.7 (**C_2**)

Data collected on the mixture

LRMS: (ESI^+) 178.2 $[M+H]^+$

HRMS: (ESI^+) *m/z* for $[C_{10}H_{12}NO_2]^+$ $[M+H]^+$ calcd: 178.0863 found: 178.0864

FT-IR: ν_{max} (neat) 2440, 1703, 1049, 733 cm^{-1}

4.4.31 5-(Methoxy(pyridine-3-yl)methyl)dihydrofuran-2(3H)-one

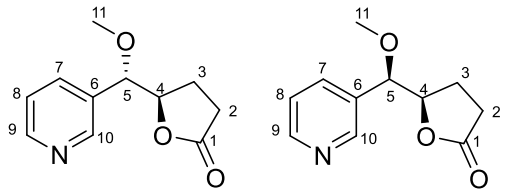

erythro:*threo* ~ 80:20 (^{1}H-NMR)

$C_{11}H_{13}NO_3$

Mol Wt: 207.1 g/mol

A solution of (*E*,*Z*)-5-(Pyridin-3-yl)pent-4-enoic acid (0.260 g, 1.50 mmol, 1.00 equiv), Et_4NBF_4 (0.080 g, 0.370 mmol, 0.250 equiv) in MeOH (15 mL) was passed through the Ammonite 8 reactor (ss cathode, C/PVDF anode) with a flow of 0.25 mL/min and a current of 80 mA (steady state V = 3.5 V). The effluent was collected and the solvent evaporated under reduced pressure. The electrolyte was recovered by precipitation in EtOAc and filtered away. The solution was concentrated under reduced pressure. The resulting clear oil was purified by column chromatography (SiO_2, DCM to DCM/MeOH = 95/5) to give the desired product as a colourless oil (0.070 g, 0.340 mmol, 22%) as a 85:15 mixture of *erythro* and *threo* diasteroisomers, respectively.

NMR data for *erythro* diastereoisomer (major)

^{1}H-NMR: (400 MHz, $CDCl_3$) δ ppm = 8.54-8.65 (m, 2H, $\mathbf{H_{9,\,10}}$), 7.73 (dt, *J* = 1.8, 7.9 Hz, 1H, $\mathbf{H_7}$), 7.35 (m, 1H, $\mathbf{H_8}$), 4.67 (m, 1H, $\mathbf{H_4}$), 4.30 (d, *J* = 4.5 Hz, 1H, $\mathbf{H_5}$), 3.33 (s, 3H, $\mathbf{H_{11}}$), 2.40-2.48 (m, 2H, $\mathbf{H_3}$), 2.07-2.18 (m, 2H, $\mathbf{H_2}$)

^{13}C-NMR: (101 MHz, $CDCl_3$) δ ppm = 176.8 ($\mathbf{C_1}$), 150.1 ($\mathbf{C_9}$), 149.0 ($\mathbf{C_{10}}$), 135.4 ($\mathbf{C_7}$), 132.4 ($\mathbf{C_6}$), 123.7 ($\mathbf{C_8}$), 82.8 ($\mathbf{C_5}$), 81.5($\mathbf{C_4}$), 57.5 ($\mathbf{C_{11}}$), 28.2 ($\mathbf{C_3}$), 24.0 ($\mathbf{C_2}$)

NMR data for *threo* diastereoisomer (minor)

^{1}H-NMR: (400 MHz, $CDCl_3$) δ ppm = 8.54-8.65 (m, 2H, $\mathbf{H_{9,\,10}}$), 7.69 (dt, *J* = 2.0, 7.9 Hz, 1H, $\mathbf{H_7}$), 7.35 (m, 1H, $\mathbf{H_8}$), 4.60 (m, 1H, $\mathbf{H_4}$), 4.48 (d, *J* = 3.8 Hz, 1H, $\mathbf{H_5}$), 3.36 (s, 3H, $\mathbf{H_{11}}$), 2.40-2.61 (m, 2H, $\mathbf{H_3}$), 2.07-2.33 (m, 2H, $\mathbf{H_2}$)

^{13}C-NMR: (101 MHz, $CDCl_3$) δ ppm = 177.0 ($\mathbf{C_1}$), 149.9 ($\mathbf{C_9}$), 148.7 ($\mathbf{C_{10}}$), 134.7 ($\mathbf{C_7}$), 132.3 ($\mathbf{C_6}$), 123.6 ($\mathbf{C_8}$), 82.3 ($\mathbf{C_5}$), 82.1 ($\mathbf{C_4}$), 57.9 ($\mathbf{C_{11}}$), 28.1 ($\mathbf{C_3}$), 21.8 ($\mathbf{C_2}$)

Data collected on the mixture of diastereoisomers

LRMS: (ESI^+) 208.2 $[M+H]^+$

HRMS: (ESI^+) *m/z* for $[C_{11}H_{14}NO_3]^+$ $[M+H]^+$ calcd: 208.0968 found: 208.0973

FT-IR: ν_{max} (neat) 1769, 1174, 715 cm^{-1}

4.4.32 (E,Z)-5-(Pyridine-3-yl)pent-4-en-1-ol

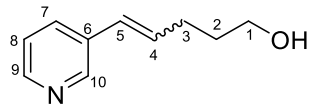

$C_{10}H_{13}NO$

Mol Wt: 163.1 g/mol

(*E*,*Z*)-5-(Pyridine-3-yl)pent-4-en-1-ol was prepared adapting the procedure of Farndon *et al.*[178]

To a solution of (*E*,*Z*)-5-(Pyridin-3-yl)pent-4-enoic acid (0.800 g, 4.50 mmol, 1.00 equiv), in anhydrous THF (10 mL), at 0 °C, was added dropwise a 1M solution of $LiAlH_4$ in THF (9.00 mL, 9.00 mmol, 2.00 equiv). The suspension was stirred for 1 h at rt. Then it was cooled down to 0 °C and water (1.60 mL) and a 10% aqueous solution of NaOH (1.20 mL) were slowly added. The mixture was filtered through celite and washed with dichloromethane. Phases were separated and the aqueous phase was extracted with dichloromethane (2 x 10 mL). The combined organic phases were dried ($MgSO_4$), filtered and solvent removed under reduced pressure. The desired product was obtained as a colourless oil without further purification (0.690 g, 4.20 mmol, 94%, 70/30 *E*/*Z*).

NMR data for *E* isomer

^{1}H-NMR: (400 MHz, $CDCl_3$) δ ppm = 8.53 (m, 1H, **H_{10}**), 8.41 (m, 1H, **H_9**), 7.60 (dt, *J* = 1.5, 8.1 Hz, 1H, **H_7**), 7.23 (m, 1H, **H_8**), 6.39 (m, 1H, **H_5**), 6.30 (m, 1H, **H_4**), 5.82 (dt, *J* = 7.2, 12.0Hz, 1H, **H_4**), 3.64 (m, 2H, **H_1**), 2.40 (m, 2H, **H_3**), 2.25 (bs, 1H, **OH**), 1.74 (m, 2H, **H_2**)

^{13}C-NMR: (101 MHz, $CDCl_3$) δ ppm = 150.0 (**C_{10}**), 147.6 (**C_9**), 135.7 (**C_7**), 134.6 (**C_4**), 133.1 (**C_6**), 125.8 (**C_5**), 123.1 (**C_8**), 62.2 (**C_1**), 32.7 (**C_2**), 25.0 (**C_3**)

NMR data for *Z* isomer

^{1}H-NMR: (400 MHz, $CDCl_3$) δ ppm = 8.53 (m, 1H, **H_{10}**), 8.41 (m, 1H, **H_9**), 7.65 (dt, *J* = 1.8, 8.1 Hz, 1H, **H_7**), 7.23 (m, 1H, **H_8**), 6.39 (m, 1H, **H_5**), 6.30 (m, 1H, **H_4**), 3.69 (m, 2H, **H_1**), 2.39 (m, 2H, **H_3**), 2.25 (bs, 1H, **OH**), 1.74 (m, 2H, **H_2**)

^{13}C-NMR: (101 MHz, $CDCl_3$) δ ppm = 148.0 (**C_{10}**), 147.9 (**C_9**), 133.2 (**C_6**), 132.7 (**C_4**), 132.5 (**C_7**), 126.8 (**C_5**), 123.4 (**C_8**), 62.2 (**C_1**), 32.0 (**C_2**), 29.4 (**C_3**)

Data collected on the mixture

LRMS: (ESI^+) 164.2 $[M+H]^+$

HRMS: (ESI^+) *m/z* for $[C_{10}H_{14}NO]^+$ $[M+H]^+$ calcd: 164.1070 found: 164.1068

FT-IR: ν_{max} (neat) 3285, 2932, 1057, 705 cm^{-1}

4.4.33 3-(Methoxy(tetrahydrofuran-2-yl)methyl)pyridine

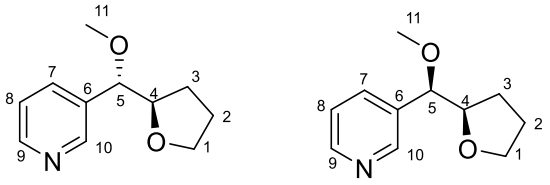

$C_{11}H_{15}NO_2$
Mol Wt: 193.1 g/mol

A solution of (*E*,*Z*)-5-(Pyridine-3-yl)pent-4-en-1-ol (0.240 g, 1.50 mmol, 1.00 equiv), Et_4NBF_4 (0.080 g, 0.370 mmol, 0.250 equiv) in MeOH (15 mL) was passed through the Ammonite 8 reactor (ss cathode, C/PVDF anode) with a flow of 0.25 mL/min and a current of 80 mA (steady state V = 3.7 V). The effluent was collected and the solvent evaporated under reduced pressure. The electrolyte was recovered by precipitation in EtOAc and filtered away. The solution was concentrated under reduced pressure. The resulting clear oil was purified by column chromatography (SiO_2, toluene/EtOAc = 4/6) to give the desired product as a colourless oil (0.090 g, 0.470 mmol, 30%).

NMR data for *erythro* diastereoisomer (major)

^{1}H-NMR: (400 MHz, $CDCl_3$) δ ppm = 8.53-8.59 (m, 2H, **H_9**, **H_{10}**), 7.69 (m, 1H, **H_7**), 7.30 (m, 1H, **H_8**), 4.15 (m, 1H, **H_5**), 4.05 (m, 1H, **H_4**), 3.69-3.89 (m, 2H, **H_1**), 3.28 (s, 3H, **H_{11}**), 1.64-1.95 (m, 4H, **H_2**, **H_3**)

^{13}C-NMR: (101 MHz, $CDCl_3$) δ ppm = 149.4 (**C_9**), 149.2 (**C_{10}**), 135.1 (**C_7**), 134.7 (**C_6**), 123.4 (**C_8**), 83.7 (**C_5**), 81.8 (**C_4**), 68.7 (**C_1**), 57.4 (**C_{11}**), 27.4 (**C_3**), 25.6 (**C_2**)

NMR data for *threo* diastereoisomer (minor)

^{1}H-NMR: (400 MHz, $CDCl_3$) δ ppm = 8.53-8.59 (m, 2H, **H_9**, **H_{10}**), 7.69 (m, 1H, **H_7**), 7.30 (m, 1H, **H_8**), 4.15 (m, 1H, **H_5**), 4.05 (m, 1H, **H_4**), 3.69-3.89 (m, 2H, **H_1**), 3.28 (s, 3H, **H_{11}**), 1.64-1.95 (m, 4H, **H_2**, **H_3**)

^{13}C-NMR: (101 MHz, $CDCl_3$) δ ppm = 149.5 (**C_9**), 149.3 (**C_{10}**), 135.0 (**C_7**), 134.4 (**C_6**), 123.5 (**C_8**), 84.2 (**C_5**), 81.7 (**C_4**), 68.7 (**C_1**), 57.2 (**C_{11}**), 28.0 (**C_3**), 25.5 (**C_2**)

Data collected on the mixture of diastereoisomers

LRMS: (ESI^+) 194.3 $[M+H]^+$

HRMS: (ESI^+) *m/z* for $[C_{11}H_{16}NO_2]^+$ $[M+H]^+$ calcd: 194.1176 found: 194.1177

FT-IR: ν_{max} (neat) 2978, 1091, 1070, 717 cm^{-1}

4.4.34 (*E*)-2-Methyl-7-phenylhept-6-en-3-ol

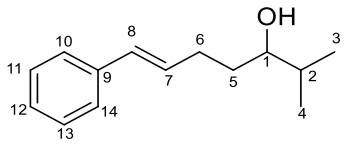

$C_{14}H_{20}O$
Mol Wt: 204.3 g/mol

(*E*)-2-Methyl-7-phenylhept-6-en-3-ol was prepared adapting the procedure of Luo *et al* [275] and Scamp *et al.*[276]

To a solution of (*E*)-5-phenylpent-4-en-1-ol (1.00 g, 6.20 mmol, 1.00 equiv) in dry CH_2Cl_2 (15 mL), DM-periodinane (3.90 g, 9.30 mmol, 1.50 equiv) was added in one portion. The reaction mixture was stirred at rt for 1 h. A solution of $Na_2C_2O_3$ sat. sol./$NaHCO_3$ sat. sol. = 1/1 was added to the reaction mixture and the system was left stirring till two distinct phases were visible. Phases were separated and the organic phase was dried ($MgSO_4$), filtered and the solvent evaporated under reduced pressure. The crude aldehyde was directly used in the second step. At -78 °C, to a stirred solution of the crude aldehyde in dry Et_2O (40 mL), a 2 M solution of isopropyl magnesium chloride in THF (4.00 mL, 8.11 mmol, 2.60 equiv) was added dropwise. Reaction mixture was stirred for 30 minutes at -78 °C and left warming up to rt over-night. The reaction mixture was cooled down at 0 °C and a 2 M aqueous solution of HCl (40 mL) was added. Phases were separated and the aqueous one was extracted with CH_2Cl_2 (2 x 30 mL). The combined organic phases were dried ($MgSO_4$), filtered and the solvent evaporated under reduced pressure. The resulting clear oil was purified by column chromatography (SiO_2, 100% toluene to toluene/EtOAc = 9/1) giving the desired product as clear oil (0.400 g, 1.90 mmol, 61%).

^{1}H-NMR: (400 MHz, $CDCl_3$) δ ppm = 7.24-7.43 (m, 5H, $\mathbf{H_{Ar}}$), 6.44 (d, *J* = 15.7 Hz, 1H, $\mathbf{H_8}$), 6.27 (dt, *J* = 15.7, 6.9 Hz, 1H, $\mathbf{H_7}$), 3.44 (m, 1H, $\mathbf{H_1}$), 2.38 (m, 2H, $\mathbf{H_6}$), 1.50-1.77 (m, 3H, $\mathbf{H_2}$, $\mathbf{H_5}$), 0.97 (d, *J* = 2.6 Hz, 3H, $\mathbf{H_3}$), 0.95 (d, *J* = 2.6 Hz, 3H, $\mathbf{H_4}$)

^{13}C-NMR: (101 MHz, $CDCl_3$) δ ppm = 137.7 ($\mathbf{C_9}$), 130.6 ($\mathbf{C_7}$), 130.2 ($\mathbf{C_8}$), 128.5 ($\mathbf{C_{ArH}}$), 126.9 ($\mathbf{C_{ArH}}$), 125.9 ($\mathbf{C_{ArH}}$), 76.2 ($\mathbf{C_1}$), 33.7 ($\mathbf{C_2}$), 33.6 ($\mathbf{C_5}$), 29.7 ($\mathbf{C_6}$), 18.8 ($\mathbf{C_4}$), 17.2 ($\mathbf{C_3}$)

LRMS: (ESI^+) 205.3 $[M+H]^+$

HRMS: (ESI^+) *m/z* for $[C_{14}H_{21}O]^+$ $[M+H]^+$ calcd: 205.1587 found: 205.1590

FT-IR: ν_{max} (neat) 3378, 2956, 962, 691 cm^{-1}

4.4.35 2-Isopropyl-5-(methoxy(phenyl)methyl)tetrahydrofuran

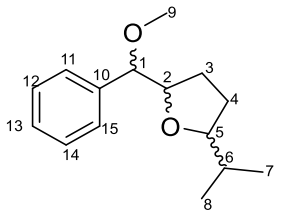

$C_{15}H_{22}O_2$
Mol Wt: 234.3 g/mol

A solution of (*E*)-2-Methyl-7-phenylept-6-en-3-ol (0.120 g, 0.490 mmol, 1.00 equiv), Et_4NBF_4 (0.050 g, 0.250 mmol, 0.500 equiv) in MeOH (5 mL) was passed through the Ammonite 8 reactor (ss cathode, C/PVDF anode) at a flow rate of 0.25 mL min^{-1} and a current of 80 mA (steady state V = 3.1 V). The effluent was collected and the solvent evaporated under reduced pressure. The electrolyte was recovered by filtration after precipitation from EtOAc. The solvent removed under reduced pressure and the resulting clear oil was purified by column chromatography (SiO_2, toluene/EtOAc = 9/1) to give the title product as a colourless oil (0.070 g, 0.290 mmol, 60%), as a mixture of diasteroisomers.

Characterisation data are reported for the mixture of stereoisomers.

^{1}H-NMR: (400 MHz, $CDCl_3$) δ ppm = 7.20-7.29 (m, 5H, **H_{Ar}**), 3.95-4.12 (m, 2H, **H_1**, **H_2**), 3.55 (m, 1H, **H_5**), 3.18 (s, 1H, **H_9**), 1.61-1.74 (m, 2H, **H_3**, **H_6**) 1.37-1.47 (m, 3H, **H_3**, **H_4**), 0.89 (d, *J* = 6.7 Hz, 3H, **H_7**), 0.77 (d, *J* = 6.7 Hz, 3H, **H_8**)

^{13}C-NMR: (101 MHz, $CDCl_3$) δ ppm = 139.0 (**C_{10}**), 128.3 (**C_{ArH}**), 128.2 (**C_{ArH}**), 127.7 (**C_{ArH}**), 87.5 (**C_1**), 85.2 (**C_5**), 82.0 (**C_2**), 56.9 (**C_9**), 32,8 (**C_6**), 29.0 (**C_4**), 28.5 (**C_3**), 19.5 (**C_8**), 17.8 (**C_7**)

LRMS: (EI) *m/z* (0.5%, $[C_{15}H_{22}O_2]^+$) 234.3, (80%, $[C_8H_9O]^\bullet$) 121.1, (80%, $[C_7H_{13}O]^{\bullet+}$) 113.1

HRMS: (EI) *m/z* for $[C_{15}H_{22}O_2]^{\bullet+}$ calcd: 234.16143 found: 234.16073

FT-IR: ν_{max} (neat) 2960, 1026, 701 cm^{-1}

4.4.36 Ethyl camphorsulfonate

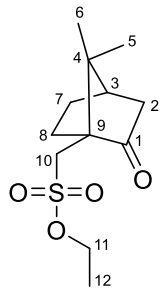

$C_{12}H_{20}O_4S$
Mol Wt: 260.3 g/mol

Ethyl camphorsulfonate was prepared following the procedure of Mekala *et al.*[206]

A solution of 1*S*-(+)-Camphorsulfonic acid (2.00 g, 8.60 mmol, 1.00 equiv) in Triethyl phosphite (2.00 mL, 9.90 mmol, 1.20 equiv) was heated at 50 °C for 2 h. Reaction mixture was directly purified by column chromatography (SiO_2, toluene/EtOAc = 7/3) to give the title Ethyl camphorsulfonate as a clear oil (1.50 g, 5.80 mmol, 65%).

Physical and spectroscopic data are consistent with reported literature.[206]

^{1}H-NMR: (400 MHz, $CDCl_3$) δ ppm = 4.31-4.38 (m, 2H, **H_{11}**), 3.62 (d, *J* = 15.1 Hz, 1H, **H_{10}**), 3.00 (d, *J* = 15.1 Hz, 1H, **H_{10}**), 2.50 (m, 1H, **H_7**), 2.40 (m, 1H, **H_2**), 2.13 (t, *J* = 4.5 Hz, 1H, **H_3**), 2.06 (m, 1H, **H_8**), 1.96 (d, *J* = 18.6 Hz, 1H, **H_2**), 1.67 (m, 1H, **H_7**), 1.38-1.49 (m, 4H, **H_8**, **H_{12}**), 1.12 (s, 3H, **H_5**), 0.98 (s, 3H, **H_6**)

^{13}C-NMR: (101 MHz, $CDCl_3$) δ ppm = 214.6 (**C_1**), 66.9 (**C_{11}**), 57.9 (**C_4**), 47.9 (**C_9**), 46.6 (**C_{10}**), 42.7 (**C_3**), 42.5 (**C_2**), 26.8 (**C_8**), 24.8 (**C_7**), 19.8 (**C_6**), 19.7 (**C_5**), 15.1 (**C_{12}**)

LRMS: (ESI^+) 261.2 $[M+H]^+$

4.4.37 Tetraethylammonium camphorsulfonate

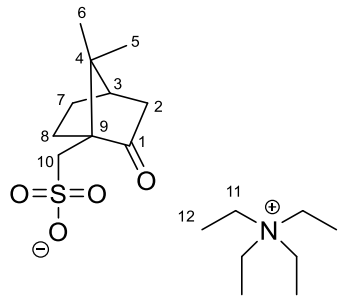

$C_{18}H_{35}NO_4S$
Mol Wt: 361.5 g/mol

Tetraethyl ammonium camphorsulfonate was prepared following the procedure of Maekawa *et al*.[202]

To a solution of Ethyl camphorsulfonate (0.500 g, 1.90 mmol, 1.00 equiv) in dry EtOH (2.00 mL), Et_3N (0.300 mL, 2.20 mmol, 1.10 equiv) was added dropwise. The mixture was heated under reflux for 3 h. EtOH and Et_3N were evaporated under reduced pressure. The resulting gel was recrystallized in EtOAc to give the title product as a white solid (0.400 g, 1.10 mmol, 58%).

Physical and spectroscopic data are consistent with reported literature.[202]

^{1}H-NMR: (400 MHz, $CDCl_3$) δ ppm = 3.39 (q, *J* = 7.1 Hz, 8H, **H_{11}**), 3.22 (d, *J* = 15.0 Hz, 1H, **H_{10}**), 2.70-2.81 (m, 2H, **H_{10}**, **H_7**), 2.27 (m, 1H, **H_2**), 1.93-2.03 (m, 2H, **H_3**, **H_8**), 1.84 (d, *J* = 18.2 Hz, 1H, **H_2**), 1.67 (m, 1H, **H_7**), 1.30-1.40 (m, 13H, **H_{12}**, **H_8**), 1.10 (s, 3H, **H_6**), 0.81 (s, 3H, **H_5**)

^{13}C-NMR: (101 MHz, $CDCl_3$) δ ppm = 217.2 (**C_1**), 58.5 (**C_4**), 52.5 (**C_{11}**), 47.8 (**C_9**), 46.8 (**C_{10}**), 43.0 (**C_2**), 42.5 (**C_3**), 27.0 (**C_8**), 24.4 (**C_7**), 20.0 (**C_6**), 19.8 (**C_5**), 7.6 (**C_{12}**)

LRMS: (ESI$^+$) 233.2 $[C_{10}H_{16}O_4S]^+$

Mp: 62-67 °C

4.4.38 4-Hydroxy-N-morpholino butanamide

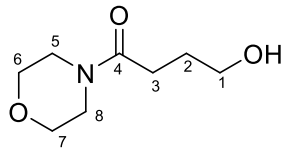

$C_8H_{15}NO_3$
Mol Wt: 173.2 g/mol

4-Hydroxy-*N*-morpholino butanamide was prepared following the procedure of Peng *et al*.[180]

A solution of γ-Butirrolactone (3.10 g, 34.8 mmol, 1.00 equiv), Morpholine (3.34 mL, 38.3 mmol, 1.10 equiv) and Trimethylamine (19.4 mL, 139.4 mmol, 4.00 equiv) was stirred under reflux over-night. The solvent was removed under reduced pressure and the resulting clear oil purified by column chromatography (SiO_2, CH_2Cl_2/MeOH = 95/5 to 9/1) to give the title amide as a brown oil (4.10 g, 23.7 mmol, 68%).

Physical and spectroscopic data are consistent with reported literature.[180]

^{1}H-NMR: (400 MHz, $CDCl_3$) δ ppm = 3.60-3.78 (m, 8H, **H_{5-8}**), 3.45-3.55 (m, 2H, **H_1**), 2.45-2.55 (m, 2H, **H_3**), 1.88-1.96 (m, 2H, **H_2**)

^{13}C-NMR: (101 MHz, $CDCl_3$) δ ppm = 171.8 (**C_4**), 66.9 (**C_{5-8}**), 66.6 (**C_{5-8}**), 62.4 (**C_{5-8}**), 46.0 (**C_1**), 42.0 (**C_{5-8}**), 30.4 (**C_3**), 27.5 (**C_2**)

LRMS: (ESI^+) 174.2 $[M+H]^+$

4.4.39 4-(Tetrahydropyranyl)-oxy-N-morpholino butanamide

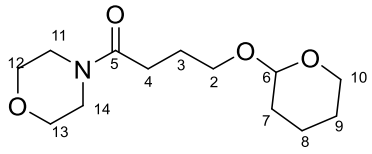

$C_{13}H_{23}NO_4$
Mol Wt:257.3 g/mol

4-(Tetrahydropyranyl)-oxy-*N*-morpholino butanamide was prepared adapting the procedure of Pesti *et al*.[181]

To a solution of 4-Hydroxy-*N*-morpholino butanamide (1.88 g, 10.9 mmol, 1.00 equiv), 3,4-Dihydro-2*H*-pyran (1.20 mL, 13.0 mmol, 1.20 equiv) in CH_2Cl_2 (20.0 mL), *p*-Toluensulfonic acid (0.080 g, 0.440 mmol, 0.040 equiv) was added in one portion and the yellow solution was stirred at rt for 3 h. Then a satured solution of $NaHCO_3$ (10.0 mL) was added; phases were separated and the aqueous phase was extracted with CH_2Cl_2 (3 x 10 mL). The combined organic phases were dried ($MgSO_4$), filtered and the solvent evaporated under reduced pressure. The red oil was purified by column chromatography (SiO_2, toluene/EtOAc=7/3 to 100% EtOAc) to give the title product as a yellow oil (2.20 g, 8.50 mmol, 79%).

^{1}H-NMR: (400 MHz, $CDCl_3$) δ ppm = 4.55 (t, *J* = 3.4 Hz, 1H, **H_6**), 3.77-3.90 (m, 2H, **H_{2a}**, **H_{10a}**), 3.60-3.71 (m, 6H, **H_{11-14}**), 3.45-3.55 (m, 4H, **H_{2b}**, **H_{10b}**, **H_{11-14}**), 2.45 (dt, *J* = 9.8, 7.2 Hz, 2H, **H_4**), 1.92-2.01 (m, 2H, **H_3**), 1.70-1.90 (m, 2H, **H_8**), 1.50-1.65 (m, 4H, **H_9**, **H_7**)

^{13}C-NMR: (101 MHz, $CDCl_3$) δ ppm = 171.4 (**C_5**), 99.1 (**C_6**), 66.9 (**C_{11-14}**), 66.7 (**C_{10}**), 62.7 (**C_2**), 45.9 (**$C_{11\ or\ 14}$**), 41.9 (**$C_{11\ or\ 14}$**), 30.8 (**C_7**), 29.7 (**C_4**), 25.4 (**C_3**, **C_9**), 19.9 (**C_8**)

LRMS: (ESI^+) 280.3 $[M+Na]^+$

4.4.40 1-Phenyl-4-(tetrahydropyranyl)oxy butanone

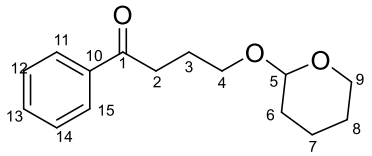

$C_{15}H_{20}O_3$
Mol Wt:248.3 g/mol

1-Phenyl-4-(tetrahydropyranyl)oxy butanone was prepared adapting the procedure of Pesti *et al*.[181]

To a solution of 4-(Tetrahydropyranyl)oxy-*N*-morpholino butanamide (1.01 g, 3.90 mmol, 1.00 equiv) in dry THF (10 mL), a 1 M solution of PhMgBr (5.10 mL, 5.10 mmol, 1.30 equiv) was added dropwise. The mixture was stirred at rt over-night. The grey solution was cooled down to 0 °C and a solution of water (10 mL) and AcOH (3 mL) was added dropwise. Phases were separated, the aqueous phase was extracted with EtOAc (3 x 10 mL) and the combined organic phases were dried ($MgSO_4$), filtered and the solvent evaporated under reduced pressure. The resulting oil was purified by column chromatography (SiO_2, toluene/EtOAc=8/2) to give the title product as a clear oil (0.500 g, 2.00 mmol, 52%).

^{1}H-NMR: (400 MHz, $CDCl_3$) δ ppm = 7.95-8.03 (m, 2H, **$H_{11,15}$**), 7.59 (m, 1H, **H_{13}**), 7.40-7.50 (m, 2H, **$H_{12,14}$**), 4.60 (m, 1H, **H_5**), 3.80-3.92 (m, 2H, **H_{4a}**, **H_{9a}**), 3.47-3.57 (m, 2H, **H_{4b}**, **H_{9b}**), 3.12 (dt, *J* = 7.4, 10.5 Hz, 2H, **H_2**), 2.03-2.12 (m, 2H, **H_3**), 1.70-1.90 (m, 2H, **H_7**), 1.49-1.65 (m, 4H, **H_6**, **H_8**)

^{13}C-NMR: (101 MHz, $CDCl_3$) δ ppm = 200.0 (**C_1**), 137.1 (**C_{10}**), 132.9 (**C_{13}**), 128.5 (**$C_{11,15}$**), 128.1 (**$C_{12,14}$**), 98.9 (**C_5**), 66.7 (**C_9**), 62.5 (**C_4**), 35.3 (**C_6**), 30.7 (**C_2**), 25.5 (**C_3**), 24.4 (**C_8**), 19.7 (**C_7**)

LRMS: (ESI^+) 249.3 $[M+H]^+$

4.4.41 4-Pheny-1-(tetrahydropyranyl)oxy-pent-4-ene

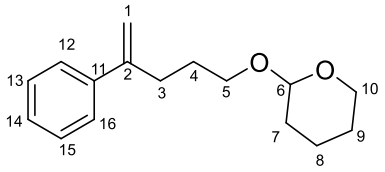

$C_{16}H_{22}O_2$
Mol Wt:246.3 g/mol

4-Phenyl-1-(tetrahydropyranyl)oxy-pent-4-ene was prepared adapting the procedure of Sha *et al*.[182]

To a suspension of Ph_3PMeBr (0.730 g, 2.03 mmol, 1.00 equiv), in dry THF (4.00 mL), at 0 °C, KO*t*Bu (0.300 g, 2.60 mmol, 1.30 equiv) was added portion-wise. The suspension was left stirring for 30 minutes and then 1-Phenyl-4-(tetrahydropyranyl)oxy butanone (0.500 g, 2.01 mmol, 1.00 equiv) previously dissolved in dry THF (1.00 mL) was added. The mixture was stirred over-night at rt. Water (5.00 mL) was added to reaction mixture, phases were separated and the aqueous phase was extracted with EtOAc (3 x 5 mL). The combined organic phases were dried ($MgSO_4$), filtered and the solvent evaporated under reduced pressure. The resulting brown oil was dissolved in hexane (10 mL) to afford the precipitation of the phosphine oxide and left stirring for 1 h at 0 °C. The solid was filtered away and solvent was evaporated under reduced pressure. The resulting clear oil was purified by column chromatography (SiO_2, hexane/EtOAc = 9/1) to give the title product as a clear oil (0.150 g, 0.600 mmol, 30%).

^{1}H-NMR: (400 MHz, $CDCl_3$) δ ppm = 7.42-7.46 (m, 2H, **$H_{12,16}$**), 7.32-7.37 (m, 2H, **$H_{13,15}$**), 7.29 (m, 1H, **H_{14}**), 5.32 (d, *J* = 1.4 Hz, 1H, **H_{1a}**), 5.11 (m, 1H, **H_{1b}**), 4.57 (m, 1H, **H_6**), 3.90 (m, 1H, **H_{10}**), 3.80 (dt, *J* = 6.5, 9.5 Hz, **H_5**), 3.51 (m, 1H, **H_{10}**), 3.44 (dt, 1H, *J* = 6.5, 9.5 Hz, **H_5**), 2.55-2.70 (m, 2H, **H_3**), 1.70-1.90 (m, 4H, **H_4**, **H_7**, **H_8**), 1.50-1.65 (m, 4H, **H_7**, **H_8**, **H_9**)

^{13}C-NMR: (101 MHz, $CDCl_3$) δ ppm = 148.0 (**C_{11}**), 141.2 (**C_2**), 128.3 (**$C_{12,16}$**), 127.3 (**C_{14}**), 126.1 (**$C_{13,15}$**), 112.4 (**C_1**), 98.8 (**C_6**), 66.9 (**C_5**), 62.2 (**C_{10}**), 31.9 (**C_3**), 30.8 (**C_7**), 28.4 (**C_4**), 25.5 (**C_9**), 19.6 (**C_8**)

LRMS: (ESI^+) 247.3 $[M+H]^+$

4.4.42 4-Phenylpent-4-en-1-ol

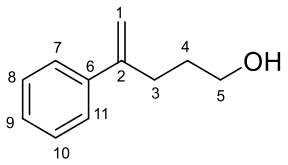

$C_{11}H_{14}O$
Mol Wt:162.2 g/mol

4-Phenylpent-4-en-1-ol was prepared adapting the procedure of Pesti *et al*.[181]

4-Phenyl-1-(tetrahydropyranyl)oxy-pent-4-ene (0.150 g, 0.610 mmol, 1.0 equiv.), was dissolved in MeOH (0.500 mL); then H_2O (0.080 mL) and *p*-Toluensulfonic acid (0.010 g, 0.061 mmol, 0.1 equiv.) were added. The mixture was left stirring at 50 °C for 3 h. Solvent was then evaporated under reduced pressure. The resulting oil was dissolved in toluene (5.00 mL) and washed with a satured solution of $NaHCO_3$ (3.00 mL). The organic phase was dried ($MgSO_4$), filtered and the solvent removed under reduced pressure. The title product was obtained as a clear oil (0.090 g, 0.550 mmol, 91%) without further purification.

Physical and spectroscopic data are consistent with reported literature. [277]

^{1}H-NMR: (400 MHz, $CDCl_3$) δ ppm = 7.40-7.45 (m, 2H, **$H_{7,11}$**), 7.31-7.37 (m, 2H, **$H_{8,10}$**), 7.28 (m, 1H, **H_9**), 5.31 (d, *J* = 1.4 Hz, 1H, **H_{1a}**), 5.12 (m, 1H, **H_{1b}**), 3.69 (t, *J* = 6.4 Hz, 2H, **H_5**), 2.59-2.66 (m, 2H, **H_3**), 1.70-1.80 (m, 2H, **H_4**)

^{13}C-NMR: (101 MHz, $CDCl_3$) δ ppm = 148.0 (**C_6**), 141.0 (**C_2**), 129.0 (**$C_{8,10}$**), 128.4 (**$C_{7,11}$**), 128.2 (**C_9**), 112.6 (**C_1**), 62.5 (**C_5**), 31.6 (**C_3**), 31.2 (**C_4**)

LRMS: (ESI^+) 162.2 $[M+H]^+$

4.4.43 Methyl-2-iodobenzoate

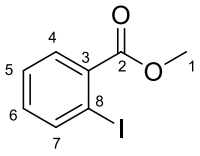

$C_8H_7IO_2$

Mol Wt: 261.9 g/mol

Methyl-2-iodobenzoate was prepared following the procedure of Gianni *et al.*[199]

To a solution of 2-Iodo-benzoic acid (1.00 g, 4.03 mmol, 1.0 equiv) in MeOH (20.0 mL) was added dropwise a concentrated (> 95%) solution of sulphuric acid (2.58 mL, 48.36 mmol, 12.0 equiv.) at rt. The solution was stirred under reflux for 3 h. The reaction mixture was then allowed to cool down to rt and the solvent removed under reduced pressure. The residue was diluted in EtOAc (20 mL) and washed with a satured solution of $NaHCO_3$ (2 x 10 mL). The organic phase was dried ($MgSO_4$), filtered and solvent removed under reduced pressure. The desired product was obtained as colourless oil without further purification (1.0 g, 3.82 mmol, 95%).

Physical and spectroscopic data are consistent with reported literature.[199]

^{1}H-NMR: (400 MHz, $CDCl_3$) δ ppm = 8.03 (dd, *J* = 1.1, 7.8 Hz, 1H, **H_7**), 7.80 (dd, *J* = 1.1, 7.8 Hz, 1H, **H_4**), 7.42 (td, *J* = 1.1, 7.8 Hz, 1H, **H_5**), 7.18 (td, *J* = 1.1, 7.8 Hz, 1H, **H_6**), 3.95 (s, 3H, **H_1**)

^{13}C-NMR: (101 MHz, $CDCl_3$) δ ppm = 167.0 (**C_2**), 141.3 (**C_7**), 135.1 (**C_3**), 132.6 (**C_6**), 130.9 (**C_4**), 127.9 (**C_5**), 94.1 (**C_8**), 52.5 (**C_1**)

LRMS: (ESI^+) 263.1 $[M+H]^+$

4.4.44 Methyl-2-(5-hydroxypent-1-yn-1-yl)benzoate

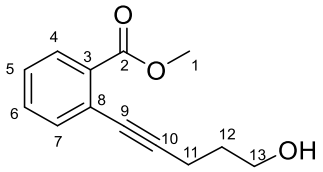

$C_{13}H_{14}O_3$

Mol Wt: 218.1 g/mol

Methyl-2-(5-hydroxypent-1-yn-1-yl)benzoate was prepared adapting the procedure of Syama *et al.*[200]

To a solution of Methyl-2-iodobenzoate (3.00 g, 11.45 mmol, 1.0 equiv), 4-Pentyn-1-ol (1.00 g, 12.6 mmol, 1.1 equiv), Et_3N (5.70 mL, 41.22 mmol, 3.6 equiv) in dry MeCN (30 mL), $Pd(PPh_3)_2Cl_2$ (0.16 g, 0.23 mmol, 2.00 mol %) and CuI (0.04 g, 0.23 mmol, 2.00 mol %) were added in one portion. Reaction mixture was stirred at rt over-night. Solvent was evaporated and then the crude was dissolved in Et_2O (20 mL), filtered and washed with water (20 mL). The organic phase was dried ($MgSO_4$), filtered and solvent removed under reduced pressure. The resulting brown oil was purified by column chromatography (SiO_2, toluene/EtOAc = 7/3 to 6/4) to give the desired product as a brown oil (1.50 g, 6.88 mmol, 60%).

^{1}H-NMR: (400 MHz, $CDCl_3$) δ ppm = 7.92 (dd, *J* = 1.1, 8.3 Hz, 1H, **H_7**), 7.53 (dd, *J* = 1.1, 8.3 Hz, 1H, **H_4**), 7.44 (td, *J* = 1.1, 8.3 Hz, 1H, **H_5**), 7.33 (td, *J* = 1.1, 8.3 Hz, 1H, **H_6**), 3.92 (s, 3H, **H_1**), 3.85-3.91 (m, 2H, **H_{13}**), 2.63 (t, *J* = 6.8 Hz, 2H, **H_{11}**), 2.23 (m, 1H, **OH**), 1.84-1.94 (m, 2H, **H_{12}**)

^{13}C-NMR: (101 MHz, $CDCl_3$) δ ppm = 166.8 (**C_2**), 134.2 (**C_4**), 131.7 (**C_5**), 130.2 (**C_7**), 127.3 (**C_6**), 124.4 (**$C_{3\text{ or }8}$**), 95.1 (**C_9**), 79.9 (**C_{10}**), 61.8 (**C_{13}**), 52.2 (**C_1**), 30.9 (**C_{12}**), 16.6 (**C_{11}**)

LRMS: (ESI^+) 219.2 $[M+H]^+$

HRMS: (ESI^+) *m/z* for $[C_{13}H_{14}NaO_3]^+$ $[M+Na]^+$ calcd: 241.0835 found: 241.0833

IR: ν_{max} (neat) 3414, 2949, 1713, 1248, 1082, 754 cm^{-1}

4.4.45 (E)-5-(2-(Hydroxymethyl)phenyl)pent-4-en-1-ol

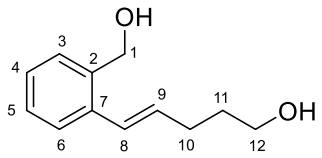

$C_{12}H_{16}O_2$

Mol Wt: 192.2 g/mol

(*E*)-5-(2-(Hydroxymethyl)phenyl)pent-4-en-1-ol was prepared adapting the procedure of Syama *et al.*[200]

To a stirred 1 M solution of $LiAlH_4$ (24 mL, 23.84 mmol, 4.0 equiv.) at 0° C, a solution of Methyl-2-(5-hydroxypent-1-yn-1-yl) benzoate (1.30 g, 5.96 mmol, 1.0 equiv.) in THF (25 mL) was added dropwise. Reaction mixture was stirred at 0° C for 30 minutes and then refluxed over-night. The solution was then cooled down to 0° C and Na_2SO_4 salt was slowly added; the emulsion was left stirring for 2 h, filtered on celite and solvent removed under reduced pressure. The resulting yellow oil was purified by column chromatography (SiO_2, toluene/EtOAc = 7/3 to 4/6) to give the desired product as a colourless oil (0.85 g, 4.42 mmol, 75%).

Physical and spectroscopic data are consistent with reported literature.[200]

^{1}H-NMR: (400 MHz, $CDCl_3$) δ ppm = 7.40 (dd, *J* = 1.5, 6.6 Hz, 1H, **H_6**), 7.26 (dd, *J* = 1.7, 7.9 Hz, 1H, **H_3**), 7.14-7.23 (m, 2H, **$H_{4,5}$**), 6.68 (d, *J* = 15.8 Hz, 1H, **H_8**), 6.09 (dt, *J* = 6.9, 15.8 Hz, 1H, **H_9**), 4.67 (s, 2H, **H_1**), 3.65 (t, *J* = 6.2 Hz, 2H, **H_{12}**), 2.24-2.33 (m, 2H, **H_{10}**), 1.35-1.75 (m, 2H, **H_{11}**)

^{13}C-NMR: (101 MHz, $CDCl_3$) δ ppm = 137.1 (**C_7**), 136.7 (**C_2**), 132.9 (**C_9**), 128.4 (**C_3**), 128.2 (**$C_{4\ or\ 5}$**), 127.2 (**C_8**), 127.1 (**$C_{4\ or\ 5}$**), 126.2 (**C_6**), 63.6 (**C_1**), 62.4 (**C_{12}**), 32.1 (**C_{11}**), 29.7 (**C_{10}**)

LRMS: (ESI^+) 193.2 $[M+H]^+$

4.4.46 2,3,4,5-Tetrahydrospiro(furan-2, 3'-isochroman)

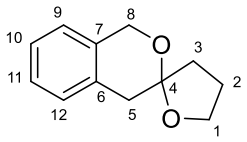

$C_{12}H_{14}O_2$

Mol Wt: 190.2 g/mol

A solution of (*E*)-5-(2-(Hydroxymethyl)phenyl)pent-4-en-1-ol (0.290 g, 1.500 mmol, 1.00 equiv), Et_4NBF_4 (0.080 g, 0.250 mmol, 0.375 equiv) in MeCN (15 mL) was passed through the Ammonite 8 reactor (ss cathode, C/PVDF anode) at a flow rate of 0.25 mL min^{-1} and a current of 80 mA (steady state V = 4.3 V). The effluent was collected and the solvent evaporated under reduced pressure. The electrolyte was recovered by filtration after precipitation from EtOAc. The solvent removed under reduced pressure and the resulting clear oil was purified by column chromatography (SiO_2, CH_2Cl_2 to CH_2Cl_2/MeOH = 95/5) to give the title product as a colourless oil (0.040 g, 0.210 mmol, 14%).

Physical and spectroscopic data are consistent with reported literature.[278]

^{1}H-NMR: (400 MHz, $CDCl_3$) δ ppm = 7.14-7.19 (m, 2H, **$H_{10,11}$**), 7.10 (m, 1H, **H_{12}**), 7.00-7.04 (m, 2H, **H_9**), 4.93 (d, *J* = 15.0 Hz, 1H, **H_8**), 4.70 (d, *J* = 15.0 Hz, 1H, **H_8**), 4.01 (t, *J* = 7.0 Hz, 2H, **H_1**), 3.23 (d, *J* = 16.7 Hz, 1H, **H_5**), 2.83 (d, *J* = 16.7 Hz, 1H, **H_5**), 2.12-2.23 (m, 2H, **$H_{2,3}$**), 1.87-2.04 (m, 2H, **$H_{2,3}$**)

^{13}C-NMR: (101 MHz, $CDCl_3$) δ ppm = 133.6 (**$C_{6\text{ or }7}$**), 131.8 (**$C_{6\text{ or }7}$**), 128.8 (**C_{12}**), 126.4 (**$C_{10\text{ or }11}$**), 126.0 (**$C_{10\text{ or }11}$**), 123.9 (**C_9**), 105.1 (**C_4**), 67.9 (**C_1**), 62.4 (**C_8**), 37.1 (**$C_{2\text{ or }3}$**), 36.0 (**C_5**), 23.7 (**$C_{2\text{ or }3}$**)

LRMS: (ESI^+) 191.2 $[M+H]^+$

4.4.47 Bibenzyl

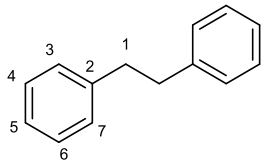

$C_{14}H_{14}$
Mol Wt:182.2 g/mol

A solution of (*E*)-Stilbene (0.270 g, 1.50 mmol, 1.00 equiv), TBABr (0.580 g, 1.80 mmol, 1.20 equiv) in THF (15 mL) (a couple of drops of MeCN were added to help electrolyte dissolution) was passed through the Ammonite 8 reactor (Ag cathode, recess C graphite anode), with a flow of 0.25 mL/min and a current of 160 mA (steady state V = 4.3 V). The effluent was collected and the solvent evaporated under reduced pressure. The crude brown oil was dissolved in CH_2Cl_2 and washed with water (3 x 10 mL). The organic phase was dried ($MgSO_4$), filtered and the solvent removed under reduced pressure. The resulting brown solid was purified by column chromatography (SiO_2, hexane 100%) to give the title product as a white solid (0.220 g, 1.20 mmol, 80%).

Physical and spectroscopic data are consistent with reported literature.[279]

^{1}H-NMR: (400 MHz, $CDCl_3$) δ ppm = 7.20-7.35 (m, 10H, **H_{Ar}**), 2.95 (s, 4H, **H_1**)

^{13}C-NMR: (101 MHz, $CDCl_3$) δ ppm = 141.8 (**C_2**), 128.5 (**$C_{3,7}$**), 128.3 (**$C_{4,6}$**), 125.9 (**C_5**), 37.9 (**C_1**)

LRMS: (EI) *m/z* (40%, $[C_{14}H_{14}]^+$) 182.4, (100%, $[C_7H_7]^{\bullet+}$) 90.9

4.4.48 1,2-Diphenyl propane

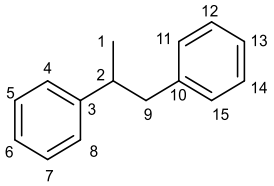

$C_{15}H_{16}$
Mol Wt:196.2 g/mol

A solution of (*E*)-α-Methylstilbene (0.290 g, 1.50 mmol, 1.00 equiv), TBABr (0.580 g, 1.80 mmol, 1.20 equiv) in THF (15 mL) (a couple of drops of MeCN were added to help electrolyte dissolution) was passed through the Ammonite 8 reactor (Ag cathode, recess C graphite anode), with a flow of 0.25 mL/min and a current of 160 mA (steady state V = 5.1 V). The effluent was collected and the solvent evaporated under reduced pressure. The crude brown oil was dissolved in CH_2Cl_2 and washed with water (3 x 10 mL). The organic phase was dried ($MgSO_4$), filtered and the solvent removed under reduced pressure. The resulting brown solid was purified by column chromatography (SiO_2, hexane 100%) to give the title product as a white solid (0.240 g, 1.22 mmol, 81%).

Physical and spectroscopic data are consistent with reported literature.[280]

^{1}H-NMR: (400 MHz, $CDCl_3$) δ ppm = 7.16-7.32 (m, 8H, **H_{Ar}**), 7.07-7.12 (m, 2H, **$H_{11,15}$**), 2.94-3.06 (m, 2H, **$H_{2,9}$**), 2.78 (dd, *J* = 7.9, 13.0 Hz, 1H, **H_9**), 1.26 (d, *J* = 6.7 Hz, 3H, **H_1**)

^{13}C-NMR: (101 MHz, $CDCl_3$) δ ppm = 147.0 (**C_3**), 140.8 (**C_{10}**), 129,2 (**$C_{11,15}$**), 128.3 (**C_{ArH}**), 128.1 (**C_{ArH}**), 127.0 (**$C_{4,8}$**), 126.0 (**C_{ArH}**), 125.8 (**C_{ArH}**), 45.0 (**C_9**), 41.9 (**C_2**), 21.1 (**C_1**)

LRMS: (EI) *m/z* (10%, $[C_{15}H_{16}]^+$) 196.4, (100%, $[C_8H_9]^{\bullet+}$) 105.1

4.4.49 5-Phenyl pentan-1-ol

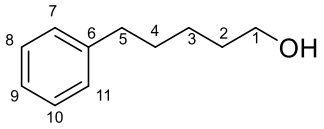

$C_{11}H_{16}O$
Mol Wt:164.2 g/mol

A solution of (*E*)-5-Phenyl-4-penten-1-ol (0.243 g, 1.50 mmol, 1.00 equiv), TBABr (0.580 g, 1.80 mmol, 1.20 equiv) in THF (15 mL) (a couple of drops of MeCN were added to help electrolyte dissolution) was passed through the Ammonite 8 reactor (Ag cathode, recess C graphite anode), with a flow of 0.25 mL/min and a current of 160 mA (steady state V = 5.0 V). The effluent was collected and the solvent evaporated under reduced pressure. The crude brown oil was dissolved in CH_2Cl_2 and washed with water (3 x 10 mL). The organic phase was dried ($MgSO_4$), filtered and the solvent removed under reduced pressure. The resulting brown solid was purified by column chromatography (SiO_2, hexane/EtOAc = 7/3 to 6/4) to give the title product as a white solid (0.148 g, 0.900 mmol, 60%).

Physical and spectroscopic data are consistent with reported literature.[281,282]

^{1}H-NMR: (400 MHz, $CDCl_3$) δ ppm = 7.17-7.31 (m, 5H, $\mathbf{H_{Ar}}$), 3.65 (t, *J* = 6.6 Hz, 2H, $\mathbf{H_1}$), 2.64 (t, *J* = 7.6 Hz, 2H, $\mathbf{H_5}$), 1.58-1.71 (m, 4H, $\mathbf{H_{2,4}}$), 1.38-1.46 (m, 2H, $\mathbf{H_3}$)

^{13}C-NMR: (101 MHz, $CDCl_3$) δ ppm = 142.6 ($\mathbf{C_6}$), 128.4 ($\mathbf{C_{7,11}}$), 128.3 ($\mathbf{C_{8,10}}$), 62.9 ($\mathbf{C_1}$), 35.9 ($\mathbf{C_5}$), 32.6 ($\mathbf{C_2}$), 31.2 ($\mathbf{C_4}$), 25.4 ($\mathbf{C_3}$)

LRMS: (EI) *m/z* (5%, $[C_{15}H_{16}]^+$) 164.2, (100%, $[C_7H_7]^{\bullet+}$) 90.9

4.4.50 4-Hydroxy-6-methoxy benzaldehyde

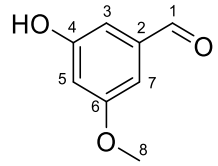

$C_8H_8O_3$
Mol Wt:152.1 g/mol

4-Hydroxy-6-methoxy benzaldehyde was prepared following the procedure of Castedo *et al*.[242]

To a suspension of NaH(60% in mineral oil, 0.180 g, 4.50 mmol, 3.00 equiv) in DMF (10 mL) at 0 °C under nitrogen atmosphere, ethanthiol (0.450 mL, 6.30 mmol, 4.20 equiv) was slowly added. Once the evolution of H2 gas ceased, the solution was refluxed for 1 h to remove the excess of Ethanethiol. Then 4,6-Dimethoxy benzaldehyde (0.250 g, 1.50 mmol, 1.00 equiv), previously dissolved in DMF (5 mL) was added and the resulting solution refluxed for 1 h. Brine (40 mL), 26% formaline (4 mL) and acetic acid (8 mL) were added and the resulting solution was extracted with EtOAc (3 x 10 mL). The combined organic layers were washed with water several times to remove DMF, dried ($MgSO_4$), filtered and the solvent removed under reduced pressure. The resulting brown solid was purified by column chromatography (SiO_2, hexane/EtOAc = 8/2 to 7/3) to give the title product as yellowish solid (0.200 g, 1.32 mmol, 87%).

^{1}H-NMR: (400 MHz, $CDCl_3$) δ ppm = 9.90 (s, 1H, **H_1**), 7.01 (dd, *J* = 1.2, 2.3 Hz, 1H, **H_7**), 6.96 (dd, *J* = 1.2, 2.3 Hz, 1H, **H_3**), 6.68 (t, *J* = 2.3 Hz, 1H, **H_5**), 5.14 (bs, 1H, **OH**), 3.86 (s, 3H, **H_8**)

^{13}C-NMR: (101 MHz, $CDCl_3$) δ ppm = 191.8 (**C_1**), 161.5 (**C_2**), 157.2 (**C_6**), 138, 5 (**C_4**), 109.1 (**C_3**), 108.1 (**C_5**), 107.1 (**C_7**), 55.7 (**C_8**)

LRMS: (ESI^+) 153.2 $[M+H]^+$

HRMS: (ESI^+) *m/z* for $[C_8H_9O_3]^+$ $[M+H]^+$ calcd: 153.0546 found: 153.0544

FT-IR: ν_{max} (neat) 3197, 1670, 1589, 1159, 716 cm^{-1}

4.4.51 6-Methoxy-4-(methoxymethyl)benzaldehyde

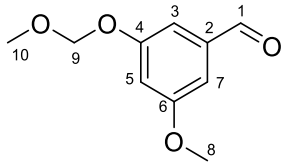

$C_{10}H_{12}O_4$
Mol Wt:196.21 g/mol

6-Methoxy-4-(methoxymethyl) benzaldehyde was prepared following the procedure of Wang *et al.*[243]

To a solution of 4-Hydroxy-6-methoxy benzaldehyde (0.400 g, 2.63 mmol, 1 equiv) in dry acetone (10 mL), under nitrogen atmosphere, K_2CO_3 (1.98 g, 14.3 mmol, 5.45 equiv) and MOMCl (1.05 mL, 13.8 mmol, 5.25 equiv) were added at room temperature. The suspension was left stirring overnight. The suspension was then filtered, the residue washed with EtOAc, and solvent removed under reduced pressure. The resulting oil was purified by column chromatography (SiO_2, hexane/EtOAc = 8/2 to 7/3) to give the title product as a colourless oil (0.400 g, 2.04 mmol, 76%).

^{1}H-NMR: (400 MHz, $CDCl_3$) δ ppm = 9.92 (s, 1H, **H_1**), 7.16 (dd, *J* = 1.2, 2.3 Hz, 1H, **H_3**), 7.08 (dd, *J* = 1.2, 2.3 Hz, 1H, **H_7**), 6.86 (t, *J* = 2.3 Hz, 1H, **H_5**), 5.22 (s, 2H, **H_9**), 3.86 (s, 3H, **H_8**), 3.50 (s, 3H, **H_{10}**)

^{13}C-NMR: (101 MHz, $CDCl_3$) δ ppm = 191.8 (**C_1**), 161.2 (**C_6**), 158.8 (**C_4**), 138.4 (**C_2**), 110.4 (**C_3**), 109.3 (**C_5**), 107.1 (**C_7**), 94.5 (**C_9**), 56.2 (**C_8**), 55.7 (**C_{10}**)

LRMS: (ESI^+) 197.3 $[M+H]^+$

HRMS: (ESI^+) *m/z* for $[C_{10}H_{12}NaO_4]^+$ $[M+Na]^+$ calcd: 219.0628 found: 219.0625

FT-IR: ν_{max} (neat) 2956, 1701, 1150, 1025 cm^{-1}

4.4.52 3-Methoxy-4-(methoxymethyl) benzaldehyde

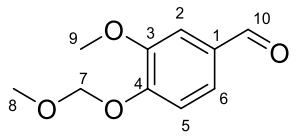

$C_{10}H_{12}O_4$
Mol Wt:196.21 g/mol

3-Methoxy-4-(methoxymethyl) benzaldehyde was prepared following the procedure of Wang *et al*.[243]

To a solution of Vanillin (1.50 g, 9.86 mmol, 1 equiv) in dry acetone (20 mL), under nitrogen atmosphere, K_2CO_3 (7.00 g, 53.7 mmol, 5.45 equiv) and MOMCl (4.00 mL, 51.8 mmol, 5.25 equiv) were added at room temperature. The suspension was left stirring overnight. The suspension was then filtered, the residue washed with EtOAc, and solvent removed under reduced pressure. The resulting oil was purified by column chromatography (SiO_2, hexane/EtOAc = 8/2 to 7/3) to give the title product as a colourless oil (1.70 g, 8.66 mmol, 88%).

Physical and spectroscopic data are consistent with reported literature.[283]

^{1}H-NMR: (400 MHz, $CDCl_3$) δ ppm = 9.88 (s, 1H, **H_{10}**), 7.42-7.45 (m, 2H, **$H_{2,5}$**), 7.27 (m, 1H, **H_6**), 5.33 (s, 2H, **H_7**), 3.96 (s, 3H, **H_9**), 3.53 (s, 3H, **H_8**)

^{13}C-NMR: (101 MHz, $CDCl_3$) δ ppm = 191.0 (**C_{10}**), 152.0 (**C_4**), 151.0 (**C_3**), 131.1 (**C_1**), 126.4 (**C_5**), 114.7 (**C_6**), 109.5 (**C_2**), 95.0 (**C_7**), 56.5 (**C_8**), 56.0 (**C_9**)

LRMS: (ESI$^+$) 197.3 $[M+H]^+$

4.4.53 3-Methoxy-4-(methoxymethyl) benzylalcohol

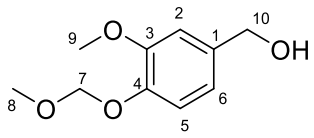

$C_{10}H_{12}O_4$
Mol Wt:196.21 g/mol

3-Methoxy-4-(methoxymethyl) benzyl alcohol was prepared following the procedure of Wang *et al*. [243]

To a solution of 3-Methoxy-4-(methoxymethoxy)benzaldehyde (1.70 g, 8.66 mmol, 1.00 equiv) in dry MeOH (20 mL) under nitrogen atmosphere, $NaBH_4$ (0.180 g, 4.76 mmol, 0.550 equiv) was added at room temperature and the mixture was left stirring for 30'. Reaction mixture was then diluted in EtOAc and water was added. Phases were then separated and the aqueous phase extracted with EtOAc (3 x 10 mL). The combined organic layers were dried ($MgSO_4$), filtered and the solvent removed under reduced pressure. The title product was obtained as a colourless oil without further purification (1.50 g, 7.57 mmol, 87%).

^{1}H-NMR: (400 MHz, $CDCl_3$) δ ppm = 7.13 (d, *J* = 8.1 Hz, 1H, **H_5**), 6.97 (d, *J* = 1.9 Hz, 1H, **H_2**), 6.88 (ddt, *J* = 0.6, 1.9, 8.1 Hz, **H_6**), 5.24 (s, 2H, **H_7**), 4.63 (d, *J* = 5.8 Hz, **H_{10}**), 3.92 (s, 3H, **H_9**), 3.54 (s, 3H, **H_8**)

^{13}C-NMR: (101 MHz, $CDCl_3$) δ ppm = 149.9 (**C_3**), 146.0 (**C_4**), 135.3 (**C_1**), 119.4 (**C_7**), 116.4 (**C_5**), 110.8 (**C_2**), 95.5 (**C_7**), 65.3 (**C_{10}**), 56.2 (**C_8**), 55.9 (**C_9**)

LRMS: (ESI^+) 221.2 $[M+Na]^+$

HRMS: (ESI^+) *m/z* for $[C_{10}H_{12}NaO_4]^+$ $[M+Na]^+$ calcd: 221.0784 found: 221.0783

FT-IR: ν_{max} (neat) 3403, 2937, 1512, 1153, 993, 729 cm^{-1}

4.4.54 Diethyl(3-methoxy-4-(methoxymethyl)benzyl) phosphonate

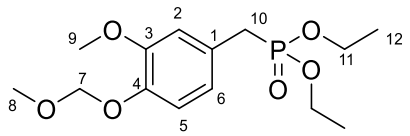

$C_{14}H_{23}O_6P$
Mol Wt:318.31 g/mol

Diethyl(3-methoxy-4-(methoxymethoxy)benzyl) phosphonate was prepared adapting the procedure of Wang *et al*.[243]

To a solution of 3-Methoxy-4-(methoxymethoxy) benzyl alcohol (0.900 g, 4.50 mmol, 1.00 equiv) in dry THF (10 mL), at 0 °C were added PPh_3 (1.20 g, 4.70 mmol, 1.05 equiv), imidazole (0.350 g, 5.22 mmol, 1.16 equiv) and iodine (1.19 g, 4.70 mmol, 1.05 equiv). The reaction mixture was left stirring at 0 °C for 40'. Then it was diluted with Et_2O and washed with a satured solution of $Na_2S_2O_3$. Phases were separated and the organic layer was dried over Na_2SO_4, filtered and the solvent removed under reduced pressure. Obtained 2.00 g of a yellowish solid directly used for the next step.

A solution of the crude solid and $P(OEt)_3$ (1.00 mL, 5.85 mmol, 0.900 equiv) under nitrogen atmosphere, in dry toluene (5 mL) was heated under reflux for 2 h. The solution was then cooled down to room temperature and the solvent removed under reduced pressure. The resulting oil was purified by column chromatography (SiO_2, EtOAc 100%) to give the title product as a colourless oil (0.600 g, 1.88 mmol, 30%).

^{1}H-NMR: (400 MHz, $CDCl_3$) δ ppm = 7.08 (dd, *J* = 0.9, 8.5 Hz, 1H, **H_5**), 6.89 (t, *J* = 2.8 Hz, 1H, **H_2**), 6.80 (m, 1H, **H_6**), 5.21 (s, 2H, **H_7**), 3.99-4.08 (m, 4H, **H_{11}**), 3.88 (s, 3H, **H_9**), 3.51 (s, 3H, **H_8**), 3.11 (d, *J* = 21.3 Hz, 2H, **H_{10}**), 1.27 (t, *J* = 7.2 Hz, 6H, **H_{12}**)

^{13}C-NMR: (101 MHz, $CDCl_3$) δ ppm = 149.6 (**C_3**), 145.5 (**C_4**), 125.7 (**C_1**, *J* = 9.5 Hz), 122.1 (**C_6**, *J* = 7.3 Hz), 116.5 (**C_5**), 113.3 (**C_2**), 95.6 (**C_7**), 62.0 (**C_{11}**), 56.1 (**C_8**), 55.9 (**C_9**), 32.7 (**C_{10}**, *J* = 139.4 Hz), 16.4 (**C_{12}**)

LRMS: (ESI^+) 319.3 $[M+H]^+$

HRMS: (ESI^+) *m/z* for $[C_{14}H_{23}NaO_6P]^+$ $[M+Na]^+$ calcd: 341.1124 found: 341.1129

FT-IR: ν_{max} (neat) 2980, 1513, 1241, 1025, 939 cm^{-1}

4.4.55 (*E*)-3,3'-Dimethoxy-4,5'-di(methoxymethyl)-stilbene

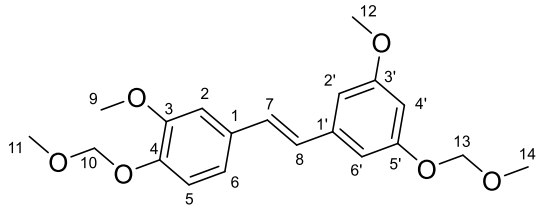

$C_{20}H_{24}O_6$
Mol Wt:360.4 g/mol

(E)-3,3'-Dimethoxy-4,5'-di(methoxymethoxy)-stilbene was prepared following the procedure of Wang *et al*.[243]

To a solution of Diethyl(3-methoxy-4-(methoxymethoxy)benzyl) phosphonate (0.400 g, 1.26 mmol, 1.00 equiv) in dry THF (10 mL), under nitrogen atmosphere and at 0 °C NaH (60% mineral oil, 0.070 g, 1.64 mmol, 1.30 equiv) was added portion-wise. The suspension was stirred at 0 °C for 10' and at room temperature for 30'. Then a solution of 3-hydroxy-5-methoxy benzaldehyde (0.250 g, 1.26 mmol, 1.00 equiv) in dry THF (2 mL) was added. After 4 h, the reaction mixture was quenched with water and then extracted with EtOAc (3 x 10 mL). The combined organic layers were dried ($MgSO_4$), filtered and the solvent removed under reduced pressure. The resulting oil was purified by column chromatography (SiO_2, hexane/EtOAc = 7/3) to give the title product as a colourless oil (0.180 g, 0.500 mmol, 40%).

^{1}H-NMR: (400 MHz, $CDCl_3$) δ ppm = 7.16 (d, *J* = 8.4 Hz, 1H, **H_5**), 7.02-7.08 (m, 3H, **$H_{2,6,7}$**), 6.95 (d, *J* = 16.2 Hz, 1H, **H_8**), 6.82 (t, *J* = 1.6 Hz, 1H, **$H_{6'}$**), 6.72 (t, *J* = 2.0 Hz, 1H, **$H_{2'}$**), 6.53 (t, *J* = 2.2 Hz, 1H. **$H_{4'}$**), 5.26 (s, 2H, **H_{10}**), 5.21 (s, 2H, **H_{13}**), 3.95 (s, 3H, **H_9**), 3.84 (s, 3H, **H_{12}**), 3.54 (s, 3H, **H_{11}**), 3.52 (s, 3H, **H_{14}**)

^{13}C-NMR: (101 MHz, $CDCl_3$) δ ppm = 160.9 (**$C_{3'}$**), 158.6 (**$C_{5'}$**), 149.8 (**C_3**), 146.4 (**C_4**), 139.5 (**C_1**), 131.8 (**$C_{1'}$**), 128.9 (**C_7**), 127.2 (**C_8**), 119.9 (**C_2**), 116.3 (**C_5**), 109.4 (**C_6**), 106.5 (**$C_{6'}$**), 105.6 (**$C_{2'}$**), 101.9 (**$C_{4'}$**), 95.5 (**C_{10}**), 94.5 (**C_{13}**), 56.2 (**C_{11}**), 56.0 (**C_{14}**), 55.9 (**C_9**), 55.4 (**C_{12}**)

LRMS: (ESI^+) 361.3 $[M+H]^+$

HRMS: (ESI^+) *m/z* for $[C_{20}H_{24}NaO_6]^+$ $[M+Na]^+$ calcd: 383.1462 found: 383.1465

FT-IR: ν_{max} (neat) 2955, 1589, 1145, 1029, 727 cm^{-1}

4.4.56 3,3’-Dimethoxy-4,5’-di(methoxymethoxy)-bibenzyl

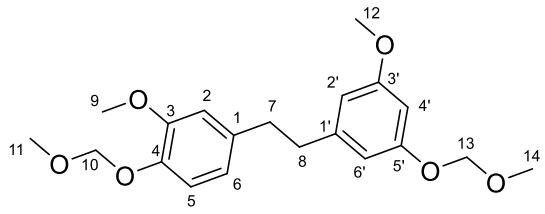

$C_{20}H_{26}O_6$
Mol Wt:362.4 g/mol

A solution of (*E*)-3,3’-Dimethoxy-4,5’-di(methoxymethoxy)-stilbene (0.180 g, 0.500 mmol, 1.00 equiv), TBABr (0.190 g, 0.600 mmol, 1.20 equiv) in THF (5 mL) (a couple of drops of MeCN were added to help electrolyte dissolution) was passed through the Ammonite 8 reactor (Ag cathode, recess C graphite anode), with a flow of 0.25 mL/min and a current of 160 mA (steady state V = 5.8 V). The effluent was collected and the solvent evaporated under reduced pressure. The crude brown oil was dissolved in CH_2Cl_2 and washed with water (3 x 10 mL). The organic phase was dried ($MgSO_4$), filtered and the solvent removed under reduced pressure. The resulting brown solid was purified by column chromatography (SiO_2, hexane/EtOAc = 8/2 to 7/3) to give the title product as a colourless oil (0.100g, 0.275 mmol, 55 %).

^{1}H-NMR: (400 MHz, $CDCl_3$) δ ppm = 7.08 (d, *J* = 8.0 Hz, 1H, **H_5**), 6.72-6.76 (m, 2H, **$H_{2,6}$**), 6.53-6.51 (m, 1H, **$H_{6'}$**), 6.48 (t, *J* = 2.3 Hz, 1H, **$H_{4'}$**), 6.42 (m, 1H, **$H_{2'}$**), 5.21 (s, 2H, **H_{10}**), 5.15 (s, 2H, **H_{13}**), 3.85 (s, 3H, **H_9**), 3.78 (s, 3H, **H_{12}**), 3.53 (s, 3H, **H_{11}**), 3.49 (s, 3H, **H_{14}**), 2.85-2.90 (m, 4H, **$H_{7,8}$**)

^{13}C-NMR: (101 MHz, $CDCl_3$) δ ppm = 160.7 (**$C_{3'}$**), 158.4 (**$C_{5'}$**), 149.6 (**C_3**), 144.7 (**C_4**), 144.2 (**$C_{1'}$**), 136.2 (**C_1**), 120.5 (**C_2**), 116.6 (**C_5**), 112.3 (**C_6**), 108.7 (**$C_{6'}$**), 107.9 (**$C_{2'}$**), 100.1 (**$C_{4'}$**), 95.7 (**C_{10}**), 94.5 (**C_{13}**), 56.1 (**C_{11}**), 56.0 (**C_{14}**), 55.8 (**C_9**), 55.3 (**C_{12}**), 38.3 (**$C_{7\text{ or }8}$**), 37.3 (**$C_{7\text{ or }8}$**)

LRMS: (ESI^+) 363.3 $[M+H]^+$

HRMS: (ESI^+) *m/z* for $[C_{20}H_{26}NaO_6]^+$ $[M+Na]^+$ calcd: 385.1622 found: 385.1628

FT-IR: ν_{max} (neat) 2937, 1593, 1145, 905 cm^{-1}

4.4.57 1,2-Diphenyl-1,2-dimethoxyethane

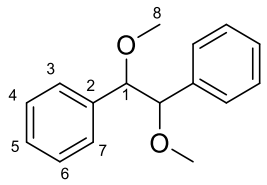

$C_{16}H_{18}O_2$
Mol Wt: 242.3 g/mol

A solution of (*E*)-Stilbene (0.090 g, 0.500 mmol, 1.00 equiv), Et_4NBF_4 (0.027 g, 0.125 mmol, 0.250 equiv) in MeOH (5 mL) was passed through the Ammonite 8 reactor (ss cathode, C/PVDF anode) with a flow of 0.25 mL/min and a current of 80 mA (steady state V = 3.3 V). The effluent was collected and the solvent evaporated under reduced pressure. The electrolyte was recovered by precipitation in EtOAc and filtered away. The solution was concentrated under reduced pressure. The resulting clear oil was purified by column chromatography (SiO_2, hexane/EtOAc = 9/1 to 8/2) to give the desired product as a colourless oil (0.050 g, 0.206 mmol, 41%).

Physical and spectroscopic data are consistent with reported literature[284].

^{1}H-NMR: (400 MHz, $CDCl_3$) δ ppm = 7.16-7.19 (m, 6H, **$H_{4,5,6}$**), 6.99-7.04 (m, 4H, **$H_{3,7}$**), 4.32 (s, 2H, **H_1**), 3.28 (s, 6H, **H_8**)

^{13}C-NMR: (101 MHz, $CDCl_3$) δ ppm = 138.2 (**C_2**), 127.9 (**C_{ArH}**), 127.6 (**C_{ArH}**), 87.7 (**C_1**), 57.2 (**C_8**)

LRMS: (EI) *m/z* (10%, $[C_{15}H_{15}O]^+$) 211.1, (25%, $[C_{10}H_{13}O_2]^{\bullet+}$) 165.1, (100%, $[C_8H_9O]^{\bullet+}$) 121.1

4.4.58 2,2-Diphenylacetaldehyde dimethylacetal

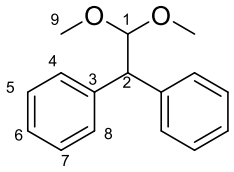

$C_{16}H_{18}O_2$
Mol Wt: 242.3 g/mol

A solution of (*E*)-Stilbene (0.090 g, 0.500 mmol, 1.00 equiv), Et_4NBF_4 (0.027 g, 0.125 mmol, 0.250 equiv) in MeOH (5 mL) was passed through the Ammonite 8 reactor (ss cathode, C/PVDF anode) with a flow of 0.25 mL/min and a current of 80 mA (steady state V = 3.3 V). The effluent was collected and the solvent evaporated under reduced pressure. The electrolyte was recovered by precipitation in EtOAc and filtered away. The solution was concentrated under reduced pressure. The resulting clear oil was purified by column chromatography (SiO_2, hexane/EtOAc = 9/1 to 8/2) to give the desired product as a colourless oil (0.040 g, 0.165 mmol, 33%).

Physical and spectroscopic data are consistent with reported literature[285].

^{1}H-NMR: (400 MHz, $CDCl_3$) δ ppm = 7.28-7.35 (m, 8H, **H_{Ar}**), 7.19-7.24 (m, 2H, **H_{Ar}**), 5.01 (d, *J* = 8.0 Hz, 1H, **H_1**), 4.25 (d, *J* = 8.0 Hz, 1H, **H_2**), 3.33 (s, 6H, **H_9**)

^{13}C-NMR: (101 MHz, $CDCl_3$) δ ppm = 141.1 (**C_3**), 128.7 (**C_{ArH}**), 128.4 (**C_{ArH}**), 126.5 (**C_{ArH}**), 106.5 (**C_1**), 54.6 (**C_2**), 54.0 (**C_9**)

LRMS: (EI) *m/z* (50%, $[C_{15}H_{15}O]^+$) 211.1, (60%, $[C_{10}H_{13}O_2]^{\bullet+}$) 165.1, (100%, $[C_3H_7O_2]^{\bullet+}$) 75.0

4.4.59 1,1,2-Triphenylethane

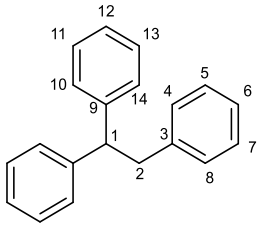

$C_{20}H_{18}$
Mol Wt: 258.3 g/mol

A solution of Triphenylethylene (0.130 g, 0.500 mmol, 1.00 equiv), TBABr (0.190 g, 0.600 mmol, 1.20 equiv) in THF (5 mL) (a couple of drops of MeCN were added to help electrolyte dissolution) was passed through the Ammonite 8 reactor (Ag cathode, recess C graphite anode), with a flow of 0.25 mL/min and a current of 160 mA (steady state V = 4.3 V). The effluent was collected and the solvent evaporated under reduced pressure. The crude brown oil was dissolved in CH_2Cl_2 and washed with water (3 x 10 mL). The organic phase was dried ($MgSO_4$), filtered and the solvent removed under reduced pressure. The resulting brown solid was purified by column chromatography (SiO_2, hexane 100% to hexane/EtOAc = 9/1) to give the title product as a colourless oil (0.100 g, 0.387 mmol, 77%).

Physical and spectroscopic data are consistent with reported literature[286].

^{1}H-NMR: (400 MHz, $CDCl_3$) δ ppm = 7.03-7.39 (m, 15H, $\mathbf{H_{Ar}}$), 4.27 (t, *J* = 7.6 Hz, 1H, $\mathbf{H_1}$), 3.41 (d, *J* = 7.6 Hz, 2H, $\mathbf{H_2}$)

^{13}C-NMR: (101 MHz, $CDCl_3$) δ ppm = 144.4 ($\mathbf{C_{Ar}}$), 140.2 ($\mathbf{C_{Ar}}$), 129.0 ($\mathbf{C_{ArH}}$), 128.3 ($\mathbf{C_{ArH}}$), 128.0 ($\mathbf{C_{ArH}}$), 126.1 ($\mathbf{C_{ArH}}$), 125.9 ($\mathbf{C_{ArH}}$), 53.1 ($\mathbf{C_1}$), 42.1 ($\mathbf{C_2}$)

LRMS: (EI) *m/z* (5%, $[C_{20}H_{18}]^+$) 258.2, (100%, $[C_{13}H_{11}]^{\bullet+}$) 167.0, (15%, $[C_7H_7]^{\bullet+}$) 90.0

4.4.60 1,1-Diphenylethane

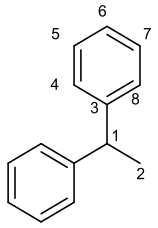

$C_{14}H_{14}$
Mol Wt: 182.2 g/mol

A solution of 1,1-Diphenylethylene (0.090 g, 0.500 mmol, 1.00 equiv), TBABr (0.190 g, 0.600 mmol, 1.20 equiv) in THF (5 mL) (a couple of drops of MeCN were added to help electrolyte dissolution) was passed through the Ammonite 8 reactor (Ag cathode, recess C graphite anode), with a flow of 0.25 mL/min and a current of 160 mA (steady state V = 4.4 V). The effluent was collected and the solvent evaporated under reduced pressure. The crude brown oil was dissolved in CH_2Cl_2 and washed with water (3 x 10 mL). The organic phase was dried ($MgSO_4$), filtered and the solvent removed under reduced pressure. The resulting brown solid was purified by column chromatography (SiO_2, hexane 100% to hexane/EtOAc = 9/1) to give the title product as a colourless oil (0.050 g, 0.274 mmol, 55%).

Physical and spectroscopic data are consistent with reported literature[287].

^{1}H-NMR: (400 MHz, $CDCl_3$) δ ppm = 7.16-7.37 (m, 10H, $\mathbf{H_{Ar}}$), 4.18 (q, *J* = 7.6 Hz, 1H, $\mathbf{H_1}$), 1.67 (d, *J* = 7.6 Hz, 3H, $\mathbf{H_2}$)

^{13}C-NMR: (101 MHz, $CDCl_3$) δ ppm = 146.4 ($\mathbf{C_3}$), 128.4 ($\mathbf{C_{ArH}}$), 127.6 ($\mathbf{C_{ArH}}$), 126.0 ($\mathbf{C_{ArH}}$), 44.8 ($\mathbf{C_1}$), 21.9 ($\mathbf{C_2}$)

LRMS: (EI) *m/z* (70%, $[C_{14}H_{14}]^+$) 181.9, (100%, $[C_{13}H_{11}]^{\bullet+}$) 167.0, (25%, $[C_6H_5]^{\bullet+}$) 77.0

4.4.61 5-(4-Methoxyphenyl)pentan-1-ol

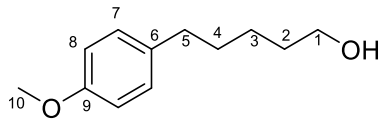

$C_{12}H_{18}O_2$
Mol Wt: 194.2 g/mol

A solution of (*E*)-5-(4-Methoxyphenyl)pent-4-en-1-ol (0.096 g, 0.500 mmol, 1.00 equiv), TBABr (0.190 g, 0.600 mmol, 1.20 equiv) in THF (5 mL) (a couple of drops of MeCN were added to help electrolyte dissolution) was passed through the Ammonite 8 reactor (Ag cathode, recess C graphite anode), with a flow of 0.25 mL/min and a current of 160 mA (steady state V = 5.0 V). The effluent was collected and the solvent evaporated under reduced pressure. The crude brown oil was dissolved in CH_2Cl_2 and washed with water (3 x 10 mL). The organic phase was dried ($MgSO_4$), filtered and the solvent removed under reduced pressure. The resulting brown solid was purified by column chromatography (SiO_2, hexane/EtOAc = 7/3 to 1/1) to give the title product as a colourless oil (0.050 g, 0.257 mmol, 51%).

Physical and spectroscopic data are consistent with reported literature[288].

^{1}H-NMR: (400 MHz, $CDCl_3$) δ ppm = 7.10 (d, *J* = 8.8 Hz, 2H, **H_7**), 6.83 (d, *J* = 8.8 Hz, 2H, **H_8**), 3.80 (s, 3H, **H_{10}**), 3.63 (t, *J* = 6.6 Hz, 2H, **H_1**), 2.58 (t, *J* = 7.8 Hz, 2H, **H_5**), 1.57-1.68 (m, 4H, **$H_{2,4}$**), 1.36-1.44 (m, 2H, **H_3**)

^{13}C-NMR: (101 MHz, $CDCl_3$) δ ppm = 157.6 (**C_9**), 134.6 (**C_6**), 129.2 (**C_7**), 113.7 (**C_8**), 62.8 (**C_1**), 55.2 (**C_9**), 34.9 (**C_5**), 32.6 (**C_2**), 31.5 (**C_4**), 25.3 (**C_3**)

LRMS: (ESI^+) 195.2 $[M+H]^+$

4.4.62 1-Phenyl-1-cyclohexane

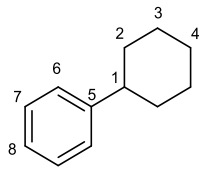

$C_{12}H_{16}$
Mol Wt: 160.2 g/mol

A solution of 1-Phenylcyclohexene (0.080 g, 0.500 mmol, 1.00 equiv), TBABr (0.190 g, 0.600 mmol, 1.20 equiv) in THF (5 mL) (a couple of drops of MeCN were added to help electrolyte dissolution) was passed through the Ammonite 8 reactor (Ag cathode, recess C graphite anode), with a flow of 0.25 mL/min and a current of 160 mA (steady state V = 5.0 V). The effluent was collected and the solvent evaporated under reduced pressure. The crude brown oil was dissolved in CH_2Cl_2 and washed with water (3 x 10 mL). The organic phase was dried ($MgSO_4$), filtered and the solvent removed under reduced pressure. The resulting brown solid was purified by column chromatography (SiO_2, hexane 100%) to give the title product as a colourless oil (0.050 g, 0.312 mmol, 62%).

Physical and spectroscopic data are consistent with reported literature[289,290].

^{1}H-NMR: (400 MHz, $CDCl_3$) δ ppm = 7.29-7.33 (m, 2H, **H_{Ar}**), 7.17-7.24 (m, 3H, **H_{Ar}**), 2.51 (m, 1H, **H_1**), 1.82-1.94 (m, 4H, **$H_{2,3}$**), 1.77 (m, 1H, **H_4**), 1.37-1.50 (m, 4H, **$H_{2,3}$**), 1.29 (m, 1H, **H_4**)

^{13}C-NMR: (101 MHz, $CDCl_3$) δ ppm = 148.1 (**C_5**), 128.3 (**C_{ArH}**), 126.8 (**C_{ArH}**), 125.8 (**C_{ArH}**), 44.6 (**C_1**), 34.5 (**$C_{2 \text{ or } 3}$**), 26.9 (**$C_{2 \text{ or } 3}$**), 26.2 (**C_4**)

LRMS: (EI) *m/z* (70%, $[C_{12}H_{16}]^+$) 160.0, (100%, $[C_8H_8]^{\bullet+}$) 103.7

4.4.63 1,2,3,4-Tetrahydronaphthalene

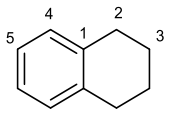

$C_{10}H_{12}$
Mol Wt: 132.2 g/mol

A solution of 2,3-Dihydronaphthalene (0.060 g, 0.500 mmol, 1.00 equiv), TBABr (0.190 g, 0.600 mmol, 1.20 equiv) in THF (5 mL) (a couple of drops of MeCN were added to help electrolyte dissolution) was passed through the Ammonite 8 reactor (Ag cathode, recess C graphite anode), with a flow of 0.25 mL/min and a current of 160 mA (steady state V = 4.3 V). The effluent was collected and the solvent evaporated under reduced pressure. The crude brown oil was dissolved in CH_2Cl_2 and washed with water (3 x 10 mL). The organic phase was dried ($MgSO_4$), filtered and the solvent removed under reduced pressure. The resulting brown solid was purified by column chromatography (SiO_2, hexane 100%) to give the title product as a colourless oil (0.050 g, 0.378 mmol, 76%).

Physical and spectroscopic data are consistent with reported literature[291,292].

^{1}H-NMR: (400 MHz, $CDCl_3$) δ ppm = 7.07-7.12 (m, 4H, **$H_{4,5}$**), 2.75-2.85 (m, 4H, **H_2**), 1.80-1.85 (m, 4H, **H_3**)

^{13}C-NMR: (101 MHz, $CDCl_3$) δ ppm = 137.1 (**C_1**), 129.1 (**C_4**), 125.4 (**C_5**), 29.4 (**C_2**), 23.2 (**C_3**)

LRMS: (EI) *m/z* (15%, $[C_{10}H_{12}]^+$) 132.2, (100%, $[C_8H_8]^{\bullet+}$) 104.2

4.4.64 Methyl(*E,Z*)-5-(9-(trifluoromethyl)phenyl)pent-4-enoate

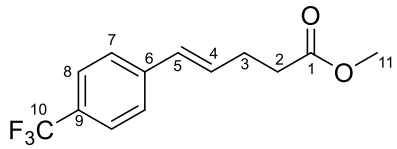

$C_{13}H_{13}F_3O_2$
Mol Wt: 258.2 g/mol

Methyl(*E*,*Z*)-5-(4-(trifluoromethyl)phenyl)pent-4-enoate was pr epared adapting the procedure of Stemp *et al*[246].

To a solution of (*E,Z*)-5-(4-Trifluoromethylphenyl)pent-4-enoic acid (0.900 g, 3.68 mmol, 1.00 equiv) in MeOH (15 mL), H_2SO_4 conc. (0.2 mL) is added dropwise. The solution is stirred open air at room temperature for 1 h. Solvent is removed under reduced pressure; the crude is dissolved in EtOAc and washed with $NaHCO_3$ sat. solution (3 x 10 mL). The organic phase was dried ($MgSO_4$), filtered and solvent removed under reduced pressure to give the titled product as a yellowish oil without further purification (0.900 g, 3.48 mmol, 95%).

NMR data for *E* isomer

^{1}H-NMR: (400 MHz, $CDCl_3$) δ ppm = 7.54 (d, *J* = 7.6 Hz, 2H, **H_8**), 7.43 (d, *J* = 7.6 Hz, 2H, **H_7**), 6.45 (d, *J* = 15.7 Hz, 1H, **H_5**), 6.33 (m, 1H, **H_4**), 3.71 (s, 3H, **H_{11}**), 2.45-2.66 (m, 4H, **$H_{2,3}$**)

^{13}C-NMR: (101 MHz, $CDCl_3$) δ ppm = 173.2 (**C_1**), 140.8 (**C_6**), 131.2 (**C_4**), 129.8 (**C_5**), 126.2 (**C_7**), 125.4 (**C_8**) 51.7 (**C_{11}**), 33.5 (**C_2**), 28.2 (**C_3**)

NMR data for *Z* isomer

^{1}H-NMR: (400 MHz, $CDCl_3$) δ ppm = 7.60 (d, *J* = 8.2 Hz, 2H, **H_8**), 7.38 (d, *J* = 8.2 Hz, 2H, **H_7**), 6.51 (d, *J* = 8.1 Hz, 1H, **H_5**), 5.74 (m, 1H, **H_4**), 3.68 (s, 3H, **H_{11}**), 2.45-2.66 (m, 4H, **$H_{2,3}$**)

Data collected on the mixture

LRMS: (ESI^+) 259.3 $[M+H]^+$

HRMS: (ESI^+) *m/z* for $[C_{13}H_{14}F_3O_2]^+$ $[M+H]^+$ calcd: 259.0940 found: 259.0940

FT-IR: ν_{max} (neat) 1735, 1321, 1108, 1065 cm^{-1}

4.4.65 Methyl(*E,Z*)-5-(7-(methoxy)phenyl)pent-4-enoate

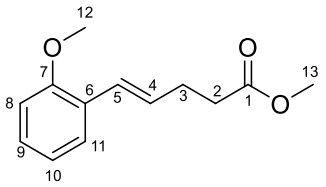

$C_{13}H_{16}O_3$
Mol Wt: 220.2 g/mol

Methyl(*E,Z*)-5-(7-(methoxy)phenyl)pent-4-enoate was prepared adapting the procedure of Stemp *et al*[246].

To a solution of (*E,Z*)-5-(7-(methoxy)phenyl)pent-4-enoic acid (0.150 g, 0.727 mmol, 1.00 equiv) in MeOH (5 mL), H_2SO_4 conc. (a couple of drops) is added. The solution is stirred open air at room temperature for 1 h. Solvent is removed under reduced pressure; the crude is dissolved in EtOAc and washed with $NaHCO_3$ sat. solution (3 x 10 mL). The organic phase was dried ($MgSO_4$), filtered and solvent removed under reduced pressure to give the titled product as a colourless oil without further purification (0.160 g, 0.726 mmol, quantitative yield).

NMR data for *E* isomer

^{1}H-NMR: (400 MHz, $CDCl_3$) δ ppm = 7.41 (dd, *J* = 7.6, 1.7 Hz, 1H, **H_{11}**), 7.22 (m, 1H, **H_9**), 6.85-6.97 (m, 2H, **$H_{8,10}$**), 6.76 (d, *J* = 16.2 Hz, 1H, **H_5**), 6.24-6.17 (m, 1H, **H_4**), 3.85 (s, 3H, **H_{12}**), 3.70 (s, 3H, **H_{13}**), 2.42-2.61 (m, 4H, **$H_{2,3}$**)

^{13}C-NMR: (101 MHz, $CDCl_3$) δ ppm = 173.5 (**C_1**), 156.3 (**C_7**), 129.9 (**C_6**), 129.0 (**C_4**), 128.1 (**C_9**), 126.5 (**C_{11}**), 125.6 (**C_5**), 120.6 (**C_{10}**), 110.7 (**C_8**), 55.4 (**C_{12}**), 51.5 (**C_{13}**), 33.9 (**C_2**), 28.7 (**C_3**)

NMR data for *Z* isomer

^{1}H-NMR: (400 MHz, $CDCl_3$) δ ppm = 7.18-7.25 (m, 2H, **$H_{9,11}$**), 6.85-6.97 (m, 2H, **$H_{8,10}$**), 6.56 (d, *J* = 11.8 Hz, 1H, **H_5**), 5.69 (m, 1H, **H_4**), 3.84 (s, 3H, **H_{12}**), 3.67 (s, 3H, **H_{13}**), 2.42-2.61 (m, 4H, **$H_{2,3}$**)

^{13}C-NMR: (101 MHz, $CDCl_3$) δ ppm = 173.5 (**C_1**), 156.9 (**C_7**), 130.2 (**C_4**), 129.9 (**C_6**), 128.3 (**C_9**), 126.4 (**C_{11}**), 125.7 (**C_5**), 120.1 (**C_{10}**), 110.4 (**C_8**), 55.4 (**C_{12}**), 51.5 (**C_{13}**), 34.1 (**C_2**), 24.1 (**C_3**)

Data collected on the mixture

LRMS: (ESI^+) 221.2 $[M+H]^+$

HRMS: (ESI^+) *m/z* for $[C_{20}H_{26}NaO_6]^+$ $[M+Na]^+$ calcd: 243.0992 found: 243.0991

FT-IR: ν_{max} (neat) 1733, 1488, 1240, 748 cm^{-1}

4.4.66 Ethyl-3-*N*-(isopropylamino)-2-butenoate

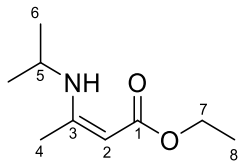

$C_9H_{17}NO_2$
Mol Wt: 171.2 g/mol

Ethyl-3-*N*-(isopropylamino)-2-butenoate was prepared adapting the procedure of Renaud *et al*[245].

To dry CH_2Cl_2 (40 mL), were successively added $FeCl_3$ (0.060 g, 0.380 mmol, 0.050 equiv), ethyl acetoacetate (1.00 g, 7.68 mmol, 1.00 equiv), and *i*-$PrNH_2$ (0.970 mL, 11.5 mmol, 1.50 equiv). the reaction mixture was stirred at room temperature, under nitrogen atmosphere for 1 day. The solvent was then evaporated and crude was purified by column chromatography (SiO_2, hexane/EtOAc = 7/3) to give the title product as a colourless oil (0.600 g, 3.50 mmol, 46%).

Physical and spectroscopic data are consistent with reported literature[293].

^{1}H-NMR: (400 MHz, $CDCl_3$) δ ppm = 8.50 (bs, 1H, **NH**), 4.40 (s, 1H, **H_2**), 4.10 (q, *J* = 7.1 Hz, 2H, **H_7**), 3.69 (m, 1H, **H_5**), 1.94 (s, 3H, **H_4**), 1.25 (t, *J* = 7.1 Hz, 3H, **H_8**), 1.21 (d, *J* = 6.4 Hz, 6H, **H_6**)

^{13}C-NMR: (101 MHz, $CDCl_3$) δ ppm = 170.6 (**C_1**), 160.8 (**C_3**), 81.7 (**C_2**), 58.1 (**C_7**), 44.4 (**C_5**), 24.1 (**C_6**), 19.2 (**C_4**), 14.6 (**C_8**)

LRMS: (ESI$^+$) 172.2 $[M+H]^+$

4.4.67 ((3-Methylbut-2-en-1-yl)oxy)benzene

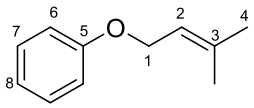

$C_{11}H_{14}O$
Mol Wt: 162.2 g/mol

((3-Methylbut-2-en-1-yl)oxy)benzene was prepared adapting the procedure of Schmidt *et al*[244].

Phenol (0.500 g, 5.30 mmol, 1.00 equiv), was added to a solution of 3,3-dimethylallyl bromide (0.950 g, 6.37 mmol, 1.20 equiv) in acetone 30 mL). K_2CO_3 (0.880 g, 6.37 mmol, 1.20 equiv) was added and the suspension was stirred under reflux, open air for 16 h. Reaction mixture was then cooled down to room temperature, filtered and solvent removed under reduced pressure. The crude mixture was purified by column chromatography (SiO_2, hexane/EtOAc = 9/1) to give the title product as a colourless oil (0.760 g, 4.68 mmol, 88%).

Physical and spectroscopic data are consistent with reported literature[244].

^{1}H-NMR: (400 MHz, $CDCl_3$) δ ppm = 7.28-7.33 (m, 2H, **H_{Ar}**), 6.93-6.98 (m, 3H, **H_{Ar}**), 5.53 (m, 1H, **H_2**), 4.54 (d, *J* = 6.7 Hz, 2H, **H_1**), 1.82 (s, 3H, **H_4**), 1.77 (s, 3H, **$H_{4'}$**)

^{13}C-NMR: (101 MHz, $CDCl_3$) δ ppm = 158.8 (**C_5**), 138.1 (**C_3**), 129.4 (**C_{ArH}**), 120.6 (**C_{ArH}**), 119.8 (**C_2**), 114.6 (**C_{ArH}**), 64.6 (**C_1**), 25.8 (**C_4**), 18.2 (**$C_{4'}$**)

LRMS: (EI) *m/z* (10%, $[C_{11}H_{14}O]^+$) 162.2, (100%, $[C_6H_5O]^{\bullet+}$) 93.9

4.4.68 Methyl-5-(7-(methoxy)phenyl)pentanoate

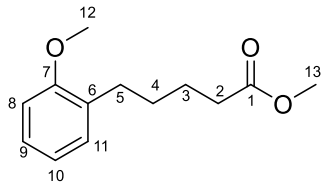

$C_{13}H_{18}O_3$
Mol Wt: 222.2 g/mol

A solution of Methyl(*E*,*Z*)-5-(7-(methoxy)phenyl)pent-4-enoate (0.110 g, 0.500 mmol, 1.00 equiv), TBABr (0.190 g, 0.600 mmol, 1.20 equiv) in THF/MeCN = 1/1 (5 mL) was passed through the Ammonite 8 reactor (Ag cathode, recess C graphite anode), with a flow of 0.25 mL/min and a current of 160 mA (steady state V = 3.7 V). The effluent was collected and the solvent evaporated under reduced pressure. The crude brown oil was dissolved in CH_2Cl_2 and washed with water (3 x 10 mL). The organic phase was dried ($MgSO_4$), filtered and the solvent removed under reduced pressure. The resulting brown solid was purified by column chromatography (SiO_2, hexane/EtOAc = 7/3) to give the title product as a colourless oil (0.010 g, 0.045 mmol, 9%).

^{1}H-NMR: (400 MHz, $CDCl_3$) δ ppm = 7.12-7.20 (m, 2H, **$H_{8,9}$**), 6.84-6.91 (m, 2H, **$H_{10,11}$**), 3.82 (s, 3H, **H_{12}**), 3.67 (s, 3H, **H_{13}**), 2.63 (t, *J* = 7.7 Hz, 2H, **H_5**), 2.36 (t. *J* = 7.0 Hz, 2H, **H_2**), 1.58-1.63 (m, 4H, **$H_{3,4}$**)

^{13}C-NMR: (101 MHz, $CDCl_3$) δ ppm = 174.2 (**C_1**), 157.4 (**C_7**), 130.5 (**C_6**), 129.7 (**C_9**), 126.9 (**C_8**), 120.3 (**C_{10}**), 110.2 (**C_{11}**), 55.2 (**C_{12}**), 51.4 (**C_{13}**), 34.0 (**C_2**), 29.7 (**C_5**), 29.3 (**$C_{3\ or\ 4}$**), 24.8 (**$C_{3\ or\ 4}$**)

LRMS: (ESI^+) 223.2 $[M+H]^+$

HRMS: (ESI^+) *m/z* for $[C_{13}H_{18}NaO_3]^+$ $[M+Na]^+$ calcd: 245.1148 found: 245.1149

FT-IR: ν_{max} (neat) 1736, 1493, 1241 cm^{-1}

4.4.69 Methyl(E)-5-(9-(fluoro)phenyl)pent-4-enoate

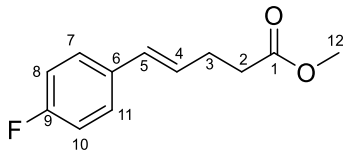

$C_{12}H_{13}FO_2$
Mol Wt: 208.2 g/mol

Methyl(*E*)-5-(9-(fluoro)phenyl)pent-4-enoate was prepared adapting the procedure of Stemp *et al*[246].

To a solution of (*E*)-5-(9-(Fluoro)phenyl) pent-4-enoic acid (0.200 g, 1.029 mmol, 1.00 equiv) in MeOH (5 mL), H_2SO_4 conc. (a couple of drops) is added. The solution is stirred open air at room temperature for 1 h. Solvent is removed under reduced pressure; the crude is dissolved in EtOAc and washed with $NaHCO_3$ sat. solution (3 x 10 mL). The organic phase was dried ($MgSO_4$), filtered and solvent removed under reduced pressure to give the titled product as a colourless oil without further purification (0.200 g, 0.961 mmol, 93%).

^{1}H-NMR: (400 MHz, $CDCl_3$) δ ppm = 7.28-7.32 (m, 2H, **$H_{7,11}$**), 6.96-7.01 (m, 2H, **$H_{8,10}$**), 6.40 (d, *J* = 15.9 Hz, 1H, **H_5**), 6.09-6.16 (m, 1H, **H_4**), 3.70 (s, 3H, **H_{12}**), 2.45-2.56 (m, 4H, **$H_{2,3}$**)

^{13}C-NMR: (101 MHz, $CDCl_3$) δ ppm = 173. 3 (**C_1**), 163.2 (*J* = 246.5 Hz, **C_9**), 133.5 (**C_6**), 129.8 (**C_5**), 128.2 (**C_4**), 127.5 (**$C_{7\ or\ 11}$**), 127.4 (**$C_{7\ or\ 11}$**), 115.4 (**$C_{8\ or\ 10}$**), 115.2 (**$C_{8\ or\ 10}$**), 51.6 (**C_{12}**), 33.8 (**C_2**), 28.1 (**C_3**)

LRMS: (ESI^+) 209.3 $[M+H]^+$

HRMS: (ESI^+) *m/z* for $[C_{20}H_{26}NaO_6]^+$ $[M+Na]^+$ calcd: 231.0792 found: 231.0794

FT-IR: ν_{max} (neat) 1734, 1507, 1224, 1157 cm^{-1}

4.4.70 *N,N*-dibutyl-*N,N*-(dibutyl-*d9*)ammonium iodide

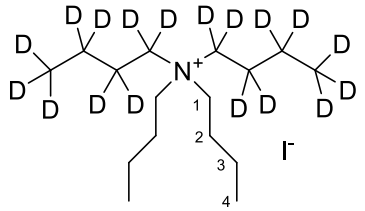

$C_{16}H_{18}D_{18}IN$
Mol Wt: 387.5 g/mol

N,*N*-dibutyl-*N*,*N*-(dibutyl-d_9)ammonium iodide was prepared adapting the procedure of Wang *et al*[243].

To a solution of 1-butanol-d_{10} (5.00 g, 59.4 mmol, 1.00 equiv) in dry CH_2Cl_2 (30 mL), at 0 °C were added PPh_3 (16.4 g, 62.4 mmol, 1.05 equiv), imidazole (4.69 g, 68.9 mmol, 1.16 equiv) and iodine (15.8 g, 62.4 mmol, 1.05 equiv). The reaction mixture was left stirring at 0 °C for 40'. Then a satured solution of $Na_2S_2O_3$ was added till the solution went colourless. Phases were separated and the organic layer was dried over Na_2SO_4, filtered and the solvent removed under reduced pressure. Obtained 7.83 g of a colourless oil directly used for the next step.

To a solution of the crude oil (1.00 g, 5.18 mmol, 8.00 equiv) in dry MeCN (10 mL), were added K_2CO_3 (0.448 g, 3.24 mmol, 5.00 equiv) and dibutylamine (0.084 g, 0.648 mmol, 1.00 equiv). The suspension was stirred at 40° C and under nitrogen atmosphere for 3 days. Then the suspension was filtered and solvent removed under reduced pressure; the resulting yellowish oil was washed with THF to give the desired product as a white solid without further purification (0.627 g, 1.62 mmol, 40%).

Data collected on the iodobutane-d_{10}

^{13}C-NMR: (101 MHz, $CDCl_3$) δ ppm = 35.5, 23.6, 12.9, 6.9

LRMS: (EI) *m/z* (10%, $[C_4D_9I]^+$) 193.0, (50%, $[C_4D_9]^{\bullet+}$) 66.2

FT-IR: ν_{max} (neat) 2957, 1245, 1189 cm^{-1}

Data collected on the *N*,*N*-dibutyl-*N*,*N*-(dibutyl-d_9)ammonium iodide

^{1}H-NMR: (400 MHz, $CDCl_3$) δ ppm = 3.37-3.41 (m, 4H, **H_1**), 1.68-1.76 (m, 4H, **H_2**), 1.45-1.55 (m, 4H, **H_3**), 1.05 (t, *J* = 7.2 Hz, 6H, **H_4**)

^{13}C-NMR: (101 MHz, $CDCl_3$) δ ppm = 59.2 (**C_1**), 24.3 (**C_2**), 19.8 (**C_3**), 13.7 (**C_4**)

LRMS: (ESI^+) 260.6 $[C_{16}H_{18}D_{18}N]^+$

HRMS: (ESI$^+$) *m/z* for $[C_{16}H_{18}D_{18}N]^+$ calcd: 260.3972 found: 260.3969

FT-IR: ν_{max} (neat) 2957, 1647, 1398, 1379 cm^{-1}

Mp: 142-149 °C

4.4.71 Phenyl(tetrahydrofuran-2-yl)methanone

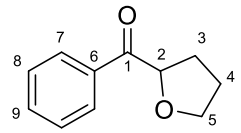

$C_{11}H_{12}O_2$
Mol Wt: 176.2 g/mol

A solution of (*E*)-5-Phenyl pent-4-en-1-ol (0.080 g, 0.500 mmol, 1.00 equiv), Et_4NBF_4 (0.027 g, 0.125 mmol, 0.250 equiv), triflic acid (0.048 g, 0.500 mmol, 1.00 equiv) in dry DMSO/CH_2Cl_2 = 2/3 (5 mL) was passed through the Ammonite 8 reactor (SS cathode, C/PVDF anode) with a flow of 0.25 mL/min and a current of 80 mA (steady state V = 2.5 V). The effluent was collected and the solvent evaporated under reduced pressure. The electrolyte was recovered by precipitation in EtOAc and filtered away. The solution was concentrated under reduced pressure. The resulting yellowish oil was purified by column chromatography (SiO_2, hexane/EtOAc = 7/3) to give the desired product as a colourless oil (0.010 g, 0.057 mmol, 11%).

Physical and spectroscopic data are consistent with reported literature[294].

^{1}H-NMR: (400 MHz, $CDCl_3$) δ ppm = 7.98-8.02 (m, 2H, **H_7**), 7.58 (m, 1H, **H_9**), 7.46-7.50 (m, 2H, **H_8**), 5.27 (dd, *J* = 5.8, 8.4 Hz, 1H, **H_2**), 3.96-4.08 (m, 2H, **H_5**), 2.31 (m, 1H, **H_3**), 2.16 (m, 1H, **H_3**), 1.95-2.02 (m, 2H, **H_4**)

^{13}C-NMR: (101 MHz, $CDCl_3$) δ ppm = 135.1 (**C_6**), 133.3 (**C_9**), 128.7 (**C_7**), 128.6 (**C_8**), 80.0 (**C_2**), 69.4 (**C_5**), 29.3 (**C_3**), 25.6 (**C_4**)

LRMS: (ESI$^+$) 177.3 $[M+H]^+$

List of References

(1) Water, E.; Treatment, W. Basic Concepts in Electrochemistry. **2012**, 114. https://doi.org/10.2118/190807-MS.

(2) Hammerich, O.; Speiser, B. *ORGANIC ELECTROCHEMISTRY Revised and Expanded-Fifth Edition*; 2016.

(3) Moeller, K. D. Synthetic Applications of Anodic Electrochemistry. *Tetrahedron* **2000**, *56* (49), 9527–9554. https://doi.org/10.1016/S0040-4020(00)00840-1.

(4) Sperry, J. B.; Wright, D. L. The Application of Cathodic Reductions and Anodic Oxidations in the Synthesis of Complex Molecules. *Chem. Soc. Rev.* **2006**, *35* (7), 605–621. https://doi.org/10.1039/b512308a.

(5) Fuchigami, Toshio; Inagi, S.; Atobe, M. *Fundamentals and Applications of Organic Electrochemistry*; 2015.

(6) Noël, T.; Cao, Y.; Laudadio, G. The Fundamentals behind the Use of Flow Reactors in Electrochemistry. *Acc. Chem. Res.* **2019**, *52* (10), 2858–2869. https://doi.org/10.1021/acs.accounts.9b00412.

(7) Frontana-Uribe, B. A.; Little, R. D.; Ibanez, J. G.; Palma, A.; Vasquez-Medrano, R. Organic Electrosynthesis: A Promising Green Methodology in Organic Chemistry. *Green Chem.* **2010**, *12* (12), 2099–2119. https://doi.org/10.1039/c0gc00382d.

(8) Couper, A. M.; Pletcher, D.; Walsh, F. C. Electrode Materials for Electrosynthesis. *Chem. Rev.* **1990**, *90* (5), 837–865. https://doi.org/10.1021/cr00103a010.

(9) Heard, D. M.; Lennox, A. J. J. Electrode Materials in Modern Organic Electrochemistry. *Angew. Chemie - Int. Ed.* **2020**, *59* (43), 18866–18884. https://doi.org/10.1002/anie.202005745.

(10) Koehl, W. J. Anodic Oxidation of Aliphatic Acids at Carbon Anodes. *J. Am. Chem. Soc.* **1964**, *86* (21), 4686–4690. https://doi.org/10.1021/ja01075a032.

(11) Sato, N.; Sekine, T.; Sugino, K. Anodic Processes of Acetate Ion in Methanol and in Glacial Acetic Acid at Various Anode Materials. *J. Electrochem. Soc.* **1968**, *115* (3), 242.

https://doi.org/10.1149/1.2411116.

(12) Svadkovskaya, G. E.; Voitkevich, S. A. Electrolytic Condensation of Carboxylic Acids. *Russ. Chem. Rev.* **1960**, *29* (3), 161–180.

(13) de Hemptinne, X.; Jungers, J. C. Sur Le Mécanisme de l'hydrogénation Électrochimique. *Zeitschrift fur Phys. Chemie* **1958**, *15* (1–6), 137–148. https://doi.org/10.1524/zpch.1958.15.1-6.137.

(14) Baizer, M. M.; Anderson, J. D. Electrolytic Reductive Coupling. *J. Electrochem. Soc.* **1964**, *111* (2), 226. https://doi.org/10.1149/1.2426088.

(15) Johnson, C. A.; Barnartt, S. On the Ratio Method of Analysis of Potentiostatic Current-Time Curves for Planar Electrodes. *J. Electrochem. Soc.* **1967**, *114* (12), 1256. https://doi.org/10.1149/1.2426462.

(16) Pietron, J. J.; Pomfret, M. B.; Chervin, C. N.; Long, J. W.; Rolison, D. R. Direct Methanol Oxidation at Low Overpotentials Using Pt Nanoparticles Electrodeposited at Ultrathin Conductive RuO 2 Nanoskins. *J. Mater. Chem.* **2012**, *22* (11), 5197–5204. https://doi.org/10.1039/c2jm15553b.

(17) Sukeri, A.; Bertotti, M. Nanoporous Gold Surface: An Efficient Platform for Hydrogen Evolution Reaction at Very Low Overpotential. *J. Braz. Chem. Soc.* **2018**, *29* (2), 226–231. https://doi.org/10.21577/0103-5053.20170132.

(18) Pu, Z.; Zhao, J.; Amiinu, I. S.; Li, W.; Wang, M.; He, D.; Mu, S. A Universal Synthesis Strategy for P-Rich Noble Metal Diphosphide-Based Electrocatalysts for the Hydrogen Evolution Reaction. *Energy Environ. Sci.* **2019**, *12* (3), 952–957. https://doi.org/10.1039/c9ee00197b.

(19) Liu, Y.; Li, X.; Zhang, Q.; Li, W.; Xie, Y.; Liu, H.; Shang, L.; Liu, Z.; Chen, Z.; Gu, L.; Tang, Z.; Zhang, T.; Lu, S. A General Route to Prepare Low-Ruthenium-Content Bimetallic Electrocatalysts for PH-UniversalHydrogen Evolution Reaction by Using Carbon Quantum Dots. *Angew. Chemie - Int. Ed.* **2020**, *132*, 1735–1743.

(20) Xu, X.; Deng, Y.; Gu, M.; Sun, B.; Liang, Z.; Xue, Y.; Guo, Y.; Tian, J.; Cui, H. Large-Scale Synthesis of Porous Nickel Boride for Robust Hydrogen Evolution Reaction Electrocatalyst. *Appl. Surf. Sci.* **2019**, *470* (September 2018), 591–595. https://doi.org/10.1016/j.apsusc.2018.11.127.

(21) Zoski; Cynthia G. *Handbook of Electrochemistry*; 2007.

(22) Bagotsky, V. S. *Fundamentals of Electrochemistry-Second Edition*; 2006.

(23) Wiebe, A.; Gieshoff, T.; Mçhle, S.; Rodrigo, E.; Zirbes, M.; Waldvogel, S. R. Electrifying Organic Synthesis. *Angew. Chemie - Int. Ed.* **2018**, *57*, 2–28. https://doi.org/10.1002/anie.201711060.

(24) Anastas, P. T. . W. J. C. *Green Chemistry: Theory and Practice*; 1998.

(25) Schäfer, H. J.; Harenbrock, M.; Klocke, E.; Plate, M.; Weiper-Idelmann, A. Electrolysis for the Benign Conversion of Renewable Feedstocks. *Pure Appl. Chem.* **2007**, *79* (11), 2047–2057. https://doi.org/10.1351/pac200779112047.

(26) Robert, F. Recent Advances in the Electrochemical Construction of Heterocycles. *Beilstein J. Org. Chem.* **2014**, *10*, 2858–2873. https://doi.org/10.3762/bjoc.10.303.

(27) Cembellín, S.; Batanero, B. Organic Electrosynthesis Towards Sustainability: Fundamentals and Greener Methodologies. *Chem. Rec.* **2021**, *21*, 1–20. https://doi.org/10.1002/tcr.202100128.

(28) Mohle, Sabine; Zirbes, Michael; Rodrigo, Eduardo; Gieshoff, Tile; Wiebe, Anton; Waldvogel, Siegfried, R. Modern Electrochemical Aspects for the Synthesis of Value-Added Organic Products. *Angew. Chemie - Int. Ed.* **2018**, *57*, 6018–6041. https://doi.org/10.1002/anie.201712732.

(29) Schafer, H. J. Electrochemical Generation of Radicals. In *Radicals in Organic Synthesis*; 2008; pp 250–297. https://doi.org/10.1002/9783527618293.ch14.

(30) Casadei, M. A.; Moracci, F. M.; Zappia, G.; Inesi, A.; Rossi, L. Electrogenerated Superoxide-Activated Carbon Dioxide. A New Mild and Safe Approach to Organic Carbamates. *J. Org. Chem.* **1997**, *62* (20), 6754–6759. https://doi.org/10.1021/jo970308h.

(31) Moeller, K. D. Synthetic Applications of Anodic Electrochemistry. *Tetrahedron* **2000**, *56* (49), 9527–9554. https://doi.org/10.1016/S0040-4020(00)00840-1.

(32) Bard, Allen J.; Inzelt, G.; Scholz, F. *Electrochemical Dictionary-2nd Edition*; 2012. https://doi.org/10.1007/978-3-642-29551-5.

(33) Francke, R.; Little, R. D. Redox Catalysis in Organic Electrosynthesis: Basic Principles and Recent Developments. *Chem. Soc. Rev.* **2014**, *43* (8), 2492–2521. https://doi.org/10.1039/c3cs60464k.

(34) Dapperheld, S.; Steckhan, E.; Brinkhaus, K. G.; Esch, T. Organic Electron Transfer Systems, II Substituted Triarylamine Cation-Radical Redox Systems – Synthesis, Electrochemical and Spectroscopic Properties, Hammet Behavior, and Suitability as Redox Catalysts. *Chem. Ber.* **1991**, *124* (11), 2557–2567. https://doi.org/10.1002/cber.19911241127.

(35) Hilt, G. Basic Strategies and Types of Applications in Organic Electrochemistry. *ChemElectroChem* **2020**, *7* (2), 395–405. https://doi.org/10.1002/celc.201901799.

(36) Uchimiya, M.; Stone, A. T. Reversible Redox Chemistry of Quinones: Impact on Biogeochemical Cycles. *Chemosphere* **2009**, *77* (4), 451–458. https://doi.org/10.1016/j.chemosphere.2009.07.025.

(37) Utley, J. H. P.; Rozenberg, G. G. Electroorganic Reactions. Part 57. DDQ Mediated Anodic Oxidation of 2-Methyl- and 2-Benzylnaphthalenes. *J. Appl. Electrochem.* **2003**, *33* (6), 525–532. https://doi.org/10.1023/A:1024474620525.

(38) Zhang, N. T.; Zeng, C. C.; Lam, C. M.; Gbur, R. K.; Little, R. D. Triarylimidazole Redox Catalysts: Electrochemical Analysis and Empirical Correlations. *J. Org. Chem.* **2013**, *78* (5), 2104–2110. https://doi.org/10.1021/jo302309m.

(39) Francke, R.; Little, R. D. Electrons and Holes as Catalysts in Organic Electrosynthesis. *ChemElectroChem* **2019**, 4373–4382. https://doi.org/10.1002/celc.201900432.

(40) Steckhan, E. Indirect Electroorganic Syntheses- A Modern Chapter of Organic Electrochemistry. *Angew. Chem., Int. Ed.* **1986**, *25*, 683–701.

(41) Putter, H.; Hannebaum, H. US Patent 6063256, 2000.

(42) Batanero, B.; Barba, F.; Sanchez-Sanchez, C. M.; Aldaz, A. Paired Electrosynthesis of Cyanoacetic Acid. *J. Org. Chem.* **2004**, *69* (15), 2423–2426.

(43) Park, K.; Pintauro, P. N.; Baizer, M. M.; Nobe, K. Flow Reactor Studies of the Paired Electro-Oxidation and Electroreduction of Glucose. *J. Electrochem. Soc.* **1985**, *132* (8), 1850–1855.

(44) Li, W.; NOnaka, T. Paired Electrosynthesis of a Nitrone. *Chem. Lett.* **1997**, *26* (12), 1271–1272.

(45) Hudlicky, T.; Claeboe, C. D.; Brammer, L. E.; Koroniak, L.; Butora, G.; Ghiviriga, I. Use of Electrochemical Methods as an Alternative to Tin Reagents for the Reduction of Vinyl Halides in Inositol Synthons. *J. Org. Chem.* **1999**, *64* (13), 4909–4913. https://doi.org/10.1021/jo990382v.

(46) Durandetti, M.; Nédélec, J. Y.; Périchon, J. An Electrochemical Coupling of Organic Halide with Aldehydes, Catalytic in Chromium and Nickel Salts. the Nozaki-Hiyama-Kishi Reaction. *Org. Lett.* **2001**, *3* (13), 2073–2074. https://doi.org/10.1021/ol016033g.

(47) Miranda, J. A.; Wade, C. J.; Little, R. D. Indirect Electroreductive Cyclization and Electrohydrocyclization Using Catalytic Reduced Nickel(II) Salen. *J. Org. Chem.* **2005**, *70* (20), 8017–8026. https://doi.org/10.1021/jo051148+.

(48) Little, D. R.; Moeller, K. D. Organic Electrochemistry as a Tool for Synthesis: Umpolung Reactions, Reactive Intermediates, and the Design of New Synthetic Methods. *Electrochem. Soc. Interface* **2002**, *11* (4), 36–42. https://doi.org/10.1149/2.f06024if.

(49) Little, R. D.; Fox, D. P.; Van Hijfte, L.; Dannecker, R.; Sowell, G.; Wolin, R. L.; Moens, L.; Baizer, M. Electroreductive Cyclization. Ketones and Aldehydes Tethered to ,/8-Unsaturated Esters (Nitriles). Fundamental Investigations. *J. Org. Chem.* **1988**, *53* (5), 2287–2294.

(50) Kolbe, H. Untersuchungen Iiber Die Elektrolyse Organischer Verbindungen. *Justus Liebigs Ann. Chem.* **1849**, *69*, 257–294.

(51) Dickinson, T.; Wynne-Jones, W. F. K. Mechanism of Kolbe ' s Electrosynthesis. *Trans. Faraday Soc.* **1962**, 382–387.

(52) Schäfer, H.-J. Recent Contributions of Kolbe Electrolysis to Organic Synthesis. *top curr. chem.* **1990**, *152*, 91–151. https://doi.org/10.1007/bfb0034365.

(53) Chen, N.; Ye, Z.; Zhang, F. Recent Progress on Electrochemical Synthesis Involving Carboxylic Acids. *Org. Biomol. Chem.* **2021**, *19* (25), 5501–5520. https://doi.org/10.1039/d1ob00420d.

(54) Behr, S.; Hegemann, K.; Schimanski, H.; Frohlic, R.; Haufe, G. Synthesis of -Lactones from Cycloocta-1 5-diene Starting Materials for Natural-Product Synthesis. *European J. Org. Chem.* **2004**, 3884–3892.

(55) Matzeit, A.; Schafer, H. J.; Amatore, C. Radical Tandem Cyclizations by Anodic Decarboxylation of Carboxylic Acids. *Synthesis (Stuttg).* **1995**, *11*, 1432–1444.

(56) Shono, T. Electroorganic Chemistry in Organic Synthesis. *Tetrahedron* **1984**, *40* (19), 811–850. https://doi.org/10.1016/S0040-4020(01)88790-1.

(57) Lee Wong, P.; Moeller, K. D. Anodic Amide Oxidations: Total Syntheses of (−)-A58365A and

(±)-A58365B. *J. Am. Chem. Soc.* **1993**, *115* (24), 11434–11445. https://doi.org/10.1021/ja00077a048.

(58) Sutterer, A.; Moeller, K. D. Reversing the Polarity of Enol Ethers: An Anodic Route to Tetrahydrofuran and Tetrahydropyran Rings [1]. *J. Am. Chem. Soc.* **2000**, *122* (23), 5636–5637. https://doi.org/10.1021/ja001063k.

(59) Liu, B.; Duan, S.; Sutterer, A. C.; Moeller, K. D. Oxidative Cyclization Based on Reversing the Polarity of Enol Ethers and Ketene Dithioacetals. Construction of a Tetrahydrofuran Ring and Application to the Synthesis of (+)-Nemorensic Acid. *J. Am. Chem. Soc.* **2002**, *124* (34), 10101–10111. https://doi.org/10.1021/ja026739l.

(60) Moeller, K. D. Intramolecular Anodic Olefin Coupling Reactions: Using Radical Cation Intermediates to Trigger New Umpolung Reactions. *Synlett* **2009**, *8*, 1208–1218. https://doi.org/10.1055/s-0028-1088126.

(61) Compton, R. G.; Laborda, E.; Ward, K. R. *Understanding Voltammetry: Simulation of Electrode Processes*; 2014.

(62) Bard, A. J.; Faulkner, L. R. Electrochemical Methods: Fundamentals and Applications. *Electrochemical Methods - Fundamentals and Applications*. 2001, pp 1–850.

(63) Elgrishi, N.; Rountree, K. J.; McCarthy, B. D.; Rountree, E. S.; Eisenhart, T. T.; Dempsey, J. L. A Practical Beginner's Guide to Cyclic Voltammetry. *J. Chem. Educ.* **2018**, *95* (2), 197–206. https://doi.org/10.1021/acs.jchemed.7b00361.

(64) Nicholson, R. S. Theory and Application of Cyclic Voltammetry for Measurement of Electrode Reaction Kinetics. *Anal. Chem.* **1965**, *37* (11), 1351–1355. https://doi.org/10.1021/ac60230a016.

(65) Barrosse-Antle, L. E.; Bond, A. M.; Compton, R. G.; O'Mahony, A. M.; Rogers, E. I.; Silvester, D. S. Voltammetry in Room Temperature Ionic Liquids: Comparisons and Contrasts with Conventional Electrochemical Solvents. *Chem. asian J.* **2010**, *5*, 202–230.

(66) Plutschack, M. B.; Pieber, B.; Gilmore, K.; Seeberger, P. H. The Hitchhiker's Guide to Flow Chemistry. *Chem. Rev.* **2017**, *117* (18), 11796–11893. https://doi.org/10.1021/acs.chemrev.7b00183.

(67) Leduc, A. B.; Jamison, T. F. Continuous Flow Oxidation of Alcohols and Aldehydes Utilizing Bleach and Catalytic Tetrabutylammonium Bromide. *Org. Process Res. Dev.* **2012**, *16* (5), 1082–1089. https://doi.org/10.1021/op200118h.

(68) Hartman, R. L. Flow Chemistry Remains an Opportunity for Chemists and Chemical Engineers. *Curr. Opin. Chem. Eng.* **2020**, *29*, 42–50. https://doi.org/10.1016/j.coche.2020.05.002.

(69) Guidi, M.; Seeberger, P. H.; Gilmore, K. How to Approach Flow Chemistry. *Chem. Soc. Rev.* **2020**, *49* (24), 8910–8932. https://doi.org/10.1039/c9cs00832b.

(70) Folgueiras-Amador, A. A.; Wirth, T. Perspectives in Flow Electrochemistry. *J. Flow Chem.* **2017**, *7* (3–4), 94–95. https://doi.org/10.1556/1846.2017.00020.

(71) Gutz, C.; Stenglein, A.; Waldvogel, S. R. Highly Modular Flow Cell for Electroorganic Synthesis. *Org. Process Res. Dev.* **2017**, *21*, 771–778. https://doi.org/10.1021/acs.oprd.7b00123.

(72) Elsherbini, M.; Wirth, T. Electroorganic Synthesis under Flow Conditions. *Acc. Chem. Res.* **2019**, *52* (12), 3287–3296. https://doi.org/10.1021/acs.accounts.9b00497.

(73) Elsherbini, M.; Winterson, B.; Alharbi, H.; Folgueiras-Amador, A. A.; Génot, C.; Wirth, T. Flow Chemistry Continuous-Flow Electrochemical Generator of Hypervalent Iodine Reagents : Synthetic Applications. *Angew. Chemie - Int. Ed.* **2019**, *58*, 9811–9815. https://doi.org/10.1002/anie.201904379.

(74) Pletcher, D.; Green, R. A.; Brown, R. C. D. Flow Electrolysis Cells for the Synthetic Organic Chemistry Laboratory. *Chem. Rev.* **2018**, *118* (9), 4573–4591. https://doi.org/10.1021/acs.chemrev.7b00360.

(75) Folgueiras-Amador, A. A.; Hodgson, J. W.; Brown, R. C. D. 13 Electrochemistry in Laboratory Flow Systems. In *Science of synthesis: Electrochemistry in organic synthesis Vol. 1*; Ackermann, L., Ed.; 2021; pp 387–434. https://doi.org/10.1055/sos-SD-236-00258.

(76) Green, R. A.; Brown, R. C. D.; Pletcher, D. Electrosynthesis in Extended Channel Length Microfluidic Electrolysis Cells. *J. Flow Chem.* **2016**, *6* (3), 191–197. https://doi.org/10.1556/1846.2016.00028.

(77) Green, R. A.; Brown, R. C. D.; Pletcher, D.; Harji, B. An Extended Channel Length Microflow Electrolysis Cell for Convenient Laboratory Synthesis. *Electrochem. commun.* **2016**, *73*, 63–66. https://doi.org/10.1016/j.elecom.2016.11.004.

(78) Folgueiras-Amador, A. A.; Teuten, A. E.; Pletcher, D.; Brown, R. C. D. A Design of Flow Electrolysis Cell for “Home” Fabrication. *React. Chem. Eng.* **2020**, *5* (4), 712–718. https://doi.org/10.1039/d0re00019a.

(79) Amri, N.; Skilton, R. A.; Guthrie, D.; Wirth, T. Efficient Flow Electrochemical Alkoxylation of Pyrrolidine-1-Carbaldehyde. *Synlett* **2019**, *30* (10), 1183–1186. https://doi.org/10.1055/s-0037-1611774.

(80) Folgueiras-Amador, A. A.; Jolley, K. E.; Birkin, P. R.; Brown, R. C. D.; Pletcher, D.; Pickering, S.; Sharabi, M.; de Frutos, O.; Mateos, C.; Rincón, J. A. The Influence of Non-Ionic Surfactants on Electrosynthesis in Extended Channel, Narrow Gap Electrolysis Cells. *Electrochem. commun.* **2019**, *100* (December 2018), 6–10. https://doi.org/10.1016/j.elecom.2019.01.009.

(81) Ke, J.; Gao, C.; Folgueiras-Amador, A. A.; Jolley, K. E.; de Frutos, O.; Mateos, C.; Rincón, J. A.; Brown, R. C. D.; Poliakoff, M.; George, M. W. Self-Optimization of Continuous Flow Electrochemical Synthesis Using Fourier Transform Infrared Spectroscopy and Gas Chromatography. *Appl. Spectrosc.* **2022**, *76* (1), 38–50. https://doi.org/10.1177/00037028211059848.

(82) Suga, S.; Okajima, M.; Fujiwara, K.; Yoshida, J. I. Electrochemical Combinatorial Organic Syntheses Using Microflow Systems. *QSAR Comb. Sci.* **2005**, *24* (6), 728–741. https://doi.org/10.1002/qsar.200440003.

(83) Chapman, M. R.; Shafi, Y. M.; Kapur, N.; Nguyen, B. N.; Willans, C. E. Electrochemical Flow-Reactor for Expedient Synthesis of Copper-N-Heterocyclic Carbene Complexes. *Chem. Commun.* **2015**, *51* (7), 1282–1284. https://doi.org/10.1039/c4cc08874c.

(84) Kuleshova, J.; Hill-Cousins, J. T.; Birkin, P. R.; Brown, R. C. D.; Pletcher, D.; Underwood, T. J. The Methoxylation of N-Formylpyrrolidine in a Microfluidic Electrolysis Cell for Routine Synthesis. *Electrochim. Acta* **2012**, *69*, 197–202. https://doi.org/10.1016/j.electacta.2012.02.093.

(85) Green, R.; Brown, R.; Pletcher, D. Understanding the Performance of a Microfluidic Electrolysis Cell for Routine Organic Electrosynthesis. *J. Flow Chem.* **2015**, *5* (1), 31–36. https://doi.org/10.1556/JFC-D-14-00027.

(86) Brown, R. C. D.; Birkin, P. R.; Pletcher, D. Microfluidic Electrolytic Cells for Routine Synthesis in the Pharmaceutical Industry.

(87) Hill-Cousins, J. T.; Kuleshova, J.; Green, R. A.; Birkin, P. R.; Pletcher, D.; Underwood, T. J.; Leach, S. G.; Brown, R. C. D. TEMPO-Mediated Electrooxidation of Primary and Secondary Alcohols in a Microfluidic Electrolytic Cell. *ChemSusChem* **2012**, *5* (2), 326–331. https://doi.org/10.1002/cssc.201100601.

(88) Kabeshov, M. A.; Musio, B.; Murray, P. R. D.; Browne, D. L.; Ley, S. V. Expedient Preparation of Nazlinine and a Small Library of Indole Alkaloids Using Flow Electrochemistry as an Enabling Technology. *Org. Lett.* **2014**, *16* (17), 4618–4621. https://doi.org/10.1021/ol502201d.

(89) Green, R. A.; R. C. D. Brown; Pletcher, D. *Cambridge Reactor Design. Ammonite Spiral Electrochemical Cells - User Guide*; 2016.

(90) Green, R. A.; Jolley, K. E.; Al-Hadedi, A. A. M.; Pletcher, D.; Harrowven, D. C.; De Frutos, O.; Mateos, C.; Klauber, D. J.; Rincón, J. A.; Brown, R. C. D. Electrochemical Deprotection of Para-Methoxybenzyl Ethers in a Flow Electrolysis Cell. *Org. Lett.* **2017**, *19* (8), 2050–2053. https://doi.org/10.1021/acs.orglett.7b00641.

(91) www.vapourtec.com https://www.vapourtec.com/products/flow-reactors/ion-electrochemical-reactor-features/.

(92) Arai, K.; Watts, K.; Wirth, T. Difluoro- and Trifluoromethylation of Electron-Deficient Alkenes in an Electrochemical Microreactor. *ChemistryOpen* **2014**, *3*, 23–28.

(93) Hartmer, M. F.; Waldvogel, S. R. Electroorganic Synthesis of Nitriles via a Halogen-Free Domino Oxidation-Reduction Sequence. *Chem. Commun.* **2015**, *51* (91), 16346–16348. https://doi.org/10.1039/c5cc06437f.

(94) Gleede, B.; Selt, M.; Gütz, C.; Stenglein, A.; Waldvogel, S. R. Large, Highly Modular Narrow-Gap Electrolytic Flow Cell and Application in Dehydrogenative Cross-Coupling of Phenols. *Org. Process Res. Dev.* **2020**, *24* (10), 1916–1926. https://doi.org/10.1021/acs.oprd.9b00451.

(95) Gomtsyan, A. HETEROCYCLES IN DRUGS AND DRUG DISCOVERY. **2012**, *48* (1), 12–15.

(96) Marson, C. M. *Saturated Heterocycles with Applications in Medicinal Chemistry*; Elsevier Ltd, 2016; Vol. 120. https://doi.org/10.1016/bs.aihch.2016.03.004.

(97) Nakatsuji, H.; Sawamura, Y.; Sakakura, A.; Ishihara, K. Cooperative Activation with Chiral Nucleophilic Catalysts and N - Haloimides : Enantioselective Iodolactonization of 4-Arylmethyl-4- Pentenoic Acids ** Angewandte. **2014**, 1–5. https://doi.org/10.1002/anie.201400946.

(98) Wang, Y.; Jiang, M.; Liu, J. T. Copper-Catalyzed Diastereoselective Synthesis of Trifluoromethylated Tetrahydrofurans. *Adv. Synth. Catal.* **2016**, *358* (8), 1322–1327. https://doi.org/10.1002/adsc.201501166.

(99) Lorente, A.; Lamariano-Merketegi, J.; Albericio, F.; Álvarez, M. Tetrahydrofuran-Containing Macrolides: A Fascinating Gift from the Deep Sea. *Chem. Rev.* **2013**, *113* (7), 4567–4610. https://doi.org/10.1021/cr3004778.

(100) Rainier, J. D. *Synthesis of Substituted Tetrahydrofurans*; 2014. https://doi.org/10.1007/978-3-642-41473-2_1.

(101) Lu, Q.; Harmalkar, D. S.; Choi, Y.; Lee, K. An Overview of Saturated Cyclic Ethers: Biological Profiles and Synthetic Strategies. *Molecules* **2019**, *24* (20). https://doi.org/10.3390/molecules24203778.

(102) Liaw, C. C.; Liou, J. R.; Wu, T. Y.; Chang, F. R.; Wu, Y. C. *Acetogenins from Annonaceae*; 2016; Vol. 101. https://doi.org/10.1007/978-3-319-22692-7_2.

(103) Saleem, M.; Hyoung, J. K.; Ali, M. S.; Yong, S. L. An Update on Bioactive Plant Lignans. *Nat. Prod. Rep.* **2005**, *22* (6), 696–716. https://doi.org/10.1039/b514045p.

(104) Miao, Y. J.; Xu, X. F.; Xu, F.; Chen, Y.; Chen, J. W.; Li, X. The Structure-Activity Relationships of Mono-THF ACGs on Mitochondrial Complex I with a Molecular Modelling Study. *Nat. Prod. Res.* **2014**, *28* (21), 1929–1935. https://doi.org/10.1080/14786419.2014.953499.

(105) Kevin, D. A.; Meujo, D. A. F.; Hamann, M. T. Polyether Ionophores: Broad-Spectrum and Promising Biologically Active Molecules for the Control of Drug-Resistant Bacteria and Parasites. *Expert Opin. Drug Discov.* **2009**, *4* (2), 109–146. https://doi.org/10.1517/17460440802661443.

(106) Avdeef, A.; Strafford, M.; Block, E.; Balogh, M. P.; Chambliss, W.; Khan, I. Drug Absorption in Vitro Model: Filter-Immobilized Artificial Membranes: 2. Studies of the Permeability Properties of Lactones in Piper Methysticum Forst. *Eur. J. Pharm. Sci.* **2001**, *14* (4), 271–280. https://doi.org/10.1016/S0928-0987(01)00191-9.

(107) Schmidt, T. J. Structure-Activity Relationships of Sesquiterpene Lactones. *Stud. Nat. Prod. Chem.* **2006**, *33* (PART M), 309–392. https://doi.org/10.1016/S1572-5995(06)80030-X.

(108) Yamamoto, H. *Lewis Acids in Organic Synthesis Vol. 1*.

(109) Faul, M. M.; Huff, B. E. Strategy and Methodology Development for the Total Synthesis of Polyether Ionophore Antibiotics. *Chem. Rev.* **2000**, *100* (6), 2407–2473. https://doi.org/10.1021/cr940210s.

(110) Lorente, A.; Lamariano-merketegi, J.; Albericio, F.; Mercedes, A. Tetrahydrofuran-

Containing Macrolides : A Fascinating Gift from the Deep Sea. **2013**. https://doi.org/10.1021/cr3004778.

(111) de la Torre, A.; Cuyamendous, C.; Bultel-Poncé, V.; Durand, T.; Galano, J. M.; Oger, C. Recent Advances in the Synthesis of Tetrahydrofurans and Applications in Total Synthesis. *Tetrahedron* **2016**, *72* (33), 5003–5025. https://doi.org/10.1016/j.tet.2016.06.076.

(112) Langer, P.; Freiberg, W. Cyclization Reactions of Dianions in Organic Synthesis. *Chem. Rev.* **2004**, *104* (9), 4125–4149. https://doi.org/10.1021/cr010203l.

(113) Sheikh, N. S. Comparative Perspective and Synthetic Applications of Transition Metal Mediated Oxidative Cyclisation of 1,5-Dienes towards Cis-2,5-Disubstituted Tetrahydrofurans. *Org. Biomol. Chem.* **2014**, *12* (47), 9492–9504. https://doi.org/10.1039/c4ob01491j.

(114) Mao, B.; Fañanás-Mastral, M.; Feringa, B. L. Catalytic Asymmetric Synthesis of Butenolides and Butyrolactones. *Chem. Rev.* **2017**, *117* (15), 10502–10566. https://doi.org/10.1021/acs.chemrev.7b00151.

(115) Marinetti, A.; Jullien, H.; Voituriez, A. Enantioselective, Transition Metal Catalyzed Cycloisomerizations. *Chem. Soc. Rev.* **2012**, *41* (14), 4884–4908. https://doi.org/10.1039/c2cs35020c.

(116) Evans, P. A.; Inglesby, P. A. Diastereoselective Rhodium-Catalyzed Ene-Cycloisomerization Reactions of Alkenylidenecyclopropanes: Total Synthesis of (-)-α-Kainic Acid. *J. Am. Chem. Soc.* **2012**, *134* (8), 3635–3638. https://doi.org/10.1021/ja210804r.

(117) Kc, S.; Basnet, P.; Thapa, S.; Shrestha, B.; Giri, R. Ni-Catalyzed Regioselective Dicarbofunctionalization of Unactivated Olefins by Tandem Cyclization/Cross-Coupling and Application to the Concise Synthesis of Lignan Natural Products. *J. Org. Chem.* **2018**, *83* (5), 2920–2936. https://doi.org/10.1021/acs.joc.8b00184.

(118) Zhang, Q.; Lu, X. Highly Enantioselective Palladium(II)-Catalyzed Cyclization of (Z)-4'-Acetoxy-2'-Butenyl 2-Alkynoates: An Efficient Synthesis of Optically Active γ-Butyrolactones [7]. *J. Am. Chem. Soc.* **2000**, *122* (31), 7604–7605. https://doi.org/10.1021/ja001379s.

(119) Mao, B.; Geurts, K.; Fañanás-Mastral, M.; Van Zijl, A. W.; Fletcher, S. P.; Minnaard, A. J.; Feringa, B. L. Catalytic Enantioselective Synthesis of Naturally Occurring Butenolides via Hetero -Allylic Alkylation and Ring Closing Metathesis. *Org. Lett.* **2011**, *13* (5), 948–951.

https://doi.org/10.1021/ol102994q.

(120) Im, H.; Kang, D.; Choi, S.; Shin, S.; Hong, S. Visible-Light-Induced C − O Bond Formation for the Construction of Five- and Six-Membered Cyclic Ethers and Lactones. *Org. Lett.* **2018**, *20*, 7437–7441. https://doi.org/10.1021/acs.orglett.8b03166.

(121) Hussein, A. A. Ru-Catalysed Oxidative Cyclisation of 1,5-Dienes: An Unprecedented Role for the Co-Oxidant. *RSC Adv.* **2020**, *10* (26), 15228–15238. https://doi.org/10.1039/d0ra02303e.

(122) Bhunnoo, R. A.; Hobbs, H.; Lainé, D. I.; Light, M. E.; Brown, R. C. D. Synthesis of the Non-Adjacent Bis-THF Core of Cis-Sylvaticin Using a Double Oxidative Cyclisation. *Org. Biomol. Chem.* **2009**, *7* (5), 1017–1024. https://doi.org/10.1039/b813201a.

(123) Yang, C. G.; Reich, N. W.; Shi, Z.; He, C. Intramolecular Additions of Alcohols and Carboxylic Acids to Inert Olefins Catalyzed by Silver(I) Triflate. *Org. Lett.* **2005**, *7* (21), 4553–4556. https://doi.org/10.1021/ol051065f.

(124) Dzudza, A.; Marks, T. J. Efficient Intramolecular Hydroalkoxylation / Cyclization of Unactivated Alkenols Mediated by Lanthanide Triflate Ionic Liquids. *Org. Chem. Front.* **2009**, *11* (7), 1523–1526.

(125) Li, Y.; Song, D.; Dong, V. M. Palladium-Catalyzed Olefin Dioxygenation. *J. Am. Chem. Soc.* **2008**, *130* (10), 2962–2964. https://doi.org/10.1021/ja711029u.

(126) McDonald, R. I.; Liu, G.; Stahl, S. S. Palladium(II)-Catalyzed Alkene Functionalization via Nucleopalladation: Stereochemical Pathways and Enantioselective Catalytic Applications. *Chem. Rev.* **2011**, *111* (4), 2981–3019. https://doi.org/10.1021/cr100371y.

(127) Cecil, A. R. L.; Brown, R. C. D. Stereoselective Synthesis of Cis-2,6-Bis-Hydroxyalkyl-Tetrahydropyrans by the Permanganate Promoted Oxidative Cyclisation of 1,6-Dienes. *Tetrahedron Lett.* **2004**, *45* (39), 7269–7271. https://doi.org/10.1016/j.tetlet.2004.08.023.

(128) Pilgrim, B. S.; Donohoe, T. J. Osmium-Catalyzed Oxidative Cyclization of Dienes and Their Derivatives. *J. Org. Chem.* **2013**, *78* (6), 2149–2167. https://doi.org/10.1021/jo302719y.

(129) Piccialli, V. Ruthenium Tetroxide and Perruthenate Chemistry. Recent Advances and Related Transformations Mediated by Other Transition Metal Oxo-Species. *Molecules* **2014**, *19* (5), 6534–6582. https://doi.org/10.3390/molecules19056534.

(130) Piccialli, V. Oxidative Cyclization of Dienes and Polyenes Mediated by Transition-Metal-Oxo

Species. *Synthesis (Stuttg).* **2007**, No. 17, 2585–2607. https://doi.org/10.1055/s-2007-983835.

(131) Baldwin, J. E.; Crossley, M. J.; Lehtonen, E. M. M. Stereospecificity of Oxidative Cycloaddition Reactions of 1,5-Dienes. *J. Chem. Soc.* **1979**, No. 20, 918–920. https://doi.org/10.1039/C39790000918.

(132) Piccialli, V.; Cavallo, N. Improved RuO4-Catalysed Oxidative Cyclisation of Geraniol-Type 1,5-Dienes to Cis-2,5-Bis(Hydroxymethyl)Tetrahydrofuranyldiols. *Tetrahedron Lett.* **2001**, *42* (28), 4695–4699. https://doi.org/10.1016/S0040-4039(01)00790-0.

(133) De Champdoré, M.; Lasalvia, M.; Piccialli, V. OsO4-Catalyzed Oxidative Cyclization of Geranyl and Neryl Acetate to Cis-2,5-Bis(Hydroxymethyl)Tetrahydrofurans. *Tetrahedron Lett.* **1998**, *39* (52), 9781–9784. https://doi.org/10.1016/S0040-4039(98)02172-8.

(134) Donohoe, T. J.; Butterworth, S. A General Oxidative Cyclization of 1,5-Dienes Using Catalytic Osmium Tetroxide. *Angew. Chemie - Int. Ed.* **2003**, *42* (8), 948–951.

(135) Brown, R. C. D.; Bataille, C. J.; Hughes, R. M.; Kenney, A.; Luker, T. J. Permanganate Oxidation of 1,5,9-Trienes: Stereoselective Synthesis of Tetrahydrofuran-Containing Fragments. *J. Org. Chem.* **2002**, *67* (8), 8079–8085.

(136) Nakatsuji, H.; Sawamura, Y.; Sakakura, A.; Ishihara, K. Cooperative Activation with Chiral Nucleophilic Catalysts and N-Haloimides: Enantioselective Iodolactonization of 4-Arylmethyl-4-Pentenoic Acids. *Angew. Chemie - Int. Ed.* **2014**, *53* (27), 6974–6977. https://doi.org/10.1002/anie.201400946.

(137) Yi, H.; Zhang, G.; Wang, H.; Huang, Z.; Wang, J.; Singh, A. K.; Lei, A. Recent Advances in Radical C-H Activation/Radical Cross-Coupling. *Chem. Rev.* **2017**, *117* (13), 9016–9085. https://doi.org/10.1021/acs.chemrev.6b00620.

(138) Snider, B. B. Manganese (III) -Based Oxidative Free-Radical Cyclizations. *Chem. Rev.* **1996**, *96*, 339–363.

(139) Dzudza, A.; Marks, T. J. Efficient Intramolecular Hydroalkoxylation of Unactivated Alkenols Mediated by Recyclable Lanthanide Lriflate Ionic Liquids: Scope and Mechanism. *Chem. - A Eur. J.* **2010**, *16* (11), 3403–3422. https://doi.org/10.1002/chem.200902269.

(140) Pandey, G.; Pal, S.; Laha, R. Direct Benzylic C-H Activation for C-O Bond Formation by Photoredox Catalysis. *Angew. Chemie - Int. Ed.* **2013**, *52* (19), 5146–5149. https://doi.org/10.1002/anie.201210333.

(141) Barthelemy, A. L.; Tuccio, B.; Magnier, E.; Dagousset, G. Alkoxyl Radicals Generated under Photoredox Catalysis: A Strategy for Anti-Markovnikov Alkoxylation Reactions. *Angew. Chemie - Int. Ed.* **2018**, *57* (42), 13790–13794. https://doi.org/10.1002/anie.201806522.

(142) Weiser, M.; Hermann, S.; Penner, A.; Wagenknecht, H. A. Photocatalytic Nucleophilic Addition of Alcohols to Styrenes in Markovnikov and Anti-Markovnikov Orientation. *Beilstein J. Org. Chem.* **2015**, *11*, 568–575. https://doi.org/10.3762/bjoc.11.62.

(143) Hamilton, D. S.; Nicewicz, D. A. Direct Catalytic Anti-Markovnikov Hydroetherification of Alkenols. *J. Am. Chem. Soc.* **2012**, *134* (45), 18577–18580. https://doi.org/10.1021/ja309635w.

(144) Sahoo, B.; Hopkinson, M. N.; Glorius, F. Combining Gold and Photoredox Catalysis: Visible Light-Mediated Oxy-and Aminoarylation of Alkenes. *J. Am. Chem. Soc.* **2013**, *135* (15), 5505–5508. https://doi.org/10.1021/ja400311h.

(145) Tsui, E.; Metrano, A. J.; Tsuchiya, Y.; Knowles, R. R. Catalytic Hydroetherification of Unactivated Alkenes Enabled by Proton-Coupled Electron Transfer. *Angew. Chemie - Int. Ed.* **2020**, *59* (29), 11845–11849. https://doi.org/10.1002/anie.202003959.

(146) Sutterer, A.; Moeller, K. D. Reversing the Polarity of Enol Ethers: An Anodic Route to Tetrahydrofuran and Tetrahydropyran Rings. *J. Am. Chem. Soc.* **2000**, *122*, 5636–5637. https://doi.org/10.1021/ja001063k.

(147) Duan, S.; Moeller, K. D. Anodic Coupling Reactions: Probing the Stereochemistry of Tetrahydrofuran Formation. A Short, Convenient Synthesis of Linalool Oxide. *Org. Lett.* **2001**, *3* (17), 2685–2688. https://doi.org/10.1021/ol0162670.

(148) Liu, B.; Duan, S.; Sutterer, A. C.; Moeller, K. D. Oxidative Cyclization Based on Reversing the Polarity of Enol Ethers and Ketene Dithioacetals. Construction of a Tetrahydrofuran Ring and Application to the Synthesis of (+)-Nemorensic Acid. *J. Am. Chem. Soc.* **2002**, *124* (34), 10101–10111. https://doi.org/10.1021/ja026739l.

(149) Xu, H. C.; Brandt, J. D.; Moeller, K. D. Anodic Cyclization Reactions and the Synthesis of (-)-Crobarbatic Acid. *Tetrahedron Lett.* **2008**, *49* (24), 3868–3871. https://doi.org/10.1016/j.tetlet.2008.04.075.

(150) Redden, A.; Perkins, R. J.; Moeller, K. D. Oxidative Cyclization Reactions: Controlling the Course of a Radical Cation-Derived Reaction with the Use of a Second Nucleophile. *Angew. Chemie - Int. Ed.* **2013**, *52* (49), 12865–12868. https://doi.org/10.1002/anie.201308739.

(151) Liu, B.; Moeller, K. D. Anodic Oxidation Reactions: The Total Synthesis of (+)-Nemorensic Acid. *Tetrahedron Lett.* **2001**, *42* (41), 7163–7165. https://doi.org/10.1016/S0040-4039(01)01506-4.

(152) Perkins, R. J.; Xu, H. C.; Campbell, J. M.; Moeller, K. D. Anodic Coupling of Carboxylic Acids to Electron-Rich Double Bonds: A Surprising Non-Kolbe Pathway to Lactones. *Beilstein J. Org. Chem.* **2013**, *9*, 1630–1636. https://doi.org/10.3762/bjoc.9.186.

(153) Tao, X. Z.; Dai, J. J.; Zhou, J.; Xu, J.; Xu, H. J. Electrochemical C−O Bond Formation: Facile Access to Aromatic Lactones. *Chem. - A Eur. J.* **2018**, *24* (27), 6932–6935. https://doi.org/10.1002/chem.201801108.

(154) Zhang, S.; Li, L.; Wu, P.; Gong, P.; Liu, R.; Xu, K. Substrate-Dependent Electrochemical Dimethoxylation of Olefins. *Adv. Synth. Catal.* **2019**, *361* (3), 485–489. https://doi.org/10.1002/adsc.201801173.

(155) Kim, Y.; Park, G. Do; Balamurugan, M.; Seo, J.; Min, B. K.; Nam, K. T. Electrochemical β-Selective Hydrocarboxylation of Styrene Using CO2 and Water. *Adv. Sci.* **2020**, *7* (3), 1–8. https://doi.org/10.1002/advs.201900137.

(156) Chung, D. S.; Park, S. H.; Lee, S. G.; Kim, H. Electrochemically Driven Stereoselective Approach Tosyn-1,2-Diol Derivatives from Vinylarenes and DMF. *Chem. Sci.* **2021**, *12* (16), 5892–5897. https://doi.org/10.1039/d1sc00760b.

(157) Zeng, X.; Miao, C.; Wang, S.; Xia, C.; Sun, W. Asymmetric 5-Endo Chloroetherification of Homoallylic Alcohols toward the Synthesis of Chiral β-Chlorotetrahydrofurans. *Chem. Commun.* **2013**, *49* (24), 2418–2420. https://doi.org/10.1039/c2cc38436a.

(158) Meyers, A. I.; Collington, E. W. An Efficient Total Synthesis of Propylure, the Highly Active Sex Attractant for the Pink Bollworm Moth *. *Tetrahedron* **1971**, *27*, 5979–5985.

(159) Liblikas, I.; Mozuraitis, R.; Santangelo, E. M.; Noreika, R.; Borg-Karlson, A. Syntheses , Characterizations , and Biological Activities of Tetradeca-4 , 8-Dien- 1-Yl Acetates as Sex Attractants of Leaf-Mining Moth of the Genus Phyllonorycter (Lepidoptera : Gracillariidae). *Chem. Biodivers.* **2009**, *6*, 1388–1403.

(160) Tian, J.; Moeller, K. D. Electrochemically Assisted Heck Reactions. *Org. Lett.* **2005**, *7*, 5381–5383. https://doi.org/10.1021/ol0519487.

(161) Yao, Q.; Kinney, E. P.; Yang, Z. Ligand-Free Heck Reaction : Pd (OAc) 2 as an Active Catalyst. *J. Org. Chem.* **2003**, *68*, 7528–7531. https://doi.org/10.1021/jo034646w.

(162) Jutand, A. *Mechanisms of the Mizoroki – Heck*; 2009.

(163) Beletskaya, I. P.; Cheprakov, A. V. Heck Reaction as a Sharpening Stone of Palladium Catalysis. *Chem. Rev.* **2000**, *100* (8), 3009–3066. https://doi.org/10.1021/cr9903048.

(164) Larock, R. C.; Leung, W.; Stolz-Dunn, S. Synthesis of Aryl-Substitued Aldehydes and Ketones via Palladium-Catalyzed Coupling of Aryl Halides and Non-Allylic Unsaturated Alcohols. *Tetrahedron Lett.* **1989**, *30* (48), 6629–6632.

(165) Colbon, P.; Ruan, J.; Purdie, M.; Mulholland, K.; Xiao, J. Double Arylation of Allyl Alcohol via a One-Pot Heck Arylation- Isomerization-Acylation Cascade. *Org. Lett.* **2011**, *13* (20), 5456–5459. https://doi.org/10.1021/ol202144z.

(166) Muzart, J. Palladium-Catalysed Reactions of Alcohols. Part B: Formation of C-C and C-N Bonds from Unsaturated Alcohols. *Tetrahedron* **2005**, *61* (17), 4179–4212. https://doi.org/10.1016/j.tet.2005.02.026.

(167) Weigel, W. K.; Dennis, T. N.; Kang, A. S.; Perry, J. J. P.; Martin, D. B. C. A Heck-Based Strategy to Generate Anacardic Acids and Related Phenolic Lipids for Isoform-Specific Bioactivity Profiling. *Org. Lett.* **2018**, *20* (19), 6234–6238. https://doi.org/10.1021/acs.orglett.8b02705.

(168) Lu, H.; Li, C.; Jiang, H.; Lizardi, C. L.; Zhang, X. P. Chemoselective Amination of Propargylic C(Sp 3) À H Bonds by Cobalt(II)-Based Metalloradical Catalysis**. *Angew. Chemie - Int. Ed.* **2014**, *53*, 7028–7032. https://doi.org/10.1002/anie.201400557.

(169) Morris, C. L.; Hu, Y.; Head, G. D.; Brown, L. J.; Whittingham, W. G.; Brown, R. C. D. Oxidative Cyclization Reactions of Trienes and Dienynes:Total Synthesis of Membrarollin. *J. Org. Chem.* **2009**, *74* (3), 981–988. https://doi.org/10.1021/jo802012a.

(170) González, M. C.; Lavaud, C.; Gallardo, T.; Zafra-Polo, M. C.; Cortes, D. New Method for the Determination of the Absolute Stereochemistry in Antitumoral Annonaceous Acetogenins. *Tetrahedron* **1998**, *54* (22), 6079–6088. https://doi.org/10.1016/S0040-4020(98)00301-9.

(171) Hoye, T. R.; Jeffrey, C. S.; Shao, F. Mosher Ester Analysis for the Determination of Absolute Configuration of Stereogenic (Chiral) Carbinol Carbons. *Nat. Protoc.* **2007**, *2* (10), 2451–2458. https://doi.org/10.1038/nprot.2007.354.

(172) Curran, D. P.; Zhang, Q.; Lu, H.; Gudipati, V. On the Proof and Disproof of Natural Product Stereostructures: Characterization and Analysis of a Twenty-Eight Member Stereoisomer Library of Murisolins and Their Mosher Ester Derivatives. *J. Am. Chem. Soc.* **2006**, *128* (30),

9943–9956. https://doi.org/10.1021/ja062469l.

(173) Hu, Y.; Cecil, A. R. L.; Frank, X.; Gleye, C.; Figadère, B.; Brown, R. C. D. Natural Cis-Solamin Is a Mixture of Two Tetra-Epimeric Diastereoisomers: Biosynthetic Implications for Annonaceous Acetogenins. *Org. Biomol. Chem.* **2006**, *4* (7), 1217–1219. https://doi.org/10.1039/b601943a.

(174) Zeng, L.; Zhang, Y.; Ye, Q.; Shi, G.; He, K.; McLaughlin, J. L. Cis-Gigantrionenin and 4-Acetyl Gigantetrocin A, Two New Bioactive Annonaceous Acetogenins from Goniothalamus Giganteus, and the Stereochemistries of Acetogenin 1,2,5-Triols. *Bioorganic Med. Chem.* **1996**, *4* (8), 1271–1279. https://doi.org/10.1016/0968-0896(96)00111-3.

(175) Hoye, Thomas R.; Zhuang, Z. P. Validation of the Proton NMR Chemical Shift Method for Determination of Stereochemistry in the Bistetrahydrofuranyl Moiety of Uvaricin-Related Acetogenins from Annonaceae: Rolliniastatin 1 (and Asimicin). *J. Org. Chem.* **1988**, *53* (23), 5578–5580.

(176) Rieser, M. J.; Hui, Y. hua; Rupprecht, J. K.; Kozlowski, J. F.; Wood, K. V.; McLaughlin, J. L.; Hanson, P. R.; Zhuang, Z.; Hoye, T. R. Determination of Absolute Configuration of Stereogenic Carbinol Centers in Annonaceous Acetogenins by 1H- and 19F-NMR Analysis of Mosher Ester Derivatives. *J. Am. Chem. Soc.* **1992**, *114* (26), 10203–10213. https://doi.org/10.1021/ja00052a018.

(177) Perkins, R. J.; Xu, H. C.; Campbell, J. M.; Moeller, K. D. Anodic Coupling of Carboxylic Acids to Electron-Rich Double Bonds: A Surprising Non-Kolbe Pathway to Lactones. *Beilstein J. Org. Chem.* **2013**, *9*, 1630–1636. https://doi.org/10.3762/bjoc.9.186.

(178) Farndon, J. J.; Young, T. A.; Bower, J. F. Stereospecific Alkene Aziridination Using a Bifunctional Amino-Reagent: An Aza-Prilezhaev Reaction. *J. Am. Chem. Soc.* **2018**, *140*, 17846–17850. https://doi.org/10.1021/jacs.8b10485.

(179) Feng, L.; Lanfranchi, D. A.; Cotos, L.; Cesar-Rodo, E.; Ehrhardt, K.; Goetz, A. A.; Zimmermann, H.; Fenaille, F.; Blandin, S. A.; Davioud-Charvet, E. Synthesis of Plasmodione Metabolites And13C-Enriched Plasmodione as Chemical Tools for Drug Metabolism Investigation. *Org. Biomol. Chem.* **2018**, *16* (15), 2647–2665. https://doi.org/10.1039/c8ob00227d.

(180) Peng, B.; Geerdink, D.; Farès, C.; Maulide, N. Chemoselective Intermolecular α-Arylation of Amides. *Angew. Chemie - Int. Ed.* **2014**, *53* (21), 5462–5466. https://doi.org/10.1002/anie.201402229.

(181) Pesti, J.; Chen, C.; Spangler, L.; Delmonte, A. J.; Benoit, S.; Berglund, D.; Bien, J.; Brodfuehrer, P.; Chan, Y.; Corbett, E.; Costello, C.; Demena, P.; Discordia, R. P.; Doubleday, W.; Gao, Z.; Gingras, S.; Grosso, J.; Haas, O.; Kacsur, D.; Lai, C.; Leung, S.; Miller, M.; Muslehiddinoglu, J.; Nguyen, N.; Qiu, J.; Olzog, M.; Reiff, E.; Thoraval, D.; Totleben, M.; Vanyo, D.; Vemishetti, P.; Wasylak, J.; Wei, C. The Process Development of Ravuconazole : An Efficient Multikilogram Scale Preparation of an Antifungal Agent 1 Abstract : *Org. Process Res. Dev.* **2009**, *13* (4), 716–728.

(182) Sha, W.; Zhang, W.; Ni, S.; Mei, H.; Han, J.; Pan, Y. Photoredox-Catalyzed Cascade Difluoroalkylation and Intramolecular Cyclization for Construction of Fluorinated γ-Butyrolactones. *J. Org. Chem.* **2017**, *82* (18), 9824–9831. https://doi.org/10.1021/acs.joc.7b01279.

(183) Xu, H. C.; Brandt, J. D.; Moeller, K. D. Anodic Cyclization Reactions and the Synthesis of (-)-Crobarbatic Acid. *Tetrahedron Lett.* **2008**, *49* (24), 3868–3871. https://doi.org/10.1016/j.tetlet.2008.04.075.

(184) Ogibin, Y. N.; Ilovaiskii, A. I.; Nikishin, G. I. The Effect of Electrolysis Conditions on the Oxidation of Styrene in Methanol. *Russ. Chem. Bull.* **1994**, *43* (9), 1536–1540. https://doi.org/10.1007/BF00697143.

(185) D'yakonov, V. A.; Trapeznikova, O. A.; De Meijere, A.; Dzhemilev, U. M. Metal Complex Catalysis in the Synthesis of Spirocarbocycles. *Chem. Rev.* **2014**, *114*, 5775–5814. https://doi.org/10.1134/S1070428019070017.

(186) Markó, I. E. Electrochemical Oxidative Cyclisation of ω-Hydroxy-Tetrahydropyrans to Spiroketals. *Tetrahedron Lett.* **2000**, *41* (22), 4383–4387. https://doi.org/10.1016/S0040-4039(00)00656-0.

(187) Borrero, N. V.; Aponick, A. Total Synthesis of Acortatarin A Using a Pd(II)-Catalyzed Spiroketalization Strategy. *J. Org. Chem.* **2012**, *77* (19), 8410–8416. https://doi.org/10.1021/jo301835e.

(188) Liu, L.; Li, Y.; Li, L.; Cao, Y.; Guo, L.; Liu, G.; Che, Y. Spiroketals of Pestalotiopsis Fici Provide Evidence for a Biosynthetic Hypothesis Involving Diversified Diels-Alder Reaction Cascades. *J. Org. Chem.* **2013**, *78* (7), 2992–3000. https://doi.org/10.1021/jo302804h.

(189) Khomutnyk, Y. Y.; Argüelles, A. J.; Winschel, G. A.; Sun, Z.; Zimmerman, P. M.; Nagorny, P. Studies of the Mechanism and Origins of Enantioselectivity for the Chiral Phosphoric Acid-Catalyzed Stereoselective Spiroketalization Reactions. *J. Am. Chem. Soc.* **2016**, *138* (1),

444–456. https://doi.org/10.1021/jacs.5b12528.

(190) Gillard, R. M.; Brimble, M. A. Benzannulated Spiroketal Natural Products: Isolation, Biological Activity, Biosynthesis, and Total Synthesis. *Org. Biomol. Chem.* **2019**, *17* (36), 8272–8307. https://doi.org/10.1039/c9ob01598a.

(191) Sperry, J.; Wilson, Z. E.; Rathwell, D. C. K.; Brimble, M. A. Isolation, Biological Activity and Synthesis of Benzannulated Spiroketal Natural Products. *Nat. Prod. Rep.* **2010**, *27* (8), 1117–1137. https://doi.org/10.1039/b911514p.

(192) Hiesinger, K.; Dar'In, D.; Proschak, E.; Krasavin, M. Spirocyclic Scaffolds in Medicinal Chemistry. *J. Med. Chem.* **2021**, *64* (1), 150–183. https://doi.org/10.1021/acs.jmedchem.0c01473.

(193) Achar, T. K.; Maiti, S.; Jana, S.; Maiti, D. Transition Metal Catalyzed Enantioselective C(Sp2)-H Bond Functionalization. *ACS Catal.* **2020**, *10* (23), 13748–13793. https://doi.org/10.1021/acscatal.0c03743.

(194) Pawlowski, R.; Skorka, P.; Stodulski, M. Radical-Mediated Non-Dearomative Strategies in Construction of Spiro Compounds. *Adv. Synth. Catal.* **2020**, *362* (21), 4462–4486. https://doi.org/10.1002/adsc.202000807.

(195) Akiyama, T.; Mori, K. Stronger Brønsted Acids: Recent Progress. *Chem. Rev.* **2015**, *115* (17), 9277–9306. https://doi.org/10.1021/acs.chemrev.5b00041.

(196) Dochain, S.; Nshimyumuremyi, J. B.; Dewez, D. F.; Body, J. F.; Elias, B.; Singleton, M. L.; Markó, I. E. Electrochemical and Photochemical Approaches for the Synthesis of the C28–C38 Fragment of Okadaic Acid. *Tetrahedron* **2019**, *75* (15), 2280–2283. https://doi.org/10.1016/j.tet.2019.02.060.

(197) Yang, W. C.; Zhang, M. M.; Feng, J. G. Recent Advances in the Construction of Spiro Compounds via Radical Dearomatization. *Adv. Synth. Catal.* **2020**, *362* (21), 4446–4461. https://doi.org/10.1002/adsc.202000636.

(198) Geske, L.; Sato, E.; Opatz, T. Anodic Oxidation as an Enabling Tool for the Synthesis of Natural Products. *Synthesis (Stuttg).* **2020**, *52* (19), 2781–2794. https://doi.org/10.1055/s-0040-1707154.

(199) Gianni, J.; Pirovano, V.; Abbiati, G. Biomolecular Chemistry. *Org. Biomol. Chem.* **2018**, *16*, 3213–3219. https://doi.org/10.1039/c8ob00436f.

(200) Syama, C.; Reddy, M. R.; Sridhar, B.; Kumar, S. K.; Reddy, C. S.; Reddy, B. V. S. 3-Dihydroisobenzofuran and Trans -Fused Hexahydropyrano [3 , 2- c] Chromene Derivatives. *Tetrahedron Lett.* **2014**, *55* (30), 4236–4239. https://doi.org/10.1016/j.tetlet.2014.05.083.

(201) Barentsen, H. M.; Sieval, A. B.; Cornelisse, J. Intramolecular Meta Photocycloaddition of Conformationally Restrained 5-Phenylpent-1-Enes. Part II: Steric and Electronic Effects Caused by 4-Mono- and 4-Disubstitution. *Tetrahedron* **1995**, *51* (27), 7495–7520. https://doi.org/10.1016/0040-4020(95)00374-H.

(202) Maekawa, H.; Itoh, K.; Goda, S.; Nishiguchi, I. Enantioselective Electrochemical Oxidation of Enol Acetates Using a Chiral Supporting Electrolyte. *Chirality* **2003**, *15* (1), 95–100. https://doi.org/10.1002/chir.10165.

(203) Moutet, J. C.; Duboc-Toia, C.; Ménage, S.; Tingry, S. A Chiral Poly(2,2'-Bipyridyl Rhodium(III) Complex) Film Electrode for Asymmetric Induction in Electrosynthesis. *Adv. Mater.* **1998**, *10* (9), 665–667. https://doi.org/10.1002/(SICI)1521-4095(199806)10:9<665::AID-ADMA665>3.0.CO;2-5.

(204) Felcmann, Christian; Greiner, G.; Rau, H.; Worner, M. Chiral Modified Electrodes. *Phys. Chem. Chem. Physiscs* **2000**, *2*, 3491–3497.

(205) Afkhami, A.; Kafrashi, F.; Ahmadi, M.; Madrakian, T. A New Chiral Electrochemical Sensor for the Enantioselective Recognition of Naproxen Enantiomers Using l -Cysteine Self-Assembled over Gold Nanoparticles on a Gold Electrode . *RSC Adv.* **2015**, *5* (72), 58609–58615. https://doi.org/10.1039/c5ra07396k.

(206) Mekala, S.; Hahn, R. C. A Scalable, Nonenzymatic Synthesis of Highly Stereopure Difunctional C 4 Secondary Methyl Linchpin Synthons. *J. Org. Chem.* **2015**, *80*, 1610–1617. https://doi.org/10.1021/jo5025392.

(207) Ashikari, Y.; Nokami, T.; Yoshida, J. I. Integrated Electrochemical-Chemical Oxidation Mediated by Alkoxysulfonium Ions. *J. Am. Chem. Soc.* **2011**, *133* (31), 11840–11843. https://doi.org/10.1021/ja202880n.

(208) Hounjet, L. J.; Stephan, D. W. Hydrogenation by Frustrated Lewis Pairs: Main Group Alternatives to Transition Metal Catalysts? *Org. Process Res. Dev.* **2014**, *18* (3), 385–391. https://doi.org/10.1021/op400315m.

(209) Pandarus, V.; Gingras, G.; Béland, F.; Ciriminna, R.; Pagliaro, M. Selective Hydrogenation of

Alkenes under Ultramild Conditions. *Org. Process Res. Dev.* **2012**, *16* (6), 1230–1234. https://doi.org/10.1021/op300079z.

(210) Nishimura, S. *Handbook of Heterogenous Catalytic Hydrogenation for Organic Synthesis*; 2001. https://doi.org/10.1055/s-2002-32521.

(211) Osborn, J. A.; Jardine, F. H.; Young, J. F.; Wilkinson, G. The Preparation and Properties of Tris(Triphenylphosphine)Halogeno-Rhodium(I) and Some Reactions Thereof Including Catalytic Homogeneous Hydrogenation of Olefins and Acetylenes and Their Derivatives. *J. Chem. Soc. A inorganic, Phys. Theor.* **1966**, No. 1, 1711–1732.

(212) Osborn, J. A.; Wilkinson, G. Tris(Triphenylphosphine)Halorhodium(I). In *Inorganic Syntheses, Volume X*; 1967; Vol. X.

(213) Meakin, P.; Jesson, J. P.; Tolman, C. A. The Nature of Chlorotris(Triphenylphosphine)Rhodium in Solution and Its Reaction with Hydrogen. *J. Am. Chem. Soc.* **1972**, *94* (9), 3240–3242.

(214) Halpern, J. Mechanistic Aspects of Homogeneous Catalytic Hydrogenation and Related Processes. *Inorganica Chim. Acta* **1981**, *50* (C), 11–19. https://doi.org/10.1016/S0020-1693(00)83716-0.

(215) Brown, J. M. Direct Homogeneous Hydrogenation. *Angew. Chemie - Int. Ed.* **1987**, *26*, 190–203.

(216) Crabtree, R. Iridium Compounds in Catalysis. *Acc. Chem. Res.* **1979**, *12* (9), 331–337. https://doi.org/10.1021/ar50141a005.

(217) Miyashita, A.; Yasuda, A.; Takaya, H.; Toriumi, K.; Ito, T.; Souchi, T.; Noyori, R. Synthesis of 2,2’-Bis(Diphenylphosphino)1,1’-Binaphtyl(BINAP), an Atropoisomeric Chiral Bis(Triaryl)Phosphine, and Its Use in the Rhodium(I)-Catalyzed Asymmetric Hydrogenation of Alpha-(Acylamino)Acrylic Acids. *J. Am. Chem. Soc.* **1980**, *102*, 7932–7934.

(218) Kurti, L.; Czako, B. *Strategic Applications of Named Reactions in Organic Synthesis*; 2005; Vol. 250. https://doi.org/10.1002/ardp.19122500151.

(219) Noyori, R.; Ohta, M.; Hsiao, Y.; Kitamura, M. Asymmetric Synthesis of Isoquinoline Alkaloids by Homogeneous Catalysis. *J. Am. Chem. Soc.* **1986**, *108* (22), 7117–7119.

(220) Meemken, F.; Baiker, A. Recent Progress in Heterogeneous Asymmetric Hydrogenation of C=O and C=C Bonds on Supported Noble Metal Catalysts. *Chem. Rev.* **2017**, *117* (17),

11522–11569. https://doi.org/10.1021/acs.chemrev.7b00272.

(221) Pasto, D. J.; Taylor, R. T. Reduction with Diimide. In *Organic Reactions*; 1991; pp 91–155. https://doi.org/10.1002/0471264180.or040.02.

(222) Lane, C. F. Reduction of Organic Compounds with Diborane. *Chem. Rev.* **1976**, *76* (6), 773–799. https://doi.org/10.5059/yukigoseikyokaishi.15.174.

(223) Shi, Z.; Li, N.; Lu, H. K.; Chen, X.; Zheng, H.; Yuan, Y.; Ye, K. Y. Recent Advances in the Electrochemical Hydrogenation of Unsaturated Hydrocarbons. *Curr. Opin. Electrochem.* **2021**, *28*, 100713. https://doi.org/10.1016/j.coelec.2021.100713.

(224) Ishifune, M.; Yamashita, H.; Kera, Y.; Yamashita, N.; Hirata, K.; Murase, H.; Kashimura, S. Electroreduction of Aromatics Using Magnesium Electrodes in Aprotic Solvents Containing Alcoholic Proton Donors. *Electrochim. Acta* **2003**, *48* (17), 2405–2409. https://doi.org/10.1016/S0013-4686(03)00259-7.

(225) Peters, B. K.; Rodriguez, K. X.; Reisberg, S. H.; Beil, S. B.; Hickey, D. P.; Kawamata, Y.; Collins, M.; Starr, J.; Chen, L.; Udyavara, S.; Klunder, K.; Gorey, T. J.; Anderson, S. L.; Neurock, M.; Minteer, S. D.; Baran, P. S. Scalable and Safe Synthetic Organic Electroreduction Inspired by Li-Ion Battery Chemistry. *Science (80-.).* **2019**, *363* (6429), 838–845. https://doi.org/10.1126/science.aav5606.

(226) da Silva, A. P.; Mota, S. D. C.; Bieber, L. W.; Navarro, M. Homogeneous Electro-Mediated Reduction of Unsaturated Compounds Using Ni and Fe as Mediators in DMF. *Tetrahedron* **2006**, *62* (23), 5435–5440. https://doi.org/10.1016/j.tet.2006.03.067.

(227) Tomida, S.; Tsuda, R.; Furukawa, S.; Saito, M.; Tajima, T. Electroreductive Hydrogenation of Activated Olefins Using the Concept of Site Isolation. *Electrochem. commun.* **2016**, *73*, 46–49. https://doi.org/10.1016/j.elecom.2016.10.015.

(228) Huang, B.; Li, Y.; Yang, C.; Xia, W. Electrochemical 1,4-Reduction of α,β-Unsaturated Ketones with Methanol and Ammonium Chloride as Hydrogen Sources. *Chem. Commun.* **2019**, *55* (47), 6731–6734. https://doi.org/10.1039/c9cc02368b.

(229) Li, B.; Ge, H. Highly Selective Electrochemical Hydrogenation of Alkynes: Rapid Construction of Mechanochromic Materials. *Sci. Adv.* **2019**, *5* (5). https://doi.org/10.1126/sciadv.aaw2774.

(230) Li, J.; He, L.; Liu, X.; Cheng, X.; Li, G. Electrochemical Hydrogenation with Gaseous Ammonia. *Angew. Chemie - Int. Ed.* **2019**, *58* (6), 1759–1763.

https://doi.org/10.1002/anie.201813464.

(231) Fukazawa, A.; Minoshima, J.; Tanaka, K.; Hashimoto, Y.; Kobori, Y.; Sato, Y.; Atobe, M. A New Approach to Stereoselective Electrocatalytic Semihydrogenation of Alkynes to Z-Alkenes Using a Proton-Exchange Membrane Reactor. *ACS Sustain. Chem. Eng.* **2019**, *7* (13), 11050–11055. https://doi.org/10.1021/acssuschemeng.9b01882.

(232) Liu, X.; Liu, R.; Qiu, J.; Cheng, X.; Li, G. Chemical-Reductant-Free Electrochemical Deuteration Reaction Using Deuterium Oxide. *Angew. Chemie - Int. Ed.* **2020**, *59* (33), 13962–13967. https://doi.org/10.1002/anie.202005765.

(233) Qin, Y.; Lu, J.; Zou, Z.; Hong, H.; Li, Y.; Li, Y.; Chen, L.; Hu, J.; Huang, Y. Metal-Free Chemoselective Hydrogenation of Unsaturated Carbon-Carbon Bonds: Via Cathodic Reduction. *Org. Chem. Front.* **2020**, *7* (14), 1817–1822. https://doi.org/10.1039/d0qo00547a.

(234) Zhang, X.; Xu, J. K.; Wang, J.; Wang, N. L.; Kurihara, H.; Kitanaka, S.; Yao, X. S. Bioactive Bibenzyl Derivatives and Fluorenones from Dendrobium Nobile. *J. Nat. Prod.* **2007**, *70* (1), 24–28. https://doi.org/10.1021/np060449r.

(235) Zhou, X. M.; Zheng, C. J.; Gan, L. S.; Chen, G. Y.; Zhang, X. P.; Song, X. P.; Li, G. N.; Sun, C. G. Bioactive Phenanthrene and Bibenzyl Derivatives from the Stems of Dendrobium Nobile. *J. Nat. Prod.* **2016**, *79* (7), 1791–1797. https://doi.org/10.1021/acs.jnatprod.6b00252.

(236) Fan, C.; Wang, W.; Wang, Y.; Qin, G.; Zhao, W. Chemical Constituents from Dendrobium Densiflorum. *Phytochemistry* **2001**, *57* (8), 1255–1258. https://doi.org/10.1016/S0031-9422(01)00168-6.

(237) Won, J. H.; Kim, J. Y.; Yun, K. J.; Lee, J. H.; Back, N. I.; Chung, H. G.; Chung, S. A.; Jeong, T. S.; Choi, M. S.; Lee, K. T. Gigantol Isolated from the Whole Plants of Cymbidium Goeringii Inhibits the LPS-Induced INOS and COX-2 Expression via NF-KB Inactivation in RAW 264.7 Macrophages Cells. *Planta Med.* **2006**, *72* (13), 1181–1187. https://doi.org/10.1055/s-2006-947201.

(238) Wu, J.; Lu, C.; Li, X.; Fang, H.; Wan, W.; Yang, Q.; Sun, X.; Wang, M.; Hu, X.; Chen, C. Y. O.; Wei, X. Synthesis and Biological Evaluation of Novel Gigantol Derivatives as Potential Agents in Prevention of Diabetic Cataract. *PLoS One* **2015**, *10* (10), 1–14. https://doi.org/10.1371/journal.pone.0141092.

(239) Charoenrungruang, S.; Chanvorachote, P.; Sritularak, B.; Pongrakhananon, V. Gigantol, a

Bibenzyl from Dendrobium Draconis, Inhibits the Migratory Behavior of Non-Small Cell Lung Cancer Cells. *J. Nat. Prod.* **2014**, *77* (6), 1359–1366. https://doi.org/10.1021/np500015v.

(240) Chen, H.; Huang, Y.; Huang, J.; Lin, L.; Wei, G. Gigantol Attenuates the Proliferation of Human Liver Cancer HepG2 Cells through the PI3K/Akt/NF-KB Signaling Pathway. *Oncol. Rep.* **2017**, *37* (2), 865–870. https://doi.org/10.3892/or.2016.5299.

(241) Crombie, L.; Jamieson, S. V. Dihydrostilbenes of Cannabis. Synthesis of Canniprene. *J. Chem. Soc. Perkin Trans. 1* **1982**, 1467–1475.

(242) Luis Castedo, I. Ben; Saá, J. M.; Seijas, J. A.; Suau, R.; Tojo, G. 4,5-O-Substituted Phenanthrenes from Cyclophanes. The Total Synthesis of Cannithrene II. *J. Org. Chem.* **1985**, *50* (13), 2236–2240. https://doi.org/10.1021/jo00213a008.

(243) Wang, Y.; Mathis, C. A.; Huang, G. F.; Holt, D. P.; Debnath, M. L.; Klunk, W. E. Synthesis and 11c-Labelling of (E,E)-1-(3',4'-Dihydroxystyryl)-4-(3'-Methoxy-4 '-Hydroxystyryl) Benzene for PET Imaging of Amyloid Deposits. *J. Label. Compd. Radiopharm.* **2002**, *45* (8), 647–664. https://doi.org/10.1002/jlcr.585.

(244) Schmidt, B.; Riemer, M.; Schilde, U. Tandem Claisen Rearrangement/6-Endo Cyclization Approach to Allylated and Prenylated Chromones. *European J. Org. Chem.* **2015**, *2015* (34), 7602–7611. https://doi.org/10.1002/ejoc.201501151.

(245) Hebbache, H.; Hank, Z.; Bruneau, C.; Renaud, J. L. Hydrogenation of β-N-Substituted and β-N,N-Disubstituted Enamino Esters in the Presence of Iridium(I) Catalyst. *Synthesis (Stuttg).* **2009**, No. 15, 2627–2633. https://doi.org/10.1055/s-0029-1217405.

(246) Stemp, G.; Ashmeade, T.; Branch, C. L.; Hadley, M. S.; Hunter, A. J.; Johnson, C. N.; Nash, D. J.; Thewlis, K. M.; Vong, A. K. K.; Austin, N. E.; Jeffrey, P.; Avenell, K. Y.; Boyfield, I.; Hagan, J. J.; Middlemiss, D. N.; Reavill, C.; Riley, G. J.; Routledge, C.; Wood, M. Design and Synthesis of Trans-N-[4-[2-(6-Cyano-1,2,3,4- Tetrahydroisoquinolin-2-Yl)Ethyl]Cyclohexyl]-4-Quinolinecarboxamide (SB- 277011): A Potent and Selective Dopamine D3 Receptor Antagonist with High Oral Bioavailability and CNS Penetration in the Rat. *J. Med. Chem.* **2000**, *43* (9), 1878–1885. https://doi.org/10.1021/jm000090i.

(247) Evans, D. H.; O'Connell, K. M.; Petersen, R. A.; Kelly, M. J. Cyclic Voltammetry. *J. Chem. Educ.* **1983**, *60* (4), 290–293. https://doi.org/10.1016/B978-0-12-409547-2.10764-4.

(248) Abdul-Rahim, O.; Simonov, A. N.; Rüther, T.; Boas, J. F.; Torriero, A. A. J.; Collins, D. J.;

Perlmutter, P.; Bond, A. M. The Observation of Dianions Generated by Electrochemical Reduction of Trans -Stilbenes in Ionic Liquids at Room Temperature. *Anal. Chem.* **2013**, *85* (12), 6113–6120. https://doi.org/10.1021/ac400915z.

(249) Bennett, B.; Chang, J.; Bard, A. J. Mechanism of the Br−/Br2 Redox Reaction on Platinum and Glassy Carbon Electrodes in Nitrobenzene by Cyclic Voltammetry. *Electrochim. Acta* **2016**, *219*, 1–9. https://doi.org/10.1016/j.electacta.2016.09.129.

(250) Schering Corporation and Pharmacopeia, I. Novel Pyrazolopyrimidines as Cyclin Dependent Kinase Inhibitors. US2004/209878, 2004, A1, 2004.

(251) Stahl, T.; Klare, H. F. T.; Oestreich, M. Main-Group Lewis Acids for C-F Bond Activation. *ACS Catal.* **2013**, *3* (7), 1578–1587. https://doi.org/10.1021/cs4003244.

(252) Uneyama, K. *Organofluorine Chemistry*; Blackwell Publishing LTD, Ed.; 2006. https://doi.org/10.2174/138527281916150731103731.

(253) Vogt, D. B.; Seath, C. P.; Wang, H.; Jui, N. T. Selective C-F Functionalization of Unactivated Trifluoromethylarenes. *J. Am. Chem. Soc.* **2019**, *141* (33), 13203–13211. https://doi.org/10.1021/jacs.9b06004.

(254) Dang, H.; Whittaker, A. M.; Lalic, G. Catalytic Activation of a Single C-F Bond in Trifluoromethyl Arenes. *Chem. Sci.* **2016**, *7* (1), 505–509. https://doi.org/10.1039/c5sc03415a.

(255) Jaroschik, F. Picking One out of Three: Selective Single C−F Activation in Trifluoromethyl Groups. *Chem. - A Eur. J.* **2018**, *24* (55), 14572–14582. https://doi.org/10.1002/chem.201801702.

(256) Andrieux, C. P.; Combellas, C.; Kanoufi, F.; Savéant, J. M.; Thiébault, A. Dynamics of Bond Breaking in Ion Radicals. Mechanisms and Reactivity in the Reductive Cleavage of Carbon-Fluorine Bonds of Fluoromethylarenes. *J. Am. Chem. Soc.* **1997**, *119* (40), 9527–9540. https://doi.org/10.1021/ja971094o.

(257) Uneyama, K.; Mizutani, G.; Maeda, K.; Kato, T. Electroreductive Defluorination of Trifluoromethyl Ketones and Trifluoroacetic Acid Derivatives. *J. Org. Chem.* **1999**, *64* (18), 6717–6723. https://doi.org/10.1021/jo990571d.

(258) Yamauchi, Y.; Fukuhara, T.; Hara, S.; Senboku, H. Electrochemical Carboxylation of α,α-Difluorotoluene Derivatives and Its Application to the Synthesis of α-Fluorinated Nonsteroidal Anti-Inflammatory Drugs. *Synlett* **2008**, *2008* (3), 438–443.

https://doi.org/10.1055/s-2008-1032069.

(259) Wu, J.; Cao, S. Nickel-Catalyzed Hydrodefluorination of Fluoroarenes and Trifluorotoluenes with Superhydride (Lithium Triethylborohydride). *ChemCatChem* **2011**, *3* (10), 1582–1586. https://doi.org/10.1002/cctc.201100083.

(260) Scott, V. J.; Çelenligil-Çetin, R.; Ozerov, O. V. Room-Temperature Catalytic Hydrodefluorination of C(Sp3)-F Bonds. *J. Am. Chem. Soc.* **2005**, *127* (9), 2852–2853. https://doi.org/10.1021/ja0426138.

(261) Panisch, R.; Bolte, M.; Müller, T. Hydrogen- and Fluorine-Bridged Disilyl Cations and Their Use in Catalytic C-F Activation. *J. Am. Chem. Soc.* **2006**, *128* (30), 9676–9682. https://doi.org/10.1021/ja061800y.

(262) Vol'pin, M. E.; Shevchenko, N. V.; Bolestova, G. I.; Zeifman, Y. V.; Fialkov, Y. A.; Parnes, Z. N. Selective Hydrogenolysis of the C-F Bond. *Mendeleev Commun.* **1991**, *1* (4), 118–119. https://doi.org/10.1070/MC1991v001n04ABEH000072.

(263) Stahl, T.; Klare, H. F. T.; Oestreich, M. C(Sp3)-F Bond Activation of CF3-Substituted Anilines with Catalytically Generated Silicon Cations: Spectroscopic Evidence for a Hydride-Bridged Ru-S Dimer in the Catalytic Cycle. *J. Am. Chem. Soc.* **2013**, *135* (4), 1248–1251. https://doi.org/10.1021/ja311398j.

(264) Nicolaou, K. C.; Chucholowski, A.; Dolle, R. E.; Randall, J. L. Reactions of Glycosyl Fluorides. Synthesis of O-, S- and N-Glycosides. *J. Chem. Soc., Chem. Commun.* **1984**, 1155–1156.

(265) Alcarazo, M.; Gomez, C.; Holle, S.; Goddard, R. Exploring the Reactivity of Carbon 0 Borane-Based Frustrated Lewis Pairs. *Angew. Chemie - Int. Ed.* **2010**, *49*, 5788–5791.

(266) Chen, K.; Berg, N.; Gschwind, R.; König, B. Selective Single C(Sp3)-F Bond Cleavage in Trifluoromethylarenes: Merging Visible-Light Catalysis with Lewis Acid Activation. *J. Am. Chem. Soc.* **2017**, *139* (51), 18444–18447. https://doi.org/10.1021/jacs.7b10755.

(267) Motohashi, H.; Mikami, K. Nickel-Catalyzed Aromatic Cross-Coupling Difluoromethylation of Grignard Reagents with Difluoroiodomethane. *Org. Lett.* **2018**, *20* (17), 5340–5343. https://doi.org/10.1021/acs.orglett.8b02264.

(268) Vasilopoulos, A.; Golden, D. L.; Buss, J. A.; Stahl, S. S. Copper-Catalyzed C-H Fluorination/Functionalization Sequence Enabling Benzylic C-H Cross Coupling with Diverse Nucleophiles. *Org. Lett.* **2020**, *22* (15), 5753–5757. https://doi.org/10.1021/acs.orglett.0c02238.

(269) Collin, D. E.; Folgueiras-Amador, A. A.; Pletcher, D.; Light, M. E.; Linclau, B.; Brown, R. C. D. Cubane Electrochemistry: Direct Conversion of Cubane Carboxylic Acids to Alkoxy Cubanes Using the Hofer–Moest Reaction under Flow Conditions. *Chem. - A Eur. J.* **2020**, *26* (2), 374–378. https://doi.org/10.1002/chem.201904479.

(270) Seiders, J. R.; Wang, L.; Floreancig, P. E. Tuning Reactivity and Chemoselectivity in Electron Transfer Initiated Cyclization Reactions : Applications to Carbon - Carbon Bond Formation. *J. Am. Chem. Soc.* **2003**, *125*, 2406–2407. https://doi.org/10.1021/ja029139v.

(271) Romano, C.; Fiorito, D.; Mazet, C. Remote Functionalization of α,β-Unsaturated Carbonyls by Multimetallic Sequential Catalysis. *J. Am. Chem. Soc.* **2019**, *141* (42), 16983–16990. https://doi.org/10.1021/jacs.9b09373.

(272) Einaru, S.; Shitamichi, K.; Nagano, T.; Matsumoto, A.; Asano, K.; Matsubara, S. Trans - Cyclooctenes as Halolactonization Catalysts. *Angew. Chemie - Int. Ed.* **2018**, *57*, 13863–13867. https://doi.org/10.1002/anie.201808320.

(273) Tan, C. K.; Le, C.; Yeung, Y. Organocatalysis Web Themed Issue. *Chem. Commun.* **2012**, *48*, 5793–5795. https://doi.org/10.1039/c2cc31148h.

(274) Musacchio, A. J.; Nguyen, L. Q.; Hudson Beard, G.; Knowles, R. R. Photoredox Method for Direct C − N Bond Formation. *J. Am. Chem. Soc.* **2014**, *136*, 12217–12220. https://doi.org/10.1021/ja5056774.

(275) Luo, Y.; Liu, H.; Su, M.; Sheng, L.; Zhou, Y.; Li, J.; Lu, W. Bioorganic & Medicinal Chemistry Letters Synthesis and Biological Evaluation of Piperamide Analogues as HDAC Inhibitors. *Bioorg. Med. Chem. Lett.* **2011**, *21* (16), 4844–4846. https://doi.org/10.1016/j.bmcl.2011.06.046.

(276) Scamp, R. J.; Jirak, J. G.; Dolan, N. S.; Guzei, I. A.; Schomaker, J. M. A General Catalyst for Site-Selective C(Sp 3)-H Bond Amination of Activated Secondary over Tertiary Alkyl C(Sp 3)-H Bonds Ryan J. Scamp, James G. Jirak, Nicholas S. Dolan, Ilia A. Guzei and Jennifer M. Schomaker*. *Org. Lett.* **2016**, *18* (12), 3014–3017.

(277) Uetake, Y.; Niwa, T.; Nakada, M. Synthesis of Cycloalkanone-Fused Cyclopropanes by Au (I) -Catalyzed Oxidative Ene-Yne Cyclizations. *Tetrahedron Lett.* **2014**, *55* (50), 6847–6850. https://doi.org/10.1016/j.tetlet.2014.10.084.

(278) Visbal, R.; Herrera, R. P.; Gimeno, M. C. Thiolate Bridged Gold(I)–NHC Catalysts: New Approach for Catalyst Design and Its Application to Trapping Catalytic Intermediates.

Chem. - A Eur. J. **2019**, *25* (69), 15837–15845. https://doi.org/10.1002/chem.201903494.

(279) Zhang, S.; Kolluru, L.; Vedula, S. K.; Whippie, D.; Jin, J. Carbon-Carbon Bond Forming Reactions via Pd-Catalyzed Detellurative Homocoupling of Diorganyl Tellurides. *Tetrahedron Lett.* **2017**, *58* (37), 3594–3597. https://doi.org/10.1016/j.tetlet.2017.07.087.

(280) Bedford, R. B.; Brenner, P. B.; Carter, E.; Carvell, T. W.; Cogswell, P. M.; Gallagher, T.; Harvey, J. N.; Murphy, D. M.; Neeve, E. C.; Nunn, J.; Pye, D. R. Expedient Iron-Catalyzed Coupling of Alkyl, Benzyl and Allyl Halides with Arylboronic Esters. *Chem. - A Eur. J.* **2014**, *20* (26), 7935–7938. https://doi.org/10.1002/chem.201402174.

(281) Ong, D. Y.; Yen, Z.; Yoshii, A.; Revillo Imbernon, J.; Takita, R.; Chiba, S. Controlled Reduction of Carboxamides to Alcohols or Amines by Zinc Hydrides. *Angew. Chemie - Int. Ed.* **2019**, *58* (15), 4992–4997. https://doi.org/10.1002/anie.201900233.

(282) Kelly, C. B.; Lambert, K. M.; Mercadante, M. A.; Ovian, J. M.; Bailey, W. F.; Leadbeater, N. E. Access to Nitriles from Aldehydes Mediated by an Oxoammonium Salt. *Angew. Chemie - Int. Ed.* **2015**, *54* (14), 4241–4245. https://doi.org/10.1002/anie.201412256.

(283) Barbuková, Z.; Kozubíková, H.; Zálešák, F.; Doležal, K.; Pospíšil, J. General Approach to Neolignan-Core of the Boehmenan Natural Product Family. *Monatshefte fur Chemie* **2018**, *149* (4), 737–748. https://doi.org/10.1007/s00706-017-2132-4.

(284) Wang, Z. J.; Lv, J. J.; Yi, R. N.; Xiao, M.; Feng, J. J.; Liang, Z. W.; Wang, A. J.; Xu, X. Nondirecting Group Sp3 C−H Activation for Synthesis of Bibenzyls via Homo-Coupling as Catalyzed by Reduced Graphene Oxide Supported PtPd@Pt Porous Nanospheres. *Adv. Synth. Catal.* **2018**, *360* (5), 932–941. https://doi.org/10.1002/adsc.201701389.

(285) Robinson, M. W. C.; Davies, A. M.; Buckle, R.; Mabbett, I.; Taylor, S. H.; Graham, A. E. Epoxide Ring-Opening and Meinwald Rearrangement Reactions of Epoxides Catalyzed by Mesoporous Aluminosilicates. *Org. Biomol. Chem.* **2009**, *7* (12), 2559–2564. https://doi.org/10.1039/b900719a.

(286) Gieshoff, T. N.; Chakraborty, U.; Villa, M.; Jacobi von Wangelin, A. Alkene Hydrogenations by Soluble Iron Nanocluster Catalysts. *Angew. Chemie - Int. Ed.* **2017**, *56* (13), 3585–3589. https://doi.org/10.1002/anie.201612548.

(287) Richter, S. C.; Oestreich, M. Bioinspired Metal-Free Formal Decarbonylation of α-Branched Aliphatic Aldehydes at Ambient Temperature. *Chem. - A Eur. J.* **2019**, *25* (36), 8508–8512. https://doi.org/10.1002/chem.201902082.

(288) Christensen, S. H.; Holm, T.; Madsen, R. Ring-Opening of Cyclic Ethers with Carbon-Carbon Bond Formation by Grignard Reagents. *Tetrahedron* **2014**, *70* (33), 4942–4946. https://doi.org/10.1016/j.tet.2014.05.026.

(289) Hashimoto, T.; Maruyama, T.; Yamaguchi, T.; Matsubara, Y.; Yamaguchi, Y. Cross-Coupling Reactions of Alkyl Halides with Aryl Grignard Reagents Using a Tetrachloroferrate with an Innocent Countercation. *Adv. Synth. Catal.* **2019**, *361* (18), 4232–4236. https://doi.org/10.1002/adsc.201900568.

(290) Liu, D.; Li, Y.; Qi, X.; Liu, C.; Lan, Y.; Lei, A. Nickel-Catalyzed Selective Oxidative Radical Cross-Coupling: An Effective Strategy for Inert Csp3-H Functionalization. *Org. Lett.* **2015**, *17* (4), 998–1001. https://doi.org/10.1021/acs.orglett.5b00104.

(291) Argouarch, G. Mild and Efficient Rhodium-Catalyzed Deoxygenation of Ketones to Alkanes. *New J. Chem.* **2019**, *43* (28), 11041–11044. https://doi.org/10.1039/c9nj02954k.

(292) Du, Z.; Sun, Z.; Zhang, W.; Miao, H.; Ma, H.; Xu, J. A Free Radical Process for Oxidation of Hydrocarbons Promoted by Nonmetal Xanthone and Tetramethylammonium Chloride under Mild Conditions. *Tetrahedron Lett.* **2009**, *50* (15), 1677–1680. https://doi.org/10.1016/j.tetlet.2009.01.077.

(293) Bartoli, G.; Cimarelli, C.; Dalpozzo, R.; Palmieri, G. A Versatile Route to β-Enamino Esters by Acylation of Lithium Enamines with Diethyl Carbonate or Benzyl Chloroformate. *Tetrahedron* **1995**, *51* (31), 8613–8622. https://doi.org/10.1016/0040-4020(95)00476-O.

(294) Watanabe, K.; Hamada, T.; Moriyama, K. Ring-Contraction Reaction of Substituted Tetrahydropyrans via Dehydrogenative Dual Functionalization by Nitrite-Catalyzed Double Activation of Bromine. *Org. Lett.* **2018**, *20* (18), 5803–5807. https://doi.org/10.1021/acs.orglett.8b02488.